REPERTOIRE SELECTION AND EFFECTOR DIFFERENTIATION DURING NKT CELL DEVELOPMENT

By

Laura Elizabeth Gordy

Dissertation

Submitted to the Faculty of the

Graduate School of Vanderbilt University

in partial fulfilment of the requirements

for the degree of

DOCTOR OF PHILOSOPHY

In

Microbiology and Immunology

May, 2012

Nashville, Tennessee

Approved:

Professor Luc Van Kaer

Professor Mark Boothby

Professor Eric Sebzda

Professor Ann Richmond

Professor Sebastian Joyce

To Mom and Dad, for their limitless love and support

& for introducing me to Mr Wizard and the wonderful world of science

and

To my love, Daniel, for being my everything

ACKNOWLEDGMENTS

The studies reported in this work were financially supported by the Immunobiology of Blood and Vascular Systems Training Grant (HL069765) and the Cellular and Molecular Microbiology Training Grant (AI007611); research grants (AI061721 and AI042284); and Core Facility grants (CA068485 and DK058404) from the National Institutes of Health.

I am especially grateful to the past Department of Microbiology and Immunology and the current Department of Pathology, Microbiology and Immunology and those whom made it a supportive and an enriching environment conducive to the growth of a budding scientist. Over the years I have had the great pleasure of working with and learning from numerous inspiring scientists. In particular I am indebted to my Dissertation Committee Chair, Luc Van Kaer, and Dissertation Committee: Mark Boothby, Eric Sebzda, and Ann Richmond, who have always had words of wisdom, confidence in my ability as a scientist, and a comforting smile during high and low points of my graduate career.

I am thankful for the many friends I have made along the way, of which many are past lab members. It is the infectious enthusiasm of one particular lab member that drew me to the Joyce lab and our years of late night experiments with loud music and countless chocolates that led me to think of her now as a big sister, Jelena Bezbradica. None of this would have been possible if not for my mentor, Professor Sebastian Joyce. Shaping me into a scientist was hard work

for him and one of the many things boss taught me is that you can always work harder and do better. We have come a long way and I have learned more about science and myself than I thought possible, for that I am forever grateful!

Finally, words cannot express my gratitude and love for my mom and dad. A loving home, support to follow my dreams and the tools to achieve them… what more could a child want? They are the reason I strive to be better at everything I do. Most importantly, I wish to thank my loving and supportive husband, Daniel, who was both my rock and my teddy bear over the course of this rollercoaster called graduate school.

TABLE OF CONTENTS

LIST OF TABLES

LIST OF FIGURES

LIST OF ABBREVIATIONS

α-galactosylceramide (αGalCer)

α-galactosyldiacylglycerol (αGalDAG)

β-glucosylceramide (βGlcCer)

β-hexosaminidase-B (HexB)

adapter protein (AP)-3

antigen presenting cells (APC)

colony stimulating factor 2 (CSF-2)

dendritic cells (DC)

diacylglycerol (DAG)

dominant negative (ΔN)

double negative (DN)

double positive (DP)

experimental autoimmune encephalomyelitis (EAE)

fetal thymic organ culture (FTOC)

follicular helper NKT (NKT_{FH})

Francisella tularensis subsp. novicida (*Ft* novicida)

GATA binding protein 3 (Gata-3)

glycosphingolipid (GSL)

Helix-loop-helix E protein (Raberger et al.)

IL-15-deficient ($IL\text{-}15^0$)

IL-17 secreting NKT (NKT-17)

IL-2 inducible tyrosine kinase (ITK)

inducible T cell costimulatory (ICOS)

interferon regulatory factor (IRF)-1

interferon-γ (IFN-γ)

Interleukin (IL)

isoglobotrihexoslyceramide (iGb3)

Jak3 (Janus kinase-3)

lipopolysaccharide (LPS)

lysophosphatidyle-choline (LPtDCho)

Macrophage inflammatory protein 1α (MIP-1α)

myeloid differentiation primary response gene (MyD88)

natural killer (NK)

natural killer T (NKT)

neuropilin-1 (Nrp-1)

NKT cell receptor (NKTCR)

pathogen associated molecular patterns (PAMPs)

pattern recognition receptors (PRRs)

phosphatidyl-ethanolamine (PtdEtN)

phosphatidyl-inositol (PtdIno)

plasmacytoid DC (pDC)

programmed death-1 (PD-1)

promyelocytic leukaemia zinc finger (PLZF)

recent thymic emigrants (RTE)

Regulated on activation, normal T expressed and secreted (RANTES)

regulatory $FoxP3^+$ NKT ($FoxP3^+$ NKTreg)l

retinoic acid orphan receptor-γt (RORγt)

runt related transcription factor 1 (Runx1)

signalling lymphocytic activation molecule (SLAM)

T cell receptor (TCR)

T-cell-specific T-box transcription factor (T-bet)

tail-deleted (TD)

Th-inducing POZ/Kruppel-like factor (ThPOK)

TIR-domain-containing-adaptor-inducing-interferon-β (Trif)

Toll-like receptors (TLRs)

tramtrack bric-a-brac-zinc finger (BTB)

transforming growth factor (TGF)

transforming growth factor-β (TGFβ)

transgenic (^{tg})

Tumour necrosis factor-α (TNF-α)

vitamin D receptor (VDR)

wild type (wt)

ZAP (ζ chain-associated protein)-70

CHAPTER I

INTRODUCTION

Prevention of disease by recognition and elimination of foreign substances and microbial and parasitic pathogens is the main objective of the immune system. As with any battle, multiple lines of defence help to sway the outcome. Thus, the vertebrate immune system has inherited the innate immune system from its predecessors and additionally evolved an adaptive immune system to defend the host against invasive molecules and organisms. The initial line of defence, i.e., the innate immune system has evolved to recognize conserved molecular patterns shared by the classes of microbes. This recognition allows for rapid responses and elimination of the pathogen. Over time pathogens have in turn evolved to evade this system of recognition. Thus, a second line of defence has evolved, the adaptive immune response. The adaptive immune response is composed of B and T lymphocytes, which are capable of recognizing a specific pathogen and maintaining memory to the same pathogen to prevent future infection and disease. One outcome of the innate immune response is to alert the adaptive immune system of a threatening situation, inform it about the nature if the incoming treat and instruct the initiation of the appropriate type of adaptive response. Alternatively, when the first line of defense fails in any of those tasks, it is important to quickly alert and bring in the second line of defense. It is at this step that natural killer T (NKT) cells are

thought to act; they act as a bridge between innate and adaptive immunity and play an important role in jump-starting the adaptive immune response.

The hallmark of innate immunity is that of microbial pattern recognition. Cells of the innate immune system such as antigen presenting cells (APCs: dendritic cells (DCs) and macrophages) and natural killer (NK) cells express an array of pattern recognition receptors (PRRs) (Medzhitov, 2001). PRRs come in a variety of flavors such as the membrane bound Toll-like receptors (TLRs) and the mannose receptor or the intracellular family of TLRs and NOD proteins. These receptors recognize the conserved pathogen associated molecular patterns (PAMPs). PAMPs include patterns commonly displayed by pathogens (e.g., viruses and bacteria) and not by the host, such as double-stranded RNA, flagellin and lipopolysaccharide (LPS), or structures found in abnormal locations within host cells (e.g., cytosolic DNA) indicating the presence of the foreign agent. Stimulation through PRRs induces a number of host defense genes including pro-inflammatory cytokines, co-stimulatory molecules and tissue repair agents. Pattern recognition and the ensuing induction of cytokines and co-stimulatory molecules are critical to permit the activation of the adaptive immune cells upon their recognition of foreign antigens displayed by MHC class I and II molecules. Interestingly, antigen recognition by NKT cells can be likened to that of pattern recognition by innate cells. This is because NKT cells express a semi-invariant T cell receptor (NKTCR) and recognize diverse ligands presented by CD1d molecules through the germline-encoded regions of the receptor (Li et al., 2010; Scott-Browne et al., 2007). Furthermore, like innate cells, NKT cells

respond to lipid antigen rapidly, within hours, and without the need for days-long priming phase seen in the typical initiation of the adaptive response.

CONVENTIONAL T CELLS VS NKT CELLS

NKT cells are a unique subset of T cells, which are developmentally divergent and functionally distinct from conventional T cells. They get their name from the fact that they express markers and functions of both conventional T cells (TCR, CD4, CD44) and NK cells (NK1.1, Ly49 family members). NKT cells can be broken down into two main subgroups, NKT type I and type II. Type I or the invariant NKT cells recognize ligands with a semi-invariant TCR consisting of an invariant mouse Vα14Jα18 (Lantz and Bendelac, 1994) (human Vα24Jα18 (Exley, 1997;Lantz, 1994)) α-chain that pairs with either Vβ8.2 (homologous to the human Vβ11), Vβ7, or Vβ2 β-chain (Arase et al., 1992; Hayakawa et al., 1992). They make up to 80% of NKT cells (Park et al., 2001) and can be identified by using multimeric α-galactosylceramide (αGalCer)-loaded CD1d molecule (MacDonald, 2000; Matsuda et al., 2000). On the other hand, type II NKT cells are a small and more diverse subset of NKT cells expressing a heterogeneous array of αβ TCRs of which two recurring TCR are Vα3.2-Jα9/Vβ8 and Vα8/Vβ8 (Park et al., 2001). Sulfatide and lyso-sulfatide have been identified as antigens for type II cells but neither is recognized by the Vα3.2-Jα9 and Vα8 NKT cells (Arrenberg et al., 2010; Roy et al., 2008). Thus, study of this population has been hindered by the limited knowledge of cell specific markers

and known agonists. Therefore, the type I invariant NKT cells will be the focus of the rest of this thesis and referred to simply as NKT cells.

Both conventional T cells and NKT cells undergo the same early thymic development but it is their divergent developmental program upon positive selection by cognate antigen (discussed later) that shapes their immunological roles. While conventional T cells develop to recognize foreign peptide in the context of MHC class I or class II molecules, NKT cells are thymus-derived lymphocytes whose functions are regulated by recognition of foreign or self glycolipid ligands presented by the MHC class I-like molecule CD1d. Additionally, developing NKT cells are unique in that upon maturation they attain a memory-like phenotype, which includes the expression of cell surface CD44, CD69, CD122 and CD127 markers and transcripts encoding effector molecules (Park et al., 2000). The NKT cell's hybrid features give insight to its role as a bridge between the adaptive and innate immune response. Upon agonistic ligand recognition, their memory-like phenotype allows NKT cells to rapidly, within 30—60 minutes, secrete large amounts of immunoregulatory cytokines and upregulate costimulatory molecules to initiate and modulate the type, magnitude and duration of the effector functions elicited by myeloid and lymphoid cells. By doing so, NKT cells regulate microbial and tumour immunity as well as autoimmune diseases (Bendelac et al., 2007; Van Kaer, 2005). Thus, NKT cells are often referred to as immunoregulatory lymphocytes, and they acquire this immunoregulatory potential during development through poorly understood processes. NKT cell frequency varies both between mouse strains

—highest in BALB/c (1—2 million in thymus, liver and spleen) and the lowest in the autoimmune disease predisposed strains NOD and SJL (0.1—0.3 million)—and between healthy human individuals —ranging from 0.01—5.0% in peripheral blood (Godfrey et al., 2010). Hence, understanding how NKT cells develop, regulate their frequency and acquire functional potential is of fundamental and clinical importance because the new insight can lead to the design of NKT cell-based therapies.

NKT CELL AGONISTS

Kirin Pharmaceuticals identified the first NKT cell antigen in a screen for anticancer agents. A glycolipid derived from a marine sponge was found to be capable of enhancing survival of tumour bearing mice. Identification of the active anti-tumor principle revealed it to be the α-linked glycolipid αGalCer (Fig. 1-1) (Morita et al., 1995). Further study into its mechanism of action revealed αGalCer's ability to robustly stimulate NKT cells, which in turn initiates and modulates the anti-tumor functions of myeloid and lymphoid cells (Carnaud et al., 1999; Kawano et al., 1997; Singh et al., 1999; Yamaguchi et al., 1996). Identification of this potent agonist enhanced the ability to track NKT cells and their functions with αGalCer-loaded CD1d tetramers or dimers (MacDonald, 2000; Matsuda et al., 2000). This advance also provided gross structural insight into what type of ligands NKT cells are able to see, and hence led to the

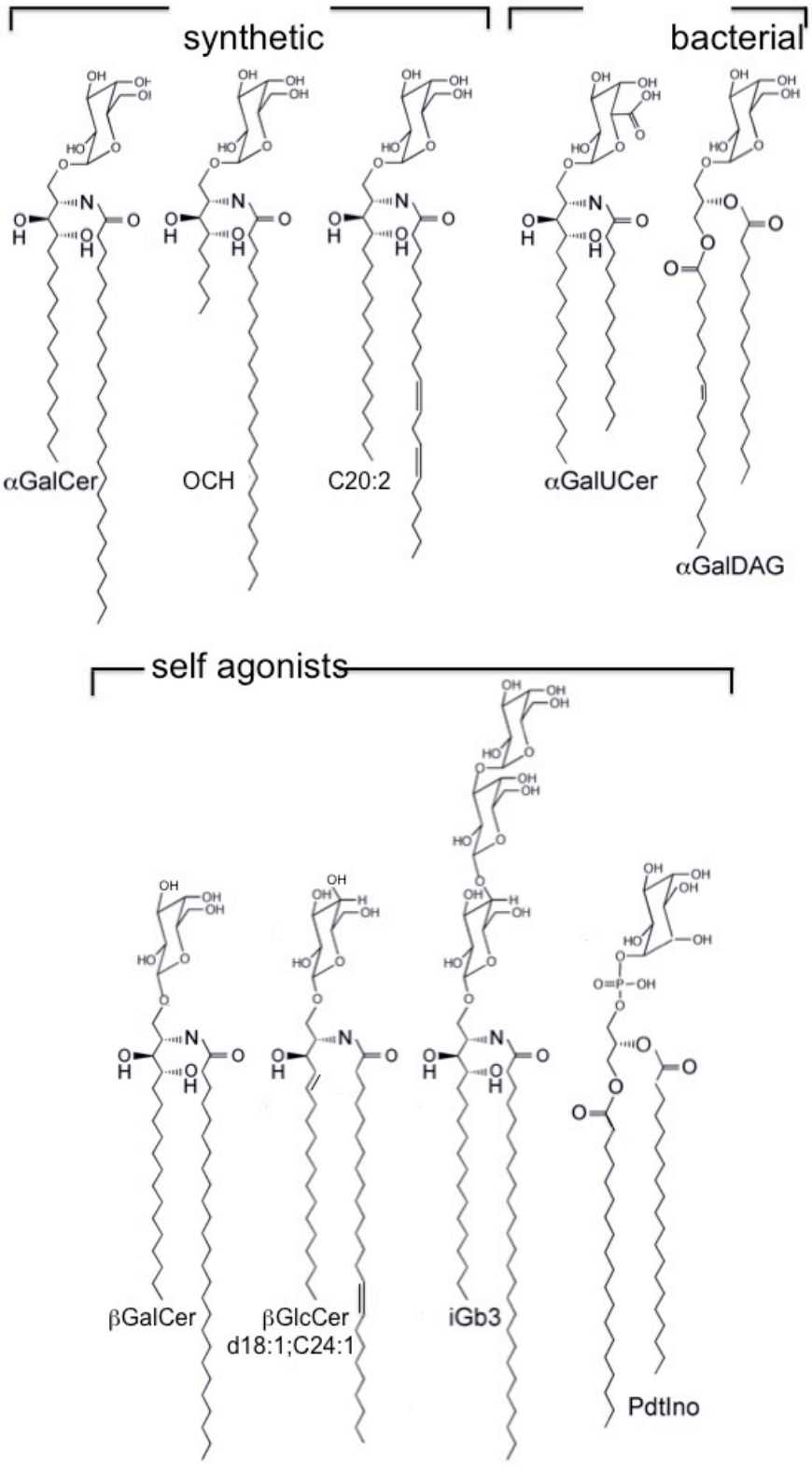

Figure 1-1. Chemical structures of NKT cell antigens

Top row: α-anomeric GSL, bottom row: β-anomeric GSL

identification of additional glycolipid exogenous antigens (Table 1-1) and endogenous agonists (Table 1-2) (Joyce et al., 2011; Venkataswamy and Porcelli, 2010).

Early studies addressing the nature of NKT cell antigens revealed autoreactivity of these cells to the cell types expressing CD1d (Bendelac et al., 1994; Bendelac et al., 1995; Exley et al., 1997). This reactivity was dependent upon proper trafficking of mouse CD1d through late endosomal vesicles, indicating that a self-antigen(s) reside therein (Chiu et al., 1999; Chiu et al., 2002; Salio et al., 2010). This raised the question: What is the endogenous selecting NKT cell ligand(s)? CD1d assembly studies revealed the ability of CD1d to bind phospholipids (De Silva et al., 2002; Joyce et al., 1998; Park et al., 2004). In turn, a few NKT cell hybridomas were identified which react to phospholipids (Gumperz et al., 2000; Rauch et al., 2003), indicating a possible role for phospholipids as selecting ligands. However, the inability of CD1d-expessing cells deficient for β-glucosylceramide (βGlcCer) synthase to activate NKT cells suggested a role for a β-GlcCer or its derived glycosphingolipid (GSL) products (Stanic et al., 2003). Initially, isoglobotrihexoslyceramide (iGb3), an endosome-resident product of β-GlcCer metabolism, was implicated as a probable candidate for the selecting ligand. This candidate emerged from studies using β-hexosaminidase-B (HexB) deficient mice. HexB is an lysosomal enzyme required for production of iGb3 from its precursor iGb4. Mice lacking HexB do not develop NKT cells and HexB-deficient DCs are incapable of stimulating NKT hybridomas (Zhou et al., 2004).

Table 1-1. Exogenous NKT cell agonists

Source	Ligand	Reference
Mycobacterium tuberculosis	phosphatidylinositol tetramannoside ($PtdInoMan_4$)	(Fischer et al., 2004)
Sphingomonas	α-galacturonosylceramide (αGalACer)	(Kinjo et al., 2005; Mattner et al., 2005; Sriram et al., 2005)
Borrelia burgdorferi	α-galactosyldiacylglycerol (αGalDAG)	(Kinjo et al., 2006)
Helicobacter pylori	cholesteryl-6-O-acyl α-glucoside	(Chang et al., 2011b)
Streptococcus pneumoniae	(DAG; 1,2-di-*O*-acyl-(α-glucopyranosyl)-(13)-glycerol) (α-galactopyranosyl)-(12)-(α-glucopyranosyl)-(13)-glycerol)	(Kinjo et al., 2011)

Table 1-2. Endogenous agonists

Source	Ligand	Reference
Glycosphingolipids	β-D-glucopyranosylsylceramide (βGlcCer; d18:1;C24:1);	(Brennan et al., 2011)
	β-D-galactopyranosylsylceramide (βGalCer)	(Parekh et al., 2004)
	β-mannosylceramide (βManCer)	(O'Konek et al., 2011)
	isoglobotrihexosylceramide (iGb3)	(Wu et al., 2003; Zhou et al., 2004)
Glycerophospholipids	phosphatidyl-inositol (PtdIno)	(Fox et al., 2009)
	phosphatidyl-ethanolamine (PtdEtN)	(Gumperz et al., 2000)
	lysophosphatidyle-choline (LPtdCho)	(Rauch et al., 2003)

While this implies iGb3 as a NKT cell antigen and points to a role as the endogenous selecting ligand, an underlying glycolipid storage disorder, which mistargets cellular lipids, in HexB-deficient mice might complicate the interpretation of the results described above (Gadola et al., 2006b). Moreover, mice lacking iGb3 synthase —the enzyme dedicated to iGb3 biosynthesis— display normal NKT cell development (Porubsky et al., 2007). Thus, while originally defective NKT cell activation in the absence of βGlcCer synthase had been attributed to the downstream effect on iGb3, the role of βGlcCer itself as an NKT cell antigen was recently brought to light. βGlcCer acts as a potent and abundant self antigen which accumulates in cells upon infection or TLR stimulation (Brennan et al., 2011). The antigen accumulation within activated APCs, is consistent with data indicating that primary NKT cells become activated in CD1d-dependent manner upon triggering of APC with microbial products such is LPS. Finally, while the search for NKT cell antigens has been focused on GSLs, a recent study revealed that in some cases NKT cells could be activated even in the absence of GSL (Pei et al., 2011), thus, revealing the need to broaden the current candidate list for NKT cell self antigens.

ANTIGEN RECOGNITION BY NKTCR

While NKT cell antigens are all glycolipids, the NKTCRs can recognize rather structurally diverse array of both foreign and self-ligands. Additionally, the ability of synthetic antigen αGalCer to stimulate all invariant NKT cells irrespective of Vβ usage raises questions about the recognition logic of the

NKTCR. A number of mutational and crystallographic studies have investigated the unique features of ligand recognition by the NKTCR (Godfrey et al., 2010; Joyce et al., 2011) Antigen recognition by conventional T cells is dependent on diagonal orientation of the TCR over peptide-MHC complex allowing critical interactions of this complex with the variable, non-germline encoded CDR loops of the TCR (Marrack et al., 2008). On the other hand, NKT cells have been shown to have a more parallel orientation of TCR to glycolipid-CD1d (Borg et al., 2007a; Borg et al., 2007b; Pellicci et al., 2009). And it is the germline-encoded surface of the TCR that is responsible for the interaction with and proper recognition of glycolipid-CD1d ligands (Li et al., 2010; Scott-Browne et al., 2007). Recognition by germline encoded CDR loops (CDR1α, CDR3α, CDR2β) is thought to drive the Vβ usage bias seen within NKTCR (Mallevaey et al., 2009). Thus, it has been proposed that the NKTCR acts like a pattern recognition receptor. It uses the conserved germline sequences to recognize multiple lipid ligands within the CD1d groove similarly, by focusing most of its recognition logic on the conserved 'hotspots' within diverse CD1d-ligand structures. Additionally, NKTCR uses some beta-chain sequences to further adapt itself to a few unique aspects of diverse CD1d-restricted ligands, presumably allowing for fine-tuning of the 'hotspot' recognition logic and the appropriate downstream response (Florence et al., 2009). This ability renders NKT cells important players in various infections and disease.

NKT CELL ACTIVATION BY ENDOGENOUS AND EXOGENOUS ANTIGENS

NKT cells are capable of responding to a wide range of pathogens because they employ two different modes of activation during an immune response: direct and indirect activation (Fig. 1-2) (Brigl and Brenner, 2010; Tupin et al., 2007). In the direct activation pathway, some microbial lipid antigens (Table 1-1) have been identified that are capable of directly activating NKT cells. This direct activation is critically dependent upon loading of such antigens onto CD1d, but appears independent of TLR signalling and of its downstream adaptor molecules: myeloid differentiation primary response gene (MyD88) and TIR-domain-containing-adaptor-inducing-interferon-β (Trif). As such, NKT cells in MyD88 and Trif deficient mice are just as responsive to *Sphingomonas* (Kinjo et al., 2005; Mattner et al., 2005) and *Borrelia* infection as are wild type mice (Kinjo et al., 2006). To rule out the contribution of the endogenous antigen iGb3 to this recognition, HexB deficient APC were analysed and also found to be equally effective in eliciting NKT cell response to *Sphingomonas* (Mattner et al., 2005). Thus, NKT cell activation is the result of direct recognition of *Sphingomonas* and *Borrelia glycolipids.*

While direct NKT cell lipid ligands have been identified from a few bacteria (see Table 1-1), several bacteria do not synthesize NKT cell ligands but nonetheless are capable of activating NKT cells. Studies reveal that these pathogens activate NKT cells through an indirect activation pathway (Fig. 1-2) (Tupin et al., 2007). Indirect activation entails four activation strategies that do not involve direct NKTCR recognition of pathogen-derived lipid ligands.

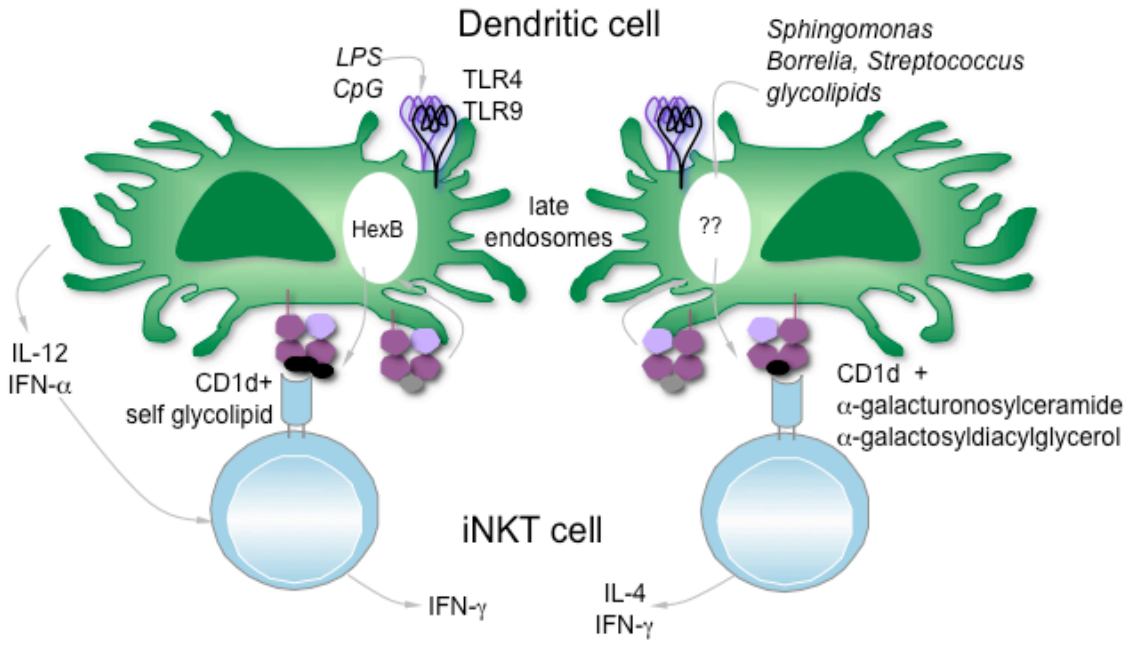

Figure 1-2. Two distinct strategies for NKT cell activation by microbes

Left: Microbes containing TLR ligands such as LPS activate NKT cells by inducing IL-12 production by DC, which amplifies weak responses elicited upon the recognition of CD1d bound with self-glycolipids by the NKT cell receptor. iGb3 has been suggested to function as an endogenous glycolipid for stimulating iNKT cell responses. The generation of iGb3 requires the action of HexB.
Right: Some microbes such as *Sphingomonas capsulata*, which belong to the class of α-Proteobacteria, synthesize α-anomeric glycolipids (Table 1-1) for their cell walls. These glycolipids, when presented by CD1d, activate NKT cells directly, without the need for endogenous iNKT cell antigens.

The first is a form of autoreactivity in which expression of weak endogenous NKT antigen in the context of stimulatory cytokines activate NKT cells. NKT cells utilize this mode of activation in the recognition of *Salmonella.* Dendritic cells stimulated by heat-killed *Salmonella* are capable of activating NKT cell in a HexB (Zhou et al., 2004), TLR, and interleukin-12 (IL-12)-dependent manner (Brigl et al., 2003). Thus, TLR activated APC in turn activate NKT cells by presenting an endogenous lipid antigen and supplying the necessary co-stimulatory cytokine IL-12 (Brigl et al., 2003; Mattner et al., 2005; Paget et al., 2007; Salio et al., 2007). Indirect recognition pathway assumes either upregulation of endogenous antigen, upregulation of CD1d or both, and the models are not mutually exclusive. Indeed a number of reports indicate that bacteria are capable of inducing upregulation of CD1d on APC (Raghuraman et al., 2006; Skold et al., 2005). This up-regulation can lead to enhanced NKT cell stimulation in the context of IL-12. Furthermore, studies by Brennan et al. (2011) revealed that there are situations where endogenous antigen is upregulated in response to TLR, and yet again, in combination with IL-12 activates NKT cells. Thus it has yet to be determined whether a change in the endogenous antigen expressed and/or the level of CD1d expression is key to NKT cell activation process.

A second form of indirect activation involves stimulation by endogenous antigen alone. NKT cell response to *Schistosoma mansoni* eggs is HexB dependent yet TLR and IL-12 independent (Faveeuw et al., 2002; Mallevaey et al., 2006). As with the previous strategy, it is unclear whether there is a change in the endogenous antigen expressed or its expression level. Additionally it is not

known whether APC are stimulated in a non-TLR-dependent manner to secrete stimulatory cytokines other than IL-12.

Thirdly, NKT cells can be stimulated by a combination of pro-inflammatory cytokines alone. *Escherichia coli* LPS is capable of stimulating NKT cells in a CD1d-independent manner. IL-12 and IL-18 production by TLR stimulated DC is critical to this process (Nagarajan and Kronenberg, 2007). Similarly, NKT cell response to murine cytomegalovirus is dependent upon IL-12 and independent of CD1d (Tyznik et al., 2008; Wesley et al., 2008).

The fourth and final endogenous-pathway activation strategy involves NKT cell activation through the cross-talk of plasmacytoid DCs (pDC) and myeloid DCs. Activated human pDC are capable of inducing an NKT cell response yet lack CD1d expression. In a study, cytokines produced by pDCs allowed NKT cells to respond to myeloid DCs (Montoya et al., 2006) by mechanisms that still remain unclear. Thus, there are numerous mechanisms by which NKT cells can be rapidly activated against a pathogen insult.

Whether activated directly or indirectly, NKT cells respond quickly with the secretion of cytokines (Carnaud et al., 1999; Singh et al., 1999). As part of their memory-like phenotype, NKT cells have stores of transcribed IL-4 and interferon-γ (IFN-γ) mRNA and perhaps other effector transcripts as well (Stetson et al., 2003). Upon stimulation with αGalCer, NKT cells begin to secrete IL-4 within a matter of an hour (Carnaud et al., 1999; Yoshimoto and Paul, 1994). This is followed by the induction and secretion of IFN-γ and by the modulation of their cell surface markers. First, the TCR is down regulated followed more slowly

by NK1.1 (Crowe et al., 2003; Eberl and MacDonald, 1998; Harada et al., 2004; Wilson et al., 2003). It is at this point the NKT cells undergo a phase of rapid proliferation and expansion. During expansion they begin to re-express the TCR and NK1.1. The previously activated NKT cells acquire an anergic or unresponsive phenotype (Hayakawa et al., 2004; Parekh et al., 2005; Uldrich et al., 2005) due to the induction of programmed death (PD)-1, an inhibitory receptor (Chang et al., 2008; Parekh et al., 2009). This anergic state to further stimulation persists for up to a month past the last stimulation during which time NKT cell numbers undergo a contraction phase (Parekh et al., 2005). Administration of αGalCer to anergic NKT cells reveals impaired proliferation and impaired IFN-γ production but not IL-4 (Parekh et al., 2005). This altered cytokine profile has implications for the therapeutic use of αGalCer. Therapies which depend upon Th2 immune responses (i.e. EAE) are not impaired while those that depend upon Th1 immune responses (i.e. anti-tumor immunity to B16 melanoma) are impaired by NKT cell anergy (Parekh et al., 2005). Anergy also impacts NKT cell response to microbes. For example, after the initial activation and expansion of NKT cells during *Mycobacterium bovis* infection, there is a contraction of NKT cell numbers and they become hypo-responsive (Chiba et al., 2008). This hypo-responsiveness occurs despite a continuing active infection (Chiba et al., 2008). Overactivation of NKT cells can be detrimental and result in immunopathology. This suggests that the controlled shutdown of an NKT cell response by contraction of cell numbers and anergy is important during a NKT cell response to microbes.

In addition to IL-4 and IFN-γ, NKT cells are capable of secreting a wide array of cytokines such as: IL-2, IL-3, IL-5, IL-6, IL-9, IL-10, IL-13, IL-17, IL-21, granulocyte macrophage colony stimulating factor (CSF-2), tumor necrosis factor (TNF)-α, macrophage inflammatory protein (MIP)-1α, MIP-1β, transforming growth factor (TGF)-β, osetopontin, lymphotactin, and RANTES (Arase et al., 1993; Bendelac et al., 1992; Coquet et al., 2008; Exley et al., 1997; Hayakawa et al., 1992). This diverse arsenal of Th1, Th2, Th17 and other cytokines give NKT cells the ability to communicate with and direct the effector functions of a variety of cell types. Obviously, it would not be beneficial for a single NKT cell to make all these cytokines at once, so models are emerging which describe phenotypically distinct subsets of NKT cells dedicated to at least some of these specialised functions. For example, IL-17 production is highly restricted to NK1.1$^-$CD4$^-$RORγ^+ NKT cells, as discussed later. This ability to quickly respond to infections and communicate with other cells of the immune system make NKT cells an important subset of immunoregulatory cells. For example, stimulation-induced cytokines and costimulatory molecules produced by NKT cells enhance IL-12 and costimulatory molecule expression by DCs (Fujii et al., 2004; Kitamura et al., 1999; Singh et al., 1999; Tomura et al., 1999). The enhanced expression of IL-12 in turn trans-activates NK cells to secrete IFN-γ (Carnaud et al., 1999; Eberl and MacDonald, 2000). In addition to NK cells, NKT cells mediate maturation of DCs, which allows transactivation and cross-priming (presentation of extracellular antigens) of cytotoxic T cells (Fujii et al., 2004; Fujii et al., 2003; Hermans et al., 2003; Nishimura et al., 2000;

Semmling et al., 2010). By trans-activating NK cells and cytotoxic T cells, NKT cells help to activate immune responses against viruses and other intracellular microbes. On the other hand, secretion of TGFβ, IL-10 and IL-2 by NKT cells has been shown to play a role in promoting T regulatory cell activation (La Cava et al., 2006). Thus, NKT cells can also initiate suppression of immune responses.

Early allergy studies revealed a role for NKT cells in B cell antibody responses. Mice lacking $CD4^+$ NKT cells were not capable of making an IgE antibody response upon polyclonal stimulation with anti-IgD antibody (Yoshimoto et al., 1995). In other immune hypersensitivity models such as lupus, NKT cells were found to stimulate B1 B cells to produce dsDNA autoantibodies (Takahashi and Strober, 2008). NKT cell mediated B cell help can also play a protective role. During infections such as *Borrelia burgdorferi* (Kumar et al., 2000), and *Streptococcus pneumoniae* (Kobrynski et al., 2005) CD1d deficiency results in impaired antibody production. Likewise, αGalCer exhibits adjuvant effect upon humoral responses (Devera et al., 2008; Ko et al., 2005). Specific responses to T cell dependent and T cell independent model antigens improved when co-administered with αGalCer (Lang et al., 2006). NKT cells provide help to B cells through direct receptor mediated interactions (i.e. CD28 and CD154) and secretion of soluble factors (i.e. IL-4, IFN-γ) (Lang, 2009). The above represent a few of many examples in which NKT cells can suppress or stimulate an immune response.

The cytokine profile of NKT cells is dependent upon a number of factors such as the lipid agonist, the APC type, and age/maturation status of the NKT cells (Matsuda et al., 2008; Parekh et al., 2004). The prototypical agonist αGalCer induces Th1, Th2 and Th17 cytokines. Conversely, a preferential Th2-like polarization is seen when NKT cells are stimulated with OCH (Fig. 1-1), a truncated αGalCer variant (Miyamoto et al., 2001) or C20-diene (Fig. 1-1), another variant with di-unsaturated acyl chain (Yu et al., 2005). It is thought that immature $NK1.1^{NEG}$ NKT cells secrete IL-4 with more mature $NK1.1^{+}$ NKT cells gaining the ability to secrete IFN-γ. This however, is an over simplification and a number of studies have begun to address the functional potential of NKT cells through the classification of subsets based on additional cell surface markers and their ability to secrete various cytokines. One such study looked at the differences in anti-tumour potential between $CD4^{+}$ and $CD4^{NEG}CD8^{NEG}$ double negative (DN) NKT cells (Crowe et al., 2005). DN NKT cells showed greater anti-tumour activity than the $CD4^{+}$ counterparts. This function of DN NKT cells was enriched within liver NKT cells compared to those from thymus and spleen (Crowe et al., 2005). Three recently identified new subsets of NKT cells include IL-17 secreting NKT (NKT-17) cells, regulatory $FoxP3^{+}$ NKT ($FoxP3^{+}$ NKTreg) cells, and follicular helper NKT (NKT_{FH}) cells. Upon stimulation, NKT-17 cells robustly secrete IL-17 a proinflammatory cytokine (Michel et al., 2007). Similar to conventional $CD4^{+}$ T_H17 cells, NKT-17 cells express RORγt (Michel et al., 2008; Rachitskaya et al., 2008) yet do not require IL-6, IL-23, and transforming growth factor-β (TGF-β) to produce IL-17. NKT-17 cells are $NK1.1^{NEG}CD4^{NEG}$ and found

distributed throughout tissue where NKT cells are ordinarily found (thymus, spleen, liver, lung, and lymph node). Another study found that all T_H17 producing NKT cells were IL-17 receptor β^+ and $CD122^{NEG}$ (Watarai et al., 2012). This population could be further subdivided into $CD4^+$ IL-25 dependent or $CD4^{NEG}$ IL-23 dependent. Recently, neuropilin-1 (Nrp-1) was identified as a marker for recent thymic emigrants (RTE) and IL-17 producing NKT cells are found within the RTE population (Milpied et al., 2011), indicating that NKT-17 cells may actually be a transitory population lost upon maturation. Another subset of NKT cells, $FoxP3^+$ NKTreg cell may be important to the establishment of immunological tolerance (Monteiro et al., 2010). Identified in mice protected from experimental autoimmune encephalomyelitis (EAE) after αGalCer administration, these cells are characterized by $FoxP3^+$ expression and potent immunosuppressive properties. As with NKT-17, $FoxP3^+$ NKTreg require certain cytokine signals for their development, specifically transforming growth factor-β (TGFβ) (Moreira-Teixeira et al., 2012). The newest subset to join the NKT cell family is that of NKT_{FH} cells. Identified as $CXCR5^+$ $PD\text{-}1^{HI}$, NKT_{FH} cells are found in germinal centers in the spleen and provide cognate help to B cells. Like conventional T_{FH}, NKT_{FH} cells development is dependent upon the transcription factor Bcl-6 (Chang et al., 2012; King et al., 2012). Further delineation of different functional subsets of NKT cells and the identification of specific developmental requirements, is critical for understanding their roles in health and disease.

ROLE IN HEALTH AND DISEASE

The ability to secrete Th1, Th2 and Th17 cytokines along with the up-regulation of costimulatory molecules make NKT cells important regulatory cells during infections (bacterial, parasitic, and viral), allergy, autoimmune disease, cancer, and allograft survival. Depending upon the antigen and/or mode of activation and/or specific NKT subset activated, a final NKT cell response can be skewed toward either Th1-, Th2-, or Th17-like, which in turn can help to ameliorate or promote disease (Diana and Lehuen, 2009; Exley et al., 2011; Tupin et al., 2007; Wu and Van Kaer, 2011).

The identification of bacterial lipid agonists implicated a role for NKT cell activation during bacterial infections. NKT cells have been shown to play protective roles in the host during several bacterial infections, either by reducing pathogen burden or by reducing immune-response mediated immunopathology. As an example for the former mode of action, NKT cells were shown to assist in the reduction of bacterial burden during *Streptococcus pneumoniae* infection (Kawakami et al., 2003). Similarly, NKT cells are important in reducing the parasite burden during *Leishmania* infections (Ishikawa et al., 2000; Mattner et al., 2006). Conversely, the protective role NKT cells play during *Trypanosoma cruzi* infection is one of preventing inflammation and immunopathology (Duthie et al., 2005a, b). Likewise, CD1d-deficient mice have increased symptoms of arthritis during *Borrelia burgdorferi* infection (Kumar et al., 2000).

A number of viruses are known to down regulate CD1d as an immune escape mechanism indicating a probable role of NKT cells during viral infections

(Lin et al., 2005; Renukaradhya et al., 2005). While a protective role for NKT cells is implicated in herpes simplex virus (Grubor-Bauk et al., 2008) and respiratory syncytial virus (Johnson et al., 2002) infections, NKT cells play a detrimental role in the induction of chronic lung disease during Sendai virus infection (Kim et al., 2008). This detrimental effect possibly emerged as a result of NKT cell's attempt to jump-start the immune response, which resulted in uncontrolled immune amplification through downstream positive feed-back loops leading to excessive lung immunopathology and disease. A detrimental role for NKT cells is also seen during *Chlamydia muridarum* infection where production of Th2 cytokines by NKT cells results in impaired bacterial clearance (Bilenki et al., 2005). All of these studies indicate a complex role NKT cells play during infections.

Non-infectious disease states such as autoimmunity and cancer are also influenced by the immunoregulatory properties of NKT cells. As with infections, NKT cells can promote or ameliorate disease. NKT cells play a role in a number of autoimmune diseases including type I diabetes, multiple sclerosis, rheumatoid arthritis, lupus, myasthenia gravis, and primary biliary cirrhosis (Wu and Van Kaer, 2009). In general, NKT cell's ability to suppress Th1 responses and skew towards Th2 is protective against autoimmune diseases. However, when this ability is mis-regulated such as in rheumatoid arthritis and primary biliary cirrhosis, NKT cells can exacerbate disease (Wu and Van Kaer, 2009). Conversely, the anti-tumour ability of NKT cells relies upon their ability to induce an inflammatory Th1 response. A number of advanced cancers reveal low

numbers of peripheral blood NKT cells whose functions are skewed toward Th2. Consistently, therapeutic ability to elicit NKT cell Th1 responses by αGalCer administration with or without specific tumor antigens, has shown greatly beneficial effects in tumor clearance by CD8 and NK cells (Dhodapkar et al., 2003; Molling et al., 2005; Molling et al., 2007; Tahir et al., 2001). Thus, NKT cells make appealing targets for treatment of autoimmune diseases and cancer.

What role do different NKT cell subsets play in various disease states? Why do certain infections/diseases induce Th1 response from NKT cells while others induce a Th2 response? How do we harness the ability of NKT cells to skew an immune response in favour of a protective role during specific diseases? A better understanding of NKT cell development, during which NKT cell subsets acquire and commit to all these functions, is therefore necessary to address the above questions and to develop/tailor NKT cell based immunotherapies.

LINEAGE COMMITTMENT

As with conventional T cells, NKT cells begin their developmental journey in the thymus (Coles and Raulet, 2000; Hammond et al., 1998; Pellicci et al., 2002). In mice, NKT cells are detected only by the 3rd postnatal day (Benlagha et al., 2005; Hammond et al., 1998). A number of studies have addressed whether NKT cells develop from an independent or common precursor pool, the same as conventional T cells. Transfer experiments revealed that NKT cells develop from $CD4^+CD8^+$ double positive (DP) thymocytes (Gapin et al., 2001). Mice deficient in RORγ, a retinoic acid orphan receptor, which is needed for DP

thymocytes to survive long enough to make distal TCR re-arrangements, including the *Vα14-to-Jα18* rearrangement, lack NKT cells (Bezbradica et al., 2005; Egawa et al., 2005). It is the distal *Vα14-to-Jα18* TCR rearrangement that commits DP thymocytes to the NKT cell lineage. Therefore, NKT cells develop from a common T cell precursor pool and go through the same early developmental stages as conventional T cells. Because of the shared early thymic developmental stages, NKT cells and T cells require the same ontogenic cues that drive development through those stages: these include IL-7Rα, common γ-chain, Jak3 (Janus kinase-3), pre-TCRα, and ZAP (ζ chain-associated protein)-70 signaling (Fig. 1-3) (Boesteanu et al., 1997; Eberl et al., 1999a; Iwabuchi et al., 2001; Peschon et al., 1994; Thomis et al., 1995).

Deletion of specific transcription factors at the DP stage greatly impairs NKT cell development. Similar to RORγt, HEB—a basic helix-loop-helix E protein, is required for the survival of DP thymocytes thereby allowing for distal TCR rearrangements (D'Cruz et al., 2010), and hence, like RORγt is critically required for NKT lineage development (Fig. 1-3, Table 1-3). Likewise, a deficiency in c-Myb, a nuclear DNA binding protein, results in the loss of NKT cell development. This too is associated with impaired TCR rearrangement and also with impaired expression of SLAM and SAP molecules, important

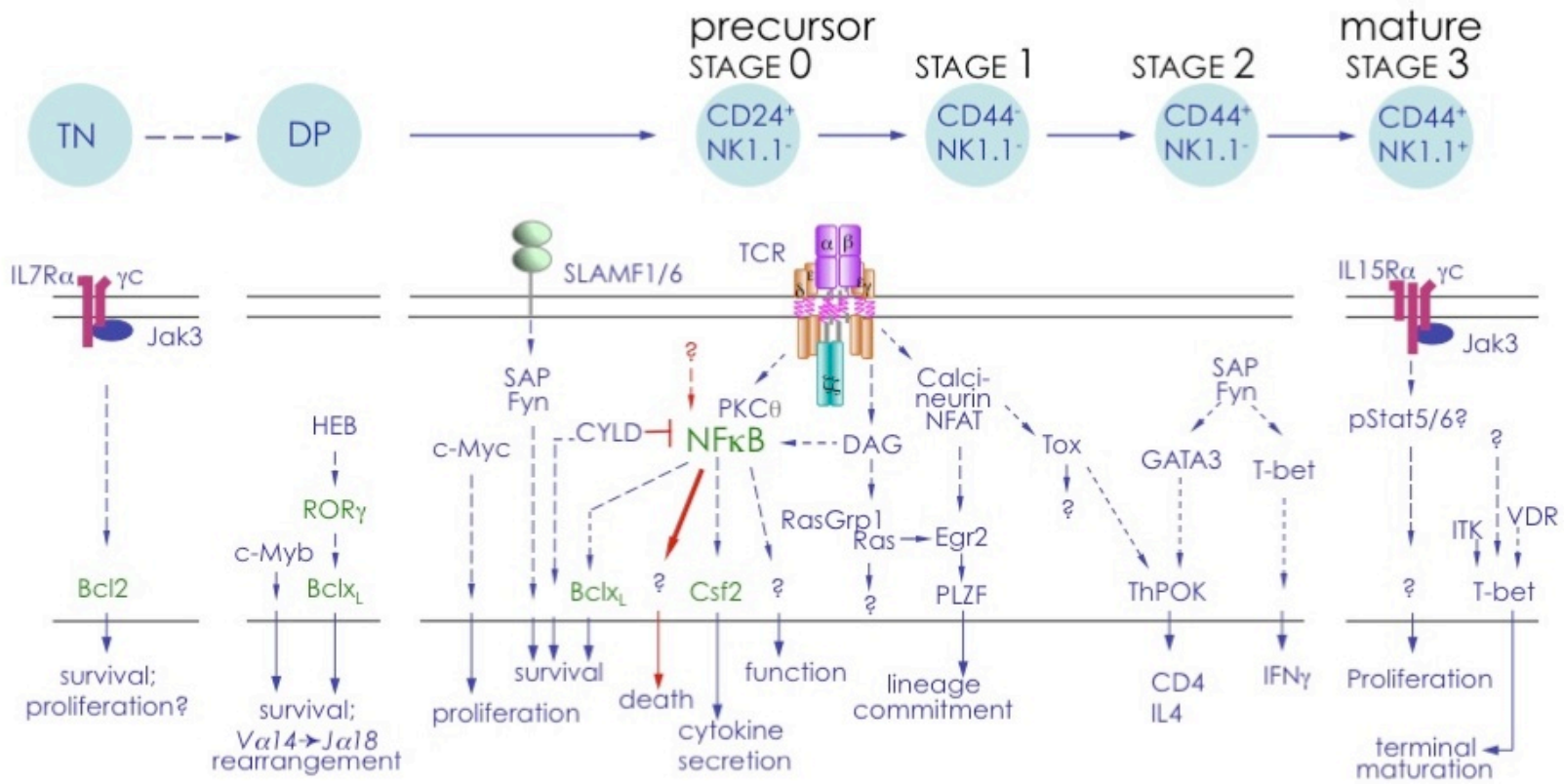
precursor
STAGE 0
STAGE 1
STAGE 2
mature
STAGE 3
TN
DP
CD24+ NK1.1-
CD44- NK1.1-
CD44+ NK1.1-
CD44+ NK1.1+
IL7Rα
γc
Jak3
SLAMF1/6
TCR
IL15Rα
γc
Jak3
SAP
Fyn
PKCθ
CYLD
NFκB
DAG
Calci-
neurin
NFAT
Tox
SAP
Fyn
HEB
RORγ
c-Myb
Bcl2
BclxL
c-Myc
BclxL
Csf2
RasGrp1
Ras
Egr2
PLZF
GATA3
T-bet
ThPOK
pStat5/6?
ITK
VDR
T-bet
survival;
proliferation?
survival;
Vα14→Jα18
rearrangement
proliferation
survival
death
cytokine
secretion
function
lineage
commitment
CD4
IL4
IFNγ
Proliferation
terminal
maturation

Figure 1-3. NKT cell developmental stages and signaling requirements

NKT cell lineage commitment occurs with HEB-RORγ_t-dependent survival for expression of the semi-invariant TCR at the DP stage. Hence, both NKT cells and conventional CD4 and CD8 T cells require the same factors to progress from the $CD3^{NEG}CD4^{NEG}CD8^{NEG}$ triple negative (TN) to DP thymocyte stage. Positive selection by DP thymocytes displaying CD1d-self-lipid complexes and SLAM-SLAM interactions at stage 0/1 induce survival. TCR-induced calcineurin-NFAT-Egr2 and Ras-Egr2 induce expression of PLZF, necessary for the NKT cell memory-like phenotype. At this stage, TCR-induced PKCθ-NFκB signalling is critical for lineage maintenance (e.g., Bcl-x_L) and effector differentiation (e.g. Csf2). Ontogenetic progression at this stage is further regulated by SAP-Fyn signalling axes culminating in GATA3 and T-bet expression, which are transcription factors essential for the elaboration of IL-4 and IFN-γ for which this lineage is best known (stages 1 and 2). Finally, stage 3 NKT cells require ITK and VDR induction of T-bet for terminal maturation. Additionally, NKT cells require IL-15 for proliferation in the periphery. Dashed arrows, intermediates not known; thick arrow, over activation.

Table 1-3. NKT cell developmental factors

Factors	Type	Necessary for	Refs
Pre-selection			
RORγt	TF	Survival (Bcl-x_L) and distal TCR re-arrangements	(Bezbradica et al., 2005; Egawa et al., 2005)
HEB	TF	Induction of RORγt	(D'Cruz et al., 2010)
c-Myb	TF	Survival and TCR re-arrangement, regulates CD1d, SLAM, SAP expression (extrinsic)	(Hu et al., 2010; Yuan et al., 2010)
miR-150	microRNA	May regulate expression level of c-Myb	(Zheng et al., 2012)
Bcl11b	TF	Lipid processing and presentation (extrinsic)	(Albu et al., 2007; Albu et al., 2011)
Developmental Stage 0			
AP-1 (Fra-2)	TF	Selection	(Lawson et al., 2009)
Runx1	TF	Selection	(Egawa et al., 2005)
c-Myc	TF	Proliferation	(Dose et al., 2006; Mycko et al., 2009)
TOX	TF	Early development	(Aliahmad and Kaye, 2008)
SAP	STM	SLAM signalling	(Chung et al., 2005; Nichols et al., 2005; Pasquier et al., 2005)
Fyn	STM	SLAM-SAP signalling	(Eberl et al., 1999b; Gadue et al., 1999)
Lck	STM	TCR signalling	(Eberl et al.,

			1999a)
Zap70	STM	TCR signalling	(Iwabuchi et al., 2001)
Ras	STM	Selection	(Hu et al., 2011; Shen et al., 2011a)
CD1d	CSM	NKT cell selection	(Bendelac, 1995; Xu et al., 2003)
Developmental Stage 1			
Egr2	TF	Survival, TCR signalling through Ras-Erk and NFAT	(Lazarevic et al., 2009; Seiler et al., 2012)
NF-κB1	TF	Survival and function, TCR signalling	(Stanic et al., 2004a)
PLZF	TF	Memory phenotype and maturation	(Kovalovsky et al., 2008; Savage et al., 2008)
RelB	TF	Survival	(Elewaut et al., 2003b)
Dock2	STM	Immunological synapse formation	(Kunisaki et al., 2006)
IKK2	STM	Inhibits IκB (NFκB inhibitor)	(Schmidt-Supprian et al., 2004)
NIK	STM	RelB signalling	(Elewaut et al., 2003b)
PKCθ	STM	TCR signalling to NFκB	(Schmidt-Supprian et al., 2004; Stanic et al., 2004b)
Bcl-10	STM	TCR signalling to NFκB	(Schmidt-Supprian et al., 2004)
CYLD	STM	Regulates NFκB signalling and IL7Rα expression	(Lee et al., 2010)
SLAMF1, SLAMF6	CSM	Selection	(Griewank et al., 2007)
TGF-βR	CSM	Proliferation/expansion	(Doisne et al., 2009a)
Dicer	Endoribo-	miRNA expression	(Fedeli et al., 2009; Zhou et al.,

	nuclease		2009)
Developmental Stage 2			
GATA-3	TF	Generation of CD4+ NKT cells, may induce TH-POK	(Kim et al., 2006)
TH-POK	TF	Generation of CD4+ NKT cells	(Engel et al., 2010)
RelA	TF	Regulates expansion and maturation through IL-7 and IL-15	(Vallabhapurapu et al., 2008)
Developmental Stage 3			
Ets-1	TF	Development (only NK1.1+ analysed)	(Walunas et al., 2000)
MEF	TF	Development (only NK1.1+ analysed)	(Lacorazza et al., 2002)
Elf-1	TF	Development and function	(Choi et al., 2011)
T-bet	TF	CD122 expression, maturation & function	(Matsuda et al., 2006; Townsend et al., 2004)
IRF1	STM	Regulates thymic IL-15 levels (extrinsic)	(Ohteki et al., 1998)
ITK	STM	Induction of T-bet	(Felices and Berg, 2008)
CD28	CSM	Expression of T-bet and CD122	(Zheng et al., 2008)
ICOS	CSM	Expression of T-bet and CD122	(Akbari et al., 2008)
TGF-βR	CSM	Expansion at early stage and maintenance of T-bet and CD122 at St3	(Doisne et al., 2009a)
Osteopontin	glycoprotein	Maturation and function	(Diao et al., 2008)
WASp	adaptor	Role unclear	(Astrakhan et al., 2009; Locci et al., 2009)
VDR	TF	T-bet expression	(Yu and Cantorna, 2008, 2011; Yue et al., 2011)

Effector differentiation			
GM-CSF	cytokine	Cytokine secretion	(Bezbradica et al., 2006a)
T-bet	TF	T_H1 cytokine production	(Matsuda et al., 2007; Matsuda et al., 2006; Townsend et al., 2004)
GATA-3	TF	T_H2 cytokine production, may induce TH-POK	(Kim et al., 2006)
TH-POK	TF	T_H2 cytokine production	(Engel et al., 2010)
Emigration & peripheral homeostasis			
$S1P_1$	CSM	Thymic emigration	(Allende et al., 2008)
LT-$\alpha\beta$	cytokine	Thymic emigration	(Franki et al., 2006)
CXCR6	CSM	Migration of NK1.1+ NKT cells in liver	(Germanov et al., 2008; Monticelli et al., 2009)
ID2	TF	Survival (Bcl-2 & Bcl-x_L) and migration of NK1.1+ NKT cells in liver by CXCR6 expression	(Boos et al., 2007; Cannarile et al., 2006; Monticelli et al., 2009)
IL-7	cytokine	Minor role compared to IL-15	(Matsuda et al., 2002)
LFA-1	CSM	Regulates migration/re-circulation of hepatic NKT cells	(Emoto et al., 1999; Ohteki et al., 1999)
PLZF	TF	Modulates expression of LFA-1	(Thomas et al., 2011)
IL-15	cytokine	Proliferation	(Matsuda et al., 2002; Ranson et al., 2003)

TF= transcription factor
STM = signal transduction molecule
CSM = cell surface molecule

co-regulators in NKT cell selection (Fig. 1-3, Table 1-3) (Hu et al., 2010; Yuan et al., 2010). Targeting of c-Myb gene expression may be mediated by microRNA-150 (miRNA-150) as deficiency in this small regulatory RNA prevents NKT cell development and maturation (Table 1-3) (Zheng et al., 2012). While RORγt, HEB, and c-Myb are required for NKTCR rearrangement, deficiency in Runx1 –runt related transcription factor 1, results in a block at the earliest known NKT cell commitment stage suggesting a possible role for Runx1 in positive selection or lineage expansion (Table 1-3) (Egawa et al., 2005). The above factors are necessary to reach lineage commitment of Vα14Jα18 NKT cells, which begins with positive selection by CD1d-positive double-positive thymocytes (Table 1-3). From this step on, NKT cells diverge from the T cell lineage and therefore we begin to uncover unique NKT cell specific developmental cues.

POSITIVE AND NEGATIVE SELECTION

Low-to-intermediate affinity self recognition and removal of potentially auto-reactive T cells is the purpose of the positive and negative selection processes during thymocyte development. Avidity of the TCR-antigen interaction is the main determinant of these processes. Positive selection occurs when developing DP thymocytes encounter self peptide-MHC that induces low to intermediate reactivity allowing further development and differentiation to single positive thymocytes. In contrast, negative selection results in elimination of developing thymocytes, which are highly reactive to self peptide-MHC. Similar to conventional T cells, NKT cells are thought to undergo both positive and

negative selection, even though genetic evidence for the latter process was lacking. Furthermore, the extent to which each of these processes plays a role in shaping the NKT cell repertoire is less well understood. Both of these questions will be addressed as a part of this study.

Self peptide-MHC expressed on thymic epithelial cells are critical for positive selection of conventional T cells. However, NKT cells are unique in their requirement for self glycolipid-CD1d expression on DP thymocytes for positive selection to occur. There are several lines of genetic evidence to support this conclusion. Absence of CD1d on double positive thymocytes within bone marrow chimeric mice results in a lack of NKT cells (Bendelac, 1995). If CD1d is re-introduced into CD1d-deficient mice by a pLCK driven transgene, NKT cell development resumes (Schumann et al., 2005; Xu et al., 2003). Molecules such as adapter protein (AP)-3 (Cernadas et al., 2003; Elewaut et al., 2003a) and lipid transfer proteins saposins (Kang and Cresswell, 2004), which are necessary for appropriate loading of endogenous glycolipids into CD1d within endosome, are also necessary for NKT cell development. Trafficking of CD1d through the intracellular endosomal and lysosomal pathways are guided by AP-3 (Sugita et al., 2002), indicating that CD1d presentation of a self-glycolipid is required for positive selection of NKT cells. Additionally, signalling lymphocytic activation molecule (SLAM) receptors slamf1 and slamf6, which are necessary co-stimulators in NKT cell selection, are expressed by cortical thymocytes and not thymic epithelia (Griewank et al., 2007). Thus, DP thymocytes supply critical

developmental signals to NKT cells through CD1d-NKTCR and SLAM-SLAM interactions (Fig. 1-3, Table 1-3).

Identifying the selecting ligand is critical to understanding NKT cell biology because positive selection is thought to bias the NKT cell TCRβ usage. Most NKT cells express TCRs containing Vβ8.2, 7 and 2 (Bendelac et al., 2007). Expression of a Vα14Jα18 transgene in CD1d-deficient mice reveals a broad TCR Vβ cell repertoire (Wei et al., 2006). Thus, the restriction is not due to the inability of the α-chain to pair with particular Vβs. Additionally, only TCRs containing Vβ7, 8.2 and 2 were capable of responding to stimulation with a putative endogenous selecting ligand iGb3 (Wei et al., 2006). Thus, the NKTCR bias is thought to be the result of positive selection. Whether one or more lipid ligands play a role in NKT cell positive selection and what affect they have on the NKTCR repertoire remains to be determined.

Several lines of somewhat indirect evidence indicate that NKT cells undergo negative selection. Neonatal mice injected intraperitoneally with high affinity antigen, αGalCer, at days 3—14 lose NKT cells in a dose dependent manner (Pellicci et al., 2003). Similarly, addition of αGalCer to fetal thymic organ culture (FTOC) also results in loss of NKT cells (Chun et al., 2003; Pellicci et al., 2003). Conversely, intrathymic injection or addition of αGalCer to adult mice and older thymocyte cultures respectively, does not affect already selected NKT cells numbers (Pellicci et al., 2003). Since older thymi contain more mature NKT cells these data indicate that if negative selection does occur during NKT cell development it is at an early stage. Conclusions from this evidence are

confounded by the fact that while αGalCer is a potent agonist; it is not an endogenous lipid encountered by NKT cells during development. Additional supportive evidence indicates that transgenic over-expression of CD1d by thymic dendritic cells abrogates NKT cell development. Conversely, lack of CD1d expression by thymic dendritic cells results in development of hyper-responsive NKT cells (Chun et al., 2003; Schumann et al., 2005). The aforementioned studies indicate that negative selection occurs in NKT cells. The genetic evidence for existence of negative selection as well as the extent to which negative selection plays a role in shaping the NKT cell repertoire is the focus of my studies that are described in Chapter II.

DIFFERENTIATION & MATURATION

A number of divergent signalling requirements for NKT development (Fig. 1-3; Table 1-3) highlight the branch point in which NKT cells begin their unique ontogenic program. Upon commitment, immature NKT cells undergo robust proliferation and further differentiation. NKT cell precursors ($CD24^{HI}CD69^{+}CD44^{-}NK1^{NEG}$; stage-0: ST0) emerge from DP thymocytes soon after expression of the semi-invariant TCR (Bendelac et al., 2007). Precursor ST0 cells proliferate extensively in a c-Myc-dependent manner (Dose et al., 2009; Mycko et al., 2009) and undergo positive selection through homotypic interactions of SLAM molecules and heterotypic interactions between the semi-invariant TCR and CD1d molecules expressed by DP thymocytes (Bendelac et al., 2007; Godfrey

et al., 2010). These interactions are necessary for a number of signalling pathways critical for NKT cell development.

As previously mentioned, SLAM family members, Slamf1 and Slamf6 (Griewank et al., 2007) are critical for positive selection of developing NKT cells. Signals initiated by interaction of SLAM receptors are transduced by a mechanism involving the SAP and Fyn signalling module (Chung et al., 2005; Eberl et al., 1999b; Gadue et al., 1999; Nichols et al., 2005; Pasquier et al., 2005). While SAP deficiency results in a severe loss of NKT cells, a lack of Fyn displays a less dramatic effect on NKT cell development, thus indicating that SLAM-SAP can mediate signals though Fyn-dependent and -independent mechanisms. In conventional T cells SLAM-SAP signals are necessary for cooperating with TCR signals in the induction of NFκB signalling (Cannons et al., 2004). NKT cell development is dependent upon cell intrinsic NFκB signalling (Elewaut et al., 2003b; Sivakumar et al., 2003; Stanic et al., 2004a), raising the question as to whether the SLAM/SAP signals are required for this induction of NFκB. Over expression of constitutively active IKKβ, essential for NFκB activation, was unable to rescue NKT cell development in SAP deficient mice (Cen et al., 2009), even though the uncontrolled/overt NFκB activation might not quite recapitulate the situation seen during positive selection in vivo. Thus, the signalling pathway downstream of SLAM-SAP remains to be defined (Fig. 1-3).

TCR stimulation initiates a number of signalling pathways critical for proper NKT cells development: PKCθ-NFκB, Ras-Erk, and calcineurin-NFAT (Fig. 1-3)

(Das et al., 2010). While the NFκB family of transcription factors modestly affects conventional T cell development, they play important roles during NKT cell development at multiple stages (Table 1-3). Disruption of NFκB signalling results in a significant impairment of NKT cell development at the earliest precursor stage (Sivakumar et al., 2003; Stanic et al., 2004a). This impairment is due to a lack of induction of lineage-specific survival factor(s) of the Bcl-2 family. Hence, the forced expression of a Bcl-x_L transgene can rescue NKT cell development in mice in which NFκB signal induction is disrupted (Stanic et al., 2004a). Interestingly, loss of upstream signal transduction molecule PKCθ resulted in a milder defect in NKT cell development (Schmidt-Supprian et al., 2004; Stanic et al., 2004b), indicating that multiple pathways are required for the activation of NFκB during NKT cell ontogeny (Fig. 1-3). On the other hand, lack of NFκB signal strength regulation as seen in mice deficient for CYLD –a deubiquitinating enzyme and negative regulator of NFκB, results in the loss of NKT cells through overt apoptosis (Lee et al., 2010) Similarly, absence of diacylglycerol (DAG) kinase α and ζ –a negative regulator of DAG, causes severe defects in NKT development as a result of overt NFκB and Ras-Erk activation (Shen et al., 2011b). Thus, both too much and too little NFκB activation is detrimental to NKT cell development indicating importance of very tight regulation of NFκB signalling in selection of appropriate NKT cells.

Infelicitous calcium signalling which leads to Ca^{2+}-calcineurin-NFAT represents another pathway involved in NKT cell development. TCR signalling results in the activation of calcineurin through Ca^{2+} influx and the release of

intracellular calcium stores. Absence of calcineurin B1 results in a significant loss of NKT cells (Fig. 1-3, Table 1-3) (Lazarevic et al., 2009). Likewise, loss of Egr-2 –a transcription factor and a target of calcineurin-NFAT, results in a developmental block after positive selection at ST0 to ST1 as a result of increased cell death (Lazarevic et al., 2009). Egr-2 is a transcription factor that can be induced by both NFAT and Ras signalling pathways. A previous report indicated that Ras signalling does not play a role in NKT cell development (Fig. 1-3, Table 1-3) (Alberola-Ila et al., 1996). However, two recent studies have indicated otherwise. Mice expressing a dominant negative Ras displayed a dramatic loss of NKT cells (Hu et al., 2011). Additionally, RasGrp1-activator of Ras, was required for proper NKT cell development (Shen et al., 2011a). Thus, Ras and NFAT signalling may both play a role in the induction of Egr-2 (Fig. 1-3).

While many pathways seem to be important to allow for proper NKT cell survival and lineage expansion, a long term goal of many studies has been to identify a master regulator of NKT cell development. One such study identified the broad complex tramtrack bric-a-brac-zinc finger (BTB-ZF; also known as promyelocytic leukaemia zinc finger or *Zbtb16*) transcription factor PLZF (Kovalovsky et al., 2008; Savage et al., 2008). PLZF-deficient mice are impaired in NKT cell development and residual NKT cells that develop do not exhibit a memory-like phenotype. Transgenic expression of PLZF in thymocytes conferred a memory-like phenotype to conventional T cells similar to that of wild type NKT cells (Raberger et al., 2008; Savage et al., 2008). Interesting however,

PLZF^{tg} T cells do not acquire the expression of NK cell markers, suggesting that not all aspects of NKT cell lineage can be imprinted by this one factor. Ras induced Erg-2 was recently shown to be a regulator of PLZF expression by NKT cells (Fig. 1-3, Table 1-3) (Seiler et al., 2012). Furthermore, recent studies reveal a role for PLZF in other cell types such as NKT cell-like Vγ1.1^{+}Vδ6.3^{+} T cells, which also express a memory-like phenotype (Alonzo et al., 2010; Kreslavsky et al., 2009). These data indicate that although PLZF is an important regulator of NKT cell development it is not, at least when acting alone, the single and sufficient lineage specific master regulator.

NKT cells develop in the thymus and attain markers typical of NK and activated/memory T cells as they mature (Fig. 1-3) (Godfrey et al., 2010). For further development and functional differentiation into ST1 (CD24^{NEG}CD44^{NEG}NK1.1^{NEG}), ST2 (CD24^{NEG}CD44^{+}NK1.1^{NEG}) and ST3 (CD24^{NEG}CD44^{+}NK1.1^{+}) NKT cells require regulation by a number of instructive signals. At ST2 and ST3, NKT cells also acquire memory T cell markers (CD44^{HI}, CD62L^{LO}, CCR7^{NEG}) as well as NK cell markers (NKG2D, Ly49 and NK1.1) and cytolytic function (granzyme B and perforin) (Bendelac et al., 2007; Godfrey and Berzins, 2007). During differentiation, NKT cells acquire the ability to produce IL-4 (ST1), IL-4 and IFN-γ (ST1 and ST2) or IL-4^{LO} and IFN-γ^{HI} (ST3) in response to TCR stimulation (Benlagha et al., 2002; Gadue and Stein, 2002). It is at the final maturation stage (ST2 TO ST3 transition) that T-cell-specific T-box transcription factor (T-bet) plays an indispensable role. T-bet deficiency results in a developmental block at ST2 (Fig. 1-3, Table 1-3) (Matsuda et al., 2006;

Townsend et al., 2004). In the absence of T-bet, NKT cells fail to proliferate due to a lack of CD122 expression and consequent inability to respond to IL-15 stimulation (Townsend et al., 2004). Furthermore, T-bet deficient NKT cells fail to activate the necessary functional NK-like properties so typical of mature NKT cells, for example the ability to produce IFN-γ (Matsuda et al., 2007; Matsuda et al., 2006). The integral role that T-bet plays during the final stages of NKT cell development can be seen in the similar NKT cell developmental defects found in the absence of various molecules/pathways which regulate T-bet expression: IL-2 inducible tyrosine kinase (ITK) (Felices and Berg, 2008), transforming growth factor-β receptor (TGF-βR) (Doisne et al., 2009b), vitamin D receptor (VDR) (Yu and Cantorna, 2008), and inducible T cell costimulatory (ICOS) (Akbari et al., 2008) (Fig. 1-3, Table 1-3). In addition to T-bet, GATA binding protein 3 (Gata-3) plays an important role in some aspects of functional development of NKT cells (Kim et al., 2006). Gata-3, (which is well know and the master regulator of Th2 functions in conventional T cells) acts possibly together with its downstream target Th-inducing POZ/Kruppel-like factor (ThPOK) within NKT cells to control the production of T_H2 cytokines (Fig. 1-3, Table 1-3) (Engel et al., 2010). While production of cytokines is regulated by transcription factors like T-bet, Gata-3 and ThPOK, secretion of these cytokines by NKT cells is regulated by CSF-2 (Fig. 1-3, Table 1-3). CSF-2 deficient mice are capable of producing, packaging, and transporting cytokines to the NKT cell-dendritic cell synapse but are unable to release the secretory vesicles (Bezbradica et al., 2006a). Thus, acquisition of

the ability to secrete cytokines is an important step for the development of functional NKT cells.

NKT cells developmentally regulate the expression of CD4 as well. NKT cells emerge from the DP positive stage as those that express CD4. As these NKT cells differentiate, a portion down regulate CD4 expression and become double negative ($CD8^-CD4^-$). Two transcription factors have been identified as key players in the development of $CD4^+$ NKT cells: Gata-3 and ThPOK. Gata-3 is essential at numerous stages of T cell development: early thymocyte differentiation, the development of conventional $CD4^+$ T cells, and differentiation of $CD4^+$ T cells to a Th2 phenotype (Hernandez-Hoyos et al., 2003; Pai et al., 2003). Likewise, it is also required for the development of $CD4^+$ NKT cells and it plays an ill-defined role in hepatic NKT cell survival and TCR-induced activation of NKT cells (Table 1-3) (Cen et al., 2009; Kim et al., 2006; Wang et al., 2006). Loss of the transcription factor Th-POK results in a normal number of NKT cells, but they completely lack CD4 expression and are functionally impaired (Table 1-3). Together, these data suggest that Gata-3 and ThPOK may function in a similar pathway (Engel et al., 2010). As discussed previously, CD4 expression has been used in the identification of new functional NKT cell subsets. Thus, identification of developmental regulators of $CD4^+$ NKT cells is an important area of future research.

One important feature that emerges from these studies is that NKT cells use more than one master regulator, found within distinct conventional lineages (CD8 T cells, CD4 T cells, NK cells, innate cells) to acquire many functions that

these lineages can perform and to generate a lymphocyte with an extraordinary functional potential. How and when this potential is controlled and regulated is currently unclear.

THYMIC EMIGRATION AND HOMING OF NKT CELLS

While a substantial fraction of ST2 cells remain in the thymus and mature to ST3, a small fraction egresses from the thymus and migrates into the spleen and liver whereupon further maturation occurs (Benlagha et al., 2002; Berzins et al., 2006; Pellicci et al., 2002). Migration to these peripheral sites depends on CXCR6 (Geissmann et al., 2005), while continued development and maintenance in the liver require LFA-1 (Ohteki et al., 1999) and Id2 (Monticelli et al., 2009) (Table 1-3). Even though mature thymic and splenic NKT cells are phenotypically similar, they behave as distinct functional populations at these sites because the developmental cues and perhaps the agonistic ligands are distinct at different sites (Berzins et al., 2006; McNab et al., 2005; McNab et al., 2007). Thus, unlike conventional T lymphocytes, which undergo complete ontogenetic maturation in the thymus but commit to effector differentiation only upon antigen recognition in the periphery, NKT cells complete both these processes both within and outside the thymus.

NKT CELL MAINTENANCE AND HOMEOSTASIS

Upon lineage commitment and the emergence of ST0 NKT precursors and

through subsequent stages of differentiation and maturation, thymic and peripheral NKT cells are maintained by complex, yet poorly understood homeostatic mechanisms involving a vast array of molecules. These molecules function either to promote survival or proliferation of NKT cells. NFκB (Stanic et al., 2004a), calcineurin (Lazarevic et al., 2009), Egr-2 (Lazarevic et al., 2009) and Id2 (Monticelli et al., 2009) mediate survival of NKT cells through the induction of Bcl-x_L and/or Bcl-2 (Table 1-3). c-Myc is critical to proliferation of NKT cells during early ontogeny (Table 1-3) (Dose et al., 2009; Mycko et al., 2009). Peripheral NKT cells, on the other hand, require IL-15 for homeostatic proliferation (Table 1-3) (Matsuda et al., 2002). A number of studies support the essential role of IL-15. Loss of interferon regulatory factor (IRF)-1, which regulates IL-15 gene expression, results in a loss of NKT cells (Ohteki et al., 1998). Additionally, defects in receptors involved in IL-15 signalling such as CD122 (Ohteki et al., 1997) and IL-15Rα (Chang et al., 2011a; Lodolce et al., 1998) exhibit impaired NKT cell homeostasis. Similarly, RelA regulates IL-15Rα expression and loss of RelA leads to defective IL-15 and IL-7-induced proliferation of NKT cells (Vallabhapurapu et al., 2008). While IL-15 is required for homeostatic proliferation in the periphery, NKT cell proliferation in the thymus appears intact in IL-15-deficient (IL-15^0) mice (Matsuda et al., 2002). Yet, the thymic NKT cell developmental defect in IL-15^0 mice is quite severe and arrests NKT cell ontogeny at ST2, with leaky progression to ST3 (Fig. 1-3) (Matsuda et al., 2002) thus implicating additional roles for IL-15 in NKT cell development. The extent to which IL-15 plays a role in NKT cell thymic ontogeny, and whether

IL-15 is essential for NKT cell survival, proliferation and/or functional maturation in the thymus or periphery is the focus of my studies described in Chapter III.

OUTSTANDING QUESTIONS

NKT cells are an important immunoregulatory cell type that can function both to enhance and suppress an immune response. They play roles in a vast number of disease states, i.e., infections, allergy, autoimmune disease, tumour immunity, and allograft survival. The innate and memory like properties of NKT cells allow them to respond quickly and vigorously to produce immunomodulatory cytokines, thus, making them ideal targets for the design of immunotherapies. Controlling the type and intensity of the immune response is crucial to any immunotherapy. Both the subtype of NKT cell responding and the conditions of activation regulate these features. Because NKT cells acquire their functional properties during development, to allow for rapid and 'ready-to-go' responses, it is critically important to have a clear understanding of the NKT cell developmental program/signalling networks involved in shaping their functional response. Using genetically deficient mice, numerous transcription factors and other signalling molecules have been identified as important regulators of NKT cell development. Yet for many of these, their precise mechanism of action and how their activity is induced and regulated remain unclear. Thus, the **central goal** of my thesis research was to delineate signals critical to shaping the functional NKT cell repertoire. To address this, two outstanding questions were defined:

1) What is the role of negative selection in sculpting a functional NKT cell repertoire?
2) What is the role of interleukin (IL)-15 in NKT cell effector differentiation and homeostasis?

What is the role of negative selection in sculpting a functional NKT cell repertoire?

Central tolerance of conventional T cells is mediated by the process of negative selection. Since NKT cells have characteristics of activated conventional T cells and they react to self-lipids, the question arises as to whether they are subjected to negative selection. The Nur77 family of nuclear orphan hormone receptors mediates negative selection in conventional T cells (Calnan et al., 1995; Cheng et al., 1997; Zhou et al., 1996). Nur77 expression is temporarily controlled in developing T cells, because it functions by translocating to the cytoplasm upon induction where it targets Bcl-2 at the mitochondria. Binding of Bcl-2 by Nur77 induces conformational changes in Bcl-2 and converts its function from anti-apoptotic to pro-apoptotic, thereby inducing cell death (Kolluri et al., 2008; Thompson et al., 2010; Thompson and Winoto, 2008). Previous studies from our group had revealed that a small population of the earliest stage of immature NKT cells expressed Nur77 (Stanic et al., 2004a). This subset was further expanded in NFκB signalling deficient mice whose NKT cells are arrested at earliest immature stage due to failure to survive during positive selection. Thus, data imply that Nur77 is expressed in NKT cells and, like in T

cells, may mediate negative selection of developing NKT cells. Whether NKT cells undergo Nur77 mediated negative selection and what role it plays in shaping the NKT cells repertoire is addressed in Chapter II.

What is the role of IL-15 in NKT cell effector differentiation and homeostasis?

The pleiotropic cytokine, IL-15 regulates the development and maintenance of several subsets of innate lymphocytes, including γδ T, CD8αα T, and NK cells (Ma et al., 2006). IL-15 is also vital to proper NKT cell development as seen by defective development of thymic and peripheral NKT cells in IL-15 deficient mice (Matsuda et al., 2002). Of note, while the peripheral defect is due to impaired homeostatic proliferation, thymic proliferation appears intact (Matsuda et al., 2002). Yet, IL-15 deficient mice develop a severe blockade in NKT cell ontogeny at ST2, with leaky progression to ST3 (Matsuda et al., 2002). Furthermore, IL-15 signals the ontogeny, effector differentiation and Mcl-1-dependent survival of an NKT-related lymphocytic lineage, NK cells (Huntington et al., 2007). Thus, IL-15 may play roles in both survival and functional maturation of thymic NKT cells during final stages, i.e., when they begin to acquire typical NK-like behavior. On the other hand, the developmental block may be due to impaired ST3 survival and not a deficiency of maturation signals. What role do IL-15 signals play during thymic NKT cell ontogeny? Is IL-15 essential for NKT cell functional maturation in the periphery? These questions will be addressed in Chapter III.

CHAPTER II

NUR77 MEDIATES NEGATIVE SELECTION IN NKT CELLS

ABSTRACT

Semi-invariant NKT cells are innate-like lymphocytes whose functions are regulated by CD1d-restricted lipid agonists. NKT cells express an invariant TCR α-chain that pairs with a limited number of β-chains. The diversity in β-chains is encoded by rearrangements between *Vβ* and the *Jβ2* cluster and relatively rarely the *Jβ1* cluster. There are two views to the events that sculpt this semi-invariant NKTCR repertoire: One view holds that positive selection alone is sufficient to shape this repertoire, whilst the other purports that both positive and negative selection together sculpt the NKT cell repertoire. Indirect evidence supports both views. By directly addressing whether negative selection plays a role in sculpting the NKT cell repertoire, we found that no NKT cells developed in mice in which negative selection was induced by over expressing Nur77 within thymocytes even when the rearranged NKTCR α-chain gene was introgressed into these mice. Conversely, Nur77ΔN^{tg} mice expressing a dominant negative mutant, which blocks negative selection, develop NKT cells but lower numbers. The NKT cells were further enriched to the wild type levels by introgression of the rearranged NKTCR α-chain gene into these mice. Strikingly, although β-chain usage remained the same, CDR3β in Nu77ΔN^{tg} mice was encoded by

rearrangements to the *Jβ1* cluster and relatively rarely to the *Jβ2* cluster. The altered CDR3β had only a modest impact on reactivity to currently known lipid agonists. Moreover, introgression of *Nur77ΔN* into mice expressing the tail-deleted CD1d mutant, which fails to positively select NKT cells, did not rescue NKT development in these mice. These data suggest that positive selection of NKT cells most likely precedes negative selection and that both together sculpt the NKT cell repertoire.

INTRODUCTION

The process of negative selection, in which highly self-reactive T cells are removed from the T cell repertoire, mediates central tolerance of T cells. Since NKT cells have characteristics of activated conventional T cells and they react to self-lipids, the question arises as to whether they are subjected to negative selection. Multiple lines of evidence suggest that NKT cells undergo negative selection (Chun et al., 2003; Pellicci et al., 2003; Schumann et al., 2005) but the extent to which it plays a role in shaping the NKT cell repertoire remains to be determined.

In conventional T cells, Nur77 and other members of the Nur77 family of nuclear orphan hormone receptors mediate negative selection (Calnan et al., 1995; Cheng et al., 1997; Zhou et al., 1996). Nur77 is a transcription factor composed of three domains: a N-terminal trans-activation domain, a Zn finger DNA-binding domain and a C-terminal ligand-binding domain. Transgenic studies

revealed that over-expression of full length Nur77 early in thymocytes results in overt negative selection and near complete loss of T cells. Conversly, over-expression of a dominant negative (ΔN) Nur77, which lacks the trans-activation domain, rescues conventional T cell development in a model of negative selection (Calnan et al., 1995; Zhou et al., 1996). A recent study has revealed the mechanism by which Nur77 induces apoptosis in thymocytes undergoing negative selection. Upon induction, Nur77 translocates to the cytoplasm where it targets Bcl-2 at the mitochondria. Binding of Bcl-2 by Nur77 induces conformational changes of Bcl-2 converting its function from anti-apoptotic to pro-apoptotic (Thompson and Winoto, 2008). Since a small population of immature NKT cells was shown to express Nur77, we decided to address whether NKT cells undergo Nur77 mediated negative selection and what role it plays in shaping the NKT cells repertoire.

RESULTS

NKT cell development is altered in Nur77^{tg} mice

Previously, we reported that a small population of NKT cells that were blocked at an early stage of development (ST0/ST1) expressed Nur77 (Stanic et al., 2004a). Nur77 family of transcription factors has been shown to mediate negative selection of conventional T cells. A tractable genetic model to study negative selection and its role in shaping the NKTCR repertoire is currently lacking. To address this issue, the previously reported Nur77 transgenic (^{tg}) mouse model (Calnan et al., 1995), used to study negative selection in

conventional T cells was revisited. Re-evaluation of thymi and spleens by flow cytometry confirmed the loss of $CD4^+$ and $CD8^+$ T cell development within $Nur77^{tg}$ mice (Fig. 2-1A,B). The percentage of total $CD3\varepsilon^+$ as well as $CD4^+$ and $CD8^+$ single positive populations were much lower in both thymus and spleen of $Nur77^{tg}$ mice compared to C57BL/6 while the percentage of thymic $CD4^+CD8^+$ DP cells remained unaltered (Fig. 2-1A). However, analysis of cell numbers revealed a near complete loss of DP thymocytes (reflecting an overall smaller size of the thymus in these mice), as well as a loss of $CD4^+$ and $CD8^+$ T cell populations in both thymus and spleen (Fig. 2-1B). These data indicate that the mouse model for overt negative selection ($Nur77^{tg}$) is functioning as previously reported (Calnan et al., 1995).

Next, NKT cell development within $Nur77^{tg}$ mice was assessed by flow cytometry. Examination of NKT cell frequency (Fig. 2-2A) and absolute numbers (Fig. 2-2B) revealed a near complete loss of NKT cells within $Nur77^{tg}$ mice. NKT cell development is critically dependent upon positive selection by CD1d positive, DP thymocytes. $Nur77^{tg}$ mice have greatly reduced total numbers of DP thymocytes (Fig. 2-1A,B). Thus, the absence of NKT cells in $Nur77^{tg}$ mice may be a result of either Nur77-mediated negative selection, lack of the canonical *Vα14*-to-*Jα18* gene rearrangement or the inability of DP thymocytes to induce positive selection of NKT cells. To test the last possibility, equal numbers of DP thymocytes from C57BL/6 or $Nur77^{tg}$ mice were used to stimulate three $V\alpha14^+$ (N37-1H5a, N38.3C3, and N38-2C12) and one $V\alpha14^-$ (N37-1A12) hybridomas. $V\alpha14^+$ NKT cell hybridomas are extremely sensitive to self antigen(s) displayed

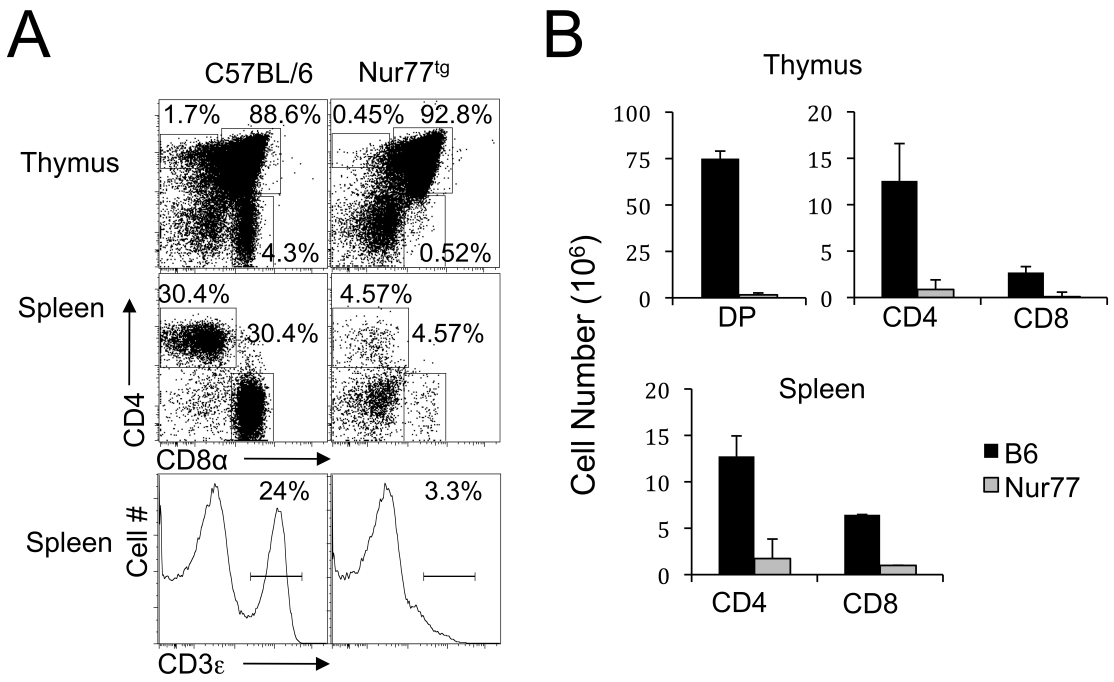

Figure 2-1. Nur77 transgenic (^{tg}) mice as models for negative selection

(A) Thymic and splenic $CD4^+$ and $CD8^+$ T cells from C57BL/6, $Nur77^{tg}$ and $Nur77\Delta N^{tg}$ mice were identified as $CD4^+$ or $CD8^+$ cells within total thymocytes or electronically gated $B220^-CD3\varepsilon^+$ splenocytes. Numbers are % of $CD4^+$ or $CD8^+$ T cells among total leukocytes. Data are representative of 3 independent experiments; *n*= 5 mice.
(B) Absolute numbers of $CD4^+$ or $CD8^+$ cells in the thymus and spleen of C57BL/6, and $Nur77^{tg}$ mice were calculated from % cells in **A** and total thymocytes or splenocytes recovered from the respective lymphoid organs. Data are representative of 3 independent experiments showing mean±sem; *n* as in **A**.

by CD1d molecules expressed by DP thymocytes. After overnight stimulation, the ability of Nur77^{tg} DP thymocytes to activate NKT cell hybridomas was measured by ELISA for secreted IL-2 in the supernatant (Fig. 2-2C). Although the reactivity varied between hybridoma lines, both the C57BL/6 and Nur77^{tg} DP thymocytes stimulated the Vα14^{+} hybridomas equally well (Fig. 2-2C). These data indicate that CD1d molecules expressed by Nur77^{tg} DP thymocytes have the potential to positively select NKT cells. This result then left remaining two possibilities open for testing: that NKT cell deficiency in Nur77^{tg} mice was due to negative selection and/or due to the lack of the canonical *Vα14*-to-*Jα18* rearrangement.

Nur77 overexpression induces apoptosis of developing NKT cells and can not be rescued by expression of rearranged Vα14 Jα18 TCR

If Nur77 mediates negative selection within NKT cells via induction of cell death, then introgression of survival factors may rescue NKT cell development in Nur77^{tg} mice. A previous study showed that negative selection of conventional T cells in Nur77^{tg} mice can not be rescued by *Bcl2* transgenesis (Rajpal et al., 2003) as Nur77 and the related Nor1 molecules bind the anti-apoptotic Bcl-2, and convert it into the pro-apoptotic factor (Thompson et al., 2010; Thompson and Winoto, 2008). We therefore, introgressed the pLck-*Bclxl* transgene into Nur77^{tg} mice. Enforced Bcl-x$_L$ over expression within early thymocytes rescued DP thymocytes from death and consequently the development of both conventional T cells and NKT cells (Fig. 2-3A and 2-3B) suggesting apoptosis as the potential underlying mechanism for NKT cell phenotype in Nur77^{tg} mice.

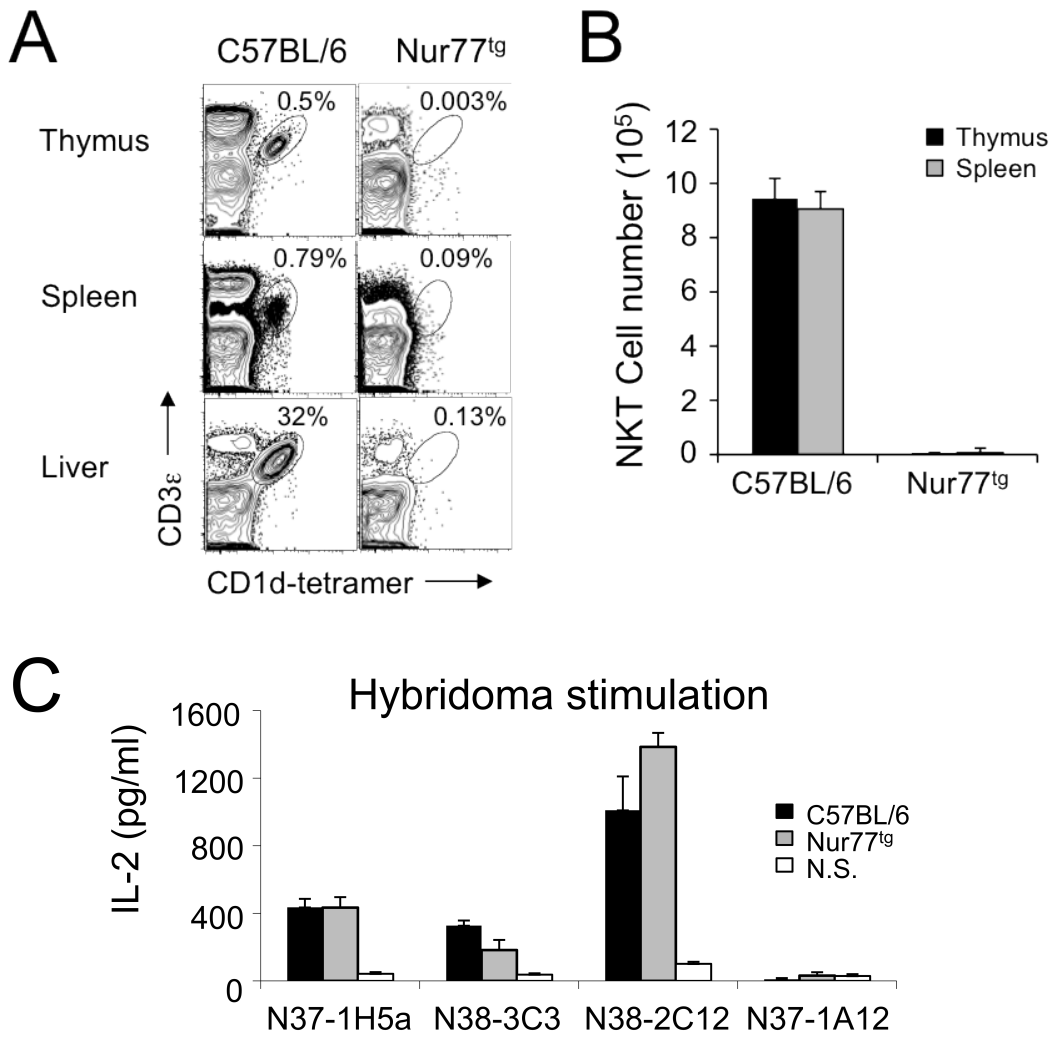

Figure 2-2. Nur77 affects the development of NKT cells

(A) Thymic, splenic and hepatic NKT cells from C57BL/6, and Nur77^{tg} mice were identified as CD3ε^{+}tetramer^{+} cells within electronically gated CD8^{LO} thymocytes or B220^{LO} splenocytes and liver mononuclear cells. Numbers are % of NKT cells among total leukocytes within each organ. Data are representative of 3 independent experiments, *n*=6.
(B) Absolute numbers of NKT cells in the thymus and spleen of C57BL/6, and Nur77^{tg} mice were calculated from % NKT cells in **A** and total thymocytes or splenocytes recovered from the respective lymphoid organs. Data are representative of 3 independent experiments showing *n* as in **A**. **(C)** The indicated hybridoma lines were incubated overnight with either C57BL/6 or Nur77^{tg} double positive thymocytes or without stimulator cells (N.S.). Using ELISA, IL-2 secreted into the supernatant was measured. Data are representative of 2 independent experiments, *n*=6.

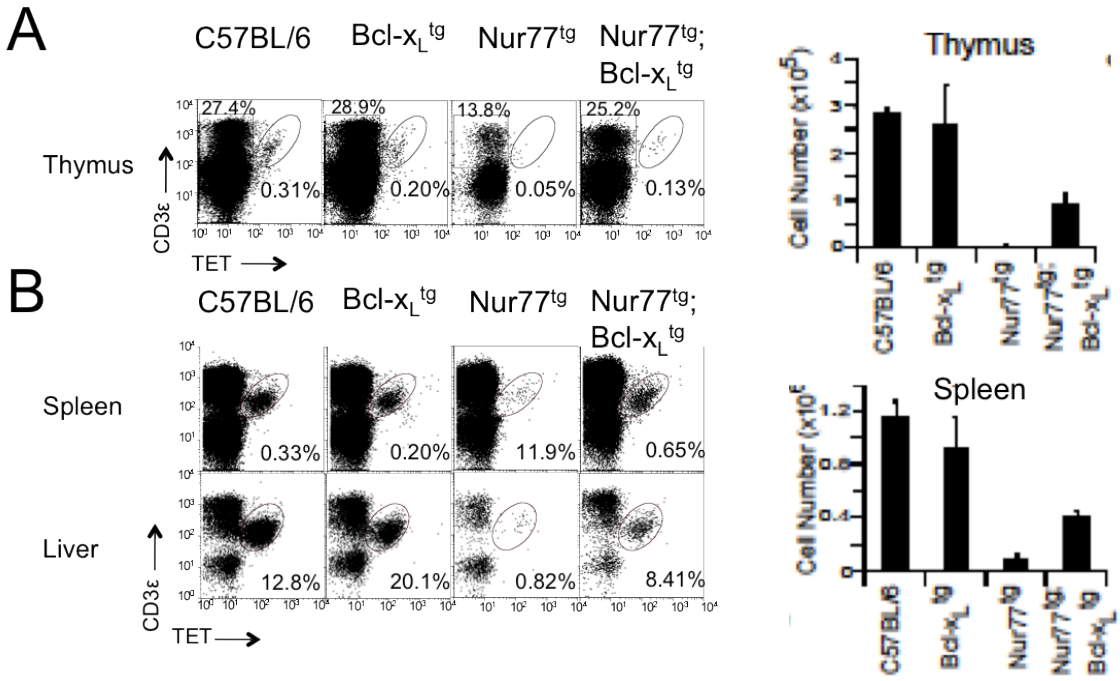

Figure 2-3. Overexpression of *Bcl-xl* restores NKT cell development in Nur77^{tg} mice

(A) Thymic NKT cells from C57BL/6 (n=2), Bcl-x$_L$^{tg} (n=2), Nur77^{tg} (n=2), and Nur77^{tg};Bcl-x$_L$^{tg} (n=5) mice were identified as CD3ε$^+$tetramer$^+$ cells within electronically gated CD8^{lo} thymocytes. Numbers are % of NKT cells among total leukocytes. Absolute NKT cell numbers (right panel) were calculated as in Fig 3-2A.

(B) Splenic and hepatic NKT cells from mice were identified as CD3ε$^+$tetramer$^+$ cells within electronically gated B220^{lo} splenocytes. Numbers are % of NKT cells among total leukocytes within each organ. Absolute NKT cell numbers were calculated as in Fig 3-2A. Data are representative of 2 independent experiments showing. *n*, as in **A**.

Since there was only partial rescue of NKT cell development within Nur77^{tg};Bcl-x_L^{tg} mice (Fig. 2-3), it is possible that Nur77^{tg} DP thymocytes poorly rearrange distal *Vα14*-to-*Jα18* gene segments, due to their premature apoptosis thereby resulting in low NKT cell precursors and total numbers. To test this, in a pilot experiment, DP thymocytes were sorted from C57BL/6, Nur77^{tg}, and Jα18^{0} (NKT deficient) thymi and their RNA was analysed by RT-PCR for the canonical *Vα14* to *Jα18* rearrangement. The specificity of the reaction was ascertained by RT-PCR for *Vα3* to *Jα18* rearrangement. The data revealed that in contrast to C57BL/6 DP thymocytes, those from Nur77^{tg} mice had not rearranged the canonical *Vα14* and *Jα18* gene segments (Fig. 2-4A), as expected from previously described animal models with similarly high DP thymocyte apoptosis (e.g., RORγt$^{-/-}$ and HEB$^{-/-}$). None of the strains tested showed *Vα3* to *Jα18* rearrangement (Fig. 2-4A), which was used as negative control. To confirm and quantify *Vα14*-to-*Jα18* re-arrangement, qRT-PCR analysis was performed on RNA isolated from CD3ε^{+} T cell-enriched C57BL/6, Nur77^{tg}, and Vα14^{tg} (from rearranged *Vα14Jα18* TCR transgenic mice (Bendelac, 1996)) thymocytes and splenocytes. Compared to C57BL/6, Nur77^{tg} CD3ε^{+} T cell-enriched thymocytes and splenocytes contained significantly lower amount of *Vα14Jα18* transcript (Fig. 2-4B). In contrast, but as expected, Vα14^{tg} CD3ε^{+} T cell-enriched thymocytes and splenocytes contained very high levels of *Vα14Jα18* transcript (Fig. 2-4B). These results suggest that a low initial pool of NKT cell precursors in DP thymocytes may have led to decreased numbers of NKT cells in Nur77^{tg} mice.

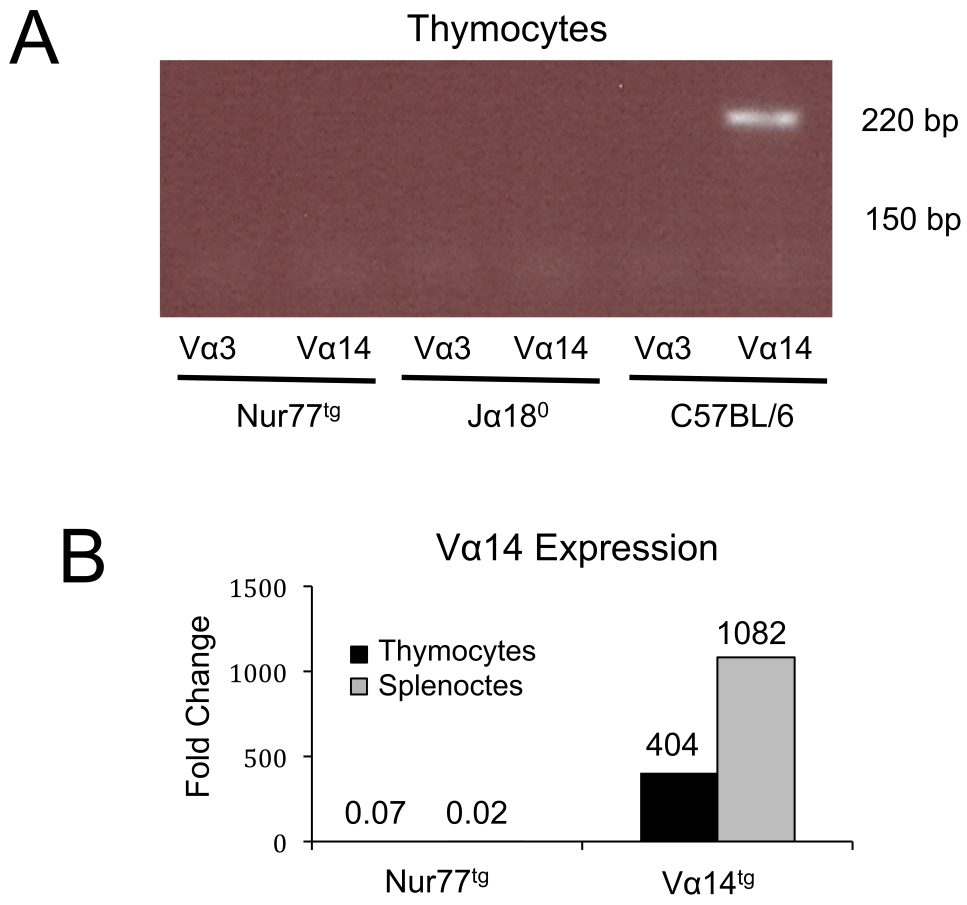

Figure 2-4. Absence of Vα14Jα18 transcript in Nur77 transgenic T cells

(A) RT-PCR assessment of *Vα3* to-*Jα18* and *Vα14*-to-*Jα18* rearrangements within Nur77^{tg} and Jα18^{0} thymocytes compared to C57BL/6 thymocytes. Data are representative of 1 experiment.

(B) Quantitative RT-PCR for Vα14Jα18 transcript within CD3ε^{+} cells magnetically enriched from Nur77^{tg} and Vα14^{tg} thymocytes, and splenocytes.

Based on the above speculation, we reasoned that forced expression of a rearranged *Vα14Jα18* transgene, which bypasses the requirement for endogenous TCR rearrangement, should rescue NKT cell development, if there was no contribution of overt negative selection to Nur77^{tg} NKT cell phenotype. Therefore, a rearranged *Vα14Jα18* TCR transgene (Vα14^{tg}) was introgressed into the Nur77^{tg} strain. The resulting mice were assessed for T cell and NKT cell development. Developing thymocytes expressed higher levels of CD3ε within both Vα14^{tg} and Nur77^{tg};Vα14^{tg} mice perhaps due to forced over expression of the TCR transgene (Fig. 2-5A). Nonetheless, as expected both Nur77^{tg} and Nur77^{tg};Vα14^{tg} mice had fewer conventional T cells in the spleen compared to C57BL/6 mice (Fig. 2-5A) and their numbers should not be affected by introgression of the NKT cell specific TCR transgene. Hence, the absolute number of T cells in both the thymus and spleen were much lower in both Nur77^{tg} and Nur77^{tg};Vα14^{tg} mice (Fig.2-5A) and those few T cells that developed were either skewed towards CD4 or did not express either CD4 or CD8 (Fig. 2-5B). Assessment of NKT cell development revealed that they were poorly represented in Nur77^{tg};Vα14^{tg} mice compared to the Vα14^{tg} controls (Fig. 2-6A and 2-6B). While Vα14^{tg};Nur77^{tg} mice have apparent higher frequency of NKT cells compared to C57BL/6 (which has intact conventional T and DP T cell compartment), a more appropriate way to compare these two strains with unequal thymic cellular composition was to compare the absolute numbers of cells, rather than frequencies, and those numbers revealed significantly reduced thymic and splenic NKT compartment in Vα14^{tg};Nur77^{tg} compared to that in both

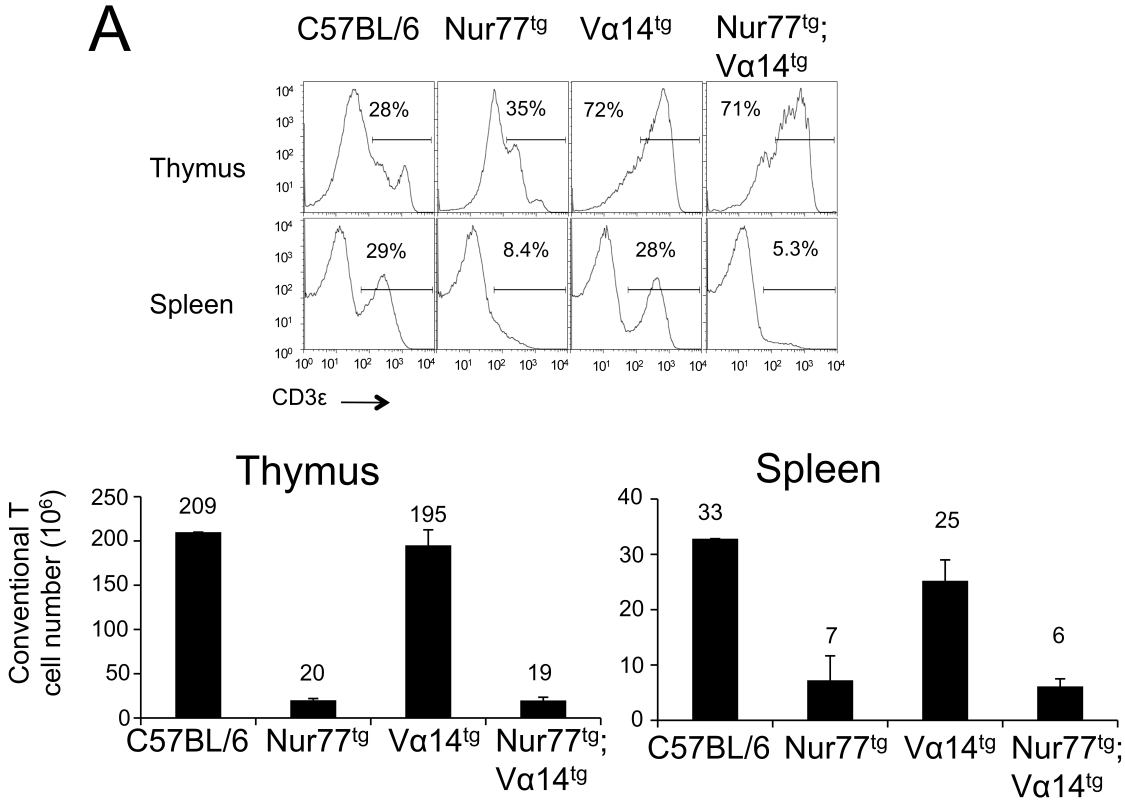

Figure 2-5. Nur77 negatively selects T cells

(A) Thymic, splenic and hepatic CD3ε$^+$ cells from C57BL/6, Nur77^{tg}, Vα14^{tg} and Nur77^{tg};Vα14^{tg}. Numbers are % of CD3ε$^+$ T cells among total leukocytes. Data are representative of 1 experiment, *n*=2. Absolute numbers of T cells in the thymus and spleen were calculated from % T cells and total cell count.

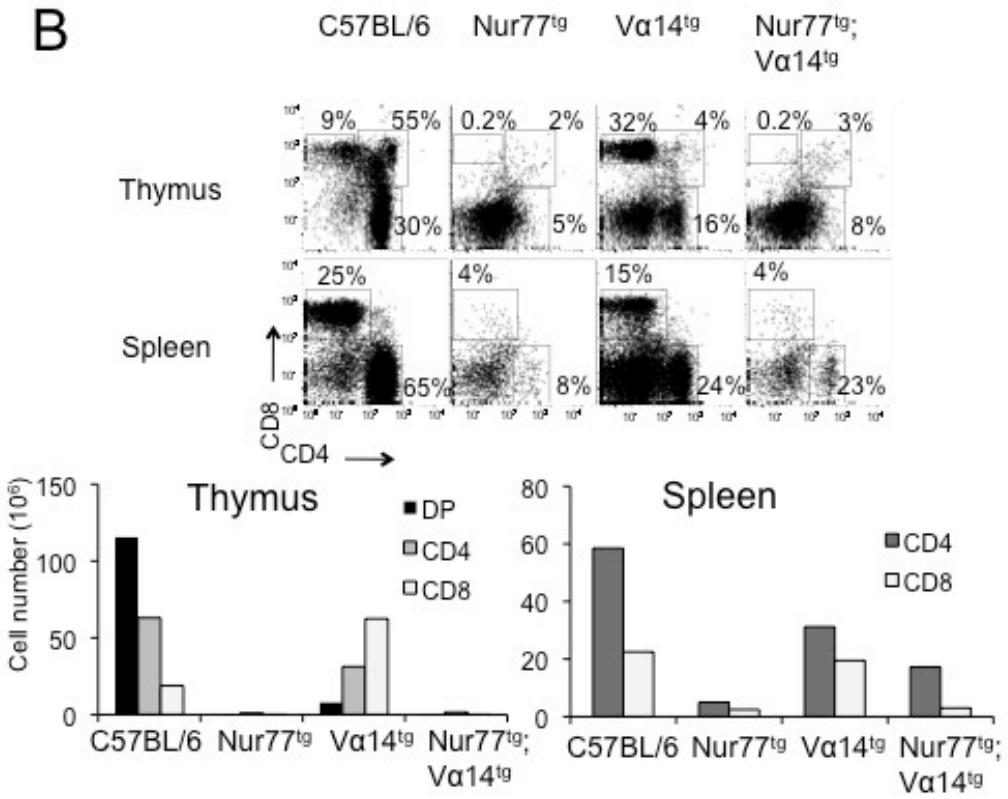

Figure 2-5 continued. Nur77 negatively selects T cells

(B) Thymic, splenic and hepatic $CD4^+$ and $CD8^+$ T cells from C57BL/6, $Nur77^{tg}$, $V\alpha14^{tg}$ and $Nur77^{tg}$;$V\alpha14^{tg}$ mice were identified as $CD4^+$ or $CD8^+$ cells within electronically gated $B220^-$ $CD3\varepsilon^+$ thymocytes or splenocytes. Numbers are % of $CD4^+$ or $CD8^+$ T cells among total leukocytes. Absolute numbers of T cells in the thymus and spleen were calculated from % T cells and total cell count. *n*=2.

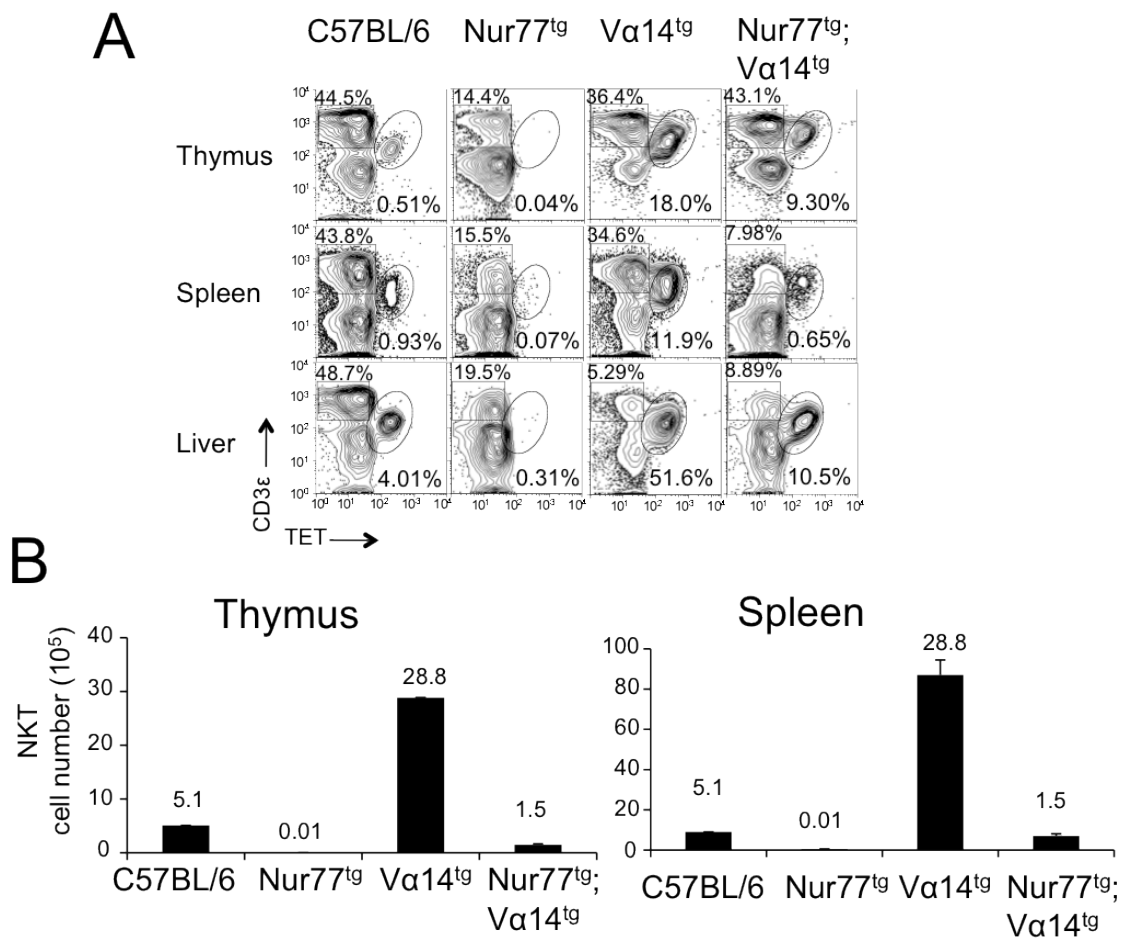

Figure 2-6. Nur77 negatively selects Vα14^{tg} NKT cells

(A) Thymic, splenic and hepatic NKT cells from C57BL/6, Nur77^{tg}, Vα14^{tg} and Nur77^{tg};Vα14^{tg} mice were identified as CD3ε^{+}tetramer^{+} cells within electronically gated CD8^{LO} thymocytes or B220^{LO} splenocytes and liver mononuclear cells. Numbers are % of NKT cells among total leukocytes within each organ. *n*=2.
(B) Absolute numbers of NKT cells in the thymus and spleen were calculated from % NKT cells in **A** and total cell count. *n* as in **A**.

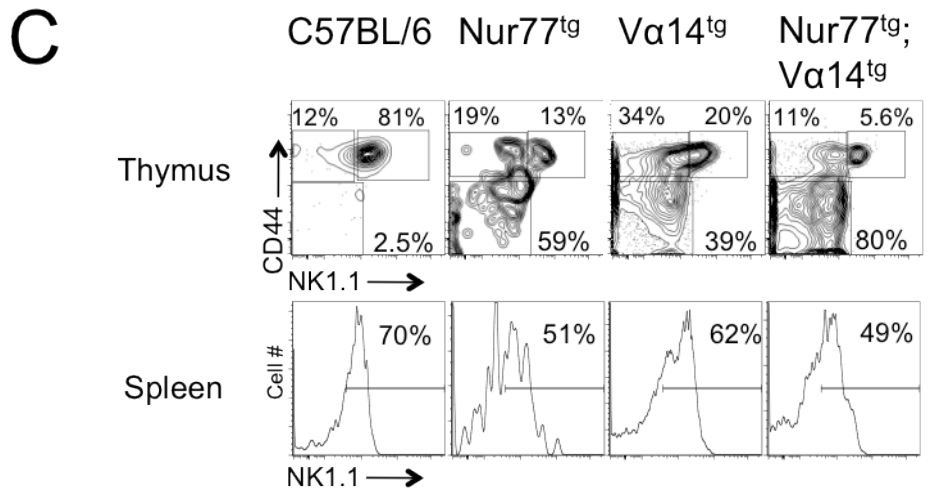

Figure 2-6, continued. Nur77 negatively selects of Vα14^{tg} NKT cells

(C) NKT cell developmental stages in C57BL/6, Nur77^{tg}, Vα14^{tg} and Nur77^{tg};Vα14^{tg} mice were identified as CD44^{NEG}NK1.1^{NEG} ST1, CD44^{+}NK1.1^{NEG} ST2, or CD44^{+}NK1.1^{+} ST3 in the thymus or as NK1.1^{NEG}tetramer^{+} or NK1.1^{+}tetramer^{+} within the splenic and hepatic MNCs. Numbers are % of cells among total NKT cells. *n*=2.

C57BL/6 and Vα14^{tg} mice (Fig. 2-6B). To determine how far the NKT cells that were detected in Nur77^{tg};Vα14^{tg} mice had progressed through development, the expression pattern of CD44 and NK1.1 markers were investigated. The data revealed that the thymic Vα14^{tg};Nur77^{tg} NKT cells were blocked at the very immature CD44^{NEG}NK1.1^{NEG} stage and contained lower frequency of CD44^{HI}NK1.1^{+} NKT cells when compared to C57BL/6 and Vα14^{tg} mice (Fig. 2-6C). Taken together, the results described above suggest that regardless of NKTCR rearrangement and despite *Vα14Jα18* transgenic TCR expression in Nur77^{tg};Vα14^{tg} mice, Nur77 is still capable of inducing negative selection during early development of NKT cells.

Dominant negative Nur77 mouse: a model for T cell negative selection

Previous reports demonstrated that thymocyte-specific expression of the dominant negative Nur77 transgene (Nur77ΔN^{tg}) blocks negative selection of conventional T cells (Calnan et al., 1995; Zhou et al., 1996). Since Nur77 plays a role in negative selection of NKT cells (Fig 2-2), this model of impaired negative selection was investigated. Mice were generated that express proximal-*Lck* promotor-enhancer driven Nur77ΔN transgene by the Vanderbilt Transgenic Mouse Shared Resource. This was accomplished by microinjection of an expression plasmid construct [generously provided by Dr. A. Winoto of UC Berkley (Fig. 2-7A) (Calnan et al., 1995)] into fertilized oocytes isolated from C57BL/6 mice. Upon breeding and PCR screening for germline transmission, three founder lines were identified. Functional redundancy between Nur77 family

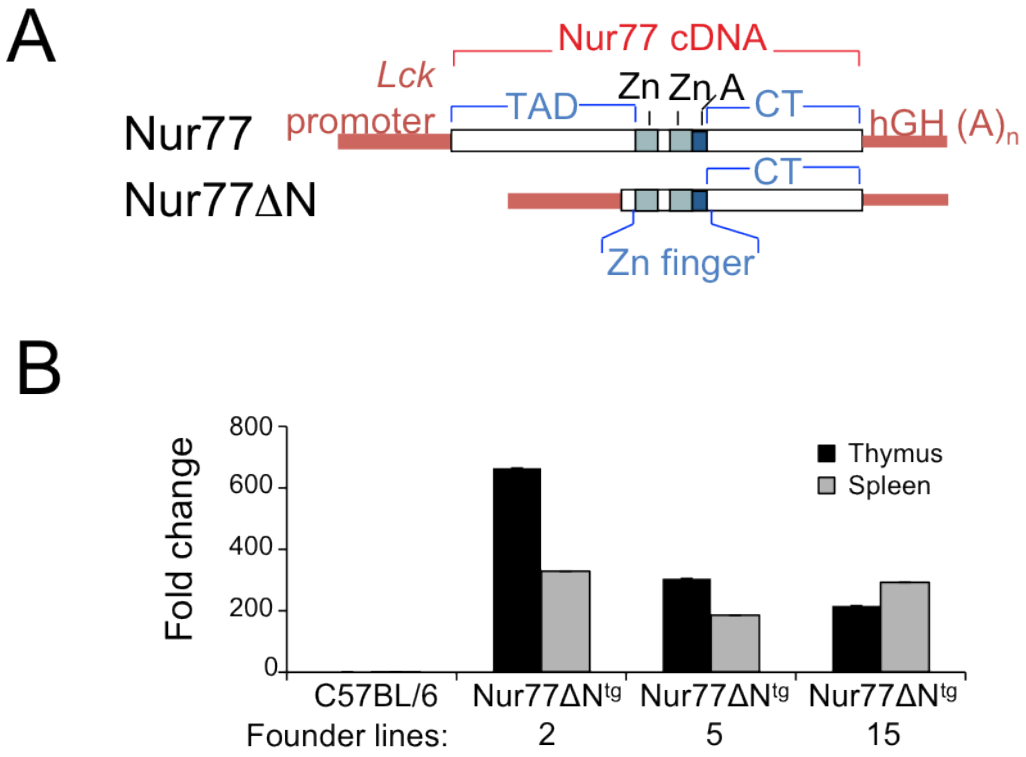

Figure 2-7. Nur77 transgenic (^{tg}) mice as models for negative selection

(A) Map of transgene constructs both driven by the *Lck*-proximal promoter. The wild-type *Nur77* construct contains full length *Nur77* cDNA made up of the transactivation domain (TAD), the zinc finger DNA binding domain (Tyznik et al., 2008), and c-terminal domain (CT). The dominant negative (ΔN) *Nur77* construct lacks the TAD. Nur77^{tg} mice and the Nur77ΔN construct were generous gifts from Dr. A. Winoto.
(B) Transcript expression levels within thymocytes and splenocytes from 3 founder lines of Nur77ΔN^{tg} mice was assessed by real-time qPCR. β-actin was used as the internal control for normalization. Data from 1 experiment; each qPCR was performed in triplicate.

members Nur77 and Nor-1 was previously shown (Cheng et al., 1997). Hence, the conventional $Nur77^{0}$ mice can not be used as appropriate model and furthermore, Nur77ΔN transgene must be expressed at high enough levels to inhibit function of both family members. Therefore, transgene expression in thymic and splenic T cells was determined in the three $Nur77\Delta N^{tg}$ founder lines by real-time qRT-PCR. Founder line #2 was determined to have the highest expression of Nur77ΔN (Fig. 2-7B). This line was used for all experiments described herein.

Evaluation of thymi and spleens confirmed the development of $CD4^{+}$ and $CD8^{+}$ T cell within $Nur77\Delta N^{tg}$ mice (Fig. 2-8). Both the frequency (Fig. 2-8A) and absolute number (Fig. 2-8B) of T cells in $Nur77\Delta N^{tg}$ mice were similar to C57BL/6 levels. As expected the frequency and absolute number of conventional T cells were low in $Nur77^{tg}$ mice as described above and in the previous studies (Calnan et al., 1995).

Next, to ascertain whether the Nur77ΔN transgene does indeed inhibit negative selection, the Nur77ΔN transgene was introgressed into a mouse model of negative selection, the TCR-HY^{tg} mouse. TCR-HY^{tg} male C57BL/6 mice do not develop $CD8^{+}$ T cells due to overt negative selection of HY specific T cells upon recognition of their cognate male minor histocompatibility antigen pHY presented by the $H2D^{b}$ (Kisielow et al., 1988). Flow cytometric analysis of blood revealed rescue of T cell development within $Nur77\Delta N^{tg}$;TCR-HY^{tg} C57BL/6 male mice (Fig. 2-8C). These data indicate that in this mouse model, Nur77ΔN

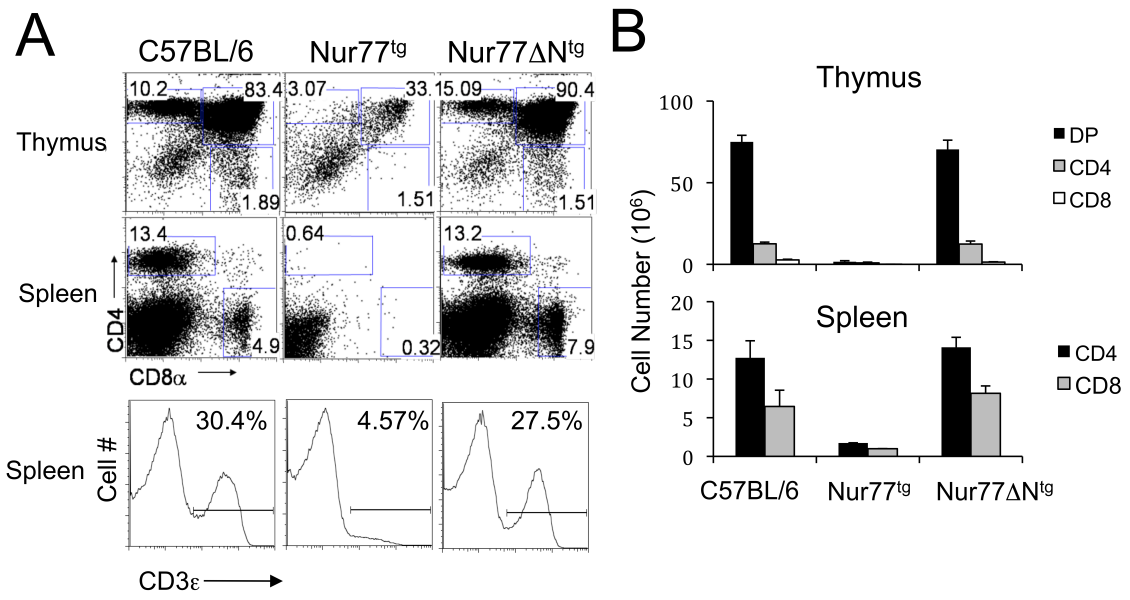

Figure 2-8. Nur77 transgenic (^{tg}) mice as models for negative selection

(A) Thymic, splenic and hepatic NKT cells from C57BL/6, Nur77^{tg}, and Nur77ΔN^{tg} mice were identified as CD3ε^{+}tetramer^{+} cells within electronically gated CD8^{LO} thymocytes or B220^{LO} splenocytes and liver mononuclear cells. Numbers are % of NKT cells among total leukocytes within each organ. Data are representative of 3 independent experiments, *n*=6.
(B) Absolute numbers of NKT cells in the thymus and spleen of C57BL/6, Nur77^{tg}, and Nur77ΔN^{tg} mice were calculated from % NKT cells in **A** and total thymocytes or splenocytes recovered from the respective lymphoid organs. Data are representative of 3 independent experiments showing *n* as in **A**.

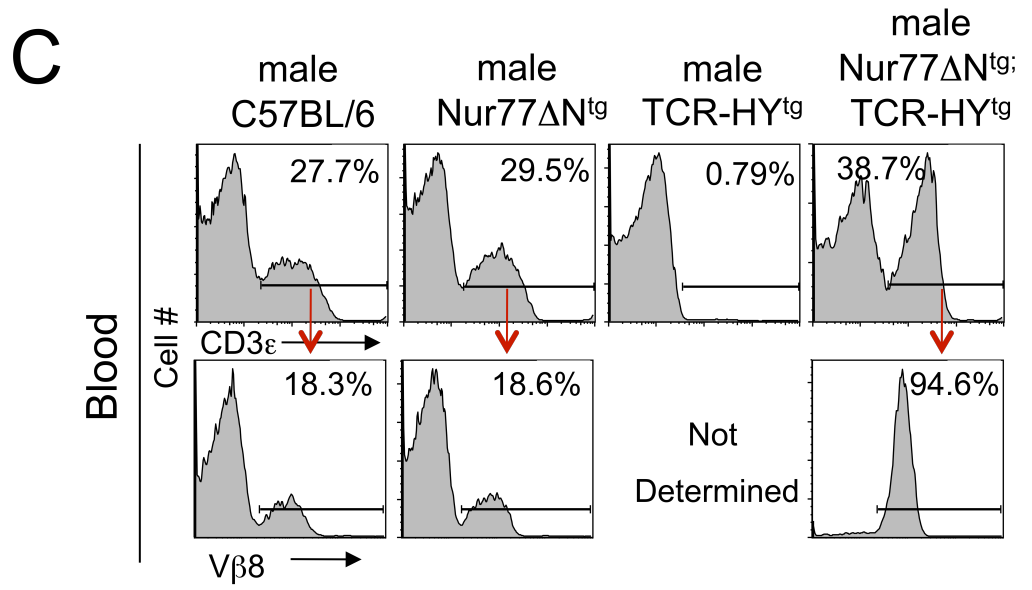

Figure 2-8, continued. Nur77 transgenic (^{tg}) mice as models for negative selection

(C) Blood from male C57BL/6 (*n*= 3), Nur77ΔN^{tg} (*n*= 3), TCR-HY^{tg} (*n*= 4), and Nur77ΔN^{tg};TCR-HY^{tg} (*n*= 9) mice was stained for presence of T cells (CD3ε^{+}) and TCR-Hy (Vβ8^{+}) transgene. Top row indicates T cells within total leukocytes. Bottom row indicates TCR-HY transgene (Vβ8^{+}) expression within electronically gated CD3ε^{+} leukocytes, when present. Numbers in top row are % of total lymphocytes and the bottom row are % of CD3ε^{+} leukocytes. Data are representative of 3 independent experiments.

functions as previously reported (Zhou et al., 1996) and, consequently, blocks negative selection of $CD8^+$ T cells.

NKT cells develop and mature in Nur77ΔN^{tg} mice

Since Nur77ΔN blocked negative selection of transgenic $CD8^+$ T cells, we wanted to examine whether the mutant transcription factor could also block negative selection of NKT cells within Nur77ΔN^{tg} mice. Should negative selection occur during NKT cell development, upon blocking negative selection one would expect one of few outcomes: the most obvious assumption would be an increase in NKT cell frequency and number due to increased survival of these lymphocytes. This was a rather unlikely outcome as levels of conventional CD4 and CD8 T cells, which also undergo Nur77-mediated negative selection, are not increased in these mice either (Fig 2-8), perhaps reflecting some other general mechanism dictating overt population size in lymphoid organs. Indeed, our data revealed that thymic CD4, CD8 and NKT cell frequency (Fig. 2-8 and 2-9A) and absolute number (Fig. 2-9B) were close to similar in Nur77ΔN^{tg} mice and C57BL/6 mice. Splenic NKT cells were about half reduced in the mutant mice compared to C57BL/6 animals (Fig. 2-9A and 2-9B) suggesting potential additional aspects of NKT cell population control in peripheral organs. Moreover, similar to C57BL/6 NKT cells, Nur77ΔN^{tg} NKT cells that develop were mature because they had attained $CD44^{HI}NK1.1^+$ phenotype (Fig. 2-9C). The reduced peripheral Nur77ΔN^{tg} NKT cell number may also be a consequence of the

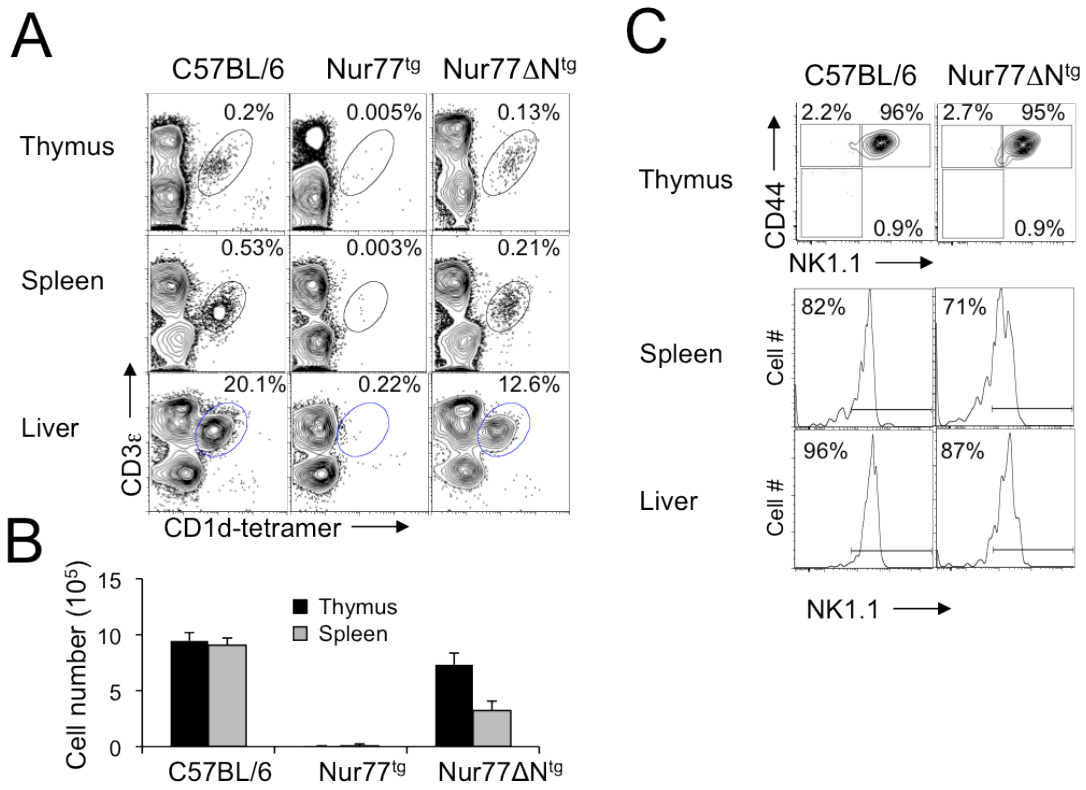

Figure 2-9. Nur77 affects the development of NKT cells

(A) Thymic, splenic and hepatic NKT cells from C57BL/6, Nur77^{tg}, and Nur77ΔN^{tg} mice were identified as CD3ε^{+}tetramer^{+} cells within electronically gated CD8^{LO} thymocytes or B220^{LO} splenocytes and liver mononuclear cells. Numbers are % of NKT cells among total leukocytes within each organ. Data are representative of 3 independent experiments, *n*=6.
(B) Absolute numbers of NKT cells in the thymus and spleen of C57BL/6, Nur77^{tg}, and Nur77ΔN^{tg} mice were calculated from % NKT cells in **A** and total thymocytes or splenocytes recovered from the respective lymphoid organs. *n* as in **A**.
(C) NKT cell developmental stages in C57BL/6 and Nur77^{tg};Vα14^{tg} mice were identified as CD44^{NEG}NK1.1^{NEG} ST1, CD44^{+}NK1.1^{NEG} ST2, or CD44^{+}NK1.1^{+} ST3 in the thymus or as NK1.1^{NEG}tetramer^{+} or NK1.1^{+}tetramer^{+} within the splenic and hepatic MNCs. Data are showing *n* as in **A**.

transgene interfering with the NKT cell developmental program in an as yet unknown manner.

Positive selection precedes Nur-77-mediated negative selection during NKT cell development

Developing conventional T cells initially undergo the process of positive selection within the cortex of the thymus. Before completing their development, those that are positively selected then undergo negative selection upon migrating to cortico-medullary boundary to eliminate highly self-reactive T cell clones. NKT cells undergo positive selection in the thymus by interacting with CD1d molecules expressed by DP thymocytes (Bendelac, 1995; Xu et al., 2003). This process is dependent upon proper endosomal CD1d trafficking and lipid presentation because NKT cells poorly, if at all develop in CD1d tail-deleted (TD) mice. Mutant CD1d-TD molecules lack the cytoplasmic tail; consequently, they do not recycle efficiently through the endo-lysosomal compartment. This recycling is essential for CD1d-restricted presentation of lipid ligand(s) that mediate positive selection of NKT cells (Chiu et al., 2002). Since our data indicate that NKT cells undergo negative selection, we queried which process occurs first, positive or negative selection. To address this question, the CD1d-TD knock-in strain was bred to the Nur77ΔN^{tg} strain. We reasoned that if negative selection occurs first, NKT cell number would increase in CD1d-TD^{KI};Nur77ΔN^{tg} mice compared to either parent strain. Alternatively, if negative selection occurs after positive selection, the new

strain should look identical to CD1d-TD^{KI} as developing NKT cells would be arrested at the failed positive selection step just like seen in CD1d-TD^{KI}. The data supported the latter scenario i.e., NKT cell frequency and absolute number were much lower in CD1d-TD^{KI};Nur77ΔN^{tg} mice when compared to Nur77ΔN^{tg} mice and more closely resembled those of NKT cells in CD1d-TD^{KI} mice (Fig. 2-10). These data indicate that positive selection of NKT cells precedes their negative selection. Because it was reported that biased usage of Vβ chains in NKTCR is shaped during positive selection, these data suggest a hypothesis, to be tested below, in which positive selection plays a dominant role in grossly shaping the NKT cell repertoire.

Block of negative selection in Nur77ΔN^{tg} mice has a modest effect on positively selected αGalCer reactive NKTCR repertoire

NKT cells express a restricted TCR Vβ repertoire composed of Vβ8.2, 7, 2, 6,10, and 14. This restriction is not due to the inability of the α-chain to pair with particular Vβ as Vα14Jα18^{tg};CD1d-deficient mice contain a broad TCR Vβ cell repertoire (Bendelac et al., 2007). Additionally, only TCRs containing Vβ7, 8.2 and 2 were capable of responding to stimulation with a putative endogenous selecting ligand iGb3 (Wei et al., 2006). Thus, the NKTCR bias is thought to be the result of positive selection. What role negative selection plays in shaping the NKT cell repertoire is currently ill defined despite the fact that there is evidence to indicate this (Chun et al., 2003; Pellicci et al., 2003). A serologic analysis using

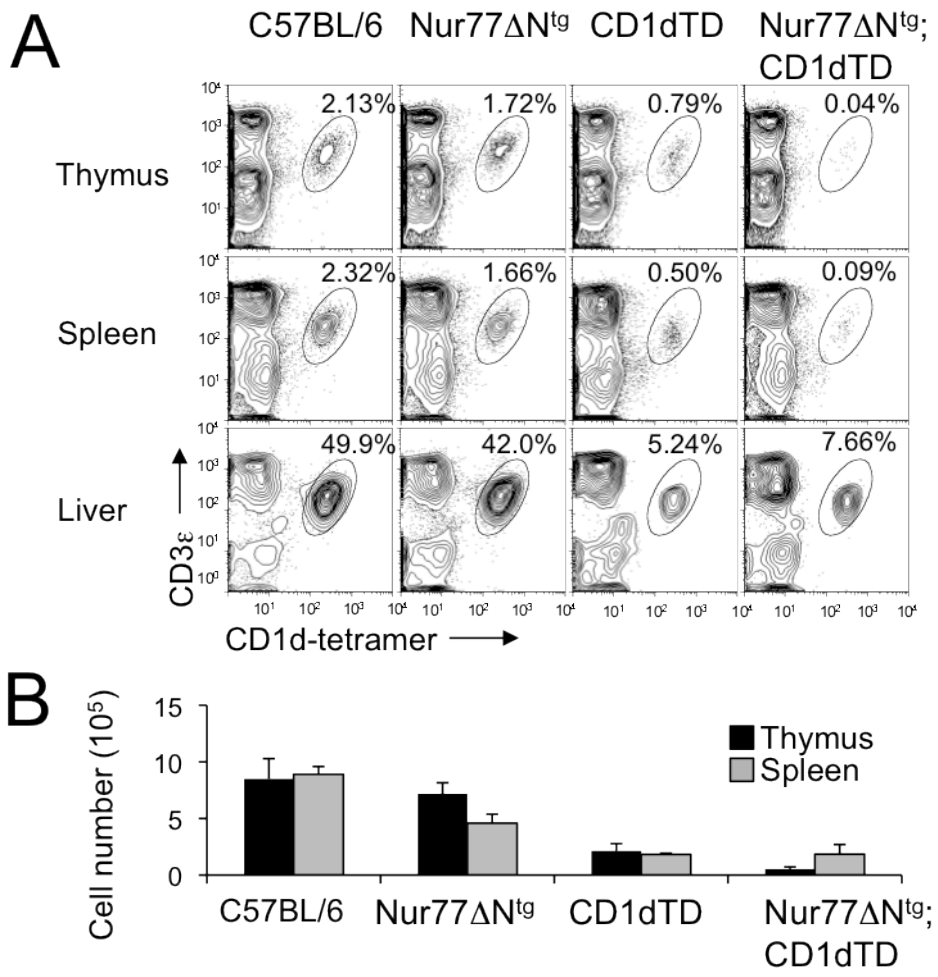

Figure 2-10. Positive selection precedes negative selection in NKT cells

(A) Thymic, splenic and hepatic NKT cells from C57BL/6 (n=7), Nur77ΔN^{tg} (n=4), CD1dTD (n=3), and Nur77ΔN^{tg};CD1dTD (n=7) mice were identified as CD3ε^{+}tetramer^{+} cells within electronically gated CD8^{LO} thymocytes or B220^{LO} splenocytes and liver mononuclear cells. Numbers are % of NKT cells among total leukocytes within each organ. Data are representative of 3 independent experiments.

(B) Absolute numbers of NKT cells in the thymus and spleen were calculated from % NKT cells in **A** and total thymocytes or splenocytes recovered from the respective lymphoid organs. Data showing *n* as in **A**.

Vβ-specific mAbs revealed that Vβ usage in C57BL/6 and Nur77ΔN^{tg} thymic NKT cells were not significantly altered (Fig. 2-11A). A similar analysis of splenic NKT cells in the two strains showed only minor differences (Fig. 2-11A) thus supporting dominant role of positive selection in restricting overall Vβ usage by NKT cells.

The TCR repertoire is shaped not only by the particular pairing of α- and β-chains but also by V(D)J rearrangements that confers extreme diversity to the complementary determining region 3 (CDR3) within the two TCR chains. Negative selection within NKT cells may not alter Vβ chain usage but may alter the length and frequency of CDR3β expressed by Nur77ΔN^{tg} NKT cells. The nature of CDR3β has been shown to influence lipid ligand recognition by NKT cells even though this part of the TCR makes very little direct contact with the CD1d-lipid complex (Li et al., 2010; Scott-Browne et al., 2007). To assess CDR3 diversity within C57BL/6 and Nur77ΔN^{tg} NKT cells, TCRs were sequenced from purified NKT cells. Preliminary data show no overlapping sequences in both strains (Table 2-1), even though the exact level of overlap (or its absence) will be tested in the repeat experiment to ensure the reproducibility of the technology in the animals of the same genotype. Regardless, Nur77ΔN^{tg} NKT cells contained generally higher percentage of re-arrangements between *Vβ*-to-*Jβ1*-cluster when compared to C57BL/6, which predominantly utilized *Jβ2*-cluster to code for CDR3β (Fig. 2-11B). This bias also rules out the randomness in our sequence analysis. The *Jβ*-cluster bias was more evident in NKTCRs made up of Vβ6 than

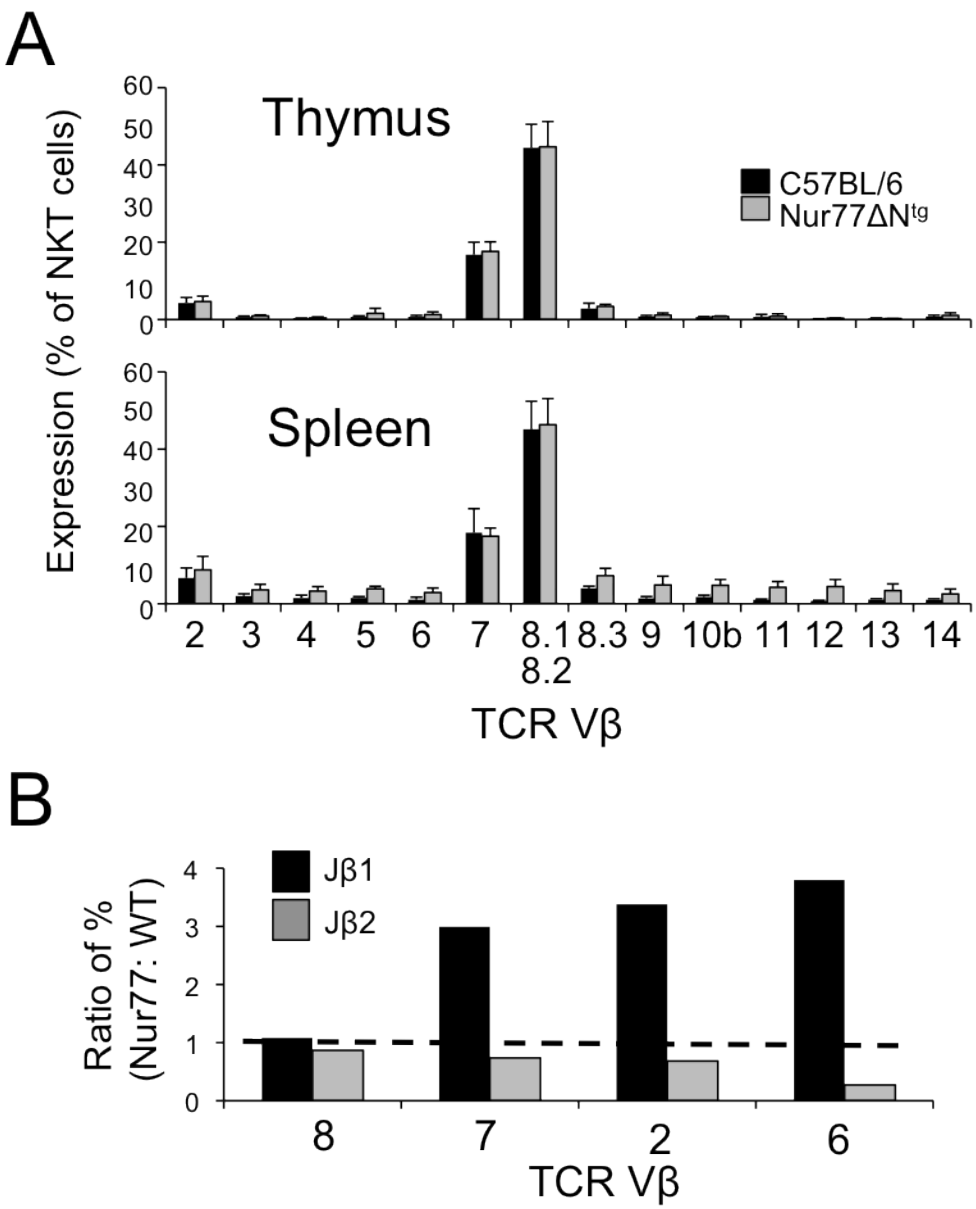

Figure 2-11. Nur77 plays a minor role in modeling the NKTCR repertoire

(A) TCR Vβ usage by thymic and splenic NKT cells from C57BL/6 and Nur77ΔN^{tg} mice was determined by flow cytometry. Shown are the percents of NKT cells expressing the indicated Vβs. Data are representative of 5 independent experiments showing *n=5.*

(B) Ratio of Nur77ΔN^{tg} to C57BL/6 percentage of Jβ expression based on sequences in Table 3-1.

Table 2-1. NKTCR CDR3 sequences

C57BL/6 TCR Vβ8						
Group	**Vβ**	**N/D/N**	**Jβ**	**Jβ-nomenclature**	**CDR length [CDR1, CDR2, CDR3]**	**Productive (P), Stop codon (S), Out of frame (O)**
1	ASSD		TNSDYT	TRBJ1-2*01	[5.6.10]	P
	ASSD		TNSDYT	TRBJ1-2*01	[5.6.10]	P
	ASSD		TNSDYT	TRBJ1-2*01	[5.6.10]	P
2	ASGD	LGGR	EDTQY	TRBJ2-5*01	[5.6.13]	P
3	ASG	GTGS	AETLY	TRBJ2-3*01	[5.6.12]	P
4	ASG	GLGAL	SAETLY	TRBJ2-3*01	[5.6.14]	P
5	ASGD		DTGQLY	TRBJ2-2*01	[5.6.10]	P
6	ASGD	V	GNTLY	TRBJ1-3*01	[5.6.10]	P
7	ASGD	AES	SYEQY	TRBJ2-7*01	[5.6.12]	P
8	AS	ALPGTGG	DEQY	TRBJ2-7*01	[5.6.13]	P
9	ASGD	QGA	DAEQF	TRBJ2-1*01	[5.6.12]	P
10	AS	TGTG	NTEVF	TRBJ1-1*01	[5.6.11]	P
11	ASGD	AIGA	SAETLY	TRBJ2-3*01	[5.6.14]	P
12	ASG	AS	SDYT	TRBJ1-2*01	[5.6.9]	P
13				TRBJ2-1*01	[5.6.X]	O
14	ASGD	RL	NQDTQY	TRBJ2-5*01	[5.6.12]	P
15	ASGD	*LGG#	#DTQY	TRBJ2-5*01	[5.6.X]	S,O
16	ASGD	AAGGG	YEQY	TRBJ2-7*01	[5.6.13]	P
17	ASGD	AGGA	NSDYT	TRBJ1-2*01	[5.6.13]	P
18	ASGD	ELGI	YEQY	TRBJ2-7*01	[5.6.12]	P
19	AS	GA	DTQY	TRBJ2-5*01	[5.6.8]	P
20	ASS	GDRG	TEVF	TRBJ1-1*01	[5.6.11]	P
21	ASGD	DWGG	SQNTLY	TRBJ2-4*01	[5.6.14]	P
22	ASG	V	SNTEVF	TRBJ1-1*01	[5.6.10]	P
23	ASGD	AGTGG	SQNTLY	TRBJ2-4*01	[5.6.15]	P
24	AS	SGTD	NNQAPL	TRBJ1-5*01	[5.6.12]	P
25	ASGD	AGTSYE	QY	TRBJ2-5*01	[5.6.12]	P
26	ASGE	RA	QNTLY	TRBJ2-4*01	[5.6.11]	P

Nur77ΔN ^{tg} TCR Vβ8						
Group	**Vβ**	**N/D/N**	**Jβ**	**Jβ-nomenclature**	**CDR length [CDR1.CDR2.CDR3]**	**Productive (P), Stop codon (S), Out of frame (O)**
1	ASG		SQNTLY	TRBJ2-4*01	[5.6.9]	P (no D segment)
	ASG		SQNTLY	TRBJ2-4*01	[5.6.9]	P (no D segment)
2	ASSD	VRGA	AETLY	TRBJ2-3*01	[5.6.13]	P
3	ASGD	AQ	AYEQY	TRBJ2-7*01	[5.6.11]	P
4	ASGD	GTGGN	NYAEQF	TRBJ2-1*01	[5.6.15]	P
5	ASGD	VGG	NSPLY	TRBJ1-6*01	[5.6.12]	P
6	ASGD	AGE	DTGQLY	TRBJ2-2*01	[5.6.13]	P
7	ASSD	AAGTG#	YEQY	TRBJ2-7*01	[5.6.X]	S, O
8	ASGD	AGES	SYEQY	TRBJ2-7*01	[5.6.13]	P
9	ASGE	QGNX	APL	TRBJ1-5*01	[5.6.11]	P
10	ASG	PGQ	TNTEVF	TRBJ1-1*01	[5.6.12]	P
11	ASGD	RDV	NTEVF	TRBJ1-1*01	[5.6.12]	P
12	ASR	GTS	SNERLF	TRBJ1-4*02	[5.6.12]	P
13	ASSD	ASTGV	NQDTQY	TRBJ2-5*02	[5.6.15]	P
14	ASGD	ADI	QDTQY	TRBJ2-5*01	[5.6.12]	P
15	ASGD		NTEVF	TRBJ1-1*01	[5.6.9]	P
16	ASSD	N	YEQY	TRBJ2-7*01	[5.6.9]	P
17	ASSD	RGG	NQAPL	TRBJ1-5*01	[5.6.12]	P
18	ASGD	AGGPV#	QF	TRBJ2-1*01	[5.6.X]	S, O
19	ASGD		NTEVF	TRBJ1-1*01	[5.6.9]	P
20	ASR		DTQY	TRBJ2-5*01	[5.6.7]	P
21	ASGD	AGQGG#	NYAEQF	TRBJ2-1*01	[5.6.X]	S, O
22	ASSE	MGG	EQY	TRBJ2-7*01	[5.6.10]	P
23	AS	SDAWGL	AEQF	TRBJ2-1*01	[5.6.12]	P
24	ASG	GT	SQNTLY	TRBJ2-4*01	[5.6.11]	P
25	ASG	QGG	AETLY	TRBJ2-3*01	[5.6.11]	P
26	ASGD	SGGD	QNTLY	TRBJ2-4*01	[5.6.13]	P
27	ASGD	AGT	ANSDYT	TRBJ1-2*01	[5.6.13]	P
28	ASGD	AGQGG	#NYAEQF	TRBJ2-1*01	[5.6.X]	S, O
29	ASGD	LTGGD	YEQY	TRBJ2-7*01	[5.6.13]	P
30	ASG	T	TNTEVF	TRBJ1-1*01	[5.6.10]	P

C57BL/6 TCR Vβ6						
Group	**Vβ**	**N/D/N**	**Jβ**	**Jβ-nomenclature**	**CDR length [CDR1.CDR2.CDR3]**	**Productive (P), Stop codon (S), Out of frame (O)**
1	ASS	PLGQA	QNTLY	TRBJ2-4*01	[5.6.13]	P
	ASS	PLGQA	QNTLY	TRBJ2-4*01	[5.6.13]	P
	ASS	PLGQA	QNTLY	TRBJ2-4*01	[5.6.13]	P
	ASS	PLGQA	QNTLY	TRBJ2-4*01	[5.6.13]	P
2	ASS	RFGS	SAETLY	TRBJ2-3*01	[5.6.13]	P
	ASS	RFGS	SAETLY	TRBJ2-3*01	[5.6.13]	P
3	ASSI	RTGG	YAEQF	TRBJ2-1*01	[5.6.13]	P
4	ASSI	S	YAEQF	TRBJ2-1*01	[5.6.10]	P
5	ASSI	WG#	SYEQY	TRBJ2-7*01	[5.6.X]	S, O
6		ARGTG	DTEVF	TRBJ1-1*01	[5.6.10]	P
7	AS	IPGLGGRG	EQY	TRBJ2-7*01	[5.6.13]	P
8	ASSI	MGR	YEQY	TRBJ2-7*01	[5.6.11]	P
9	ASSM	GLG#	SYEQY	TRBJ2-7*01	[5.6.X]	S, O
10	ASX	XSXXHT	LY	TRBJ1-3*01	[5.6.11]	S
11	ASSI	DRS	SYEQY	TRBJ2-7*01	[5.6.12]	P
12	ASS	PRQ	DSDYT	TRBJ1-2*01	[5.6.11]	P

Nur77ΔN ^{tg} TCR Vβ6						
Group	**Vβ**	**N/D/N**	**Jβ**	**Jβ-nomenclature**	**CDR length [CDR1.CDR2.CDR3]**	**Productive (P), Stop codon (S), Out of frame (O)**
1	ASSI	TGGA	DSDYT	TRBJ1-2*01	[5.6.13]	P
	ASSI	TGGA	DSDYT	TRBJ1-2*01	[5.6.13]	P
	ASSI	TGGA	DSDYT	TRBJ1-2*01	[5.6.13]	P
	ASS	TGGA	DSDYT	TRBJ1-2*01	[5.6.13]	P
2	ASS	RDRGKG	NTEVF	TRBJ1-1*01	[5.6.14]	P
	ASS	RDRGKG	NTEVF	TRBJ1-1*01	[5.6.14]	P
	ASS	RDRGKG	NTEVF	TRBJ1-1*01	[5.6.14]	P
	ASS	RDRGKG	NTEVF	TRBJ1-1*01	[5.6.14]	P
3	ASS	RGR	EVF	TRBJ1-1*01	[5.6.9]	P
	ASS	RGR	EVF	TRBJ1-1*01	[5.6.9]	P
	ASS	RGR	EVF	TRBJ1-1*01	[5.6.9]	P
4	ASS	PLG	AETLY	TRBJ2-3*01	[5.6.11]	P
	ASS	PLG	AETLY	TRBJ2-3*01	[5.6.11]	P
5	ASSI	PA#		TRBJ2-3*01	[5.6.X]	O (PHE 118 not identified)
6	ASSI	VQ	SQNTLY	TRBJ2-4*01	[5.6.12]	P
7	ASSM	RD#	#NERLF	TRBJ1-4*02	[5.6.X]	O
8	ASS	TLQA	NSDYT	TRBJ1-2*01	[5.6.12]	P
9	ASR	DRGR	DSDYT	TRBJ1-2*01	[5.6.12]	P
10	ASSI	PES	NSDYT	TRBJ1-2*01	[5.6.12]	P
11	AS	AGTGPS		TRBJ1-6*01	[5.6.8]	P

C57BL/6 TCR Vβ2						
Group	**Vβ**	**N/D/N**	**Jβ**	**Jβ-nomenclature**	**CDR length [CDR1.CDR2.CDR3]**	**Productive (P), Stop codon (S), Out of frame (O)**
1	TCSA	DWG	EQY	TRBJ2-7*01	[6.6.10]	P
	TCSA	DWG	EQY	TRBJ2-7*01	[6.6.10]	P
	TCSA	DWG	EQY	TRBJ2-7*01	[6.6.10]	P
	TCSA	DWG	EQY	TRBJ2-7*01	[6.6.10]	P
2	TCSAD	R	DQDTQY	TRBJ2-5*01	[6.6.12]	P
3	TCSAE	WV	EQY	TRBJ2-7*01	6.6.10]	P
4	TCSA	AGIQ	DTQY	TRBJ2-5*01	[6.6.12]	P
5	TCSAD	GGV	YEQY	TRBJ2-7*01	[6.6.12]	P
6	TCSAD	GGLGGH	NYAEQF	TRBJ2-1*01	[6.6.17]	P
7	TCSAD	GVG	NERLF	TRBJ1-4*02	[6.6.13]	P
8	TCSAD	GRGL	DTQY	TRBJ2-5*01	[6.6.13]	P
9	TCSA	A	GAETLY	TRBJ2-3*01	[6.6.11]	P
10	TCR	GTGG	KNTLY	TRBJ2-4*01	[6.6.12]	P
11	TCSA	LDWGVS	SAETLY	TRBJ2-3*01	[6.6.16]	P

Nur77ΔN ^{tg} TCR Vβ2						
Group	**Vβ**	**N/D/N**	**Jβ**	**Jβ-nomenclature**	**CDR length [CDR1.CDR2.CDR3]**	**Productive (P), Stop codon (S), Out of frame (O)**
1	TCSAD	QG	TLY	TRBJ2-3*01	[6.6.10]	P
	TCSAD	QG	TLY	TRBJ2-3*01	[6.6.10]	P
2	TCSAD	RLG	SAETLY	TRBJ2-3*01	[6.6.14]	P
3	TCS	GTG	NTEVF	TRBJ1-1*01	[6.6.11]	P
4	TCSA	DRG	DTEVF	TRBJ1-1*01	[6.6.12]	P
5	TCS	DIRE	EVF	TRBJ1-1*01	[6.6.10]	P
6	TCSAD	HG	SQNTLY	TRBJ2-4*01	[6.6.13]	P
7	TCSA	RDF	SAETLY	TRBJ2-3*01	[6.6.13]	P
8	TCS	PDRGS	SAETLY	TRBJ2-3*01	[6.6.14]	P
9		PAVQINWGA#	EQY	TRBJ2-7*01	[6.6.X]	S, O
10	TCS	GD	SQNTLY	TRBJ2-4*01	[6.6.11]	P
11	TCSAD	LG	QDTQY	TRBJ2-5*01	[6.6.12]	P
12	TCSAD	S	NERLF	TRBJ1-4*02	[6.6.11]	P
13	TCSAE	TVW	EQY	TRBJ2-7*01	[6.6.11]	P

C57BL/6 TCR Vβ7						
Group	**Vβ**	**N/D/N**	**Jβ**	**Jβ-nomenclature**	**CDR length [CDR1.CDR2.CDR3]**	**Productive (P), Stop codon (S), Out of frame (O)**
1	ASSL	GH	SNERLF	TRBJ1-4*02	[5.6.12]	P
	ASSL	GH	SNERLF	TRBJ1-4*01	[5.6.12]	P
2	AS	H	TNTGQLY	TRBJ2-2*01	[5.6.10]	P
3	ASSLS	R	SQNTLY	TRBJ2-4*01	[5.6.12]	P
4	ASS	XQGXX	AEQF	TRBJ2-1*01	[5.6.12]	P
5	A	TQG	SAETLY	TRBJ2-3*01	[5.6.10]	P
6	ASSL	TGD	ANTGQLY	TRBJ2-2*01	[5.6.14]	P
7	AR	TGP	ANTGQLY	TRBJ2-2*01	[5.6.12]	P
8	ASS	SPTG	ANTGQLY	TRBJ2-2*01	[5.6.14]	P
9	AS	H	TNTGQLY	TRBJ2-2*01	[5.6.10]	P
10	ASS	TGQGG	NTLY	TRBJ2-4*01	[5.6.12]	P
11	ASS	XXGGK	AETLY	TRBJ2-3*01	[5.6.13]	P
12	ASSL		DTQY	TRBJ2-5*01	[5.6.8]	P (no D segment)
13	ASSL	AGTG	DERLF	TRBJ1-4*02	[5.6.13]	P
14	ASSLS	YGG	GAETLY	TRBJ2-3*01	[5.6.14]	P

the high affinity Vβ7 and Vβ2. Thus, highly self reactive NKTCR containing Jβ1 may be negatively selected in wild type mice while they survive in Nur77ΔN^{tg}. These data indicate that Nur77 plays a minor role in shaping the αGalCer reactive NKT cell repertoire.

C57BL/6 and Nur77ΔN^{tg} NKT cells react differently to a variety of lipid agonists

The purpose of negative selection is to remove highly self-reactive T cells from the repertoire to prevent potential autoimmune responses. Therefore, whether Nur77ΔN^{tg} NKT cells show altered reactivity to currently known self lipid agonists was determined. Since conventional T cells also express the Nur77ΔN^{tg}, it was important to rule out any reactivity that may be contributed by conventional T cells in the functional assays. Thus, Nur77ΔN^{tg} mice were made deficient for NKT cells by crossing them with Jα18^{0} mice (Fig. 2-13A). Splenocytes stimulated in vitro with different amounts of the known potent NKT cell agonist αGalCer resulted in similar or slightly reduced IFN-γ secreted into the culture supernatants when Nur77ΔN^{tg} splenocytes were compared to C57BL/6 cells (Fig. 2-12B). The slight reduction in response may be due to the reduced overall numbers of NKT cells within Nur77ΔN^{tg} spleens. Additionally, IFN-γ was not found in the culture supernatant when Nur77ΔN^{tg};Jα18^{0} splenocytes stimulated as above, suggesting that the IFN-γ response to αGalCer stimulation in vitro is NKT cell dependent.

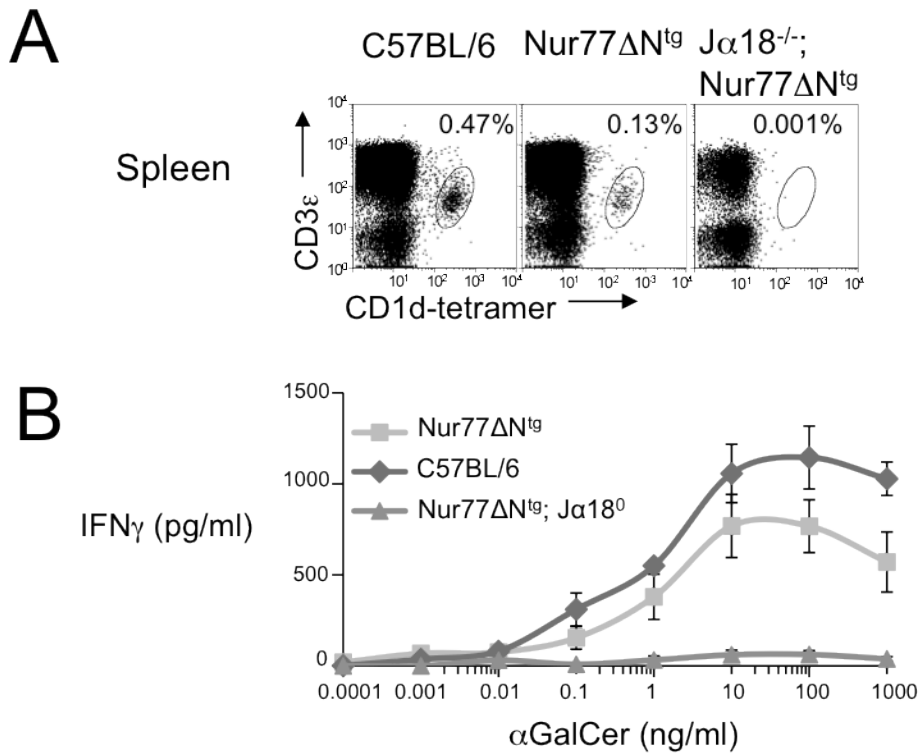

Figure 2-12. Defective Nur77 expression alters *in vitro* NKT cell response to antigens

(A) Splenic NKT cells from C57BL/6 (*n*=7), Nur77ΔN^{tg} (*n*=11), and Nur77ΔN^{tg};Jα18^{0} (*n*=6) mice were identified as CD3ε^{+}tetramer^{+} cells within electronically gated CD8^{LO} thymocytes or B220^{LO} splenocytes. Numbers are % of NKT cells among total mononuclear leukocytes within each organ. Total splenocytes from mice in **A** were cultured 5 days with titrated amounts αGalCer **(B).** Using ELISA, IFN-γ secreted into the supernatant was measured. Data are representative of 4 independent experiments; *n* as in **A**.

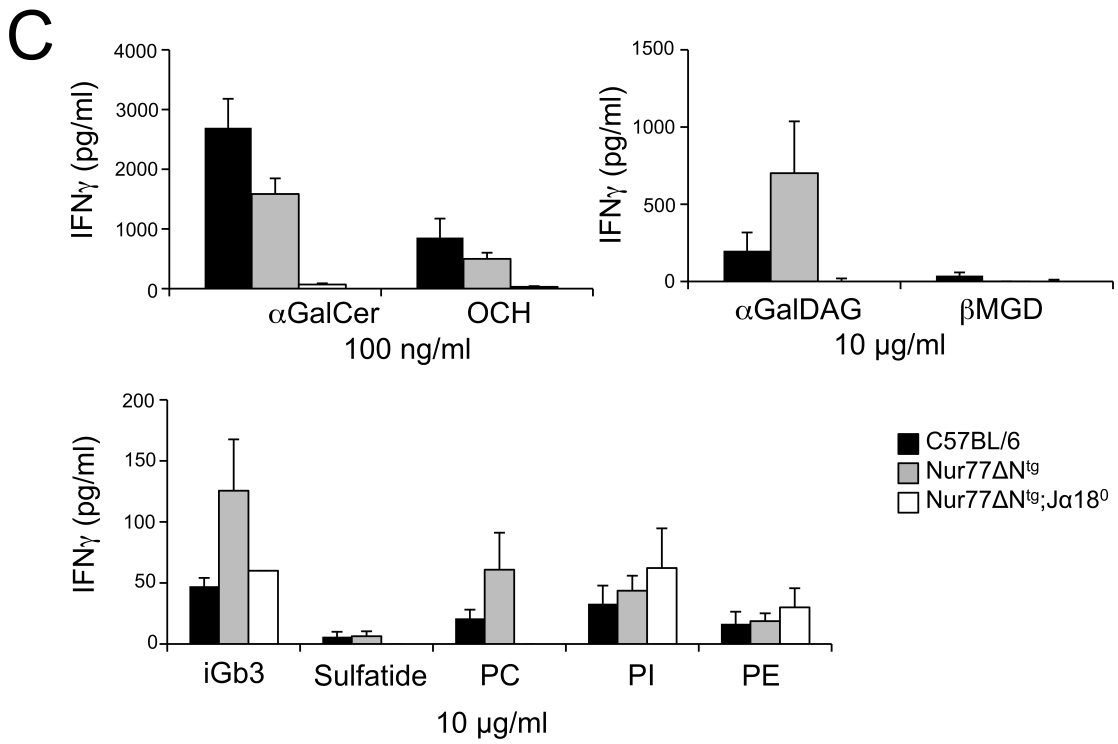

Figure 2-12, continued. Defective Nur77 expression alters *in vitro* NKT cell response to antigens

Total splenocytes from mice in **A** were cultured 5 days with indicated lipids.
(C) Using ELISA, IFN-γ secreted into the supernatant was measured. Data are representative of 4 independent experiments; *n* as in **A**.

Since αGalCer is an extremely potent NKT cell antigen, any variation in reactivity might be difficult to detect due to the robustness of the response. Therefore, we reasoned that weaker NKT cell lipid agonists might allow a better assessment of NKT cell responses in Nur77ΔN^{tg} mice. Thus, a panel of lipids composed of an αGalCer variant (OCH), a known microbial glycolipid ligand (αGalDAG), the putative selecting antigen (iGb3), and a number of self lipids (sulfatide, PtdCho, PtdIno, and PtdEtN) were used in preliminary experiments to stimulate C57BL/6 and Nur77ΔN^{tg} NKT cells in vitro (Fig. 2-12C). αGalCer and OCH elicited slightly lower IFN-γ response from Nur77ΔN^{tg} splenocytes when compared to C57BL/6 cells (Fig. 3-12C). Nonetheless, the weaker agonists such as iGb3 and αGalDAG elicited higher IFN-γ response from Nur77ΔN^{tg} splenocytes when compared to C57BL/6 cells (Fig. 2-12C) despite the reduced numbers of NKT cells in Nur77ΔN^{tg} splenocytes (Fig. 2-9). Additionally, the self-lipid PtdCho elicited a slightly increased IFN-γ response within Nur77ΔN^{tg} but not C57BL/6 cultures (Fig. 2-12C). Thus, negative selection of NKT cells does moderately impact reactivity to self lipid agonists. One caveat of this analysis is that it uses all known NKT cell agonists and those were discovered by studying already selected NKT cell repertoire of wild type mice. Hence, it would be interesting to test in the future the more unbiased panel of cellular lipids using either splenocytes of the NKT cell clones generated from Nur77ΔN^{tg} mice to identify any previously unanticipated NKT cell specificities.

An NKT cell response can be assessed both by measuring the robustness of secreted cytokines and by following the kinetics of cytokine response. Upon in vivo stimulation with αGalCer, NKT cells rapidly secrete IL-4, which peaks within 2 hours, followed by IFN-γ and the down regulation of the TCR (Bendelac et al., 2007). Therefore, in vivo splenic and hepatic NKT cell responses in C57BL/6 and Nur77ΔN^{tg} mice were assessed at 2 and 4 hours post αGalCer injection. TCR down-regulation was delayed beyond 4 hours in hepatic NKT cells of Nur77ΔN^{tg} mice whereas splenic NKTCR down regulation was the same in both strains (Fig. 2-13A). Robust IFN-γ response was elicited from both splenic and hepatic NKT cells at 2 hours in C57BL/6 and Nur77ΔN^{tg} mice (Fig. 2-13B). At 4 hours, IFN-γ response begins to wane in livers of the C57BL/6 mice but still remains on-going in liver of Nur77ΔN^{tg} (Fig.2-13B). IL-4 response was the same in both strains in both organs (Fig.2-13B). These functional data indicate that Nur77ΔN expression affects hepatic NKT cell function. Whether this reflects altered NKTCR repertoire or intrinsic role of Nur77 in hepatic NKT cells requires further investigation.

DISCUSSION

Here we provide evidence for the role of Nur77 in mediating negative selection during NKT cell development. First, overexpression of Nur77 results in the massive apoptosis of NKT cells as well as CD4, CD8 and DP thymocytes, all of which could be rescued by overexpression of the anti-apoptotic protein Bcl-x_L.

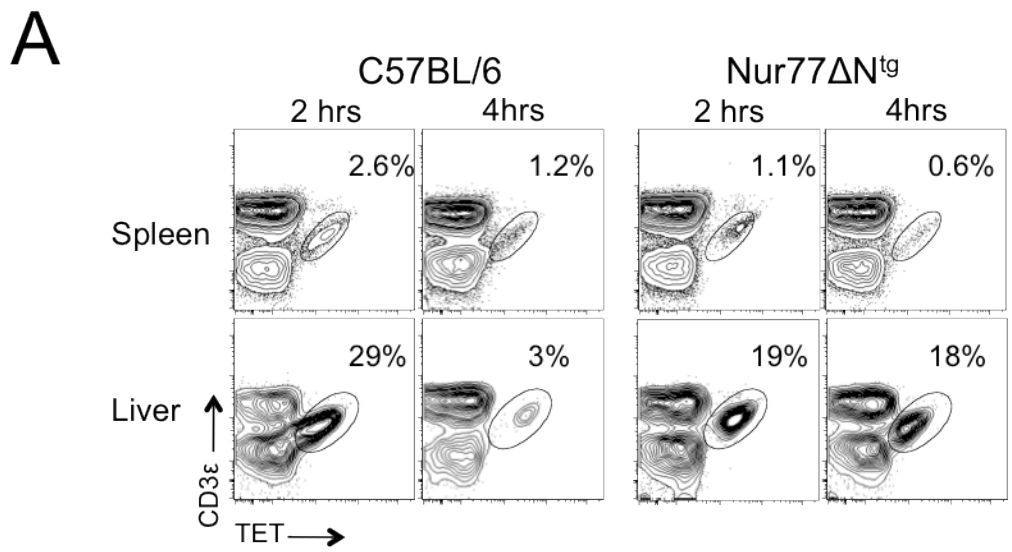

Figure 2-13. Comparable in vivo functional NKT cell response in C57BL/6 and Nur77 defective mice

C57BL/6 (*n*=4) and Nur77ΔN^{tg} (*n*=4) mice were injected i.p. with 5 μg αGalCer (open) or vehicle (shaded). After 2 and 4 hrs, splenic and hepatic NKT (B220^{LO}CD3ε^{+}tetramer^{+}) cells were electronically gated **(A).**

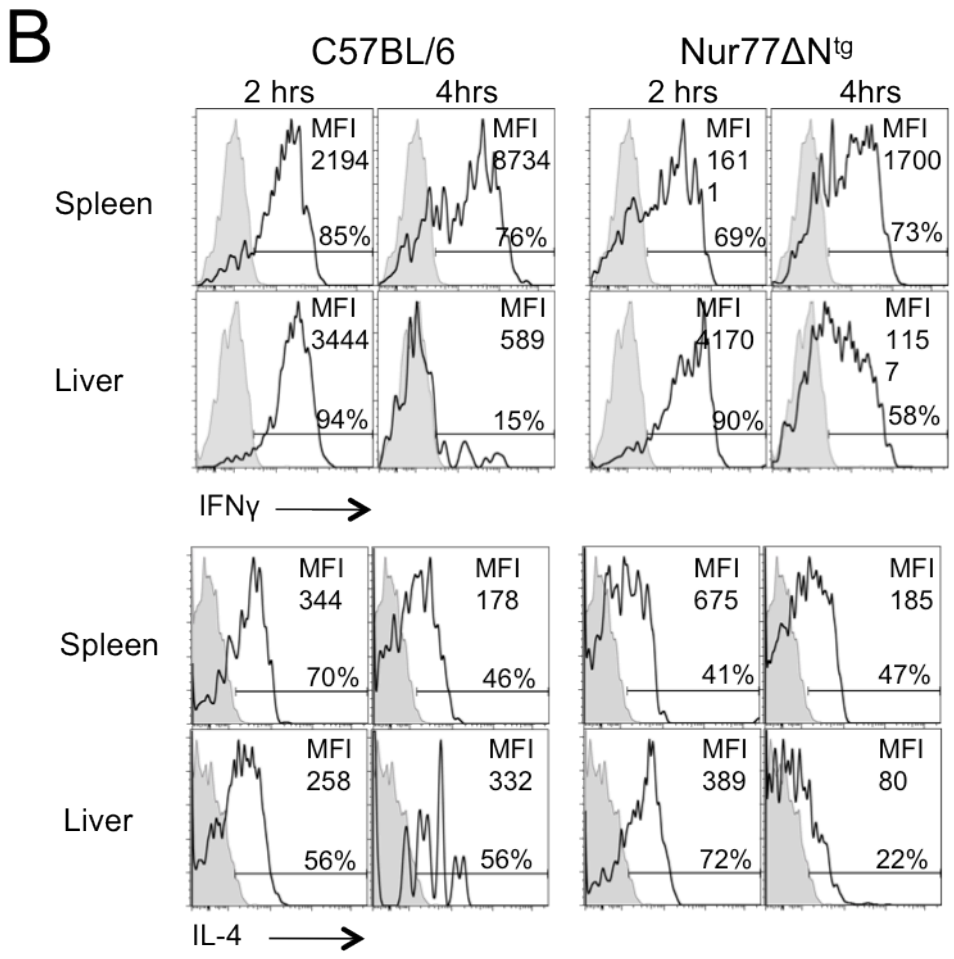

Figure 2-13, continued. Comparable in vivo functional NKT cell response in C57BL/6 and Nur77 defective mice

(B) Intracellular IL-4 and IFN-γ expression within gated NKT cells in **A**. Numbers refer to ΔMFI and % of NKT cells. Data are representative of 2 independent experiments.

Second, positive selection precedes negative selection in NKT cells and hence play dominant role in shaping NKT cell Vβ repertoire. Inhibition of Nur77-mediated negative selection, results in the alteration of CDR3β sequences in NKTCR and reveals increased TCR *Jβ1*-cluster usage over *Jβ2*-cluster, which is predominantly used by C57BL/6 NKT cells. Preliminary analyses revealed that this subtle alteration in NKTCR does not affect recognition of high affinity NKT antigens but does increase reactivity to the weaker self-lipid ligands. From these data we propose that Nur77 induces negative selection of NKT cells during thymic development, and that negative selection, together with positive selection, sculpts the NKT cell repertoire and, thereby, impacts their function.

In this study we re-generated two previously described mouse models used to over-induce ($Nur77^{tg}$) or to suppress ($Nur77\Delta N^{tg}$) negative selection of developing thymocytes (Calnan et al., 1995). As was seen with conventional T cells, we discovered dramatic loss of NKT cells in $Nur77^{tg}$ mice. We investigated three possible mechanisms to explain the loss of NKT cells in these mice: a defect in positive selection owing to decreased DP thymocytes, which mediate this process; a DP thymocyte intrinsic impairment in the rearrangement of the canonical *Vβ14*-to-*Jβ18* segments; and a defect in NKT cell survival. Two experiments ruled out the role of a DP cell defect in the loss of NKT cells. First, $Nur77^{tg}$ DP thymocytes were equally capable of stimulating NKT cell hybridomas, which are sensitive to the purported positively selecting endogenous lipid antigen, ruling out a defect in positive selection of NKT cells in $Nur77^{tg}$ mice. Second, we found that the DP thymocytes did not rearrange the canonical *Vβ14*-

to-*Jβ18* segments. Nonetheless, complementation of this defect by the introgression of a rearranged *Vα14Jα18* transgene into Nur77^{tg} mice failed to rescue NKT cell development. Hence, the lack of NKT cells in Nur77^{tg} mice was not due to the inability of DP cells to make the necessary TCR rearrangements. Finally, introgression of the Bcl-x_L transgene into Nur77^{tg} mice partially rescued NKT cell development within Nur77^{tg} mice, indicating a role of Nur77 in inducing NKT cell death. From these results we conclude that Nur77 mediates negative selection of NKT cells, just like it does in conventional CD4 and CD8 T cells.

Mice in which negative selection was blocked (Nur77ΔN^{tg} mice) developed NKT cells, but their number was somewhat reduced in the spleen and liver. One possible explanation for the low peripheral NKT cell number could be that negative selection may not play a major role in shaping the NKT cell ontogeny. This however, would be inconsistent with the data discussed above. Therefore, an alternative explanation might be an incomplete block of Nur77 function in the Nur77ΔN^{tg} mouse line used in this study. Although this line expresses the highest level of Nur77ΔN^{tg} among the three founder lines generated, other parts of Nur77 that were not deleted in the dominant negative mutant might play a role in mediating negative selection. A number of studies have implicated the Nur77 transactivation domain in mediating negative selection induced apoptosis (Kuang et al., 1999; Rajpal et al., 2003). Therefore, the deletion of this domain from Nur77, as in the Nur77ΔN transgene used in this study, should have blocked negative selection. However, one study has shown that the binding of Nur77 to Bcl-2 and the consequent conversion of the anti-apoptotic Bcl-2 to a proapoptotic

form requires the C-terminal ligand binding domain of Nur77 (Thompson et al., 2010; Thompson and Winoto, 2008). The dominant negative Nur77 transgene encodes a protein that lacks the transactivation domain but contains the C-terminal domain. It is unclear whether such a mutant would be able to convert the anti-apoptotic to pro-apoptotic Bcl-2, and whether this part of Nur77 function would or not require an intact transactivation domain. Based on these reports, we predict that the Nur77ΔN transgene, as it still contains the Bcl-2 binding C-terminal domain may largely but not completely block all pathways leading to negative selection. This therefore, results in a milder phenotype such that some developing NKT cells continue to undergo negative selection. The role that the C-terminal domain plays in negative selection of NKT cells and shaping the NKT cell repertoire will be an area for future research.

When does positive and negative selection of NKT cells occur? Previous studies have suggested that during NKT cell development there is a defined period of susceptibility to negative selection. Both the addition of αGalCer to foetal thymic organ culture (FTOC) at later stages of culture and intrathymic injection of adult mice with αGalCer do not result in the depletion of NKT cells, raising the question as to which development stage do NKT cells undergo negative selection (Pellicci et al., 2003). Conventional T cells are sensitive to negative selection as long as they are in a semi-immature state (HSA^{HI}). Previous reports have shown that an immature population of NKT cells that were HSA^{HI} also expressed Nur77, suggesting that negative selection occurs during a very early stage of NKT cell development (Moran et al., 2011; Stanic et al., 2004a). In

agreement with this report is the finding that the residual NKT cells which develop in Nur77^{tg};Vα14^{tg} are blocked at the immature CD44^{LOW}NK1.1^{LOW} ST1. This suggests that NKT cells undergo negative selection at very early stage in development. Additionally, analysis of CD1d-TD^{KI};Nur77ΔN^{tg} revealed a complete absence of NKT cells despite a block of negative selection, indicating that positive selection (which is altered in CD1d-TD^{KI} mice) occurs before negative selection within NKT cells.

NKT cells have a very limited TCR Vβ repertoire. A number of studies have implicated positive selection as the sole process by which the NKT cell repertoire is selected (Mallevaey et al., 2009; Pellicci et al., 2009; Wei et al., 2006). The role of negative selection however, has been much less clear. Analysis of Nur77ΔN^{tg} mice revealed that TCR Vβ usage in NKT cells is very similar to C57BL/6 mice. This is consistent with our data suggesting that positive selection precedes negative selection and with published data suggesting that positive selection actually shapes Vβ usage in NKT cells. A previous study has shown that the CDR2β loop in the NKTCR is responsible for CD1d/glycolipid recognition and in particular for strong recognition by Vβ8.2, Vβ7, and Vβ2 (Florence et al., 2009; Gui et al., 2001; Mallevaey et al., 2009). Mallevaey et al. (2009) study also found that CDR3β could play a role in increasing or decreasing the affinity of NKTCR/CD1d/glycolipid interactions. Thus, we decided to look at whether Nur77ΔN^{tg} NKT cells expressed altered CDR3β compared to C57BL/6.

The junctions of V-D-J rearrangements codes for the CDR3β region of the TCR. Whereas C57BL/6 NKT cells predominately use the *Jβ2*-cluster for this

rearrangement, Nur77ΔN^{tg} NKT cells retained the usage of *Jβ1*-cluster for this purpose. Though limited by a small sample size, the data here suggests that negative selection also impacts NKT cell repertoire, although apparently in a more subtle way than positive selection does. A major limitation to these studies is the assumption that NKT cells rescued from negative selection will also be reactive to tetrameric CD1d-αGalCer that was used to sort and analyse cells in these experiments. Future studies involving the use of tetramers of CD1d loaded with endogenous lipid ligands will be important for teasing out additional populations of NKT cells not detected with tetrameric CD1d-αGalCer.

The role of negative selection is to remove highly self-reactive T cells from the repertoire. Thus, by blocking negative selection, one would expect to find altered antigen reactivity within the emerging T cell pool. In vitro stimulation studies revealed an increased response to αGalDAG and modestly increased, but nonetheless, significantly higher response to iGb3 and PtdCho by Nur77ΔN^{tg} NKT cells when compared to C57BL/6 NKT cells. This increased reactivity is not the result of overt sensitivity of Nur77ΔN^{tg} NKT cells to lipids caused by the expression of the mutant transcription factor, as reactivity to αGalCer and OCH was not increased when compared to C57BL/6 NKT cell response. In vivo stimulation resulted in persistent hepatic NKT cell response in Nur77ΔN^{tg} mice compared to the response in C57BL/6 mice. Additional experiments will be required to determine if this is due to a delay in activation or reflects the prolonged responsive state of Nur77ΔN^{tg} NKT cells.

Altered reactivity, especially increased response to a pathogen derived lipid antigen such as *Borrelia burgdorferi*-derived αGalDAG can have deleterious effects. The role of NKT cells in the immune system is generally one of protection from pathogens and autoimmune disease. However, NKT cells have also been found to have detrimental affects during immune responses to pathogens such as *Salmonella enterica* and Sendai virus (Tupin et al., 2007) and in exacerbating autoimmune diseases such as rheumatoid arthritis and primary biliary cirrhosis (Wu and Van Kaer, 2009). Thus, NKT cells' potential to induce detrimental cytokine storm by rapidly and robustly secreting cytokines has to be kept in check. Therefore, negative selection is an important mechanism of central tolerance that is accomplished during NKT cell development.

In conclusion, NKT cells undergo Nur77 mediated negative selection during development. While positive selection broadly shapes the NKT cell repertoire, negative selection fine-tunes this repertoire. A properly shaped repertoire is important for the necessary and appropriate immune responses initiated by NKT cells.

CHAPTER III

IL-15 REGULATES HOMEOSTASIS AND TERMINAL MATURATION OF NKT CELLS

ABSTRACT

Semi-invariant NKT cells are thymus-derived innate lymphocytes that modulate microbial and tumor immunity as well as autoimmune diseases. These immunoregulatory properties of NKT cells are acquired during their development. Much has been learnt regarding the molecular and cellular cues that promote NKT cell development, yet how these cells are maintained in the thymus and the periphery and how they acquire functional competence are incompletely understood. We found that IL-15 induced several Bcl-2 family survival factors in thymic and splenic NKT cells in vitro. Yet, IL15-mediated thymic and peripheral NKT cell survival critically depended on Bcl-x_L expression. Additionally, IL-15 regulated thymic developmental stage 2 (ST2) to ST3 lineage progression and terminal NKT cell differentiation. Global gene expression analyses and validation revealed that IL-15 regulated *Tbx21* (T-bet) expression in thymic NKT cells. The loss of IL-15 also resulted in poor expression of key effector molecules such as IFN-γ, granzyme A and C as well as several NK cell receptors in NKT cells. Strikingly, the maturation of $CD44^+NK1^-$ st2 precursors to st3 $CD44^+NK1^+$ NKT cells was essential for protecting mice from the lethal disease caused by *Francisella tularensis*. Taken together, our findings reveal a critical role for IL-15

in NKT cell survival, which is mediated by Bcl-x_L, and effector differentiation, which is consistent with a role of T-bet in regulating terminal maturation, and protection from runaway inflammation caused by a lethal bacterial infection

INTRODUCTION

IL-15 is a pleiotropic cytokine that regulates the development and maintenance of several subsets of innate lymphocytes, including $\gamma\delta$ T, CD8$\alpha\alpha$ T, NK and NKT cells (Ma et al., 2006). Furthermore, IL-15 signals the ontogeny, effector differentiation and Mcl-1-dependent survival of NK cells (Huntington et al., 2007). Moreover, thymic and peripheral NKT cells develop poorly in IL-15-deficient (IL-15^0) mice (Matsuda et al., 2002). In the periphery, this is due to impaired NKT cell homeostatic proliferation (Matsuda et al., 2002). In the thymus, NKT cell proliferation appears intact, yet IL-15^0 mice develop a severe blockade in NKT cell ontogeny at ST2, with leaky progression to ST3 (Matsuda et al., 2002). What role IL-15 signals play during thymic NKT cell ontogeny and whether IL-15 is essential for NKT cell functional maturation in the periphery remain unknown.

Here we provide evidence that thymic and peripheral NKT cell survival critically depends on IL-15. One important downstream target of IL-15 appears to be Bcl-x_L. Furthermore, we describe a new function for IL-15 by which it regulates ST2 to ST3 lineage progression and terminal NKT cell maturation, which is consistent with a role of T-bet in regulating ST2 to ST3 transition and terminal differentiation. Strikingly, IL15-dependent terminal maturation was essential for

mice to survive *Francisella tularensis* subsp. novicida (*Ft* novicida) and *F. tularensis* subsp. holartica-derived live vaccine strain (LVS) infection.

RESULTS

IL-15 induces Bcl-2 family survival factors within thymic but not peripheral NKT cells

Previous reports demonstrated that NKT cell frequency is significantly lower in mice lacking IL-15 compared to wild type mice due to altered NKT cell homeostasis within the thymus and spleen (Kennedy et al., 2000; Matsuda et al., 2002). Whilst IL-15 regulates proliferation of splenic NKT cells, its role in homeostasis of the thymic subset has remained unclear (Matsuda et al., 2002). A re-evaluation confirmed that NKT cell frequency was altered in the absence of IL-15 and, hence, their numbers were reduced in the thymus, spleen and liver (Fig. 3-1A). Likewise, in vivo BrdU incorporation experiments revealed that splenic but not thymic NKT cell proliferation was impaired in IL-15^0 mice (Fig. 3-1B). These data indicate that, in addition to its role in cell proliferation, IL-15 plays another role(s) during thymic NKT cell ontogeny.

Previous studies have suggested that IL-15 induces anti-apoptotic Bcl-2 family members, including Bcl-2, Bcl-x_L and Mcl-1, to prevent apoptosis and to regulate homeostasis in vivo (Ma et al., 2006). For example, IL-15 promotes the survival of NK cells by inducing the survival factor Mcl-1 (Huntington et al., 2007). An examination of the expression of the Bcl-2 family of survival factors by flow

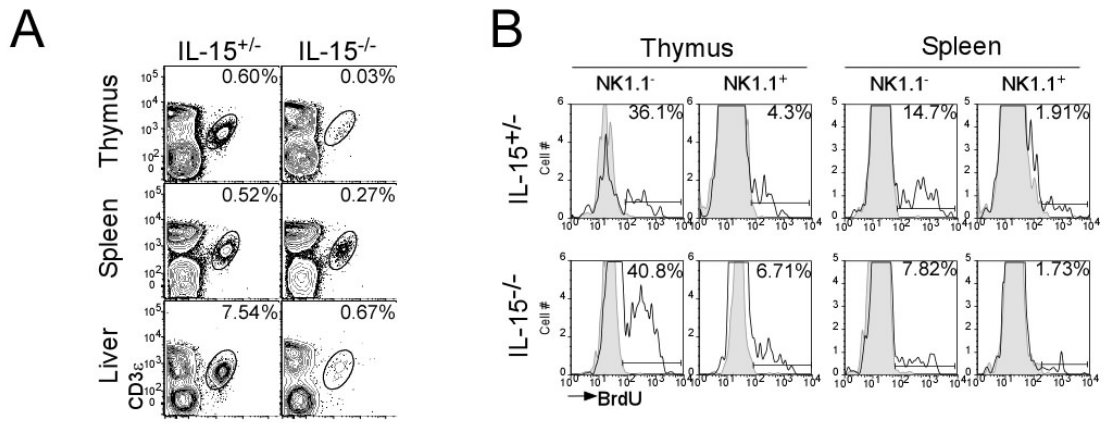

Figure 3-1. Defective NKT cell development and maintenance in IL-15^0 mice

(A) Thymic, splenic and hepatic NKT cells from C57BL/6 (*n*=13) and B6-IL-15^0 (*n*=9) mice were identified as CD3ε$^+$tetramer$^+$ cells within electronically gated CD8^{LO} thymic, B220^{LO} splenic or liver mononuclear cells (MNCs). Numbers are % NKT cells among total leukocytes within each organ. Data are representative of 9 independent experiments.

(B) C57BL/6 and IL-15^0 mice were injected i.p. with 2 mg BrdU daily for three consecutive days and sacrificed one day later. BrdU incorporation was determined by flow cytometry after extracellular lineage specific staining and intracellular labeling with anti-BrdU Alexa-647 mAb. Overlaid histograms are of NKT cells identified as in **A** from vehicle (shaded) or BrdU injected (open) mice. The histograms show the expression levels of BrdU within NK1.1^{NEG} (left) and NK1.1$^+$ (Gadola et al., 2006a) NKT cells within the thymus and spleen. Data are representative of 3 independent experiments; *n*=6.

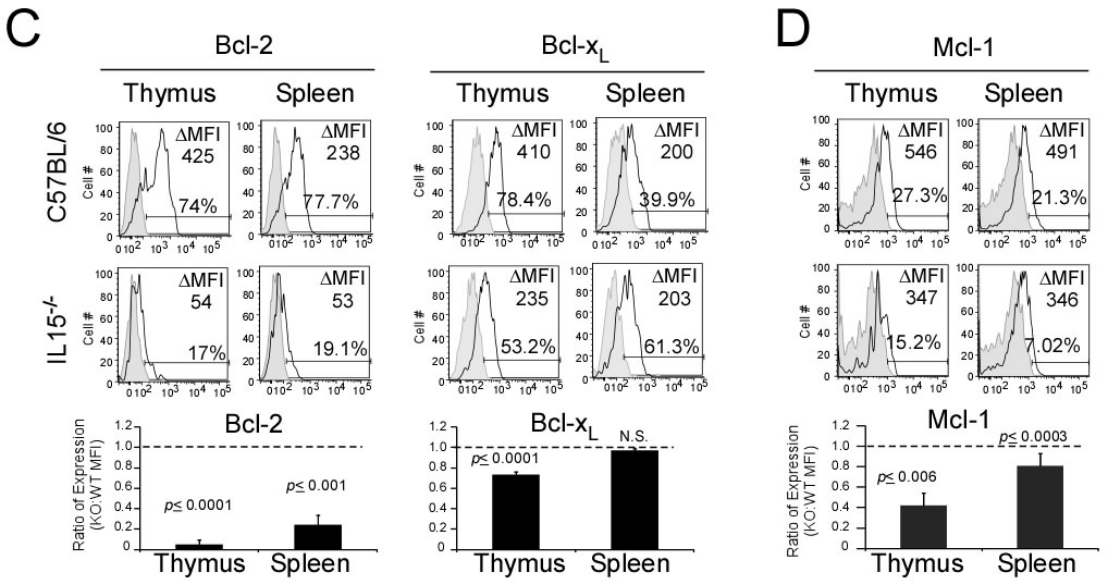

Figure 3-1, continued: Defective NKT cell development and maintenance in IL-15^0 mice

(C&D) Thymic and splenic MNCs from C57BL/6 and B6-IL-15^0 mice were assessed for intracellular expression of Bcl-2, Bcl-x$_L$ (**C**) and Mcl-1 (**D**), detected with specific mAb within electronically gated B220^{LO}CD3ε$^+$tetramer$^+$ cells. Numbers refer to the difference in mean fluorescence intensity (ΔMFI) between isotype control (shaded) and specific mAb (open) staining. Data are representative of 3 independent experiments; *n=5*. The flow data were acquired on two different instruments (FACSCalibur and LSR-II) in different experiments. Though the actual mean fluorescence intensity varied, the represented trend remained the same. Therefore, we have chosen to represent the ratio of expression between wild type and IL-15^0 NKT cells. The ratio of Bcl-2, Bcl-x$_L$ and Mcl-1 expression by IL-15^0 and wild type NKT cells is shown. A ratio of ~1 indicates no difference in expression; a ratio <1 indicates lower expression in IL-15^0 NKT cells.

cytometry revealed that intracellular Bcl-2 expression was dramatically reduced in IL-15^0 thymic and splenic NKT cells (Fig. 3-1C). Although not as dramatic, intracellular Bcl-x_L and Mcl-1 expression levels were also reduced either in thymic (Bcl-x_L) or in both thymic and splenic (Mcl-1) IL-15^0 NKT cells when compared with wild type NKT cells (Fig. 3-1C,D).

To test whether IL-15 induces survival factors in NKT cells, wild type thymocytes and splenocytes were cultivated in the absence or presence of exogenous rhIL-15 for 5 days and Bcl-2, Bcl-x_L and Mcl-1 expression in fresh or cultivated NKT cells (with or without rhIL-15) was evaluated using flow cytometry. Both fresh NKT cells and those cultivated without rhIL-15 were included as controls because expression of these survival factors changes during the 5d culture. The data revealed that IL-15 up-regulated the expression of Bcl-2 and Bcl-x_L but not Mcl-1 in thymic NKT cells to levels above those expressed by freshly isolated NKT cells (Fig. 3-2A,B). Very few NKT cells cultivated without IL-15 expressed the three survival factors and, hence, when compared to this control, IL-15 also appeared to induce Mcl-1 expression in thymic NKT cells (Fig. 3-2B). IL-15 also modestly induced Bcl-2 and Bcl-x_L expression within splenic NKT cells but not to the levels found in freshly isolated NKT cells; their expression was above control NKT cells cultured in medium without rhIL-15 (Fig. 3-2A,B). These data indicate that IL-15 has the potential to induce or maintain the expression of survival factors of the Bcl-2 family in thymic or splenic NKT cells, respectively, and, hence, to support NKT cell survival during development.

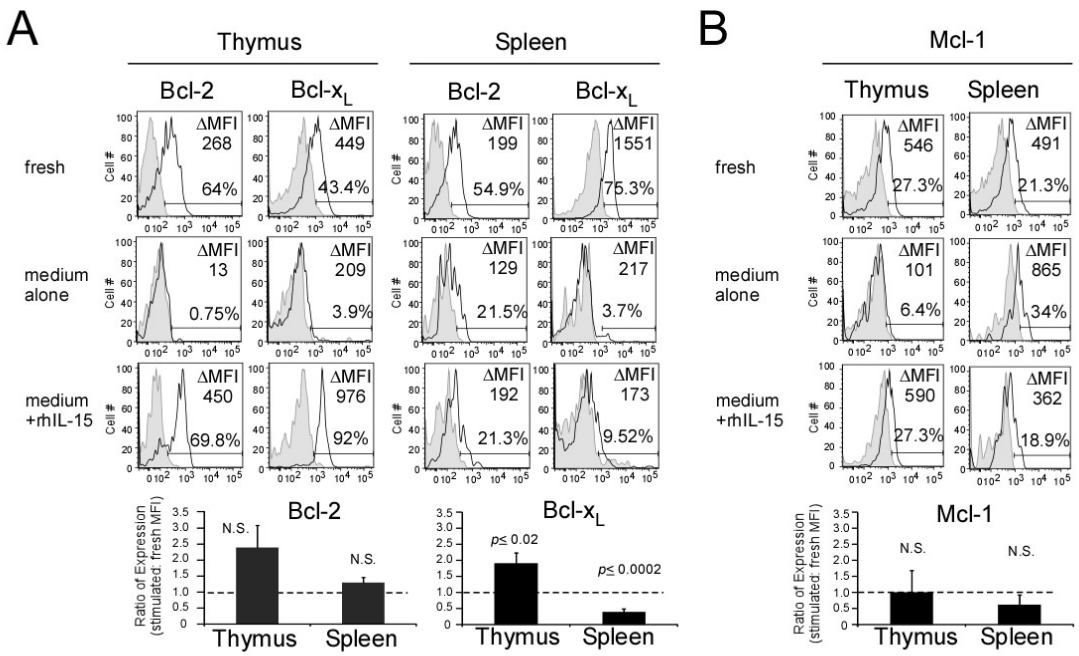

Figure 3-2. IL-15 up-regulates expression of the survival factors Bcl-2, Bcl-x_L, and Mcl-1 within thymic and splenic NKT cells

Thymic and splenic MNCs from C57BL/6 mice were cultivated in vitro in the absence or presence of 100 ng/mL of rhIL-15. After 5 days, intracellular expression of **(A)** Bcl-2, Bcl-x_L and **(B)** Mcl-1 was detected with specific mAb within electronically gated $B220^{LO}CD3\varepsilon^{+}$tetramer^{+} cells. Numbers refer to the difference in mean fluorescence intensity (ΔMFI) between isotype control (shaded) and specific mAb (open). Data are representative of 3 independent experiments, *n=5*. As for Figure 1, the flow data were acquired on two different instruments in different experiments. Hence, the ratio of IL-15-induced Bcl-2, Bcl-x_L and Mcl-1 expression NKT cells in comparison to un-stimulated, freshly isolated NKT cells is shown. A ratio of $\leq$1 indicates no induction; a ratio >1 indicates IL-15-induced expression.

Bcl-x_L over expression in IL-15^0 mice supports NKT cell survival

We took a genetic approach to further investigate the role of IL-15-induced genes in the survival of thymic and peripheral NKT cells. Thus, *Bcl-2* and *Bcl-xl* transgenes were independently introgressed into IL-15^0 mice. Analysis of the resulting mice at age 6—8 wks, when thymic and splenic cellularity is similar between the different strains, revealed that enforced Bcl-x_L but not Bcl-2 over expression rescued the frequency and absolute numbers of thymic, splenic and hepatic NKT cells in IL-15^0 mice (Fig. 2-3A,B).

Because the *Bcl2* (*Ig*μ) and *Bclxl* (p*Lck*) transgenes are under the control of different promoters (Chao et al., 1995; Strasser et al., 1991), we assessed the expression patterns of both transgenes within different thymocyte subsets. The data revealed that both transgenes were expressed as early as the $CD4^-8^-$ double negative stage of development, through the DP stage, and within CD4 and CD8 single positive thymocytes (Fig. 3-3C). Consistent with Bcl-2 expression during early thymocyte development, *Bcl-2* transgene introgression into IL-7 receptor-α null mice, which poorly if at all develop conventional T and NKT cells (Boesteanu et al., 1997; Peschon et al., 1994), rescued the development of both lineages (Fig. 3-3D). Therefore, the failure of Bcl-2 over expression to restore NKT cell numbers in IL-15^0 mice was not due to the lack of proper transgene expression or functionality, but most likely due to the fact that Bcl-2 plays a minor role when compared to Bcl-x_L in conveying IL-15 signals for NKT cell survival. Together, the above data indicate that IL-15 relays specific, Bcl-x_L-dependent survival signals during NKT cell ontogeny.

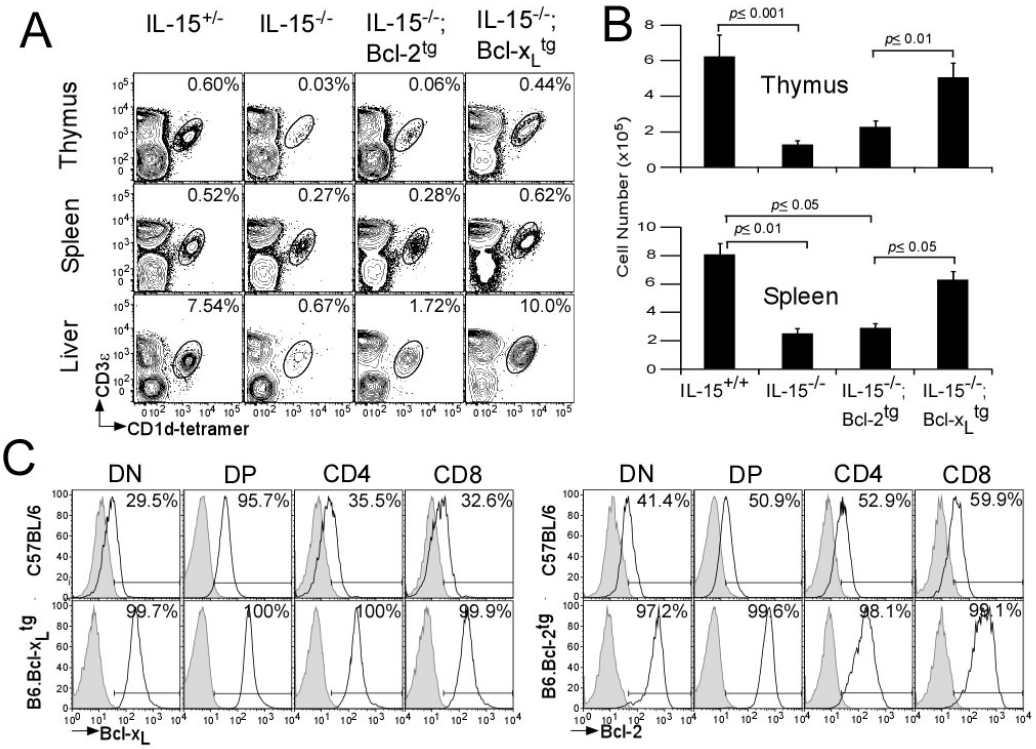

Figure 3-3. Bcl-x_L over expression restores NKT cell development in IL-15^0 mice

(A) Thymic, splenic and hepatic NKT cells from C57BL/6 (*n*=8), B6-IL-15^0 (*n*=10), B6-IL-15^0;Bcl-2^{tg} (*n*=6), and B6-IL-15^0;Bcl-$x_L{}^{tg}$ (*n*=16) mice were identified as $CD3\varepsilon^+$tetramer$^+$ cells within electronically gated $CD8^{LO}$ thymic, $B220^{LO}$ splenic or liver MNCs. Numbers are % NKT cells among total leukocytes.
(B) Absolute numbers of NKT cells in the thymus and spleen of C57BL/6, B6-IL-15^0, B6-IL-15^0;Bcl-2^{tg}, and B6-IL-15^0;Bcl-$x_L{}^{tg}$ mice were calculated from % NKT cells in **A** and total cell count. Data are representative of 6 independent experiments showing *n*, as in **A**. *p* value was calculated by one-way ANOVA with Tukey's post-test.
(C) Intracellular expression of the hBcl-x_L and hBcl-2 transgene within DN, DP, $CD4^+CD8^{NEG}$ and $CD8^+CD4^+$ thymocytes of B6.C-Bcl-$x_L{}^{tg}$ (right panels) and B6-Bcl-2^{tg} (left panels) mice. Over-laid histograms represent isotype control (shaded) and specific mAb (open). Data are representative of 3 independent experiments; *n*=5.

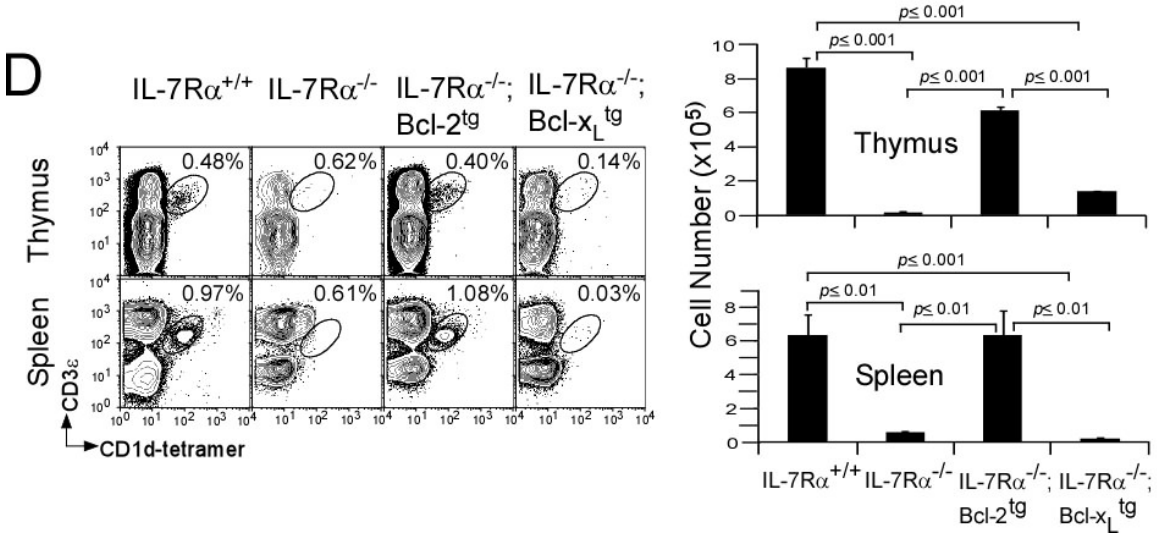

Figure 3-3, continued: Bcl-x_L over expression restores NKT cell development in IL-15^0 mice

(D) Thymic and splenic NKT cells from IL-7R$\alpha^{+/-}$ (*n*=3), IL-7Rα^0 (*n*=3), IL-7Rα^0;Bcl-2^{tg} (*n*=3) and IL-7Rα^0;Bcl-x_L^{tg} (*n*=2) mice were identified as CD3ε^+tetramer$^+$ cells within electronically gated $CD8^{LO}$ thymocytes or $B220^{LO}$ splenocytes and liver MNCs. Numbers are % NKT cells among total leukocytes. Absolute NKT cell number was calculated from % NKT cells and total MNC number. Data are representative of 2 independent experiments. Note that because IL-7Rα^0 thymic size is small due to low cellularity, % NKT cells appears artificially high despite extremely low NKT cell numbers. *P value* was calculated by one-way ANOVA with Tukey's post-test.

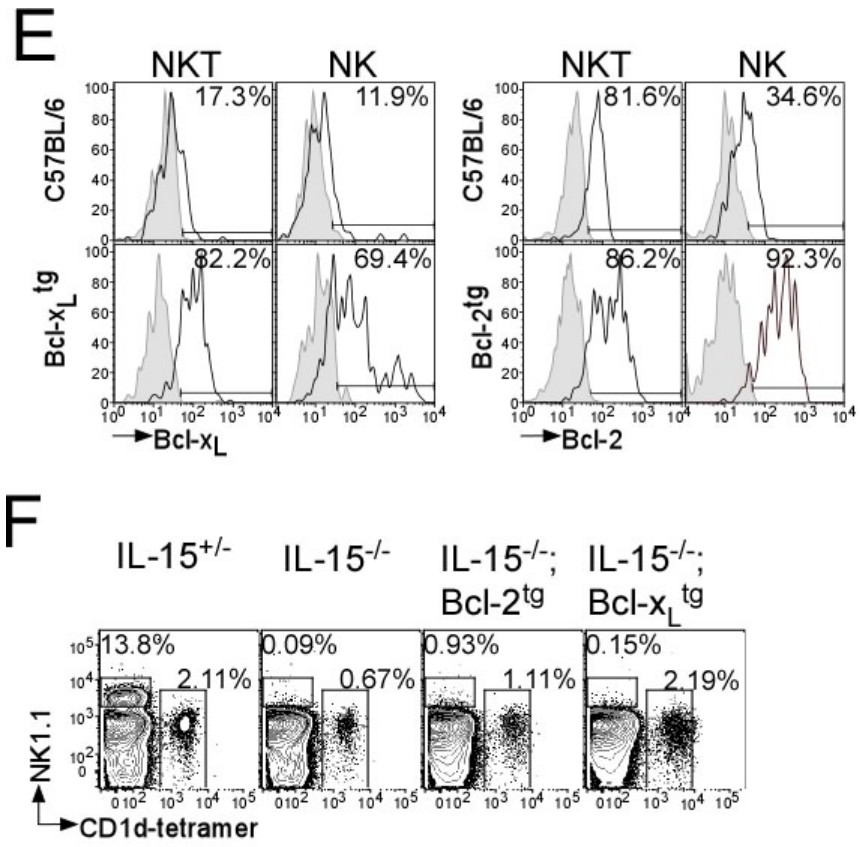

Figure 3-3, continued: Bcl-x_L over expression restores NKT cell development in IL-15^0 mice

(E) Intracellular expression of the hBcl-x_L and hBcl-2 transgenes within NKT and NK cells of B6.C-Bcl-x_L^{tg} and B6-Bcl-2^{tg} mice. Overlaid histograms represent isotype control (shaded) and specific mAb (open) staining. Data are representative of 2 independent experiments; *n* as in **C**.
(F) Splenic and hepatic NK and NKT cells from C57BL/6 (*n*=6), B6-IL-15^0 (*n*=7), B6-IL-15^0;Bcl-2^{tg} (*n*=4), and B6-IL-15^0;Bcl-x_L^{tg} (*n*=10) mice were identified as NK1.1^+tetramer^{NEG} and NK1.1^+tetramer$^+$ cells, respectively, within electronically gated B220^{LO} splenic or hepatic MNCs. Data are representative of 4 independent experiments.

A previous study reported that IL-15-induced Mcl-1 specifically supported NK cell survival in vivo and in vitro (Huntington et al., 2007) and that over expression of Bcl-2 in mice lacking IL-2Rβ—the common β-chain of IL-2 and IL-15 receptors—or in IL-15^0 mice repopulates NK cells in vivo (Minagawa et al., 2002; Nakazato et al., 2007). Because NKT and NK cells are closely related innate lymphocyte lineages and because both lineages use IL-15 for survival, we ascertained whether IL-15 induces survival of the two cell types by similar mechanism(s). This question was addressed because *Bcl-2* and *Bcl-x_L* transgenes were expressed in NK cells from B6-Bcl-2^{tg} and C-Bcl-$x_L{}^{tg}$ mice (Fig. 3-3E). We found that, as previously reported (Minagawa et al., 2002; Nakazato et al., 2007), Bcl-2 partially rescued hepatic but not splenic NK cells. Nonetheless, Bcl-x_L over expression rescued NKT but not hepatic or splenic NK cells in IL-15^0 mice (Fig. 3-3F), which is consistent with the reported model in which NK cells predominantly utilize Mcl-1 for IL-15-induced survival (Huntington et al., 2007). Thus, IL-15 appears to regulate survival of distinct lineages in a unique, cell type-specific manner, with Bcl-x_L serving as an IL-15-induced survival factor for NKT cells.

Because Bcl-x_L is required for DP thymocyte survival and *Vα14* to *Jα18* rearrangement (Bezbradica et al., 2005), it is possible that IL-15^0 DP thymocytes poorly rearrange these distal gene segments, thereby resulting in low NKT cell numbers. To test this, *Vα14* to *Jα18* rearrangement within DP thymocytes flow sorted from wild type, IL-15^0, Jα18^0 and CD1dTD—which rearrange *Vα14* to

Jα18 gene segments but are deficient in positive selection of NKT cells (Chiu et al., 2002) —mice was quantified. No defect in the canonical *Vα14* to *Jα18* rearrangement was seen in IL-15^0 DP thymocytes (Fig. 3-4). Likewise, the more distal *Vα8* to *Jα5* rearrangement was also unaffected in IL-15^0 DP thymocytes as gauged by non-quantitative PCR (Fig. 3-4B). Interestingly, however, ~1.5-fold higher *Vα14* to *Jα18* rearrangement was observed in DP thymocytes of IL-15^0;Bcl-x_L^{tg} mice (Fig. 3-4A), which was statistically insignificant. This result suggests that any increase in the initial pool of NKT cell precursors in DP thymocytes of IL-15^0;Bcl-x_L^{tg} mice less likely led to increased numbers of NKT cells in these mice.

IL-15 regulates terminal maturation of NKT cells

Because IL-15 deficiency reduced the numbers of thymic $CD44^+NK1.1^-$ ST2 and $CD44^+NK1.1^+$ ST3 NKT cells, and because forced Bcl-x_L over expression in IL-15^0 mice rescued total thymic and peripheral NKT cell numbers (Fig. 3-3), whether IL-15 has additional roles in NKT cell ontogeny was ascertained. Therefore, we determined whether IL-15 regulates terminal maturation of developing NKT cells as well, particularly at ST3 where NKT cells acquire most of their NK cell-like effector functions. Thus, the phenotype of IL-15^0;Bcl-x_L^{tg} NKT cells was compared to wild type and IL-15^0 NKT cells. Surprisingly, akin to IL-15^0

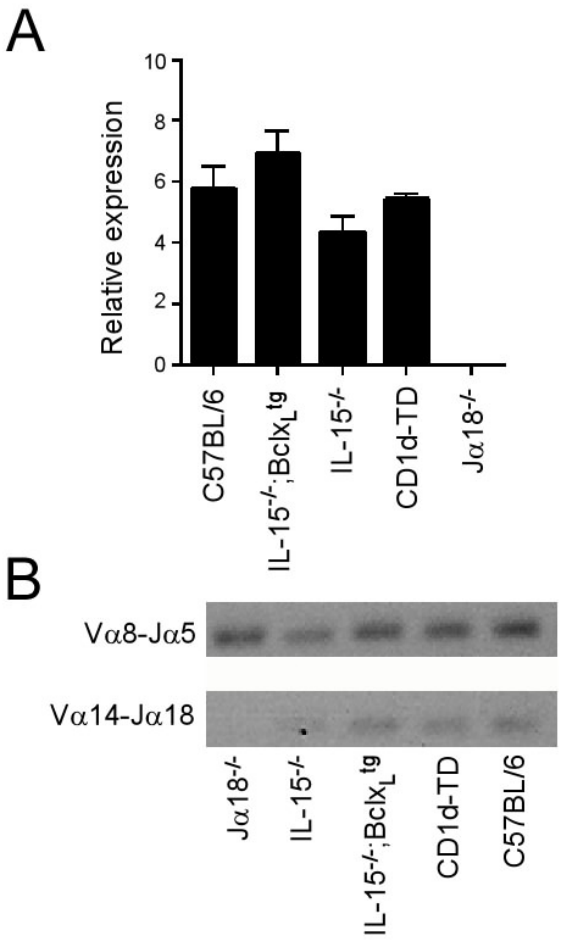

Figure 3-4. Normal TCRα rearrangement in IL-15^0 mice

(A) *Vα14*-to-*Jα18* rearrangement within DP thymocytes flow sorted from the indicated strains was assessed by real-time qPCR represented as mean±sd of 2 independent experiments. β-actin was used as the internal control for normalization. *p* value calculated by two-tailed, unpaired T-test indicated that *Vα14*-to-*Jα18* rearrangement in C57BL/6, B6-IL-15^0 and B6-IL-15^0;Bcl-x$_L^{tg}$ DP thymocytes was significant only when compared to that in B6-J18^0 DP cells. The ~1.5-fold increased *Vα14*-to-*Jα18* rearrangement seen in B6-IL-15^0;Bcl-x$_L^{tg}$ DP thymocytes compared to the others was statistically insignificant ($p \leq 0.0997$.
(B) RT-PCR assessment of *Vα8*-to-*Jα5* and *Vα14*-to-*Jα18* rearrangements. Data are representative of 2 experiments.

NKT cells, phenotypic ST2 to ST3 transition, as measured by acquisition of the NK1.1 surface marker was still partially impaired in IL-15^0;Bcl-$x_L{}^{tg}$ mice (Fig. 3-5A,B), despite near wild type numbers of NKT cells in these mice. Additional phenotypic analyses revealed that expression patterns of few other mature NKT cell markers such as NKG2D, Ly6C, CD69, and Ly49C/I reflected those of thymic NKT cells that were blocked at ST2 (Fig. 3-5C) as these markers are predominantly expressed by NK1.1^+ NKT cells (see Fig. 3-6A). Of those markers, the expression of Ly6C was also altered in hepatic, but not splenic NKT cells in IL-15^0 and IL-15^0;Bcl-$x_L{}^{tg}$ mice (Fig. 3-5C). Thus, IL-15 is required not only for lineage survival but also for terminal maturation of NKT cells, especially of the thymic subset. Furthermore, the differential requirement for IL-15 in terminal differentiation (e.g., acquisition of Ly6C, NK1.1) of some (thymic and/or hepatic) but not all (splenic) NKT cells suggests that distinct signals instruct NKT cell maturation in distinct lymphoid organs.

IL-15 regulates multiple gene expression changes during ST2 to ST3 NKT cell transition

To define the mechanism by which IL-15 regulates terminal maturation of thymic NKT cells, microarray experiments were performed. For this, wild type and IL-15^0 thymic NKT cells were flow sorted, and the derived RNA was subjected to hybridisation to a mouse microarray chip containing 60,000 genes; hybridisation was performed in duplicate (IL-15^0) or triplicate (wild type). The

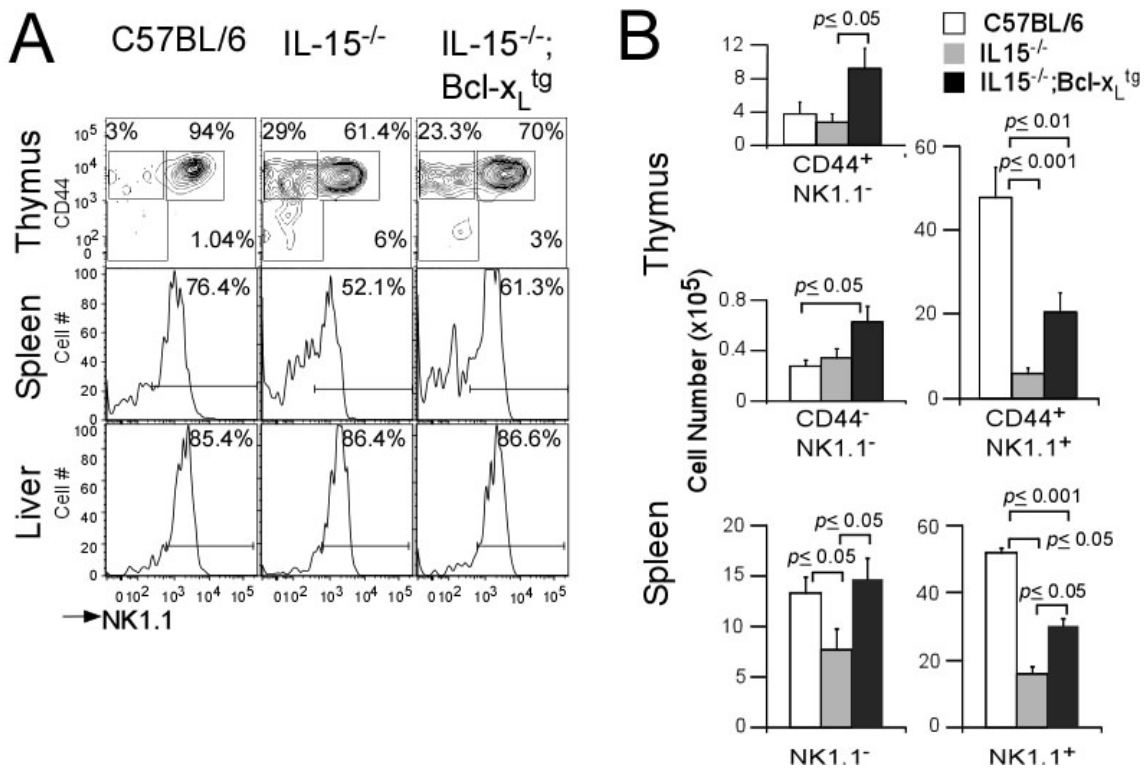

Figure 3-5. IL-15 regulates terminal maturation of NKT cells

(A) NKT cell developmental stages in C57BL/6 (*n*=9), B6-IL-15^{0} (*n*=6), and B6-IL-15^{0};Bcl-x$_{L}^{tg}$ (*n*=13) mice were identified as CD44^{NEG}NK1.1^{NEG} ST1, CD44^{+}NK1.1^{NEG} ST2, or CD44^{+}NK1.1^{+} ST3 in the thymus or as NK1.1^{NEG}tetramer^{+} or NK1.1^{+}tetramer^{+} within the splenic and hepatic MNCs. Numbers are % of cells among total NKT cells. Data are representative of 6 independent experiments.

(B) Absolute numbers of thymic NKT cells within ST1, ST2 and ST3 were calculated as in Fig. 3D. Data are representative of 6 independent experiments showing the *n*, same as in **A**. *p* value was calculated by one-way ANOVA with Tukey's post-test.

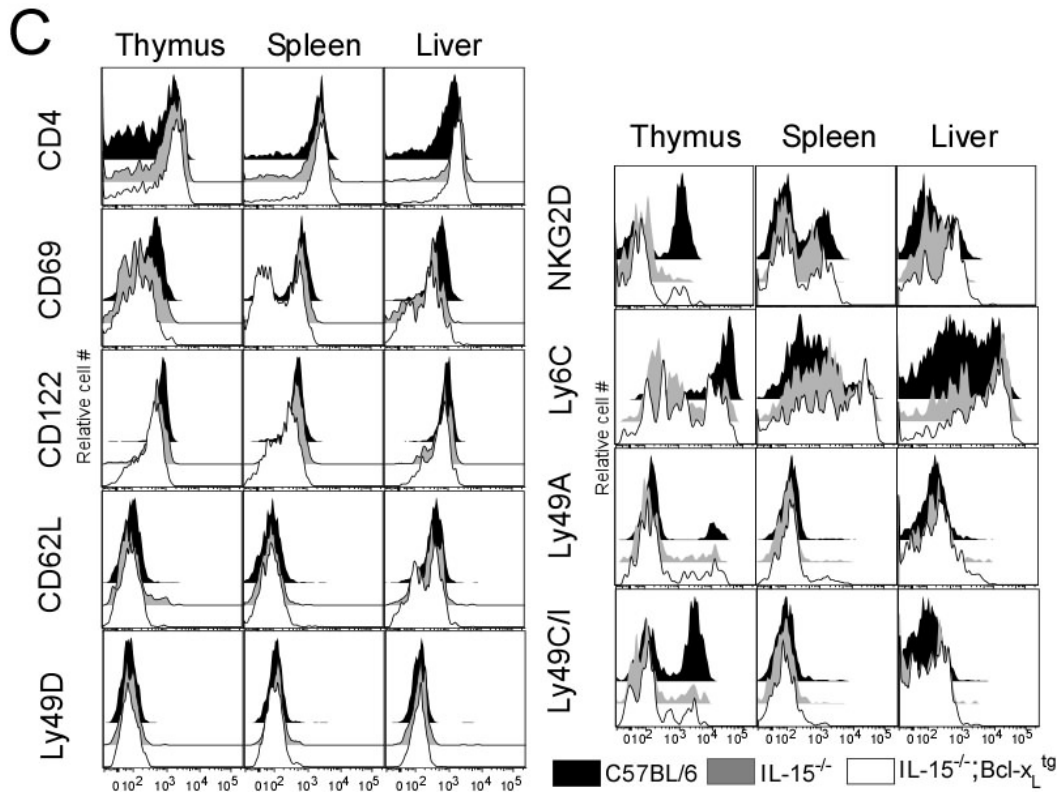

Figure 3-5 continued: IL-15 regulates terminal maturation of NKT cells

(C) Expression of lineage-specific markers by thymic, splenic, and hepatic NKT cells from C57BL/6 (*n*=6), B6-IL-15^{0} (*n*=6), and B6-IL-15^{0};Bcl-x_L^{tg} (*n*=6) mice as determined by flow cytometry after staining with specific mAb. Data are representative of 3 independent experiments.

microarray data are available at GEO (http://www.ncbi.nlm.nih.gov/geo/query/acc.cgi?token=dtgxpkoosiokmpm&acc=); accession number: GSE32568. Select genes differentially expressed (minimally $\log_2$ fold change >+1.5/<-1.5 and nominal *P*-value <0.001) in wild type and IL-15^0 NKT cells (Fig 3-6A) were then validated by quantitative (q), real-time PCR. We found that *Tbx21* (T-bet) was up-regulated in wild type NKT cells compared to IL-15^0 NKT cells (Fig. 3-6A,B). This finding is consistent with the previously reported IL-15-induced *Tbx21*-encoded T-bet expression in NKT cells in vitro (Townsend et al., 2004). Furthermore, multiple *Tbx21*-regulated genes —such as *Ifng*, *Gzma* (granzyme A), *Gzmc*, *Hopx* (homeobox domain only containing protein x), and several NK cell receptor genes: *Klra3* (NKG2E), *Klrb1c* (NK1.1), *Klrc1* (NKG2A/B), and *Klrk1* (NKG2D) (Matsuda et al., 2006; Townsend et al., 2004)— were up-regulated in wild type thymic NKT cells, which predominantly consists of ST3 NKT cells (Fig 3-6B). Consistent with the lack of intracellular Bcl-2 in IL-15^0 NKT cells (Fig. 3-1C), the *Bcl2* gene was poorly expressed in these cells (Fig. 3-6B). Conversely, *Zbtb16* (PLZF), *Tcf7* (TCF1) and *Rorc* (RORγt) genes, all signatures of ST1 and ST2 NKT cells were up-regulated in IL-15^0 thymic NKT cells (Fig. 3-6C), consistent with developmental arrest at ST2. Because T-bet is a critical regulator of differentiation in other lineages with cytotoxic properties (CTL and NK cells), our results are consistent with a role of *Tbx21* in regulating ST2 to ST3 transition.

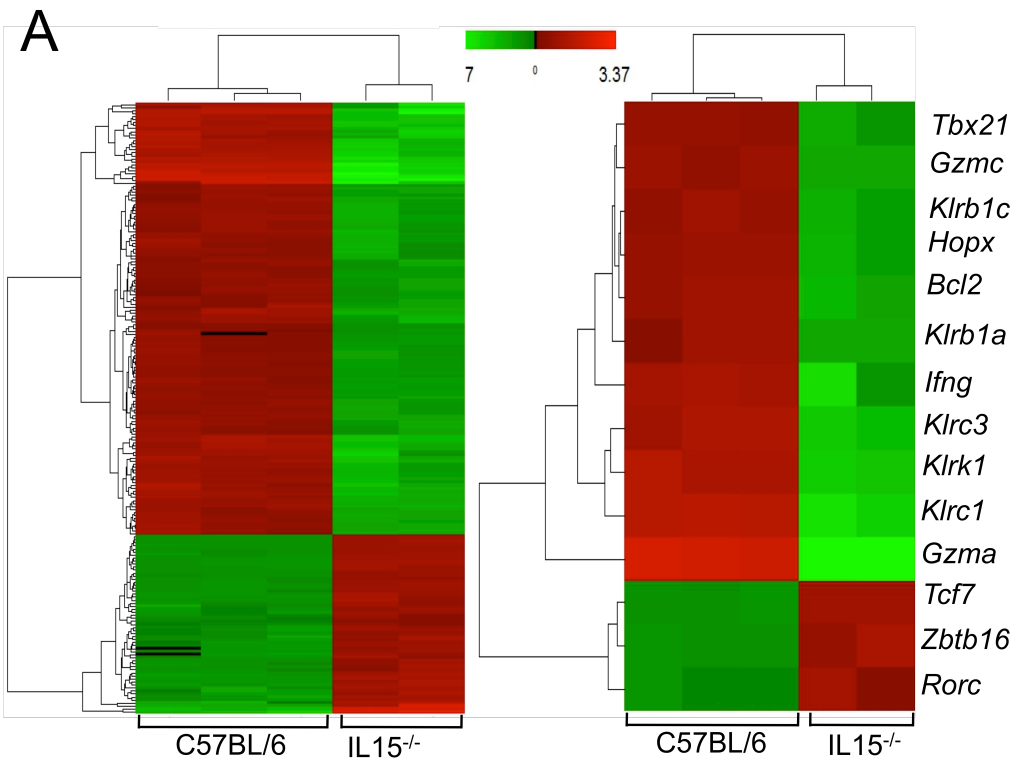

Figure 3-6. IL-15 induces *Tbx21* and T-bet-regulated genes in developing NKT cells

A. Cluster analysis of all genes differentially expressed in C57BL/6 (*n*=3) and IL-15^0 (*n*=2) NKT cells a microarray experiment. Differential expression was defined as those genes that showed $\log_2$ fold change ≥1.5/≤-1.5 with a nominal *p* value <0.001. The microarray data can be accessed at http://www.ncbi.nlm.nih.gov/geo/query/acc.cgi?token= dtgxpkoosiokmpm&acc= using the accession number GSE32568.

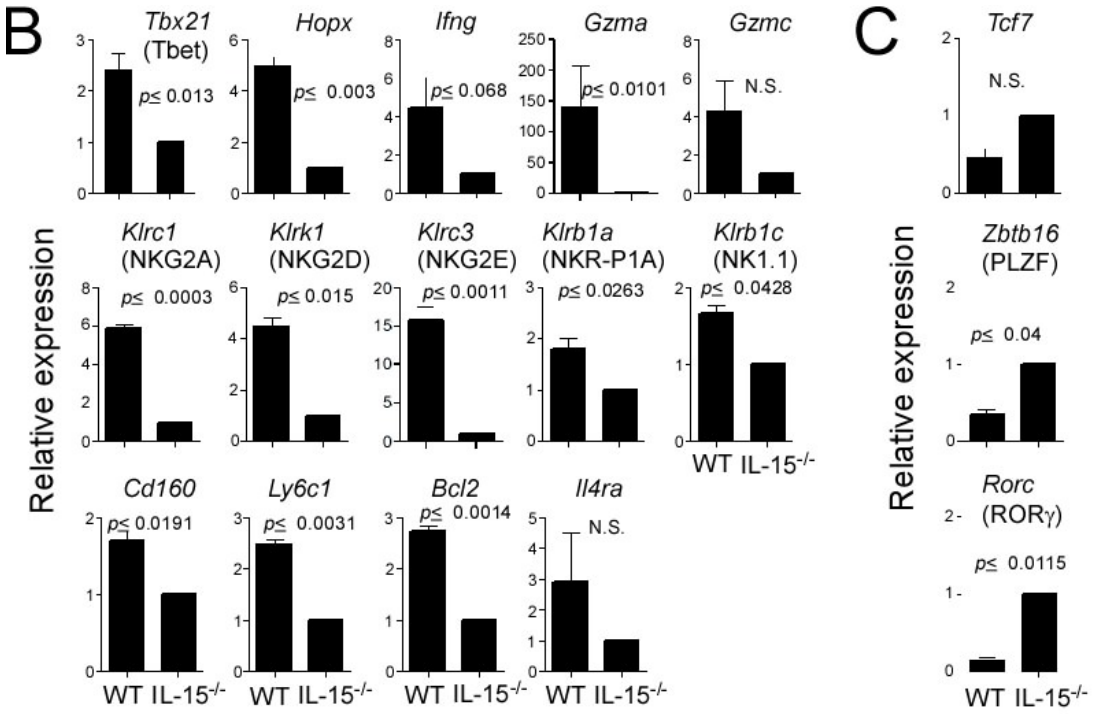

Figure 3-6 continued: IL-15 induces *Tbx21* and T-bet-regulated genes in developing NKT cells

B&C. Select differentially expressed genes identified in **A** were validated by qPCR using RNA isolated from flow sorted C57BL/6 and B6-IL-15^0 mice. Genes up-regulated in B6-derived thymic NKT cells (**B)** and genes up-regulated in B6-IL-15^0-derived NKT cells (**C**) are shown. β-actin was used to normalise expression levels. Data represent mean±sd of 2 independent experiments; each qPCR was performed in duplicate for an *n* value of 4 to calculate the *p* value by unpaired T test.

IL-15 regulates functional maturation of NKT cells

Terminally mature NKT cells produce the highest amounts of effector cytokines. Because phenotypically this subset of NKT cells appears impaired in IL-15^0 and IL-15^0;Bcl-x_L^{tg} mice, we determined whether they were functionally competent. For this purpose, the potent NKT cell ligand αGalCer (Kawano et al., 1997) was administered i.p. into IL-$15^{+/-}$, IL-15^0 and IL-15^0;Bcl-x_L^{tg} mice and 4 hrs later, intracellular and serum IL-4 and IFN-γ responses were monitored. Compared to IL-$15^{+/-}$ mice, significantly fewer splenic and hepatic NKT cells from IL-15^0 and IL-15^0;Bcl-x_L^{tg} mice expressed intracellular IL-4 and IFN-γ in response to in vivo stimulation (Fig. 3-7A,B). Furthermore, NKT cells that expressed IL-4 (splenic) and IFN-γ (splenic and hepatic) in IL-15^0 and IL-15^0;Bcl-x_L^{tg} mice, expressed these cytokines at significantly lower levels compared to those in IL-$15^{+/-}$ mice (Fig. 3-7A,B). Consistent with this expression pattern, the serum IFN-γ and IL-4 responses were also poor in IL-15^0 and IL-15^0;Bcl-x_L^{tg} mice compared to their IL-$15^{+/-}$ counterparts (Fig. 3-7C,D). Thus, IL-15 signalling is required for fully competent NKT cell responses in vivo.

IFN-γ and IL-4 responses by NKT cells require transcriptional regulation by T-bet and Gata-3 (Cen et al., 2009; Wang et al., 2006). T-bet is also required for the terminal maturation of thymic NKT cells, as T-bet deficiency blocked NKT cell ontogeny at the ST2 to ST3 transition (Townsend et al., 2004), similar to that seen with IL-15 deficiency (Fig. 3-5). Because *Tbx21* expression is reduced in IL-15^0 NKT cells and IL-15 induces *Tbx21* expression in NK cells in vitro (Townsend et al., 2004), we investigated whether impaired NKT cell function in IL-15^0 and

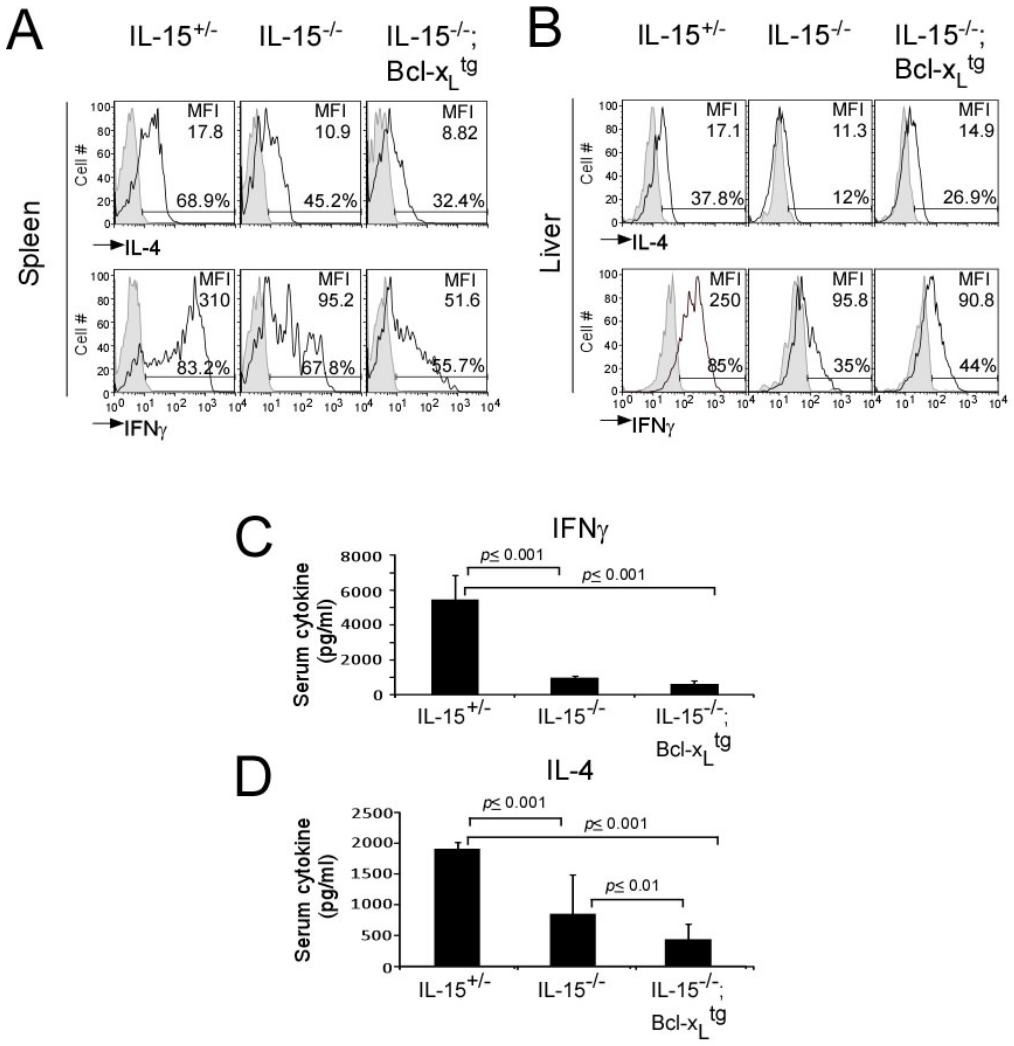

Figure 3-7. IL-15 regulates functional maturation of NKT cells

A&B. C57BL/6 (*n*=6), B6-IL-15^{0} (*n*=6), and B6-IL-15^{0};Bcl-x$_{L}^{tg}$ (*n*=12) mice were injected i.p. with 5 μg αGalCer (open) or vehicle (shaded). After 4 hrs, splenic (**A**) and hepatic (**B**) B220^{LO}CD3ε^{+}tetramer^{+} cells were electronically gated and intracellular IL-4 and IFN-γ expression was monitored. Numbers refer to ΔMFI. Data are representative of 4 independent experiments.

C&D. Using ELISA, serum IFN-γ **(C)** and IL-4 **(D)** responses to in vivo NKT cell stimulation in the above experiment were measured. *p* value was calculated by one-way ANOVA with Tukey's post-test.

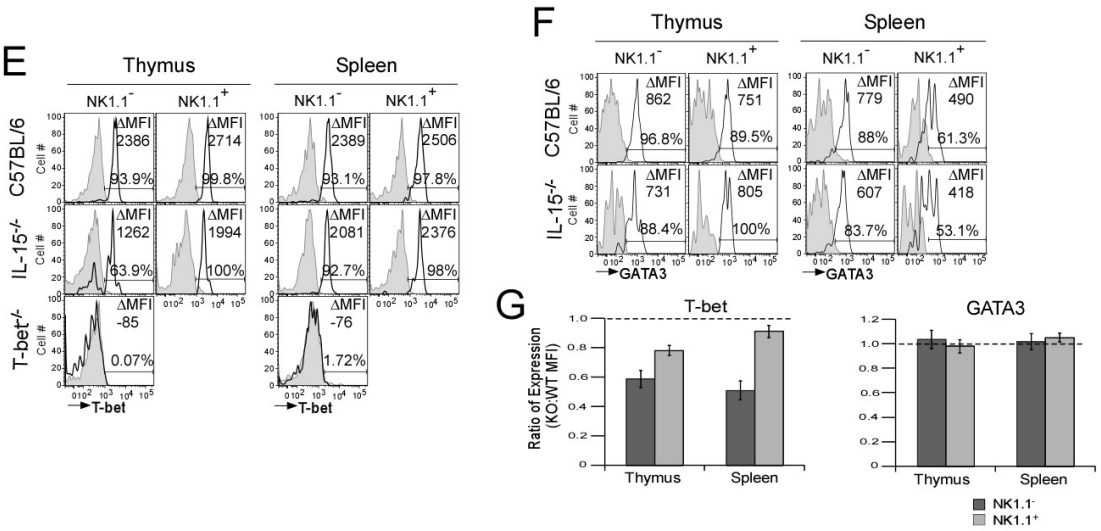

Figure 3-7 continued: IL-15 regulates functional maturation of NKT cells

E&F. Thymic and splenic MNCs from C57BL/6 and B6-IL-15^0 mice were analyzed for intracellular T-bet (**E**) and Gata-3 (**F**) expression within electronically gated CD8^{LO}CD3ε$^+$tetramer^0 thymocytes or B220^{LO}CD3ε$^+$tetramer$^+$ splenocytes. Numbers refer to the ΔMFI between isotype control (shaded) and specific mAb (open). Data are representative of 2 independent experiments; *n*=5.

(**G**) The ratio of T-bet and Gata-3 expression by IL-15^0 and wild type NKT cells is shown. A ratio of ~1 (e.g., Gata-3) indicates no difference in expression; a ratio <1 (e.g., T-bet) indicates lower expression in IL-15^0 NKT cells.

IL-15^0;Bcl-x_L^{tg} mice was due to altered levels of T-bet and Gata-3 expression. For this, thymic and splenic NK1.1^- and NK1.1^+ NKT cells from wild type and IL-15^0 mice were probed for intracellular expression of T-bet and Gata-3. We found that the level of T-bet expression was reduced by 30% (splenic) to 50% (thymic) in IL-15^0 compared to wild type NKT cells (Fig. 3-7E,G). Additionally, a slightly reduced percentage of thymic, but not splenic, NKT cells expressed T-bet in IL-15^0 mice. Similarly, intracellular Gata-3 expression was ~15—20% lower in thymic and splenic NK1.1^- NKT cells but about similar in NK1.1^+ NKT cells of IL-15^0 mice compared to their wild type counterparts (Fig. 3-7F,G), consistent with somewhat more preserved IL-4 production in IL-15^0 NKT cells when compared to IFN-γ response. In wild type NKT cells, Gata-3 expression level was constant, whilst T-bet levels increased with ST3 differentiation (Fig. 3-7G). Hence, the reduced T-bet expression (Fig. 3-7E) in IL-15^0 mice is consistent with reduced ST3 NKT cells in these mice. Thus, IL-15 signals are partially required for T-bet and Gata-3 expression in NKT cells and, possibly, for the robust IFN-γ and IL-4 cytokine responses seen in wild type but not in IL-15^0 and IL-15^0;Bcl-x_L^{tg} mice.

IL15-dependent NKT cell effector maturation is essential to survive lethal F. tularensis infection

If, as shown above, IL-15 deficiency results in a block in the development of functional NKT cells, IL-15^0 mice should be more susceptible to microbial infection that depends on NKT cells for protection. *Francisella tularensis (Ft)* subspecies tularensis—the causative agent of lethal tularaemia in humans—is a

Gram-negative bacterium that is easily bio-weaponized. IFN-γ and TNF-α are critical for protective, sterilizing immunity against *Ft.* Previously, the human live vaccine strain (LVS) derived from Ft spp. holarctica was shown to stimulate IFN-γ from $CD3^{+}NK1.1^{+}$ NKT cells (Fuller et al., 2006). Significantly, in pilot experiments, we found that both *Ft* novicida and LVS activated NKT cells and induced intracellular IFN-γ expression (Gilchuk,P., Spencer,C.T. and Joyce, S. unpublished data).

IL-15^{0} mice inoculated with either *Ft* novicida or LVS did indeed show a survival defect compared with wild type animals (Fig. 3-8A). As IL-15 deficiency also suppresses the development of NK cells—a major component of the innate response against microbes—Jα18^{0} mice, which specifically lack NKT but not NK cells, were similarly inoculated with these bacteria. IL-15^{0} mice yielded an almost identical survival curve as Jα18^{0} animals, suggesting that the susceptibility of IL-15^{0} mice to *Ft* novicida and LVS was due to the lack of functional NKT cells.

Infection of mice with other pathogens, such as *Sphingomonas* and *Ehrlichia,* results in a NKT cell-dependent release of cytokines including IFN-γ and protection from death (Kinjo et al., 2005; Mattner et al., 2005). To determine the role of NKT cells in protecting mice against lethal *Ft novicida and LVS* infection, the serum levels of three proinflammatory cytokines previously known to be critical for the control of Ft infection—IFN-γ, TNF-α and IL-6—was determined. We found that many more Jα18^{0} and IL-15^{0} mice secreted copious amounts of proinflammatory cytokines such as IFN-γ, TNF-α and IL-6 (Fig. 3-8B). This finding is consistent with the increased susceptibility of many more Jα18^{0}

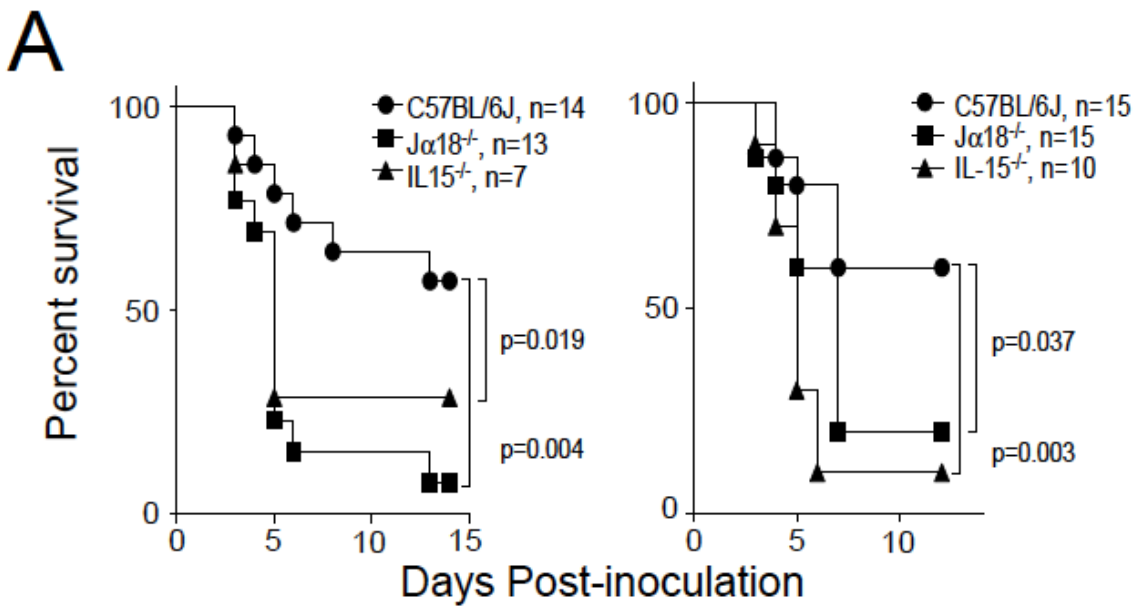

Figure 3-8. NKT cells are essential for tempering lethal disease caused by *Francisella infection*

(A) Kaplan-Meier plots detail the survival of C57BL/6 (*n*=14—15), B6-Jα18^0 (*n*=13—15) and B6-IL-15^0 (*n*=7—10) inoculated with 1 LD_{50} *Ft* spp. novicida (left) or LVS (Gadola et al.). Significance values were calculated by Mantel-Cox comparison of individual survival curves (*$p<0.04$; **$p<0.004$).

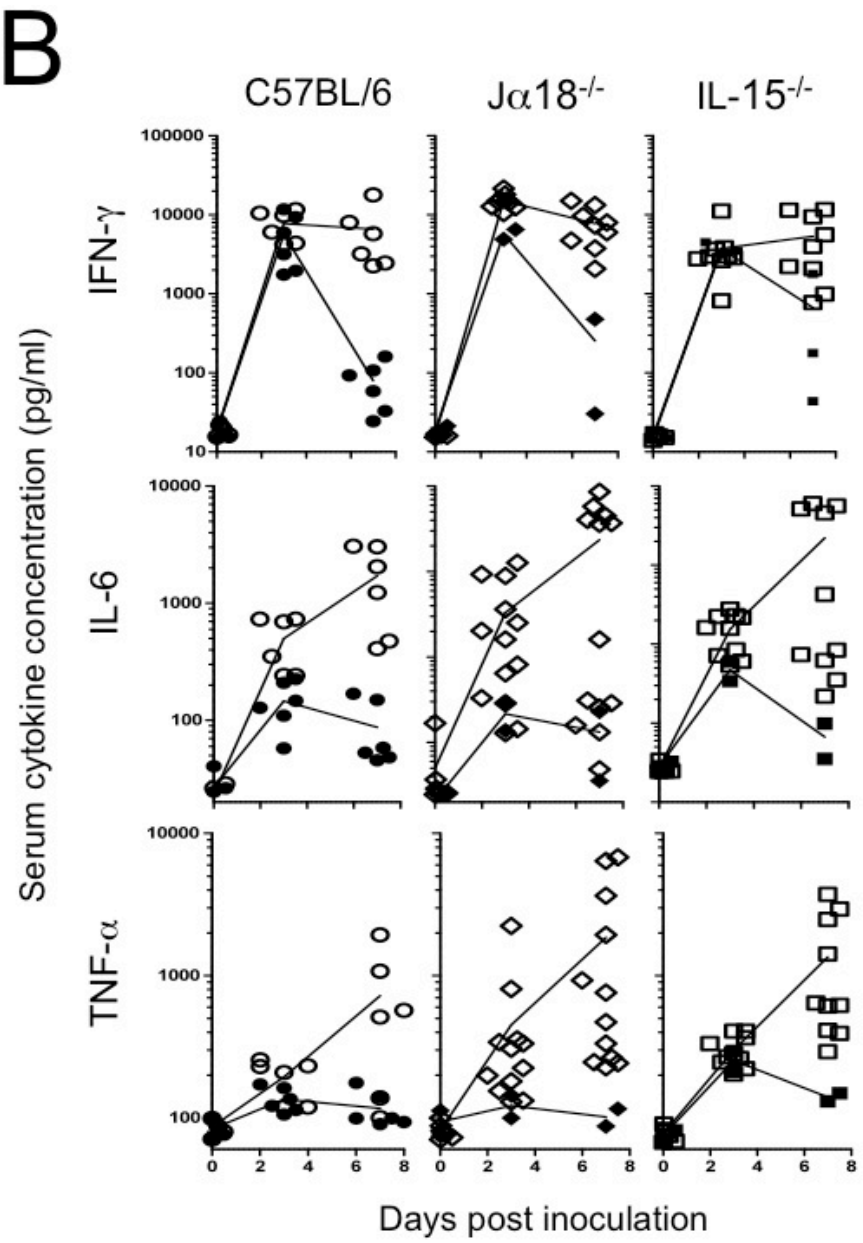

Figure 3-8, continued: NKT cells are essential for tempering lethal disease caused by *Francisella infection*

(B) Serum cytokine levels were measured by CBA assay and plotted according to whether the animals survived (solid symbols) or succumbed (open symbols) to the infection.

and IL-15^0 mice to infection when compared to wild type controls (Fig 3-8). Conversely, more wild type mice succeeded in tempering this cytokine storm and consequently survived the infection (Fig. 3-8). Taken together these data suggest that mice lacking NKT cells (J$\alpha 18^0$) or even just lacking the terminally differentiated st3 NKT cells (IL-15^0) are unable to control runaway inflammation and, hence, succumb to *Ft* novicida and LVS infection.

DISCUSSION

We describe three unique features of IL-15 that are essential for functional NKT cell development: One, it induces survival of thymic and peripheral NKT cells by regulating Bcl-x_L and Bcl-2 expression. Two, IL-15 regulates T-bet expression and signals ST3 NKT cell induction and differentiation. And three, it regulates effector differentiation that is consistent with the role of T-bet in this process. Fully differentiated functional NKT cells are essential for tempering runaway inflammation caused by *F. tularensis* infection. Thus, IL-15 plays a central role in NKT cell development and function.

It appears as though NKT cells narrowly escape death at each stage of their development: Immediately after positive selection they turn-on Nur77 expression in ST0 NKT cells (Moran et al., 2011), perhaps owing to high avidity interactions with their cognate ligand, viz., CD1d-self lipid complexes, addressed in Chapter II. In T cells, the transcription factor Nur77, in addition to inducing an apoptotic program, when targeted to the mitochondrion binds to the otherwise anti-

apoptotic factor Bcl-2, and by changing its conformation, converts it into a pro-apoptotic protein (Thompson et al., 2010). Therefore, onward development of NKT cells perhaps requires survival signal(s) to protect the lineage from death. We have identified one such survival signal to be IL-15. It induces both Bcl-2 and Bcl-x_L within thymic NKT cells in vitro. Yet, only genetic overexpression of Bcl-x_L but not Bcl-2 confers survival potential to ST1 and ST2, but not ST3, NKT cells. These data are consistent with a previous report showing that enforced Bcl-2 expression does not rescue NKT cell development in IL-15Rβ-null mice (Minagawa et al., 2002). A recent report suggested that forced Bcl-2 overexpression or introgression of Bim-deficiency modestly rescues NKT cell development in the IL-15-presenting IL-15Rα-null mice (Chang et al., 2011a). The differences in survival mechanisms in these three animal models currently remain unknown.

The global gene expression analysis of wild type and IL-15-deficient NKT cells, as well as our published data (Stanic et al., 2004a), indicate that ST3 but not ST0—2 NKT cells express high levels of Bcl-2. Hence, it is possible that Bcl-2 functions as an important survival factor only upon commitment and development into ST3 NKT cells. Because the ST3 NKT cells are absent in IL-15-, IL-15Rα- and IL-15Rβ-null mice, another factor must be necessary to support NKT cell survival up to this stage. Our data suggest Bcl-x_L provides that function. The failure of transgenic Bcl-2 to do so in this study perhaps reflects the need for an IL-15-induced, ST3-specific accessory factor to execute its function.

Previous studies have demonstrated that thymic and peripheral NKT cells represent distinct functional subsets (Berzins et al., 2006; McNab et al., 2005; McNab et al., 2007). The factor(s) that impacts differentiation of these two subsets remained incompletely defined. We found that most thymic NKT cells in IL-15^0;Bcl-$x_L{}^{tg}$ mice were blocked at the ST2-to-ST3 ontogenetic transition and lacked activation/memory marker expression as were IL-15^0 NKT cells. In striking contrast, splenic and hepatic NKT cells in IL-15^0 and IL-15^0;Bcl-$x_L{}^{tg}$ mice underwent almost complete phenotypic maturation, suggesting that developmental cues in the thymus and periphery are somewhat distinct. In contrast, gene expression analyses indicated reduced T-bet expression in both thymic and splenic NKT cells of IL-15^0 mice. T-bet was previously shown to regulate the ST2-to-ST3 NKT ontogenetic transition (Matsuda et al., 2006; Townsend et al., 2004). Thus, reduced T-bet expression is consistent with the ST2-to-ST3 developmental block in IL-15^0 NKT cells. Furthermore, low levels of T-bet may in part explain the poor expression of NK cell receptors as well as the deficiency in ST3-specific IFN-γ response in IL-15^0 mice. Taken together, we conclude that IL-15 differentially impacts central and peripheral NKT cell maturation in vivo.

It is noteworthy that T-bet belongs to a group of transcription factors whose functions are regulated not only by their presence or absence but also by absolute levels. An example of such regulation is seen in effector CD8 T cell fate determination via graded expression of T-bet (Joshi et al., 2007). Differentiation into effector and memory CD8 T cell fates was dictated by the levels of T-bet,

where high T-bet expression induced an effector cell fate, whilst lower T-bet level directed cells into the memory pool. Such a model would in principle be consistent with a past report (Chang et al., 2011a) and ours suggesting that partially reduced levels of T-bet expression in IL-15^0 mice could indeed significantly impair the NKT cell differentiation programme. Finally, because T-bet regulates expression of IL-15/IL-2Rβ (CD122) on NKT cells (this report and Matsuda et al., 2006), and therefore IL-15 responsiveness, the two factors (IL-15 and T-bet) generate a positive feedback regulatory loop. The property of all such loops is that small changes in gene expression are amplified by self-sustained and self-amplified system oscillation. Therefore, we predict that the reduced but not the complete absence of T-bet observed in IL-15^0 NKT cells may be sufficient to prevent complete effector differentiation.

The importance of NKT cell function(s) is implicated in multiple infectious diseases. However, their role is poorly defined. Because NKT cells acquire most of their NK cell-like properties at the last ST3 stage of their differentiation, and because IL-15 seems to regulate acquisition of these properties, we speculated that IL-15-encoded NKT cell functions are important in controlling in vivo responses to infections. IL-15^0 mice, which have deficits in NKT cell effector differentiation, provide a model to ascertain how NKT cells regulate immunity to infectious diseases. This study revealed that protection from the mouse and human pathogen *Ft* novicida and LVS, respectively, critically depended on NKT cells in general and on IL-15-regulated NKT cell functions in particular. Thus, many more IL-15^0 mice than wild type mice succumbed to both *F. tularensis*

infections owing to defective NKT cell effector differentiation. Further analyses revealed that all the mice that succumbed to *F. tularensis* infection also secreted very high proinflammatory serum cytokines. Because the bacterial load in the lung and liver of IL-15^0 mice was not higher than wild type animals (Spencer, C.T., and Joyce, S., unpublished data), we conclude that NKT cells play very little role in regulating bacterial clearance but play a critical role in tempering runaway inflammation caused by *F. tularensis* infection and/or increasing host tolerance to an on-going inflammation. This will be an exciting area for future investigations.

In conclusion, IL-15 functions by supporting survival of developing NKT cells and perhaps by inducing *Tbx21* expression as an ST3-specific differentiation factor in NKT cells. NKT cells share this feature with NK cells and T cells, and are expected to collaborate with these lineages in executing *Tbx21*-induced functions in vivo. Fully mature NKT cells function to temper runaway inflammation caused by certain bacterial infections that cause lethal disease in humans.

CHAPTER IV

CONCLUSION AND FUTURE DIRECTIONS

NKT cells develop in the thymus from common precursors that give rise to conventional T cells. Commitment to the NKT cell lineage occurs at the DP stage where their ontogenetic program diverges from that of conventional CD4 and CD8 T cells (Bezbradica et al., 2005; Egawa et al., 2005). Soon after commitment, NKT cells are positively selected by interactions with DP thymocytes through the semi-invariant TCR and CD1d-self lipid ligand(s) (Bendelac et al., 1995; Xu et al., 2003). It is currently thought that positive selection alone sculpts the semi-invariant NKT cell repertoire. Nonetheless, several groups have reported that negative selection can also contribute to the development of a function NKT cell repertoire (Chun et al., 2003; Pellicci et al., 2003). These conclusions were predicated on indirect experimental approaches to evaluate the role of positive and negative selection processes in sculpting the NKT cell repertoire. And as such, the question had remained whether NKT cell precursors underwent negative selection and what impact this process had on NKT cell biology. Shortly after the selection process, this lineage undergoes a series of progressive maturation steps that culminate in effector differentiation. The signals and how they are integrated during NKT cell effector differentiation had remained ill-defined. I have answered these two critical questions in NKT cell biology in an effort to advance the field.

To directly address whether NKT cells undergo negative selection, I re-generated and then investigated a previously described mouse model in which thymocytes are forced to undergo negative selection. In this model, Nur77, which is induced transiently in wild type thymocytes undergoing negative selection, is expressed constitutively as a transgene within developing T cells such that signalling through the TCR results in apoptotic cell death (Calnan et al., 1995). I chose this model because a prior study from our group found that Nur77 was expressed in a subset of immature ST0 ($CD24^{HI}CD44^{NEG}NK1.1^{NEG}$)/ST1 ($CD44^{NEG}NK1.1^{NEG}$) NKT cells which were particularly enriched in NFκB signalling deficient mice due to their failure to induce survival signal and therefore progress further through the ontogeny. As a consequence, the thymus, spleen and liver of these mice did not contain NKT cells (Stanic et al., 2004a). Investigations of many strains of mice that I generated during the course of this study revealed the role for Nur77 in negative selection of NKT cells. The most compelling evidence that NKT cells undergo negative selection came when I introgressed a fully rearranged *Vα14Jα18* transgene into the $Nur77^{tg}$ mouse. The doubly transgenic mice developed very few NKT cells compared to *Vα14Jα18* TCR transgenic mice. Those few escapees NKT cells that developed in the doubly transgenic mice were arrested at the $CD44^{NEG}NK1.1^{NEG}$ stage (ST0/1) although some had progressed to the $CD44^{NEG}NK1.1^{NEG}$ (ST2) and relatively fewer to the $CD44^{NEG}NK1.1^{NEG}$ (ST3) stages.

In additional studies using another mouse model in which thymocytes were protected from negative selection, I addressed the impact of negative selection on NKT cell biology. These studies involving the mutant Nur77ΔN^{tg} mice revealed differences in NKTCR repertoire and function. Nonetheless, the observed differences were subtle and, hence, these findings did not conclusively reveal a significant impact of negative selection on NKT cell biology, at least not as tested using currently known NKT cell antigens. I propose that the unique, rearranged TCR β-chain genes be cloned from wild type and Nur77ΔN^{tg} mice. When introduced into wild type mice, TCR β-chain genes isolated from Nur77ΔN^{tg} mice would be expected to undergo negative selection; hence, NKT cells bearing the introduced TCR β-chain will not develop. In contrast, the same TCR β-chain when introduced into Nur77ΔN^{tg} mice will generate NKT cells expressing that TCR. If they do, then the functional consequence of expressing the NKTCR that would otherwise be negatively selected in wild type mice can be interrogated. Such questions as,

a. whether novel NKT cell agonists are recognized by the Nur77ΔN^{tg} NKT cells;

b. whether the novel NKT cells confer protective advantage to microbial or parasitic pathogens; and

c. whether the new mouse strain develops autoimmune diseases and, if so, which organs are affected?

should be interrogated.

The most significant advance I made is related to understanding what cytokine signals induce NKT cell effector differentiation and how these signals are integrated to instruct this process. Our group had previously demonstrated that IL-15-deficient mice poorly developed mature ST3 ($CD44^{HI}NK1.1^{+}$) T cells in the thymus (Kennedy et al., 2000). Studies from other groups had indicated that IL-15-deficient peripheral, splenic and hepatic NKT cells had proliferative defects and, hence, affected NKT cell homeostasis in the peripheral lymphoid organs (Chang et al., 2011a; Matsuda et al., 2002; Ranson et al., 2003; Wu et al., 2008). The role of IL-15 in the thymus had remained undefined, however. Thus I discovered that the introgression of the human Bcl-x_L transgene into the IL-15-null mice increased NKT cell frequency and number in the thymus and the periphery. This result indicated that IL-15 provides a survival signal to developing NKT cells. How this survival signal(s) is relayed within NKT cell, and who delivers it, currently remains undefined. The survival issue is an important question in NKT cell biology because both their selection and peripheral functions are driven by the recognition of self lipid ligands, which would normally in other cell lineages (B or T) result in elimination of auto-reactive clones. Reports from several groups, including ours, have indicated that NKT cells narrowly escape death at multiple stages reviewed by (Bendelac et al., 2007). Elucidating the underlying survival signalling processes will reveal how the immune system protects the host from autoimmune diseases while at the same time uses this border-line autoreactivity to defend it from infectious diseases and chronic inflammation.

Most interestingly however, the NKT cells that arose in IL-15^0;Bcl-x_L mice were immature in that they were developmentally blocked between $CD44^{HI}NK1.1^{NEG}$ ST2 to $CD44^{HI}NK1.1^{+}$ ST3 transition. This result indicated that IL-15 played additional roles, beyond just survival, in NKT cell development. To understand the underlying ontogenetic defect, I investigated the gene expression program in wild type and IL-15^0 NKT cells. From this line of investigation, I discovered several key steps in NKT cell differentiation program. I found that the transcription factor gene *Tbx21* was poorly expressed in IL-15^0 NKT cells. This result was consistent with the reduced T-bet protein expression within peripheral IL-15^0 NKT cells. T-bet was previously shown to regulate NKT cell maturation; a deficiency in this transcription factor also blocked NKT cell development at ST2, i.e., at the same stage where NKT cell development was arrested in IL-15-null mice (Matsuda et al., 2007; Matsuda et al., 2006; Townsend et al., 2004). Furthermore, IL-15 null NKT cells poorly transcribed their *Ifng* locus, a locus that is transcriptionally regulated by T-bet. Consistent with this finding, IL-15^0 NKT cells poorly, if at all, responded to its cognate ligand, CD1d-αGalCer, in vivo. Gene expression analyses revealed defects in additional T-bet regulated genes that encode proteins that mediate NKT cell effector functions. These included *Gzma, Gzmc*, *Hopx, and Krl(a,b,c,k)* that were down regulated in IL-15-deficient NKT cells (Figure 4-1).

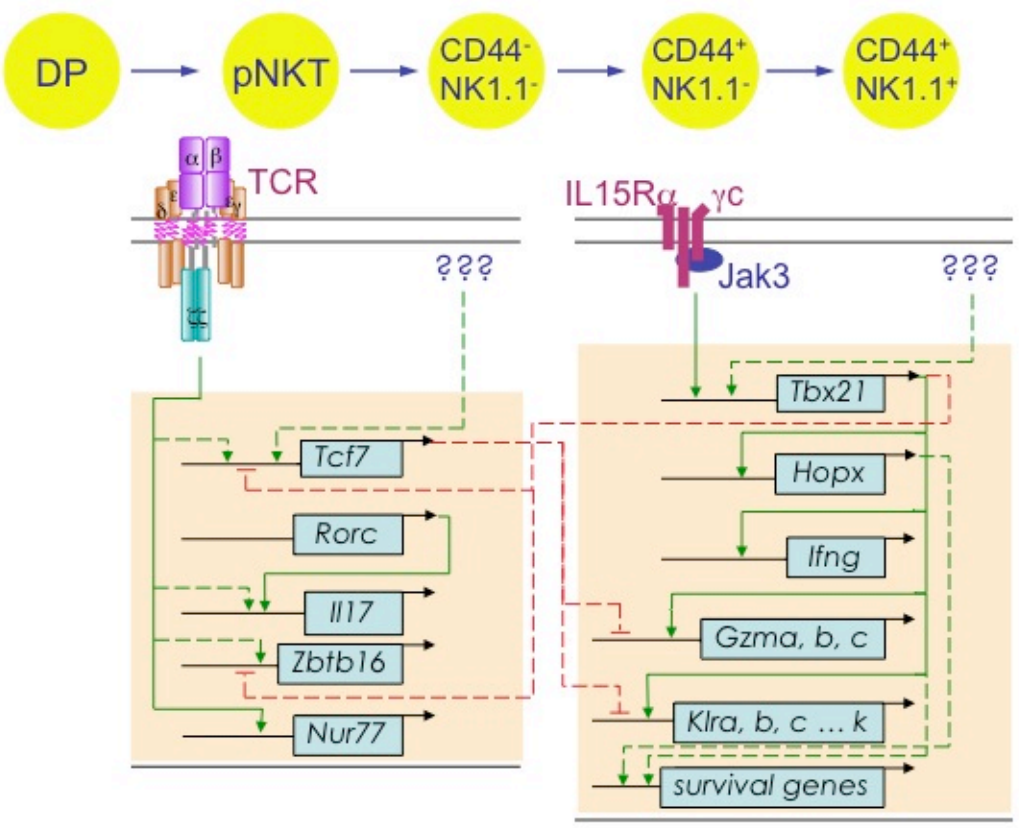

Figure 4-1. Gene regulatory network

Model for gene regulatory network functioning during NKT cell maturation, based upon gene expression analysis. IL-15 induces *Tbx21* expression and its downstream target genes *Hopx, Ifng, Gzm(a,b,c), Klr(a,b,c,k)* (solid lines). and may regulate proposed targets (dashed lines). During NKT cell development NKTCR mediated signals are important for the upregulation of genes such as *Tcf7, Il17, Zbtb16, and Nur77.* Yet expression of *Zbtb16* is reduced in mature NKT cells and *Tcf7* is known to repress expression of effector molecules (granzyme A and B, and Klrg1) found in mature NKT cells. While Tbet functions as activator of gene expression, it can work in combination with other factors as a repressor. Thus, we propose that *Tbx21,* which is critical for NKT cell maturation, may directly or indirectly repress expression of *Tcf7* and *Zbtb16.*

On the other hand, transcription factors such as *Tcf7* (encoding T cell factor 7), *Rorc* (encoding RORγt) and *Zbtb16* (encoding PLZF), which are expressed by immature ST0—ST2 NKT cells, were abundant in IL-15-null NKT cells and conversely were poorly expressed in wild type NKT cells, indicating perhaps the enrichment of these stages in developmentally arrested IL15-null NKT cells. These data confirmed that IL-15 signalling was critical for functional maturation of NKT cells. The IL-15 signal is thus integrated and relayed into the nucleus to induce *Tbx21* expression (amongst other genes) whose product in turn regulated the expression of multiple genes encoding effector molecules including IFN-γ, granzyme B and NK cell receptors (Figure 4-1).

Finally, the data emerging from the global gene expression analysis as described above lent to a draft gene regulatory network that specifies ontogenetic progression and effector differentiation of NKT cells (Figure 4-1). This draft gene regulatory network provides a framework to direct further studies on NKT cell lineage progression and effector differentiation. Questions of significant interest include,

a. Elucidation of the mechanism(s) underlying IL-15 signal integration and how it is relayed to the nucleus; especially whether this mechanism is distinct from conventional T cells and NK cells or similar to one or the other lineage.

b. How are NKT cell lineage specific transcription factors switched on and off as development progresses from immature to mature stages: Does IL-15-induced *Tbx21* expression in combination with other transcription factor(s) or

switch off *Zbtb16* expression with the help of repressor(s)? In this regard it is noteworthy that T-bet in combination with Bcl-6 can act as a repressor (Oestreich et al., 2011) in conventional T cells and is thought to regulate effector differentiation in CD4 T cells. Conversely, BLIMP-1 can repress *Tbx21* thereby attenuating Th1 differentiation (Cimmino et al., 2008). Similarly, it is possible that T-bet represses Tcf-7 expression to induce the expression of effector genes as they mature to ST3 NKT cells as Tcf-7 is known to repress granzyme A and B, perforin and Klrg1 gene expression in $CD8^+$ T cells (Zhou et al., 2010).

SUMMARY

During NKT cell ontogeny, the integration of numerous developmental signals dictate the subtype and function of the developing cells. This thesis explored the role of negative selection in sculpting a functional NKT cell repertoire; and the role of IL-15 in NKT cell effector differentiation and homeostasis. I found that NKT cells undergo Nur77 mediated negative selection during development. I found that positive selection precedes negative selection during NKT cell development, and hence plays a major role in shaping global NKT cell Vβ repertoire. This repertoire is then further fine-tuned, particularly within CDR region during negative selection presumably to eliminate highest auto-reactive clones. Additionally I found that IL-15 functions by supporting survival of developing thymic NKT cells and is necessary for complete maturation perhaps by inducing T-bet expression as a ST3-specific differentiation factor in

NKT cells. NKT cells play key roles in regulating immune responses in health and disease. What ligands NKT cells recognize and how they respond to those ligands is determined by the signals that shape the NKTCR repertoire and its functional maturation. Thus, my findings provide important new insights into NKT cell ontogeny and have implications for NKT cell mediated immune responses.

CHAPTER V

MATERIALS AND METHODS

Mice

The mouse strains used in this study and their sources are listed in Table 4-1. B6-IL-15^0, B6.129-IL-$7\alpha^0$, B6-$J18^0$, B6-$V\alpha14^{tg}$, B6.129-CD1dTD mice and B6-$Nur77^{tg}$ (Bendelac et al., 1996; Boesteanu et al., 1997; Calnan et al., 1995; Chiu et al., 2002; Cui et al., 1997; Kennedy et al., 2000) were generous gifts from J. Peschon (Immunex), M. Taniguchi (RIKEN, Japan), A. Bendelac (U Chicago), and A. Winoto (UC Berkley), respectively. B6-IL-15^0 and B6.129-IL-$7R\alpha^0$ mice were bred with B6-Eμ36-Bcl-2^{tg} (Strasser et al., 1991) and C-Lck-Bcl-$x_L{}^{tg}$ (Chao et al., 1995) mice. B6.C-IL-15^0;Bcl-$x_L{}^{tg}$ mice were backcrossed to B6-IL-15^0 mice for 6 generations. C57BL/6 and B6-TCR-Hy^{tg} were purchased from the Jackson Laboratory (Bar Harbor, Maine) and Taconic respectively. B6-Nur77ΔN^{tg} were generated by the Vanderbilt Transgenic Mouse facility, which injected Nur77ΔN^{tg} plasmid DNA into B6 pronucleus generating transgenic founder mice. Founders were bred to C57BL/6 and 3 founder lines were identified with germline transmission. B6-Nur77ΔN^{tg} mice were bred with J$\alpha18^0$ and TCR-Hy^{tg} mice. B6-$Nur77^{tg}$ mice were bred with $V\alpha14^{tg}$ mice. All mouse crosses and experiments were performed under approved by Institutional Animal Care and Use Committee protocols.

Table 4-1. Mouse strains used in this study

Mouse strain	Source/Reference
C57BL/6	The Jackson Laboratory
B6.129-Jα18^{0}	(Cui et al., 1997)
B6.129CD1dTD	(Chiu et al., 2002)
B6-Vα14^{tg}	(Bendelac et al., 1996)
B6-Eμ36-Bcl-2^{tg}	The Jackson Laboratory
C-Lck-Bcl-x_L^{tg}	The Jackson Laboratory
B6-IL-15^{0}	(Kennedy et al., 2000)
B6.C-IL15^{0};Eμ36-Bcl-2^{tg}	This study
B6.C-IL15^{0};Bcl-x_L^{tg}	This study
B6.129-IL-7Rα^{0}	(Boesteanu et al., 1997; Peschon et al., 1994)
B6.129-IL-7Rα^{0};Eμ36-Bcl-2^{tg}	This study
B6.129-IL-7Rα^{0};Bcl-x_L^{tg}	This study
B6-Nur77^{tg}	(Calnan et al., 1995)
B6-Nur77^{tg};Bcl-x_L^{tg}	This study
B6-Nur77ΔN^{tg};Vα14^{tg}	This study
B6-Nur77ΔN^{tg}	This study
B6-TCR-HY^{tg}	Taconic
B6-Nur77ΔN^{tg};TCR-HY^{tg}	This study
B6-Nur77ΔN^{tg};CD1dTD^{KI}	This study
B6-Nur77ΔN^{tg};Jα18^{0}	This study

Antibodies and Reagents

All antibodies used for the identification of NKT cells were from BD Pharmingen as described (Bezbradica et al., 2006b). Anti-BrdU-Alexa-647 (PRB-1; Invitrogen), anti-human Bcl-x_L-PE and IgG3 isotype control-PE (7B25 and B10; Southern Biotech), anti-mouse Bcl-2-PE (3F11) and Armenian hamster IgG1κ isotype control-PE (A19-3), anti-human Bcl-2-PE (6C8) and Armenian hamster IgG2λ isotype control-PE (Ha4/8), anti-Mcl-1 rabbit polyclonal (Rockland), chicken anti-rabbit-Alexa-647 (Invitrogen), anti-T-bet-Alexa-647 (eBio4B10; eBiosciences) and mouse IgG1 isotype control-Alexa-647 (P3; eBioscience), anti-Gata-3-Alexa-647 (L50-823) and mouse IgG1κ isotype control-Alexa-647 (MOPC-21), anti-PLZF (D-9, Santa Cruz), mouse IgG1 isotype control (eBioscience), anti-mouse IgG-FITC (eBiosciences), and TCR Vβ Screening Panel-FITC (BD Pharmingen) antibodies were purchased. α-galactosylceramide (αGalCer; KRN7000) was generously provided by Kirin Brewery Company (Gunma, Japan) or purchased from Funakoshi Co. Ltd. (Tokyo, Japan). Mouse αGalCer-loaded CD1d monomers were obtained from the NIH Tetramer Facility (Emory University). Preparation of αGalCer-loaded CD1d tetramer from monomer and their use are described elsewhere (Bezbradica et al., 2006b).

Flow Cytometry

Antibodies and staining procedures for the identification of NKT cells were as described elsewhere (Bezbradica et al., 2006b). NKT cells were identified as $CD3\varepsilon^{+}$tetramer^{+} cells among $B220^{LO}$ splenocytes and hepatic mononuclear cells or $CD8^{LO}$ thymocytes. Four-color flow cytometry was performed with a FACSCalibur instrument (Becton-Dickinson) whilst seven-color flow cytometry was performed with a LSR-II instrument (Becton-Dickinson). Data were analyzed with FlowJo software (Treestar Inc.). Absolute NKT cell numbers were calculated from % tetramer^{+} cells and total number of cells recovered from each organ.

Ex Vivo Stimulation of Thymocytes and Splenocytes with IL-15

Thymocytes and splenocytes were stimulated in vitro with 100 ng/ml recombinant human (rh) IL-15 (Miltenyi) for 5 days. Cells were then collected and stained with specific mAb for intracellular expression of Bcl-2, Bcl-x_L, and Mcl-1.

Intracellular Flow Cytometry

Cells were fixed and permeabilized with cytofix/cytoperm solution for intracellular staining or with cytofix/cytoperm plus (both from BD Pharmingen) for intra-nuclear BrdU staining according to the manufacturer's protocol. Staining for intracellular IFN-γ and IL-4 also used GolgiStop (BD Pharmingen). Staining for intracellular T-bet, Gata-3, and PLZF used "Foxp3 staining buffer kit" (eBioscience). Intra-cellular and intra-nuclear staining was performed according to the manufacturer's protocol.

Thymocyte sorting

Thymic NKT cells were enriched by magnetic sorting using a Pan-T cell isolation kit in combination with CD8 beads (Miltenyi) as instructed by the manufacturer. Enriched NKT cells from 5—10 mice were pooled and further purified by flow sorting CD3ε^+tetramer$^+$ cells (FACSAria; Becton-Dickinson). CD4 and CD8 double positive (DP) thymocytes were flow sorted as above. Freshly purified NKT cells and DP thymocytes were >98% pure as judged by CD3ε^+tetramer$^+$ and CD4/CD8 specific staining (data not shown).

RNA preparation, microarray hybridization and analyses

Freshly purified NKT cells were washed and lysed by passage through a Qiashedder column (Qiagen). Total RNA was extracted per the manufacturer's instructions (RNeasy, Qiagen). RNA yield was quantified spectrophotometrically (Nanodrop ND-1000) and aliquots electrophoresed to determine sample purity and concentration (Agilent 2100 Bioanalyzer). Microarray hybridizations were performed using One-colour hybridization on SurePrint G3 Mouse GE 60K Microarray (Agilent) by the Functional Genomics and Shared Resources Core (Vanderbilt University). Scanning was performed using a GenePix® 4000B Microarray Scanner (Molecular Devices). The resulting images were processed with Agilent Feature Extraction software to generate raw probe intensity data, which was subsequently normalised by the quantile method (Bolstad et al., 2003). Differential expression analysis was carried out with an empirical Bayes

approach on linear model using limma package (Smyth, 2004, 2005). In this study, we defined differentially expressed genes as those whose $\log_2$ fold change values were $\geq$ +1.5 or $\geq$ -1.5 and whose nominal *P*-values were less than 0.001 (Huang, 2011). Next we performed hierarchical clustering of the differentially expressed genes using the R AMAP Package (http://cran.r-project.org/web/packages/amap/). The microarray data are available at GEO (http://www.ncbi.nlm.nih.gov/geo/query/acc.cgi?token=dtgxpkoosiokmpm&acc=); accession number: GSE32568.

Real time quantitative PCR

RNA was reverse transcribed with MuLV RT Reverse Transcriptase (Applied Biosystems) according to manufacturer's protocol. qPCR was performed in the presence of IQ RealTime Sybr Green PCR Supermix and target gene-specific primers (Table 5-2) in an iQ5 thermocycler (Biorad). qPCR for Nur77 and β-actin was performed in the presence Taqman Universal Mastermix II and Nur77 (4331182) and β-actin (4331182) Taqman probe sets (Invitrogen) in an iQ5 thermocycler (Biorad). Results were analyzed using iQ5 software. Data were first normalized against β-actin control. As the CT values are obtained as $\log_2$ values, the normalised delta CT values of wild type samples were subtracted from normalised delta CT values of $IL15^0$ or $Nur77\Delta N^{tg}$ samples. The resulting $\log_2$ delta delta CT values were transformed yielding relative expression, which enabled comparison between cells isolated from the two strains. For this, $IL15^0$

Table 5-2. qPCR primer pairs used to validate gene expression data

Gene	Forward primer	Reverse primer
T-bet	CCGCGCGAGGACTACGCATT	CTTGCCGCTCTGGTACCGCC
HOPX	CCACGCTGTGCCTCATCGCA	GGCCTGGCTCCCTAGTCCGT
NKG2E	GCATCTGAAGGCCAGCAGGCA	AGATCCATTCCTTTGGACAAAGAGC
GZMA	TGACTGCTGCCCACTGTAACG	CGGCATCTGGTTCCTGGTTTCACA
GZMC	GTTGGTGGGAAGAAGATGTTCTGC	GATGTTGTGAGCCCCCAGTGTGA
NK1.1	GCCCACAAGACTGGCTTTTACACCGAG	GTCTGAAGCACAGCTCTCAGGAGTCAC
NKG2A	CGAAGCAAAGGCACAGATCAATTCC	GCTGACCTCTGCCCTTCCGAAG
NKG2D	AGCAAATGGCTCCTGGCAGTGG	ACACCGCCCTTTTCATGCAGAT
NKRP1A	TGCCAGACATGAACTGGAAGTGGA	TGGCAGATCCAACGGTTGTCTGA
IL4RA	ACCAGATGGAACTGTGGGCTGA	AGCAGCCATTCGTCGGACACAT
CD160	GGACCTACCAGTGCTGTGCCAGA	TGGCTGAAGTCAGGGTGTGACC
IFN-γ	CCTTCTTCAGCAACAGCAAGGCGAA	GCAACAGCTGGTGGACCACTCG
Ly6c1	CCTCTGATGGATTCTGCATTGCTC	GCTGCAACAGGAAGTCCTCTCCCT
Bcl-2	CAGGGAGATGTCACCCCTGGTGG	CAGAGTGATGCAGGCCCCGACC
PLZF	TGCGGTGCCCAGTTCTCAAAGG	TGGGGAAGGTGCGGTTGCAC
Tcf7	CCTGCGGATATAGACAGCACTTC	TGTCCAGGTACACCAGATCCCA
RORC	GTGGAGTTTGCCAAGCGGCTTT	CCTGCACATTCTGACTAGGACG
IRF4	GAACGAGGAGAAGAGCGTCTTC	GTAGGAGGATCTGGCTTGTCGA
ACTB	CATTGCTGACAGGATGCAGAAGG	TGCTGGAAGGTGGACAGTGAGG
Vα14-Jα18	AGGTCTTGTGTCCCTGACAG	CAGGTATGACAATCAGCTGAGTCC

sample, called the Calibrator was set to 1, and relative expression calculated as fold change in gene expression in wild type cells relative to the Calibrator.

TCRα re-arrangement

cDNA was prepared from total RNA isolated from DP thymocytes. qPCR for Vα14 to Jα18 rearrangement was performed as described above using the following forward (^{F}) and reverse (^{R}) primers: Vα14^{F} (5'-AGGTCTTGTGTCCCTG-ACAG-3'), Jα18^{R} (5'-CAGGTATGACAATCAGCTGAGTCC-3'), Vα8^{F} (5'-TCACA-GACAACAAGAGGACC-3'), and Jα5^{R} (5'-AGTGAGCTGCCCCACAACCT-3'). PCR products were separated by agarose gel electrophoresis and visualized by ethidium bromide staining. Alternatively, RNA was obtained from C57BL/6, Nur77tg and Jα18ko thymocytes per the manufacturer's instructions (RNeasy; Qiagen) and reverse transcribed using protocol described above. PCR reaction was performed using Vα3, Vα14 and Jα18 specific primers (Table 5-3) with 30 amplification cycles. PCR products were separated by agarose gel electrophoresis and visualized by ethidium bromide staining.

Table 5-3. PCR primers for Vβ-gene specific amplification and sequencing

Gene name	Forward primer
Vβ2	TACAGACCCCACAGTGACTTTGC
Vβ6	CCCTCCAAACTATGAACAAGTGG
Vβ7	GAACAGGCCTGGTGGACATGAAAG
Vβ8	CAAAACACATGGAGGCTGCAGTCA
Vβ9	CAGCCACTTTTGTGGATACTACGG
Vβ10	TTCCTATTGGTACAAGCAAGACTCT
Vβ11	GAGCAGAACCAACAAATGTGGTG
Vβ13	AGATCTATGGGCTCCAGGCTCTTCTTCGTGCTC
Vβ15	GTGGAACTTCCATGAGGATGGAGT
Vβ17	AGATCTGAATGGATCCTAGACTTCTTTGCTGTGTG
Cβ	GGGTGGAGTCACATTTCTCAGATC
Vα3	CCCAGTGGTTCAAGGAGTGA
Vα14	AGGTCTTGTGTCCCTGACAG
Jα18	CAGGTATGACAATCAGCTGAGTCC
pJET1.2-for	CGACTCACTATAGGGAGAGCGGC
pJET1.2-rev	AAGAACATCGATTTTCCATGGCAG

Statistics

Comparisons of normally distributed continuous data were performed by one-way ANOVA with Tukey's post test to determine significance. The significance of gene expression analyzed by qPCR was determined by unpaired T test. Statistical significance of *Vα14-Jα18* rearrangement by qPCR was calculated by two-tailed, unpaired T-test. Comparisons were performed using GraphPad (Prism).

Cytokine Responses

Individual, age (6—10 weeks old)-matched mice were either injected i.p. with 5 μg αGalCer or vehicle (0.1% Tween-20 in PBS). After 2, 4, or 6 hrs, serum, splenocytes and hepatic mononuclear cells were prepared. Cells were stained with anti-CD3ε mAb, tetramer and anti-IFN-γ or anti-IL-4 mAb and analyzed by flow cytometry.

Ft *novicida and LVS Growth and Mouse Infection*

Frozen aliquots of *Ft* novicida and LVS were inoculated in triplicate into 35 ml LB broth and grown for 12 hrs at 37°C with 250 rpm agitation. Cultures were pooled and the density determined to be $3x10^9$ and $9x10^9$ cfu/ml, respectively, for *Ft* novicida and LVS. Bacteria were serially diluted into sterile PBS and an aliquot was plated to calculate the injected dose. Mice were injected with 50 μl diluted

bacteria (~68,000 cfu *Ft* novicida or ~10^6 cfu LVS) i.d. on the right dorsal region. Blood collection was performed by retroorbital bleed (d0, 1, 3 and 5 post-inoculation) or cardiac puncture for terminal bleeds. Animals were monitored daily for weight loss and multiple times daily for progression of disease. Animals losing more than 20% of their initial body weight were humanely euthanized. Kaplan-Meier plots detail the survival of animals following infection. The indicated significance values were calculated by Mantel-Cox comparison of individual survival curves. Serum cytokine levels were determined by cytokine bead array (CBA) assay using mouse Th1, Th2, Th17 cytokine kit (BD Bioscience) according to the manufacturer's instructions.

Hybridoma stimulation

All Vα14$^+$ mouse NKT hybridomas N38-3C3, N37-1H5a, N38-2C12, and Vα14$^-$ mouse hybridoma N37-1A12 have been described (Bezbradica et al., 2006b; Stanic et al., 2003). 5x10^5 sorted double positive thymocytes were cultured overnight with 5x10^4 hybridomas. Cell-free supernatant was harvested and IL-2 secreted during co-culture was determined by ELISA.

Analysis of TCR CDR3β sequence diversity

Freshly purified NKT cells obtained from C57BL/6 and Nur77DN mice were washed and lysed by passage through a Qiashedder column (Qiagen). Total RNA was extracted per the manufacturer's instructions (RNeasy; Qiagen). RNA

yield was quantified spectrophotometrically (Nanodrop ND-1000). RNA was reverse transcribed with MuLV RT Reverse Transcriptase (Applied Biosystems) according to the manufacturer's protocol. PCR was performed by using the cDNA template resulting from the above RT reaction using the V-gene specific forward primers and C-gene specific primer (Table 5-3). PCR products were separated by agarose gel electrophoresis, purified from gel and cloned into sequencing vector pJET1.2. Nucleotide sequences of TCR were determined by Sanger sequencing using pJET1.2 vector specific primers (Table 5-3). Analysis of TCR CDR3 structure, variable (V), diverse (D) and joining (J) segment usage and the functionality of the whole V-gene sequences was performed using IMGT/V-QUEST program (www.imgt.org/IMGT_vquest/share/textes/). Sequencing was performed by the Vanderbilt DNA Sequencing Facility.

Ex Vivo Stimulation of Splenocytes with Lipids

Splenocytes were stimulated in vitro with titrating doses of αGalCer , 100 ng/ml OCH or 10 μg/ml of αGalDAG, iGb3, Sulfatide, PtdCho, PtdIno or PtdEtN for 5 days. Sandwich ELISA was performed as described (Bezbradica et al., 2006b) to monitor supernatant IFNγ response.

REFERENCES

Akbari, O., Stock, P., Meyer, E.H., Freeman, G.J., Sharpe, A.H., Umetsu, D.T., and DeKruyff, R.H. (2008). ICOS/ICOSL interaction is required for CD4+ invariant NKT cell function and homeostatic survival. J Immunol *180*, 5448-5456.

Alberola-Ila, J., Hogquist, K.A., Swan, K.A., Bevan, M.J., and Perlmutter, R.M. (1996). Positive and negative selection invoke distinct signaling pathways. J Exp Med *184*, 9-18.

Albu, D.I., Feng, D., Bhattacharya, D., Jenkins, N.A., Copeland, N.G., Liu, P., and Avram, D. (2007). BCL11B is required for positive selection and survival of double-positive thymocytes. J Exp Med *204*, 3003-3015.

Albu, D.I., VanValkenburgh, J., Morin, N., Califano, D., Jenkins, N.A., Copeland, N.G., Liu, P., and Avram, D. (2011). Transcription factor Bcl11b controls selection of invariant natural killer T-cells by regulating glycolipid presentation in double-positive thymocytes. Proc Natl Acad Sci U S A *108*, 6211-6216.

Aliahmad, P., and Kaye, J. (2008). Development of all CD4 T lineages requires nuclear factor TOX. J Exp Med *205*, 245-256.

Allende, M.L., Zhou, D., Kalkofen, D.N., Benhamed, S., Tuymetova, G., Borowski, C., Bendelac, A., and Proia, R.L. (2008). S1P1 receptor expression regulates emergence of NKT cells in peripheral tissues. FASEB J *22*, 307-315.

Alonzo, E.S., Gottschalk, R.A., Das, J., Egawa, T., Hobbs, R.M., Pandolfi, P.P., Pereira, P., Nichols, K.E., Koretzky, G.A., Jordan, M.S., and Sant'Angelo, D.B. (2010). Development of promyelocytic zinc finger and ThPOK-expressing innate gamma delta T cells is controlled by strength of TCR signaling and Id3. J Immunol *184*, 1268-1279.

Arase, H., Arase, N., Nakagawa, K., Good, R.A., and Onoe, K. (1993). NK1.1+ CD4+ CD8- thymocytes with specific lymphokine secretion. Eur J Immunol *23*, 307-310.

Arase, H., Arase, N., Ogasawara, K., Good, R.A., and Onoe, K. (1992). An NK1.1+ CD4+8- single-positive thymocyte subpopulation that expresses a highly skewed T-cell antigen receptor V beta family. Proc Natl Acad Sci U S A *89*, 6506-6510.

Arrenberg, P., Halder, R., Dai, Y., Maricic, I., and Kumar, V. (2010). Oligoclonality and innate-like features in the TCR repertoire of type II NKT

cells reactive to a beta-linked self-glycolipid. Proc Natl Acad Sci U S A *107*, 10984-10989.

Astrakhan, A., Ochs, H.D., and Rawlings, D.J. (2009). Wiskott-Aldrich syndrome protein is required for homeostasis and function of invariant NKT cells. J Immunol *182*, 7370-7380.

Bain, G., Engel, I., Robanus Maandag, E.C., te Riele, H.P., Voland, J.R., Sharp, L.L., Chun, J., Huey, B., Pinkel, D., and Murre, C. (1997). E2A deficiency leads to abnormalities in alphabeta T-cell development and to rapid development of T-cell lymphomas. Mol Cell Biol *17*, 4782-4791.

Bendelac, A. (1995). Positive selection of mouse NK1+ T cells by CD1-expressing cortical thymocytes. J Exp Med *182*, 2091-2096.

Bendelac, A., Hunziker, R.D., and Lantz, O. (1996). Increased interleukin 4 and immunoglobulin E production in transgenic mice overexpressing NK1 T cells. J Exp Med *184*, 1285-1293.

Bendelac, A., Killeen, N., Littman, D.R., and Schwartz, R.H. (1994). A subset of CD4+ thymocytes selected by MHC class I molecules. Science *263*, 1774-1778.

Bendelac, A., Lantz, O., Quimby, M.E., Yewdell, J.W., Bennink, J.R., and Brutkiewicz, R.R. (1995). CD1 recognition by mouse NK1+ T lymphocytes. Science *268*, 863-865.

Bendelac, A., Matzinger, P., Seder, R.A., Paul, W.E., and Schwartz, R.H. (1992). Activation events during thymic selection. J Exp Med *175*, 731-742.

Bendelac, A., Savage, P.B., and Teyton, L. (2007). The biology of NKT cells. Annu Rev Immunol *25*, 297-336.

Benlagha, K., Kyin, T., Beavis, A., Teyton, L., and Bendelac, A. (2002). A thymic precursor to the NK T cell lineage. Science *296*, 553-555.

Benlagha, K., Wei, D.G., Veiga, J., Teyton, L., and Bendelac, A. (2005). Characterization of the early stages of thymic NKT cell development. J Exp Med *202*, 485-492.

Berzins, S.P., McNab, F.W., Jones, C.M., Smyth, M.J., and Godfrey, D.I. (2006). Long-term retention of mature NK1.1+ NKT cells in the thymus. J Immunol *176*, 4059-4065.

Bezbradica, J.S., Gordy, L.E., Stanic, A.K., Dragovic, S., Hill, T., Hawiger, J., Unutmaz, D., Van Kaer, L., and Joyce, S. (2006a). Granulocyte-macrophage

colony-stimulating factor regulates effector differentiation of invariant natural killer T cells during thymic ontogeny. Immunity *25*, 487-497.

Bezbradica, J.S., Hill, T., Stanic, A.K., Van Kaer, L., and Joyce, S. (2005). Commitment toward the natural T (iNKT) cell lineage occurs at the CD4+8+ stage of thymic ontogeny. Proc Natl Acad Sci U S A *102*, 5114-5119.

Bezbradica, J.S., Stanic, A.K., and Joyce, S. (2006b). Characterization and functional analysis of mouse invariant natural T (iNKT) cells. Curr Protoc Immunol *Chapter 14*, Unit 14 13.

Bilenki, L., Wang, S., Yang, J., Fan, Y., Joyee, A.G., and Yang, X. (2005). NK T cell activation promotes Chlamydia trachomatis infection in vivo. J Immunol *175*, 3197-3206.

Boesteanu, A., De Silva, A.D., Nakajima, H., Leonard, W.J., Peschon, J.J., and Joyce, S. (1997). Distinct roles for signals relayed through the common cytokine receptor γ chain and interleukin 7 receptor α chain in natural T cell development. J Exp Med *186*, 331-336.

Bolstad, B.M., Irizarry, R.A., Astrand, M., and Speed, T.P. (2003). A comparison of normalization methods for high density oligonucleotide array data based on variance and bias. Bioinformatics *19*, 185-193.

Boos, M.D., Yokota, Y., Eberl, G., and Kee, B.L. (2007). Mature natural killer cell and lymphoid tissue-inducing cell development requires Id2-mediated suppression of E protein activity. J Exp Med *204*, 1119-1130.

Borg, N.A., Kjer-Nielsen, L., McCluskey, J., and Rossjohn, J. (2007a). Structural insight into natural killer T cell receptor recognition of CD1d. Adv Exp Med Biol *598*, 20-34.

Borg, N.A., Wun, K.S., Kjer-Nielsen, L., Wilce, M.C., Pellicci, D.G., Koh, R., Besra, G.S., Bharadwaj, M., Godfrey, D.I., McCluskey, J., and Rossjohn, J. (2007b). CD1d-lipid-antigen recognition by the semi-invariant NKT T-cell receptor. Nature *448*, 44-49.

Brennan, P.J., Tatituri, R.V., Brigl, M., Kim, E.Y., Tuli, A., Sanderson, J.P., Gadola, S.D., Hsu, F.F., Besra, G.S., and Brenner, M.B. (2011). Invariant natural killer T cells recognize lipid self antigen induced by microbial danger signals. Nat Immunol *12*, 1202-1211.

Brigl, M., and Brenner, M.B. (2010). How invariant natural killer T cells respond to infection by recognizing microbial or endogenous lipid antigens. Semin Immunol *22*, 79-86.

Brigl, M., Bry, L., Kent, S.C., Gumperz, J.E., and Brenner, M.B. (2003). Mechanism of CD1d-restricted natural killer T cell activation during microbial infection. Nat Immunol *4*, 1230-1237.

Calnan, B.J., Szychowski, S., Chan, F.K., Cado, D., and Winoto, A. (1995). A role for the orphan steroid receptor Nur77 in apoptosis accompanying antigen-induced negative selection. Immunity *3*, 273-282.

Cannarile, M.A., Lind, N.A., Rivera, R., Sheridan, A.D., Camfield, K.A., Wu, B.B., Cheung, K.P., Ding, Z., and Goldrath, A.W. (2006). Transcriptional regulator Id2 mediates CD8+ T cell immunity. Nat Immunol *7*, 1317-1325.

Cannons, J.L., Yu, L.J., Hill, B., Mijares, L.A., Dombroski, D., Nichols, K.E., Antonellis, A., Koretzky, G.A., Gardner, K., and Schwartzberg, P.L. (2004). SAP regulates T(H)2 differentiation and PKC-theta-mediated activation of NF-kappaB1. Immunity *21*, 693-706.

Carnaud, C., Lee, D., Donnars, O., Park, S.H., Beavis, A., Koezuka, Y., and Bendelac, A. (1999). Cutting edge: Cross-talk between cells of the innate immune system: NKT cells rapidly activate NK cells. J Immunol *163*, 4647-4650.

Cen, O., Ueda, A., Guzman, L., Jain, J., Bassiri, H., Nichols, K.E., and Stein, P.L. (2009). The adaptor molecule signaling lymphocytic activation molecule-associated protein (SAP) regulates IFN-gamma and IL-4 production in V alpha 14 transgenic NKT cells via effects on GATA-3 and T-bet expression. J Immunol *182*, 1370-1378.

Cernadas, M., Sugita, M., van der Wel, N., Cao, X., Gumperz, J.E., Maltsev, S., Besra, G.S., Behar, S.M., Peters, P.J., and Brenner, M.B. (2003). Lysosomal localization of murine CD1d mediated by AP-3 is necessary for NK T cell development. J Immunol *171*, 4149-4155.

Chang, C.L., Lai, Y.G., Hou, M.S., Huang, P.L., and Liao, N.S. (2011a). IL-15Rα of radiation-resistant cells Is necessary and sufficient for thymic invariant NKT cell survival and functional maturation. J Immunol *187*, 1235-1242.

Chang, P.P., Barral, P., Fitch, J., Pratama, A., Ma, C.S., Kallies, A., Hogan, J.J., Cerundolo, V., Tangye, S.G., Bittman, R.*, et al.* (2012). Identification of Bcl-6-dependent follicular helper NKT cells that provide cognate help for B cell responses. Nat Immunol *13*, 35-43.

Chang, W.S., Kim, J.Y., Kim, Y.J., Kim, Y.S., Lee, J.M., Azuma, M., Yagita, H., and Kang, C.Y. (2008). Cutting edge: Programmed death-1/programmed death ligand 1 interaction regulates the induction and maintenance of invariant NKT cell anergy. J Immunol *181*, 6707-6710.

Chang, Y.J., Kim, H.Y., Albacker, L.A., Lee, H.H., Baumgarth, N., Akira, S., Savage, P.B., Endo, S., Yamamura, T., Maaskant, J.*, et al.* (2011b). Influenza infection in suckling mice expands an NKT cell subset that protects against airway hyperreactivity. J Clin Invest *121*, 57-69.

Chao, D.T., Linette, G.P., Boise, L.H., White, L.S., Thompson, C.B., and Korsmeyer, S.J. (1995). Bcl-XL and Bcl-2 repress a common pathway of cell death. J Exp Med *182*, 821-828.

Cheng, L.E., Chan, F.K., Cado, D., and Winoto, A. (1997). Functional redundancy of the Nur77 and Nor-1 orphan steroid receptors in T-cell apoptosis. EMBO J *16*, 1865-1875.

Chiba, A., Dascher, C.C., Besra, G.S., and Brenner, M.B. (2008). Rapid NKT cell responses are self-terminating during the course of microbial infection. J Immunol *181*, 2292-2302.

Chiu, Y.H., Jayawardena, J., Weiss, A., Lee, D., Park, S.H., Dautry-Varsat, A., and Bendelac, A. (1999). Distinct subsets of CD1d-restricted T cells recognize self-antigens loaded in different cellular compartments. J Exp Med *189*, 103-110.

Chiu, Y.H., Park, S.H., Benlagha, K., Forestier, C., Jayawardena-Wolf, J., Savage, P.B., Teyton, L., and Bendelac, A. (2002). Multiple defects in antigen presentation and T cell development by mice expressing cytoplasmic tail-truncated CD1d. Nat Immunol *3*, 55-60.

Choi, H.J., Geng, Y., Cho, H., Li, S., Giri, P.K., Felio, K., and Wang, C.R. (2011). Differential requirements for the Ets transcription factor Elf-1 in the development of NKT cells and NK cells. Blood *117*, 1880-1887.

Chun, T., Page, M.J., Gapin, L., Matsuda, J.L., Xu, H., Nguyen, H., Kang, H.S., Stanic, A.K., Joyce, S., Koltun, W.A.*, et al.* (2003). CD1d-expressing dendritic cells but not thymic epithelial cells can mediate negative selection of NKT cells. J Exp Med *197*, 907-918.

Chung, B., Aoukaty, A., Dutz, J., Terhorst, C., and Tan, R. (2005). Signaling lymphocytic activation molecule-associated protein controls NKT cell functions. J Immunol *174*, 3153-3157.

Cimmino, L., Martins, G.A., Liao, J., Magnusdottir, E., Grunig, G., Perez, R.K., and Calame, K.L. (2008). Blimp-1 attenuates Th1 differentiation by repression of ifng, tbx21, and bcl6 gene expression. J Immunol *181*, 2338-2347.

Coles, M.C., and Raulet, D.H. (2000). NK1.1+ T cells in the liver arise in the thymus and are selected by interactions with class I molecules on CD4+CD8+ cells. J Immunol *164*, 2412-2418.

Coquet, J.M., Chakravarti, S., Kyparissoudis, K., McNab, F.W., Pitt, L.A., McKenzie, B.S., Berzins, S.P., Smyth, M.J., and Godfrey, D.I. (2008). Diverse cytokine production by NKT cell subsets and identification of an IL-17-producing CD4-NK1.1- NKT cell population. Proc Natl Acad Sci U S A *105*, 11287-11292.

Crowe, N.Y., Coquet, J.M., Berzins, S.P., Kyparissoudis, K., Keating, R., Pellicci, D.G., Hayakawa, Y., Godfrey, D.I., and Smyth, M.J. (2005). Differential antitumor immunity mediated by NKT cell subsets in vivo. J Exp Med *202*, 1279-1288.

Crowe, N.Y., Uldrich, A.P., Kyparissoudis, K., Hammond, K.J., Hayakawa, Y., Sidobre, S., Keating, R., Kronenberg, M., Smyth, M.J., and Godfrey, D.I. (2003). Glycolipid antigen drives rapid expansion and sustained cytokine production by NK T cells. J Immunol *171*, 4020-4027.

Cui, J., Shin, T., Kawano, T., Sato, H., Kondo, E., Toura, I., Kaneko, Y., Koseki, H., Kanno, M., and Taniguchi, M. (1997). Requirement for Vα14 NKT cells in IL-12-mediated rejection of tumors. Science *278*, 1623-1626.

D'Cruz, L.M., Knell, J., Fujimoto, J.K., and Goldrath, A.W. (2010). An essential role for the transcription factor HEB in thymocyte survival, Tcra rearrangement and the development of natural killer T cells. Nat Immunol *11*, 240-249.

Das, R., Sant'Angelo, D.B., and Nichols, K.E. (2010). Transcriptional control of invariant NKT cell development. Immunol Rev *238*, 195-215.

De Silva, A.D., Park, J.J., Matsuki, N., Stanic, A.K., Brutkiewicz, R.R., Medof, M.E., and Joyce, S. (2002). Lipid protein interactions: the assembly of CD1d1 with cellular phospholipids occurs in the endoplasmic reticulum. J Immunol *168*, 723-733.

Devera, T.S., Shah, H.B., Lang, G.A., and Lang, M.L. (2008). Glycolipid-activated NKT cells support the induction of persistent plasma cell responses and antibody titers. Eur J Immunol *38*, 1001-1011.

Dhodapkar, M.V., Geller, M.D., Chang, D.H., Shimizu, K., Fujii, S., Dhodapkar, K.M., and Krasovsky, J. (2003). A reversible defect in natural killer T cell function characterizes the progression of premalignant to malignant multiple myeloma. J Exp Med *197*, 1667-1676.

Diana, J., and Lehuen, A. (2009). NKT cells: friend or foe during viral infections? Eur J Immunol *39*, 3283-3291.

Diao, H., Iwabuchi, K., Li, L., Onoe, K., Van Kaer, L., Kon, S., Saito, Y., Morimoto, J., Denhardt, D.T., Rittling, S., and Uede, T. (2008). Osteopontin regulates development and function of invariant natural killer T cells. Proc Natl Acad Sci U S A *105*, 15884-15889.

Doisne, J.M., Bartholin, L., Yan, K.P., Garcia, C.N., Duarte, N., Le Luduec, J.B., Vincent, D., Cyprian, F., Horvat, B., Martel, S*., et al.* (2009a). iNKT cell development is orchestrated by different branches of TGF-beta signaling. J Exp Med *206*, 1365-1378.

Doisne, J.M., Becourt, C., Amniai, L., Duarte, N., Le Luduec, J.B., Eberl, G., and Benlagha, K. (2009b). Skin and peripheral lymph node invariant NKT cells are mainly retinoic acid receptor-related orphan receptor (gamma)t+ and respond preferentially under inflammatory conditions. J Immunol *183*, 2142-2149.

Dose, M., Khan, I., Guo, Z., Kovalovsky, D., Krueger, A., von Boehmer, H., Khazaie, K., and Gounari, F. (2006). c-Myc mediates pre-TCR-induced proliferation but not developmental progression. Blood *108*, 2669-2677.

Dose, M., Sleckman, B.P., Han, J., Bredemeyer, A.L., Bendelac, A., and Gounari, F. (2009). Intrathymic proliferation wave essential for Vα14+ natural killer T cell development depends on c-Myc. Proc Natl Acad Sci U S A *106*, 8641-8646.

Duthie, M.S., Kahn, M., White, M., Kapur, R.P., and Kahn, S.J. (2005a). Both CD1d antigen presentation and interleukin-12 are required to activate natural killer T cells during Trypanosoma cruzi infection. Infect Immun *73*, 1890-1894.

Duthie, M.S., Kahn, M., White, M., Kapur, R.P., and Kahn, S.J. (2005b). Critical proinflammatory and anti-inflammatory functions of different subsets of CD1d-restricted natural killer T cells during Trypanosoma cruzi infection. Infect Immun *73*, 181-192.

Eberl, G., Fehling, H.J., von Boehmer, H., and MacDonald, H.R. (1999a). Absolute requirement for the pre-T cell receptor alpha chain during NK1.1+ TCRalphabeta cell development. Eur J Immunol *29*, 1966-1971.

Eberl, G., Lowin-Kropf, B., and MacDonald, H.R. (1999b). NKT cell development is selectively impaired in Fyn- deficient mice. J Immunol (Cutting Edge) *163*, 4091-4094.

Eberl, G., and MacDonald, H.R. (1998). Rapid death and regeneration of NKT cells in anti-CD3epsilon- or IL-12-treated mice: a major role for bone marrow in NKT cell homeostasis. Immunity *9*, 345-353.

Eberl, G., and MacDonald, H.R. (2000). Selective induction of NK cell proliferation and cytotoxicity by activated NKT cells. Eur J Immunol *30*, 985-992.

Egawa, T., Eberl, G., Taniuchi, I., Benlagha, K., Geissmann, F., Hennighausen, L., Bendelac, A., and Littman, D.R. (2005). Genetic evidence supporting selection of the Valpha14i NKT cell lineage from double-positive thymocyte precursors. Immunity *22*, 705-716.

Elewaut, D., Lawton, A.P., Nagarajan, N.A., Maverakis, E., Khurana, A., Honing, S., Benedict, C.A., Sercarz, E., Bakke, O., Kronenberg, M., and Prigozy, T.I. (2003a). The adaptor protein AP-3 is required for CD1d-mediated antigen presentation of glycosphingolipids and development of Valpha14i NKT cells. J Exp Med *198*, 1133-1146.

Elewaut, D., Shaikh, R.B., Hammond, K.J., De Winter, H., Leishman, A.J., Sidobre, S., Turovskaya, O., Prigozy, T.I., Ma, L., Banks, T.A.*, et al.* (2003b). NIK-dependent RelB activation defines a unique signaling pathway for the development of V alpha 14i NKT cells. J Exp Med *197*, 1623-1633.

Emoto, M., Mittrucker, H.W., Schmits, R., Mak, T.W., and Kaufmann, S.H. (1999). Critical role of leukocyte function-associated antigen-1 in liver accumulation of CD4+NKT cells. J Immunol *162*, 5094-5098.

Engel, I., Hammond, K., Sullivan, B.A., He, X., Taniuchi, I., Kappes, D., and Kronenberg, M. (2010). Co-receptor choice by V alpha14i NKT cells is driven by Th-POK expression rather than avoidance of CD8-mediated negative selection. J Exp Med *207*, 1015-1029.

Exley, M., Garcia, J., Balk, S.P., and Porcelli, S. (1997). Requirements for CD1d recognition by human invariant Valpha24+ CD4-CD8- T cells. J Exp Med *186*, 109-120.

Exley, M.A., Lynch, L., Varghese, B., Nowak, M., Alatrakchi, N., and Balk, S.P. (2011). Developing understanding of the roles of CD1d-restricted T cell subsets in cancer: reversing tumor-induced defects. Clin Immunol *140*, 184-195.

Faveeuw, C., Angeli, V., Fontaine, J., Maliszewski, C., Capron, A., Van Kaer, L., Moser, M., Capron, M., and Trottein, F. (2002). Antigen presentation by CD1d contributes to the amplification of Th2 responses to Schistosoma mansoni glycoconjugates in mice. J Immunol *169*, 906-912.

Fedeli, M., Napolitano, A., Wong, M.P., Marcais, A., de Lalla, C., Colucci, F., Merkenschlager, M., Dellabona, P., and Casorati, G. (2009). Dicer-dependent microRNA pathway controls invariant NKT cell development. J Immunol *183*, 2506-2512.

Felices, M., and Berg, L.J. (2008). The Tec kinases Itk and Rlk regulate NKT cell maturation, cytokine production, and survival. J Immunol *180*, 3007-3018.

Fischer, K., Scotet, E., Niemeyer, M., Koebernick, H., Zerrahn, J., Maillet, S., Hurwitz, R., Kursar, M., Bonneville, M., Kaufmann, S.H., and Schaible, U.E. (2004). Mycobacterial phosphatidylinositol mannoside is a natural antigen for CD1d-restricted T cells. Proc Natl Acad Sci U S A *101*, 10685-10690.

Florence, W.C., Xia, C., Gordy, L.E., Chen, W., Zhang, Y., Scott-Browne, J., Kinjo, Y., Yu, K.O., Keshipeddy, S., Pellicci, D.G.*, et al.* (2009). Adaptability of the semi-invariant natural killer T-cell receptor towards structurally diverse CD1d-restricted ligands. EMBO J *28*, 3579-3590.

Fox, L.M., Cox, D.G., Lockridge, J.L., Wang, X., Chen, X., Scharf, L., Trott, D.L., Ndonye, R.M., Veerapen, N., Besra, G.S.*, et al.* (2009). Recognition of lyso-phospholipids by human natural killer T lymphocytes. PLoS Biol *7*, e1000228.

Franki, A.S., Van Beneden, K., Dewint, P., Hammond, K.J., Lambrecht, S., Leclercq, G., Kronenberg, M., Deforce, D., and Elewaut, D. (2006). A unique lymphotoxin {alpha}beta-dependent pathway regulates thymic emigration of V{alpha}14 invariant natural killer T cells. Proc Natl Acad Sci U S A *103*, 9160-9165.

Fujii, S., Liu, K., Smith, C., Bonito, A.J., and Steinman, R.M. (2004). The linkage of innate to adaptive immunity via maturing dendritic cells in vivo requires CD40 ligation in addition to antigen presentation and CD80/86 costimulation. J Exp Med *199*, 1607-1618.

Fujii, S., Shimizu, K., Smith, C., Bonifaz, L., and Steinman, R.M. (2003). Activation of natural killer T cells by alpha-galactosylceramide rapidly induces the full maturation of dendritic cells in vivo and thereby acts as an adjuvant for combined CD4 and CD8 T cell immunity to a coadministered protein. J Exp Med *198*, 267-279.

Fuller, C.L., Brittingham, K.C., Hepburn, M.J., Martin, J.W., Petitt, P.L., Pittman, P.R., and Bavari, S. (2006). Dominance of human innate immune responses in primary Francisella tularensis live vaccine strain vaccination. J Allergy Clin Immunol *117*, 1186-1188.

Gadola, S.D., Koch, M., Marles-Wright, J., Lissin, N.M., Shepherd, D., Matulis, G., Harlos, K., Villiger, P.M., Stuart, D.I., Jakobsen, B.K.*, et al.* (2006a). Structure and binding kinetics of three different human CD1d-alpha-galactosylceramide-specific T cell receptors. J Exp Med *203*, 699-710.

Gadola, S.D., Silk, J.D., Jeans, A., Illarionov, P.A., Salio, M., Besra, G.S., Dwek, R., Butters, T.D., Platt, F.M., and Cerundolo, V. (2006b). Impaired selection of invariant natural killer T cells in diverse mouse models of glycosphingolipid lysosomal storage diseases. J Exp Med *203*, 2293-2303.

Gadue, P., Morton, N., and Stein, P.L. (1999). The Src family tyrosine kinase Fyn regulates natural killer T cell development. J Exp Med *190*, 1189-1196.

Gadue, P., and Stein, P.L. (2002). NK T cell precursors exhibit differential cytokine regulation and require Itk for efficient maturation. J Immunol *169*, 2397-2406.

Gapin, L., Matsuda, J.L., Surh, C.D., and Kronenberg, M. (2001). NKT cells derive from double-positive thymocytes that are positively selected by CD1d. Nat Immunol *2*, 971-978.

Geissmann, F., Cameron, T.O., Sidobre, S., Manlongat, N., Kronenberg, M., Briskin, M.J., Dustin, M.L., and Littman, D.R. (2005). Intravascular immune surveillance by CXCR6+ NKT cells patrolling liver sinusoids. PLoS Biol *3*, e113.

Germanov, E., Veinotte, L., Cullen, R., Chamberlain, E., Butcher, E.C., and Johnston, B. (2008). Critical role for the chemokine receptor CXCR6 in homeostasis and activation of CD1d-restricted NKT cells. J Immunol *181*, 81-91.

Godfrey, D.I., and Berzins, S.P. (2007). Control points in NKT-cell development. Nat Rev Immunol *7*, 505-518.

Godfrey, D.I., Stankovic, S., and Baxter, A.G. (2010). Raising the NKT cell family. Nat Immunol *11*, 197-206.

Griewank, K., Borowski, C., Rietdijk, S., Wang, N., Julien, A., Wei, D.G., Mamchak, A.A., Terhorst, C., and Bendelac, A. (2007). Homotypic interactions mediated by Slamf1 and Slamf6 receptors control NKT cell lineage development. Immunity *27*, 751-762.

Grubor-Bauk, B., Arthur, J.L., and Mayrhofer, G. (2008). Importance of NKT cells in resistance to herpes simplex virus, fate of virus-infected neurons, and level of latency in mice. J Virol *82*, 11073-11083.

Gui, M., Li, J., Wen, L.J., Hardy, R.R., and Hayakawa, K. (2001). TCR beta chain influences but does not solely control autoreactivity of V alpha 14J281T cells. J Immunol *167*, 6239-6246.

Gumperz, J.E., Roy, C., Makowska, A., Lum, D., Sugita, M., Podrebarac, T., Koezuka, Y., Porcelli, S.A., Cardell, S., Brenner, M.B., and Behar, S.M. (2000). Murine CD1d-restricted T cell recognition of cellular lipids. Immunity *12*, 211-221.

Hammond, K., Cain, W., van Driel, I., and Godfrey, D. (1998). Three day neonatal thymectomy selectively depletes NK1.1+ T cells. Int Immunol *10*, 1491-1499.

Harada, M., Seino, K., Wakao, H., Sakata, S., Ishizuka, Y., Ito, T., Kojo, S., Nakayama, T., and Taniguchi, M. (2004). Down-regulation of the invariant Valpha14 antigen receptor in NKT cells upon activation. Int Immunol *16*, 241-247.

Hayakawa, K., Lin, B.T., and Hardy, R.R. (1992). Murine thymic CD4+ T cell subsets: a subset (Thy0) that secretes diverse cytokines and overexpresses the V beta 8 T cell receptor gene family. J Exp Med *176*, 269-274.

Hayakawa, Y., Berzins, S.P., Crowe, N.Y., Godfrey, D.I., and Smyth, M.J. (2004). Antigen-induced tolerance by intrathymic modulation of self-recognizing inhibitory receptors. Nat Immunol *5*, 590-596.

Hermans, I.F., Silk, J.D., Gileadi, U., Salio, M., Mathew, B., Ritter, G., Schmidt, R., Harris, A.L., Old, L., and Cerundolo, V. (2003). NKT cells enhance CD4+ and CD8+ T cell responses to soluble antigen in vivo through direct interaction with dendritic cells. J Immunol *171*, 5140-5147.

Hernandez-Hoyos, G., Anderson, M.K., Wang, C., Rothenberg, E.V., and Alberola-Ila, J. (2003). GATA-3 expression is controlled by TCR signals and regulates CD4/CD8 differentiation. Immunity *19*, 83-94.

Hu, T., Gimferrer, I., Simmons, A., Wiest, D., and Alberola-Ila, J. (2011). The Ras/MAPK pathway is required for generation of iNKT cells. PLoS One *6*, e19890.

Hu, T., Simmons, A., Yuan, J., Bender, T.P., and Alberola-Ila, J. (2010). The transcription factor c-Myb primes CD4+CD8+ immature thymocytes for selection into the iNKT lineage. Nat Immunol *11*, 435-441.

Huntington, N.D., Puthalakath, H., Gunn, P., Naik, E., Michalak, E.M., Smyth, M.J., Tabarias, H., Degli-Esposti, M.A., Dewson, G., Willis, S.N.*, et al.* (2007).

Interleukin 15-mediated survival of natural killer cells is determined by interactions among Bim, Noxa and Mcl-1. Nat Immunol *8*, 856-863.

Ishikawa, H., Hisaeda, H., Taniguchi, M., Nakayama, T., Sakai, T., Maekawa, Y., Nakano, Y., Zhang, M., Zhang, T., Nishitani, M.*, et al.* (2000). CD4(+) v(alpha)14 NKT cells play a crucial role in an early stage of protective immunity against infection with Leishmania major. Int Immunol *12*, 1267-1274.

Iwabuchi, K., Iwabuchi, C., Tone, S., Itoh, D., Tosa, N., Negishi, I., Ogasawara, K., Uede, T., and Onoe, K. (2001). Defective development of NK1.1+ T-cell antigen receptor alphabeta+ cells in zeta-associated protein 70 null mice with an accumulation of NK1.1+ CD3- NK-like cells in the thymus. Blood *97*, 1765-1775.

Johnson, T.R., Hong, S., Van Kaer, L., Koezuka, Y., and Graham, B.S. (2002). NK T cells contribute to expansion of CD8(+) T cells and amplification of antiviral immune responses to respiratory syncytial virus. J Virol *76*, 4294-4303.

Joshi, N.S., Cui, W., Chandele, A., Lee, H.K., Urso, D.R., Hagman, J., Gapin, L., and Kaech, S.M. (2007). Inflammation directs memory precursor and short-lived effector CD8(+) T cell fates via the graded expression of T-bet transcription factor. Immunity *27*, 281-295.

Joyce, S., Girardi, E., and Zajonc, D.M. (2011). NKT cell ligand recognition logic: molecular basis for a synaptic duet and transmission of inflammatory effectors. J Immunol *187*, 1081-1089.

Joyce, S., Woods, A.S., Yewdell, J.W., Bennink, J.R., De Silva, A.D., Boesteanu, A., Balk, S.P., Cotter, R.J., and Brutkiewicz, R.R. (1998). Natural ligand of mouse CD1d1: cellular glycosylphosphatidylinositol. Science *279*, 1541-1544.

Kang, S.J., and Cresswell, P. (2004). Saposins facilitate CD1d-restricted presentation of an exogenous lipid antigen to T cells. Nat Immunol *5*, 175-181.

Kawakami, K., Yamamoto, N., Kinjo, Y., Miyagi, K., Nakasone, C., Uezu, K., Kinjo, T., Nakayama, T., Taniguchi, M., and Saito, A. (2003). Critical role of Valpha14+ natural killer T cells in the innate phase of host protection against Streptococcus pneumoniae infection. Eur J Immunol *33*, 3322-3330.

Kawano, T., Cui, J., Koezuka, Y., Toura, I., Kaneko, Y., Motoki, K., Ueno, H., Nakagawa, R., Sato, H., Kondo, E.*, et al.* (1997). CD1d-restricted and TCR-mediated activation of Vα14 NKT cells by glycosylceramides. Science *278*, 1626-1629.

Kennedy, M.K., Glaccum, M., Brown, S.N., Butz, E.A., Viney, J.L., Embers, M., Matsuki, N., Charrier, K., Sedger, L., Willis, C.R.*, et al.* (2000). Reversible defects in natural killer and memory CD8 T cell lineages in interleukin 15-deficient mice. J Exp Med *191*, 771-780.

Kim, E.Y., Battaile, J.T., Patel, A.C., You, Y., Agapov, E., Grayson, M.H., Benoit, L.A., Byers, D.E., Alevy, Y., Tucker, J.*, et al.* (2008). Persistent activation of an innate immune response translates respiratory viral infection into chronic lung disease. Nat Med *14*, 633-640.

Kim, P.J., Pai, S.Y., Brigl, M., Besra, G.S., Gumperz, J., and Ho, I.C. (2006). GATA-3 regulates the development and function of invariant NKT cells. J Immunol *177*, 6650-6659.

King, I.L., Fortier, A., Tighe, M., Dibble, J., Watts, G.F., Veerapen, N., Haberman, A.M., Besra, G.S., Mohrs, M., Brenner, M.B., and Leadbetter, E.A. (2012). Invariant natural killer T cells direct B cell responses to cognate lipid antigen in an IL-21-dependent manner. Nat Immunol *13*, 44-50.

Kinjo, Y., Illarionov, P., Vela, J.L., Pei, B., Girardi, E., Li, X., Li, Y., Imamura, M., Kaneko, Y., Okawara, A.*, et al.* (2011). Invariant natural killer T cells recognize glycolipids from pathogenic Gram-positive bacteria. Nat Immunol *12*, 966-974.

Kinjo, Y., Tupin, E., Wu, D., Fujio, M., Garcia-Navarro, R., Benhnia, M.R., Zajonc, D.M., Ben-Menachem, G., Ainge, G.D., Painter, G.F.*, et al.* (2006). Natural killer T cells recognize diacylglycerol antigens from pathogenic bacteria. Nat Immunol *7*, 978-986.

Kinjo, Y., Wu, D., Kim, G., Xing, G.W., Poles, M.A., Ho, D.D., Tsuji, M., Kawahara, K., Wong, C.H., and Kronenberg, M. (2005). Recognition of bacterial glycosphingolipids by natural killer T cells. Nature *434*, 520-525.

Kisielow, P., Bluthmann, H., Staerz, U.D., Steinmetz, M., and von Boehmer, H. (1988). Tolerance in T-cell-receptor transgenic mice involves deletion of nonmature CD4+8+ thymocytes. Nature *333*, 742-746.

Kitamura, H., Iwakabe, K., Yahata, T., Nishimura, S., Ohta, A., Ohmi, Y., Sato, M., Takeda, K., Okumura, K., Van Kaer, L.*, et al.* (1999). The natural killer T (NKT) cell ligand alpha-galactosylceramide demonstrates its immunopotentiating effect by inducing interleukin (IL)-12 production by dendritic cells and IL-12 receptor expression on NKT cells. J Exp Med *189*, 1121-1128.

Ko, S.Y., Ko, H.J., Chang, W.S., Park, S.H., Kweon, M.N., and Kang, C.Y. (2005). alpha-Galactosylceramide can act as a nasal vaccine adjuvant

inducing protective immune responses against viral infection and tumor. J Immunol *175*, 3309-3317.

Kobrynski, L.J., Sousa, A.O., Nahmias, A.J., and Lee, F.K. (2005). Cutting edge: antibody production to pneumococcal polysaccharides requires CD1 molecules and CD8+ T cells. J Immunol *174*, 1787-1790.

Kolluri, S.K., Zhu, X., Zhou, X., Lin, B., Chen, Y., Sun, K., Tian, X., Town, J., Cao, X., Lin, F.*, et al.* (2008). A short Nur77-derived peptide converts Bcl-2 from a protector to a killer. Cancer Cell *14*, 285-298.

Kovalovsky, D., Uche, O.U., Eladad, S., Hobbs, R.M., Yi, W., Alonzo, E., Chua, K., Eidson, M., Kim, H.J., Im, J.S.*, et al.* (2008). The BTB-zinc finger transcriptional regulator PLZF controls the development of invariant natural killer T cell effector functions. Nat Immunol *9*, 1055-1064.

Kreslavsky, T., Savage, A.K., Hobbs, R., Gounari, F., Bronson, R., Pereira, P., Pandolfi, P.P., Bendelac, A., and von Boehmer, H. (2009). TCR-inducible PLZF transcription factor required for innate phenotype of a subset of gammadelta T cells with restricted TCR diversity. Proc Natl Acad Sci U S A *106*, 12453-12458.

Kuang, A.A., Cado, D., and Winoto, A. (1999). Nur77 transcription activity correlates with its apoptotic function in vivo. Eur J Immunol *29*, 3722-3728.

Kumar, H., Belperron, A., Barthold, S.W., and Bockenstedt, L.K. (2000). Cutting edge: CD1d deficiency impairs murine host defense against the spirochete, Borrelia burgdorferi. J Immunol *165*, 4797-4801.

Kunisaki, Y., Tanaka, Y., Sanui, T., Inayoshi, A., Noda, M., Nakayama, T., Harada, M., Taniguchi, M., Sasazuki, T., and Fukui, Y. (2006). DOCK2 is required in T cell precursors for development of Valpha14 NK T cells. J Immunol *176*, 4640-4645.

La Cava, A., Van Kaer, L., and Fu Dong, S. (2006). CD4+CD25+ Tregs and NKT cells: regulators regulating regulators. Trends Immunol *27*, 322-327.

Lacorazza, H.D., Miyazaki, Y., Di Cristofano, A., Deblasio, A., Hedvat, C., Zhang, J., Cordon-Cardo, C., Mao, S., Pandolfi, P.P., and Nimer, S.D. (2002). The ETS protein MEF plays a critical role in perforin gene expression and the development of natural killer and NK-T cells. Immunity *17*, 437-449.

Lang, G.A., Exley, M.A., and Lang, M.L. (2006). The CD1d-binding glycolipid alpha-galactosylceramide enhances humoral immunity to T-dependent and T-independent antigen in a CD1d-dependent manner. Immunology *119*, 116-125.

Lang, M.L. (2009). How do natural killer T cells help B cells? Expert Rev Vaccines *8*, 1109-1121.

Lantz, O., and Bendelac, A. (1994). An invariant T cell receptor alpha chain is used by a unique subset of major histocompatibility complex class I-specific CD4+ and CD4-8- T cells in mice and humans. J Exp Med *180*, 1097-1106.

Lawson, V.J., Maurice, D., Silk, J.D., Cerundolo, V., and Weston, K. (2009). Aberrant selection and function of invariant NKT cells in the absence of AP-1 transcription factor Fra-2. J Immunol *183*, 2575-2584.

Lazarevic, V., Zullo, A.J., Schweitzer, M.N., Staton, T.L., Gallo, E.M., Crabtree, G.R., and Glimcher, L.H. (2009). The gene encoding early growth response 2, a target of the transcription factor NFAT, is required for the development and maturation of natural killer T cells. Nat Immunol *10*, 306-313.

Lee, A.J., Zhou, X., Chang, M., Hunzeker, J., Bonneau, R.H., Zhou, D., and Sun, S.C. (2010). Regulation of natural killer T-cell development by deubiquitinase CYLD. EMBO J *29*, 1600-1612.

Li, Y., Girardi, E., Wang, J., Yu, E.D., Painter, G.F., Kronenberg, M., and Zajonc, D.M. (2010). The Valpha14 invariant natural killer T cell TCR forces microbial glycolipids and CD1d into a conserved binding mode. J Exp Med *207*, 2383-2393.

Lin, Y., Roberts, T.J., Wang, C.R., Cho, S., and Brutkiewicz, R.R. (2005). Long-term loss of canonical NKT cells following an acute virus infection. Eur J Immunol *35*, 879-889.

Locci, M., Draghici, E., Marangoni, F., Bosticardo, M., Catucci, M., Aiuti, A., Cancrini, C., Marodi, L., Espanol, T., Bredius, R.G.*, et al.* (2009). The Wiskott-Aldrich syndrome protein is required for iNKT cell maturation and function. J Exp Med *206*, 735-742.

Lodolce, J.P., Boone, D.L., Chai, S., Swain, R.E., Dassopoulos, T., Trettin, S., and Ma, A. (1998). IL-15 receptor maintains lymphoid homeostasis by supporting lymphocyte homing and proliferation. Immunity *9*, 669-676.

Ma, A., Koka, R., and Burkett, P. (2006). Diverse functions of IL-2, IL-15, and IL-7 in lymphoid homeostasis. Annu Rev Immunol *24*, 657-679.

MacDonald, H.R. (2000). CD1d-glycolipid tetramers: A new tool to monitor natural killer T cells in health and disease. J Exp Med *192*, F15-20.

Mallevaey, T., Scott-Browne, J.P., Matsuda, J.L., Young, M.H., Pellicci, D.G., Patel, O., Thakur, M., Kjer-Nielsen, L., Richardson, S.K., Cerundolo, V.*, et al.* (2009). T cell receptor CDR2 beta and CDR3 beta loops collaborate functionally to shape the iNKT cell repertoire. Immunity *31*, 60-71.

Mallevaey, T., Zanetta, J.P., Faveeuw, C., Fontaine, J., Maes, E., Platt, F., Capron, M., de-Moraes, M.L., and Trottein, F. (2006). Activation of invariant NKT cells by the helminth parasite schistosoma mansoni. J Immunol *176*, 2476-2485.

Marrack, P., Scott-Browne, J.P., Dai, S., Gapin, L., and Kappler, J.W. (2008). Evolutionarily conserved amino acids that control TCR-MHC interaction. Annu Rev Immunol *26*, 171-203.

Matsuda, J.L., Gapin, L., Sidobre, S., Kieper, W.C., Tan, J.T., Ceredig, R., Surh, C.D., and Kronenberg, M. (2002). Homeostasis of Vα14*i* NKT cells. Nat Immunol *3*, 966-974.

Matsuda, J.L., George, T.C., Hagman, J., and Gapin, L. (2007). Temporal dissection of T-bet functions. J Immunol *178*, 3457-3465.

Matsuda, J.L., Mallevaey, T., Scott-Browne, J., and Gapin, L. (2008). CD1d-restricted iNKT cells, the 'Swiss-Army knife' of the immune system. Curr Opin Immunol *20*, 358-368.

Matsuda, J.L., Naidenko, O.V., Gapin, L., Nakayama, T., Taniguchi, M., Wang, C.R., Koezuka, Y., and Kronenberg, M. (2000). Tracking the response of natural killer T cells to a glycolipid antigen using CD1d tetramers. J Exp Med *192*, 741-754.

Matsuda, J.L., Zhang, Q., Ndonye, R., Richardson, S.K., Howell, A.R., and Gapin, L. (2006). T-bet concomitantly controls migration, survival, and effector functions during the development of Valpha14i NKT cells. Blood *107*, 2797-2805.

Mattner, J., Debord, K.L., Ismail, N., Goff, R.D., Cantu, C., 3rd, Zhou, D., Saint-Mezard, P., Wang, V., Gao, Y., Yin, N.*, et al.* (2005). Exogenous and endogenous glycolipid antigens activate NKT cells during microbial infections. Nature *434*, 525-529.

Mattner, J., Donhauser, N., Werner-Felmayer, G., and Bogdan, C. (2006). NKT cells mediate organ-specific resistance against Leishmania major infection. Microbes Infect *8*, 354-362.

McNab, F.W., Berzins, S.P., Pellicci, D.G., Kyparissoudis, K., Field, K., Smyth, M.J., and Godfrey, D.I. (2005). The influence of CD1d in postselection NKT cell maturation and homeostasis. J Immunol *175*, 3762-3768.

McNab, F.W., Pellicci, D.G., Field, K., Besra, G., Smyth, M.J., Godfrey, D.I., and Berzins, S.P. (2007). Peripheral NK1.1 NKT cells are mature and functionally distinct from their thymic counterparts. J Immunol *179*, 6630-6637.

Medzhitov, R. (2001). Toll-like receptors and innate immunity. Nat Rev Immunol *1*, 135-145.

Michel, M.L., Keller, A.C., Paget, C., Fujio, M., Trottein, F., Savage, P.B., Wong, C.H., Schneider, E., Dy, M., and Leite-de-Moraes, M.C. (2007). Identification of an IL-17-producing NK1.1(neg) iNKT cell population involved in airway neutrophilia. J Exp Med *204*, 995-1001.

Michel, M.L., Mendes-da-Cruz, D., Keller, A.C., Lochner, M., Schneider, E., Dy, M., Eberl, G., and Leite-de-Moraes, M.C. (2008). Critical role of ROR-gammat in a new thymic pathway leading to IL-17-producing invariant NKT cell differentiation. Proc Natl Acad Sci U S A *105*, 19845-19850.

Milpied, P., Massot, B., Renand, A., Diem, S., Herbelin, A., Leite-de-Moraes, M., Rubio, M.T., and Hermine, O. (2011). IL-17-producing invariant NKT cells in lymphoid organs are recent thymic emigrants identified by neuropilin-1 expression. Blood *118*, 2993-3002.

Minagawa, M., Watanabe, H., Miyaji, C., Tomiyama, K., Shimura, H., Ito, A., Ito, M., Domen, J., Weissman, I.L., and Kawai, K. (2002). Enforced expression of Bcl-2 restores the number of NK cells, but does not rescue the impaired development of NKT cells or intraepithelial lymphocytes, in IL-2/IL-15 receptor beta-chain-deficient mice. J Immunol *169*, 4153-4160.

Miyamoto, K., Miyake, S., and Yamamura, T. (2001). A synthetic glycolipid prevents autoimmune encephalomyelitis by inducing TH2 bias of natural killer T cells. Nature *413*, 531-534.

Molling, J.W., Kolgen, W., van der Vliet, H.J., Boomsma, M.F., Kruizenga, H., Smorenburg, C.H., Molenkamp, B.G., Langendijk, J.A., Leemans, C.R., von Blomberg, B.M.*, et al.* (2005). Peripheral blood IFN-gamma-secreting Valpha24+Vbeta11+ NKT cell numbers are decreased in cancer patients independent of tumor type or tumor load. Int J Cancer *116*, 87-93.

Molling, J.W., Langius, J.A., Langendijk, J.A., Leemans, C.R., Bontkes, H.J., van der Vliet, H.J., von Blomberg, B.M., Scheper, R.J., and van den Eertwegh, A.J. (2007). Low levels of circulating invariant natural killer T cells predict poor

clinical outcome in patients with head and neck squamous cell carcinoma. J Clin Oncol *25*, 862-868.

Monteiro, M., Almeida, C.F., Caridade, M., Ribot, J.C., Duarte, J., Agua-Doce, A., Wollenberg, I., Silva-Santos, B., and Graca, L. (2010). Identification of regulatory Foxp3+ invariant NKT cells induced by TGF-beta. J Immunol *185*, 2157-2163.

Monticelli, L.A., Yang, Y., Knell, J., D'Cruz, L.M., Cannarile, M.A., Engel, I., Kronenberg, M., and Goldrath, A.W. (2009). Transcriptional regulator Id2 controls survival of hepatic NKT cells. Proc Natl Acad Sci U S A *106*, 19461-19466.

Montoya, C.J., Jie, H.B., Al-Harthi, L., Mulder, C., Patino, P.J., Rugeles, M.T., Krieg, A.M., Landay, A.L., and Wilson, S.B. (2006). Activation of plasmacytoid dendritic cells with TLR9 agonists initiates invariant NKT cell-mediated cross-talk with myeloid dendritic cells. J Immunol *177*, 1028-1039.

Moran, A.E., Holzapfel, K.L., Xing, Y., Cunningham, N.R., Maltzman, J.S., Punt, J., and Hogquist, K.A. (2011). T cell receptor signal strength in Treg and iNKT cell development demonstrated by a novel fluorescent reporter mouse. J Exp Med *208*, 1279-1289.

Moreira-Teixeira, L., Resende, M., Devergne, O., Herbeuval, J.P., Hermine, O., Schneider, E., Dy, M., Cordeiro-da-Silva, A., and Leite-de-Moraes, M.C. (2012). Rapamycin combined with TGF-beta converts human invariant NKT cells into suppressive Foxp3+ regulatory cells. J Immunol *188*, 624-631.

Morita, M., Motoki, K., Akimoto, K., Natori, T., Sakai, T., Sawa, E., Yamaji, K., Koezuka, Y., Kobayashi, E., and Fukushima, H. (1995). Structure-activity relationship of alpha-galactosylceramides against B16-bearing mice. J Med Chem *38*, 2176-2187.

Mycko, M.P., Ferrero, I., Wilson, A., Jiang, W., Bianchi, T., Trumpp, A., and MacDonald, H.R. (2009). Selective requirement for c-Myc at an early stage of Vα14i NKT cell development. J Immunol *182*, 4641-4648.

Nagarajan, N.A., and Kronenberg, M. (2007). Invariant NKT cells amplify the innate immune response to lipopolysaccharide. J Immunol *178*, 2706-2713.

Nakazato, K., Yamada, H., Yajima, T., Kagimoto, Y., Kuwano, H., and Yoshikai, Y. (2007). Enforced expression of Bcl-2 partially restores cell numbers but not functions of TCRgammadelta intestinal intraepithelial T lymphocytes in IL-15-deficient mice. J Immunol *178*, 757-764.

Nichols, K.E., Hom, J., Gong, S.Y., Ganguly, A., Ma, C.S., Cannons, J.L., Tangye, S.G., Schwartzberg, P.L., Koretzky, G.A., and Stein, P.L. (2005). Regulation of NKT cell development by SAP, the protein defective in XLP. Nat Med *11*, 340-345.

Nishimura, T., Kitamura, H., Iwakabe, K., Yahata, T., Ohta, A., Sato, M., Takeda, K., Okumura, K., Van Kaer, L., Kawano, T.*, et al.* (2000). The interface between innate and acquired immunity: glycolipid antigen presentation by CD1d-expressing dendritic cells to NKT cells induces the differentiation of antigen-specific cytotoxic T lymphocytes. Int Immunol *12*, 987-994.

O'Konek, J.J., Illarionov, P., Khursigara, D.S., Ambrosino, E., Izhak, L., Castillo, B.F., 2nd, Raju, R., Khalili, M., Kim, H.Y., Howell, A.R.*, et al.* (2011). Mouse and human iNKT cell agonist beta-mannosylceramide reveals a distinct mechanism of tumor immunity. J Clin Invest *121*, 683-694.

Oestreich, K.J., Huang, A.C., and Weinmann, A.S. (2011). The lineage-defining factors T-bet and Bcl-6 collaborate to regulate Th1 gene expression patterns. J Exp Med *208*, 1001-1013.

Ohteki, T., Ho, S., Suzuki, H., Mak, T.W., and Ohashi, P.S. (1997). Role for IL-15/IL-15 receptor β-chain in natural killer 1.1+ T cell receptor-αβ+ cell development. J Immunol *159*, 5931-5935.

Ohteki, T., Maki, C., Koyasu, S., Mak, T.W., and Ohashi, P.S. (1999). Cutting edge: LFA-1 is required for liver NK1.1+TCR alpha beta+ cell development: evidence that liver NK1.1+TCR alpha beta+ cells originate from multiple pathways. J Immunol *162*, 3753-3756.

Ohteki, T., Yoshida, H., Matsuyama, T., Duncan, G.S., Mak, T.W., and Ohashi, P.S. (1998). The transcription factor interferon regulatory factor 1 (IRF-1) is important during the maturation of natural killer 1.1+ T cell receptor-alpha/beta+ (NK1+ T) cells, natural killer cells, and intestinal intraepithelial T cells. J Exp Med *187*, 967-972.

Paget, C., Mallevaey, T., Speak, A.O., Torres, D., Fontaine, J., Sheehan, K.C., Capron, M., Ryffel, B., Faveeuw, C., Leite de Moraes, M.*, et al.* (2007). Activation of invariant NKT cells by toll-like receptor 9-stimulated dendritic cells requires type I interferon and charged glycosphingolipids. Immunity *27*, 597-609.

Pai, S.Y., Truitt, M.L., Ting, C.N., Leiden, J.M., Glimcher, L.H., and Ho, I.C. (2003). Critical roles for transcription factor GATA-3 in thymocyte development. Immunity *19*, 863-875.

Parekh, V.V., Lalani, S., Kim, S., Halder, R., Azuma, M., Yagita, H., Kumar, V., Wu, L., and Kaer, L.V. (2009). PD-1/PD-L blockade prevents anergy induction and enhances the anti-tumor activities of glycolipid-activated invariant NKT cells. J Immunol *182*, 2816-2826.

Parekh, V.V., Singh, A.K., Wilson, M.T., Olivares-Villagomez, D., Bezbradica, J.S., Inazawa, H., Ehara, H., Sakai, T., Serizawa, I., Wu, L.*, et al.* (2004). Quantitative and qualitative differences in the in vivo response of NKT cells to distinct alpha- and beta-anomeric glycolipids. J Immunol *173*, 3693-3706.

Parekh, V.V., Wilson, M.T., Olivares-Villagomez, D., Singh, A.K., Wu, L., Wang, C.R., Joyce, S., and Van Kaer, L. (2005). Glycolipid antigen induces long-term natural killer T cell anergy in mice. J Clin Invest *115*, 2572-2583.

Park, J.J., Kang, S.J., De Silva, A.D., Stanic, A.K., Casorati, G., Hachey, D.L., Cresswell, P., and Joyce, S. (2004). Lipid-protein interactions: biosynthetic assembly of CD1 with lipids in the endoplasmic reticulum is evolutionarily conserved. Proc Natl Acad Sci U S A *101*, 1022-1026.

Park, S.H., Benlagha, K., Lee, D., Balish, E., and Bendelac, A. (2000). Unaltered phenotype, tissue distribution and function of Valpha14(+) NKT cells in germ-free mice. Eur J Immunol *30*, 620-625.

Park, S.H., Weiss, A., Benlagha, K., Kyin, T., Teyton, L., and Bendelac, A. (2001). The mouse CD1d-restricted repertoire is dominated by a few autoreactive T cell receptor families. J Exp Med *193*, 893-904.

Pasquier, B., Yin, L., Fondaneche, M.C., Relouzat, F., Bloch-Queyrat, C., Lambert, N., Fischer, A., de Saint-Basile, G., and Latour, S. (2005). Defective NKT cell development in mice and humans lacking the adapter SAP, the X-linked lymphoproliferative syndrome gene product. J Exp Med *201*, 695-701.

Pei, B., Speak, A.O., Shepherd, D., Butters, T., Cerundolo, V., Platt, F.M., and Kronenberg, M. (2011). Diverse endogenous antigens for mouse NKT cells: self-antigens that are not glycosphingolipids. J Immunol *186*, 1348-1360.

Pellicci, D.G., Hammond, K.J., Uldrich, A.P., Baxter, A.G., Smyth, M.J., and Godfrey, D.I. (2002). A natural killer T (NKT) cell developmental pathway iInvolving a thymus-dependent NK1.1(-)CD4(+) CD1d-dependent precursor stage. J Exp Med *195*, 835-844.

Pellicci, D.G., Patel, O., Kjer-Nielsen, L., Pang, S.S., Sullivan, L.C., Kyparissoudis, K., Brooks, A.G., Reid, H.H., Gras, S., Lucet, I.S.*, et al.* (2009). Differential recognition of CD1d-alpha-galactosyl ceramide by the V beta 8.2 and V beta 7 semi-invariant NKT T cell receptors. Immunity *31*, 47-59.

Pellicci, D.G., Uldrich, A.P., Kyparissoudis, K., Crowe, N.Y., Brooks, A.G., Hammond, K.J., Sidobre, S., Kronenberg, M., Smyth, M.J., and Godfrey, D.I. (2003). Intrathymic NKT cell development is blocked by the presence of alpha-galactosylceramide. Eur J Immunol *33*, 1816-1823.

Peschon, J.J., Morrissey, P.J., Grabstein, K.H., Ramsdell, F.J., Maraskovsky, E., Gliniak, B.C., Park, L.S., Ziegler, S.F., Williams, D.E., Ware, C.B.*, et al.* (1994). Early lymphocyte expansion is severely impaired in interleukin 7 receptor-deficient mice. J Exp Med *180*, 1955-1960.

Porubsky, S., Speak, A.O., Luckow, B., Cerundolo, V., Platt, F.M., and Grone, H.J. (2007). Normal development and function of invariant natural killer T cells in mice with isoglobotrihexosylceramide (iGb3) deficiency. Proc Natl Acad Sci U S A *104*, 5977-5982.

Raberger, J., Schebesta, A., Sakaguchi, S., Boucheron, N., Blomberg, K.E., Berglof, A., Kolbe, T., Smith, C.I., Rulicke, T., and Ellmeier, W. (2008). The transcriptional regulator PLZF induces the development of CD44 high memory phenotype T cells. Proc Natl Acad Sci U S A *105*, 17919-17924.

Rachitskaya, A.V., Hansen, A.M., Horai, R., Li, Z., Villasmil, R., Luger, D., Nussenblatt, R.B., and Caspi, R.R. (2008). Cutting edge: NKT cells constitutively express IL-23 receptor and RORgammat and rapidly produce IL-17 upon receptor ligation in an IL-6-independent fashion. J Immunol *180*, 5167-5171.

Raghuraman, G., Geng, Y., and Wang, C.R. (2006). IFN-beta-mediated up-regulation of CD1d in bacteria-infected APCs. J Immunol *177*, 7841-7848.

Rajpal, A., Cho, Y.A., Yelent, B., Koza-Taylor, P.H., Li, D., Chen, E., Whang, M., Kang, C., Turi, T.G., and Winoto, A. (2003). Transcriptional activation of known and novel apoptotic pathways by Nur77 orphan steroid receptor. EMBO J *22*, 6526-6536.

Ranson, T., Vosshenrich, C.A., Corcuff, E., Richard, O., Laloux, V., Lehuen, A., and Di Santo, J.P. (2003). IL-15 availability conditions homeostasis of peripheral natural killer T cells. Proc Natl Acad Sci U S A *100*, 2663-2668.

Rauch, J., Gumperz, J., Robinson, C., Skold, M., Roy, C., Young, D.C., Lafleur, M., Moody, D.B., Brenner, M.B., Costello, C.E., and Behar, S.M. (2003). Structural features of the acyl chain determine self-phospholipid antigen recognition by a CD1d-restricted invariant NKT (iNKT) cell. J Biol Chem *278*, 47508-47515.

Renukaradhya, G.J., Webb, T.J., Khan, M.A., Lin, Y.L., Du, W., Gervay-Hague, J., and Brutkiewicz, R.R. (2005). Virus-induced inhibition of CD1d1-mediated

antigen presentation: reciprocal regulation by p38 and ERK. J Immunol *175*, 4301-4308.

Roy, K.C., Maricic, I., Khurana, A., Smith, T.R., Halder, R.C., and Kumar, V. (2008). Involvement of secretory and endosomal compartments in presentation of an exogenous self-glycolipid to type II NKT cells. J Immunol *180*, 2942-2950.

Salio, M., Silk, J.D., and Cerundolo, V. (2010). Recent advances in processing and presentation of CD1 bound lipid antigens. Curr Opin Immunol *22*, 81-88.

Salio, M., Speak, A.O., Shepherd, D., Polzella, P., Illarionov, P.A., Veerapen, N., Besra, G.S., Platt, F.M., and Cerundolo, V. (2007). Modulation of human natural killer T cell ligands on TLR-mediated antigen-presenting cell activation. Proc Natl Acad Sci U S A *104*, 20490-20495.

Savage, A.K., Constantinides, M.G., Han, J., Picard, D., Martin, E., Li, B., Lantz, O., and Bendelac, A. (2008). The transcription factor PLZF directs the effector program of the NKT cell lineage. Immunity *29*, 391-403.

Schmidt-Supprian, M., Tian, J., Grant, E.P., Pasparakis, M., Maehr, R., Ovaa, H., Ploegh, H.L., Coyle, A.J., and Rajewsky, K. (2004). Differential dependence of CD4+CD25+ regulatory and natural killer-like T cells on signals leading to NF-kappaB activation. Proc Natl Acad Sci U S A *101*, 4566-4571.

Schumann, J., Pittoni, P., Tonti, E., Macdonald, H.R., Dellabona, P., and Casorati, G. (2005). Targeted expression of human CD1d in transgenic mice reveals independent roles for thymocytes and thymic APCs in positive and negative selection of Valpha14i NKT cells. J Immunol *175*, 7303-7310.

Scott-Browne, J.P., Matsuda, J.L., Mallevaey, T., White, J., Borg, N.A., McCluskey, J., Rossjohn, J., Kappler, J., Marrack, P., and Gapin, L. (2007). Germline-encoded recognition of diverse glycolipids by natural killer T cells. Nat Immunol *8*, 1105-1113.

Seiler, M.P., Mathew, R., Liszewski, M.K., Spooner, C., Barr, K., Meng, F., Singh, H., and Bendelac, A. (2012). Elevated and sustained expression of the transcription factors Egr1 and Egr2 controls NKT lineage differentiation in response to TCR signaling. Nat Immunol *13*, 264-271.

Semmling, V., Lukacs-Kornek, V., Thaiss, C.A., Quast, T., Hochheiser, K., Panzer, U., Rossjohn, J., Perlmutter, P., Cao, J., Godfrey, D.I.*, et al.* (2010). Alternative cross-priming through CCL17-CCR4-mediated attraction of CTLs toward NKT cell-licensed DCs. Nat Immunol *11*, 313-320.

Shen, S., Chen, Y., Gorentla, B.K., Lu, J., Stone, J.C., and Zhong, X.P. (2011a). Critical roles of RasGRP1 for invariant NKT cell development. J Immunol *187*, 4467-4473.

Shen, S., Wu, J., Srivatsan, S., Gorentla, B.K., Shin, J., Xu, L., and Zhong, X.P. (2011b). Tight regulation of diacylglycerol-mediated signaling is critical for proper invariant NKT cell development. J Immunol *187*, 2122-2129.

Singh, N., Hong, S., Scherer, D.C., Serizawa, I., Burdin, N., Kronenberg, M., Koezuka, Y., and Van Kaer, L. (1999). Cutting edge: activation of NK T cells by CD1d and alpha-galactosylceramide directs conventional T cells to the acquisition of a Th2 phenotype. J Immunol *163*, 2373-2377.

Sivakumar, V., Hammond, K.J., Howells, N., Pfeffer, K., and Weih, F. (2003). Differential requirement for Rel/nuclear factor kappa B family members in natural killer T cell development. J Exp Med *197*, 1613-1621.

Skold, M., Xiong, X., Illarionov, P.A., Besra, G.S., and Behar, S.M. (2005). Interplay of cytokines and microbial signals in regulation of CD1d expression and NKT cell activation. J Immunol *175*, 3584-3593.

Smyth, G.K. (2004). Linear models and empirical bayes methods for assessing differential expression in microarray experiments. Stat Appl Genet Mol Biol *3*, Article3.

Smyth, G.K. (2005). Limma: Linear models for Microarray Data (New York: Springer).

Sriram, V., Du, W., Gervay-Hague, J., and Brutkiewicz, R.R. (2005). Cell wall glycosphingolipids of Sphingomonas paucimobilis are CD1d-specific ligands for NKT cells. Eur J Immunol *35*, 1692-1701.

Stanic, A.K., Bezbradica, J.S., Park, J.J., Matsuki, N., Mora, A.L., Van Kaer, L., Boothby, M.R., and Joyce, S. (2004a). NF-κB controls cell fate specification, survival, and molecular differentiation of immunoregulatory natural T lymphocytes. J Immunol *172*, 2265-2273.

Stanic, A.K., Bezbradica, J.S., Park, J.J., Van Kaer, L., Boothby, M.R., and Joyce, S. (2004b). Cutting edge: the ontogeny and function of Va14Ja18 natural T lymphocytes require signal processing by protein kinase C theta and NF-kappa B. J Immunol *172*, 4667-4671.

Stanic, A.K., De Silva, A.D., Park, J.J., Sriram, V., Ichikawa, S., Hirabyashi, Y., Hayakawa, K., Van Kaer, L., Brutkiewicz, R.R., and Joyce, S. (2003). Defective presentation of the CD1d1-restricted natural Va14Ja18 NKT

lymphocyte antigen caused by beta-D-glucosylceramide synthase deficiency. Proc Natl Acad Sci U S A *100*, 1849-1854.

Stetson, D.B., Mohrs, M., Reinhardt, R.L., Baron, J.L., Wang, Z.E., Gapin, L., Kronenberg, M., and Locksley, R.M. (2003). Constitutive cytokine mRNAs mark natural killer (NK) and NK T cells poised for rapid effector function. J Exp Med *198*, 1069-1076.

Strasser, A., Harris, A.W., and Cory, S. (1991). bcl-2 transgene inhibits T cell death and perturbs thymic self-censorship. Cell *67*, 889-899.

Sugita, M., Cao, X., Watts, G.F., Rogers, R.A., Bonifacino, J.S., and Brenner, M.B. (2002). Failure of trafficking and antigen presentation by CD1 in AP-3-deficient cells. Immunity *16*, 697-706.

Tahir, S.M., Cheng, O., Shaulov, A., Koezuka, Y., Bubley, G.J., Wilson, S.B., Balk, S.P., and Exley, M.A. (2001). Loss of IFN-gamma production by invariant NK T cells in advanced cancer. J Immunol *167*, 4046-4050.

Takahashi, T., and Strober, S. (2008). Natural killer T cells and innate immune B cells from lupus-prone NZB/W mice interact to generate IgM and IgG autoantibodies. Eur J Immunol *38*, 156-165.

Thomas, S.Y., Scanlon, S.T., Griewank, K.G., Constantinides, M.G., Savage, A.K., Barr, K.A., Meng, F., Luster, A.D., and Bendelac, A. (2011). PLZF induces an intravascular surveillance program mediated by long-lived LFA-1-ICAM-1 interactions. J Exp Med *208*, 1179-1188.

Thomis, D.C., Gurniak, C.B., Tivol, E., Sharpe, A.H., and Berg, L.J. (1995). Defects in B lymphocyte maturation and T lymphocyte activation in mice lacking Jak3. Science *270*, 794-797.

Thompson, J., Burger, M.L., Whang, H., and Winoto, A. (2010). Protein kinase C regulates mitochondrial targeting of Nur77 and its family member Nor-1 in thymocytes undergoing apoptosis. Eur J Immunol *40*, 2041-2049.

Thompson, J., and Winoto, A. (2008). During negative selection, Nur77 family proteins translocate to mitochondria where they associate with Bcl-2 and expose its proapoptotic BH3 domain. J Exp Med *205*, 1029-1036.

Tomura, M., Yu, W.G., Ahn, H.J., Yamashita, M., Yang, Y.F., Ono, S., Hamaoka, T., Kawano, T., Taniguchi, M., Koezuka, Y., and Fujiwara, H. (1999). A novel function of Valpha14+CD4+NKT cells: stimulation of IL-12 production by antigen-presenting cells in the innate immune system. J Immunol *163*, 93-101.

Townsend, M.J., Weinmann, A.S., Matsuda, J.L., Salomon, R., Farnham, P.J., Biron, C.A., Gapin, L., and Glimcher, L.H. (2004). T-bet regulates the terminal maturation and homeostasis of NK and Vα14*i* NKT cells. Immunity *20*, 477-494.

Tupin, E., Kinjo, Y., and Kronenberg, M. (2007). The unique role of natural killer T cells in the response to microorganisms. Nat Rev Microbiol *5*, 405-417.

Tyznik, A.J., Tupin, E., Nagarajan, N.A., Her, M.J., Benedict, C.A., and Kronenberg, M. (2008). Cutting edge: the mechanism of invariant NKT cell responses to viral danger signals. J Immunol *181*, 4452-4456.

Uldrich, A.P., Crowe, N.Y., Kyparissoudis, K., Pellicci, D.G., Zhan, Y., Lew, A.M., Bouillet, P., Strasser, A., Smyth, M.J., and Godfrey, D.I. (2005). NKT cell stimulation with glycolipid antigen in vivo: costimulation-dependent expansion, Bim-dependent contraction, and hyporesponsiveness to further antigenic challenge. J Immunol *175*, 3092-3101.

Vallabhapurapu, S., Powolny-Budnicka, I., Riemann, M., Schmid, R.M., Paxian, S., Pfeffer, K., Korner, H., and Weih, F. (2008). Rel/NF-kappaB family member RelA regulates NK1.1- to NK1.1+ transition as well as IL-15-induced expansion of NKT cells. Eur J Immunol *38*, 3508-3519.

Van Kaer, L. (2005). α-Galactosylceramide therapy for autoimmune diseases: prospects and obstacles. Nat Rev Immunol *5*, 31-42.

Venkataswamy, M.M., and Porcelli, S.A. (2010). Lipid and glycolipid antigens of CD1d-restricted natural killer T cells. Semin Immunol *22*, 68-78.

Walunas, T.L., Wang, B., Wang, C.R., and Leiden, J.M. (2000). Cutting edge: the Ets1 transcription factor is required for the development of NK T cells in mice. J Immunol *164*, 2857-2860.

Wang, Z.Y., Kusam, S., Munugalavadla, V., Kapur, R., Brutkiewicz, R.R., and Dent, A.L. (2006). Regulation of Th2 cytokine expression in NKT cells: unconventional use of Stat6, GATA-3, and NFAT2. J Immunol *176*, 880-888.

Watarai, H., Sekine-Kondo, E., Shigeura, T., Motomura, Y., Yasuda, T., Satoh, R., Yoshida, H., Kubo, M., Kawamoto, H., Koseki, H., and Taniguchi, M. (2012). Development and function of invariant natural killer T cells producing t(h)2- and t(h)17-cytokines. PLoS Biol *10*, e1001255.

Wei, D.G., Curran, S.A., Savage, P.B., Teyton, L., and Bendelac, A. (2006). Mechanisms imposing the Vbeta bias of Valpha14 natural killer T cells and consequences for microbial glycolipid recognition. J Exp Med *203*, 1197-1207.

Wesley, J.D., Tessmer, M.S., Chaukos, D., and Brossay, L. (2008). NK cell-like behavior of Valpha14i NK T cells during MCMV infection. PLoS Pathog *4*, e1000106.

Wilson, M.T., Johansson, C., Olivares-Villagomez, D., Singh, A.K., Stanic, A.K., Wang, C.R., Joyce, S., Wick, M.J., and Van Kaer, L. (2003). The response of natural killer T cells to glycolipid antigens is characterized by surface receptor down-modulation and expansion. Proc Natl Acad Sci U S A *100*, 10913-10918.

Wu, D.Y., Segal, N.H., Sidobre, S., Kronenberg, M., and Chapman, P.B. (2003). Cross-presentation of disialoganglioside GD3 to natural killer T cells. J Exp Med *198*, 173-181.

Wu, L., and Van Kaer, L. (2009). Natural killer T cells and autoimmune disease. Curr Mol Med *9*, 4-14.

Wu, L., and Van Kaer, L. (2011). Natural killer T cells in health and disease. Front Biosci (Schol Ed) *3*, 236-251.

Wu, Z., Xue, H.H., Bernard, J., Zeng, R., Issakov, D., Bollenbacher-Reilley, J., Belyakov, I.M., Oh, S., Berzofsky, J.A., and Leonard, W.J. (2008). The IL-15 receptor {alpha} chain cytoplasmic domain is critical for normal IL-15Ralpha function but is not required for trans-presentation. Blood *112*, 4411-4419.

Xu, H., Chun, T., Colmone, A., Nguyen, H., and Wang, C.R. (2003). Expression of CD1d under the control of a MHC class Ia promoter skews the development of NKT cells, but not CD8+ T cells. J Immunol *171*, 4105-4112.

Yamaguchi, Y., Motoki, K., Ueno, H., Maeda, K., Kobayashi, E., Inoue, H., Fukushima, H., and Koezuka, Y. (1996). Enhancing effects of (2S,3S,4R)-1-O-(alpha-D-galactopyranosyl)-2-(N-hexacosanoylamino) -1,3,4-octadecanetriol (KRN7000) on antigen-presenting function of antigen-presenting cells and antimetastatic activity of KRN7000-pretreated antigen-presenting cells. Oncol Res *8*, 399-407.

Yoshimoto, T., Bendelac, A., Hu-Li, J., and Paul, W.E. (1995). Defective IgE production by SJL mice is linked to the absence of CD4+, NK1.1+ T cells that promptly produce interleukin 4. Proc Natl Acad Sci U S A *92*, 11931-11934.

Yoshimoto, T., and Paul, W.E. (1994). CD4pos, NK1.1pos T cells promptly produce interleukin 4 in response to in vivo challenge with anti-CD3. J Exp Med *179*, 1285-1295.

Yu, K.O., Im, J.S., Molano, A., Dutronc, Y., Illarionov, P.A., Forestier, C., Fujiwara, N., Arias, I., Miyake, S., Yamamura, T.*, et al.* (2005). Modulation of

CD1d-restricted NKT cell responses by using N-acyl variants of alpha-galactosylceramides. Proc Natl Acad Sci U S A *102*, 3383-3388.

Yu, S., and Cantorna, M.T. (2008). The vitamin D receptor is required for iNKT cell development. Proc Natl Acad Sci U S A *105*, 5207-5212.

Yu, S., and Cantorna, M.T. (2011). Epigenetic reduction in invariant NKT cells following in utero vitamin D deficiency in mice. J Immunol *186*, 1384-1390.

Yuan, J., Crittenden, R.B., and Bender, T.P. (2010). c-Myb promotes the survival of CD4+CD8+ double-positive thymocytes through upregulation of Bcl-xL. J Immunol *184*, 2793-2804.

Yue, X., Izcue, A., and Borggrefe, T. (2011). Essential role of Mediator subunit Med1 in invariant natural killer T-cell development. Proc Natl Acad Sci U S A *108*, 17105-17110.

Zheng, Q., Zhou, L., and Mi, Q.S. (2012). MicroRNA miR-150 Is Involved in Valpha14 Invariant NKT Cell Development and Function. J Immunol *188*, 2118-2126.

Zheng, X., Zhang, H., Yin, L., Wang, C.R., Liu, Y., and Zheng, P. (2008). Modulation of NKT cell development by B7-CD28 interaction: an expanding horizon for costimulation. PLoS One *3*, e2703.

Zhou, D., Mattner, J., Cantu, C., 3rd, Schrantz, N., Yin, N., Gao, Y., Sagiv, Y., Hudspeth, K., Wu, Y.P., Yamashita, T.*, et al.* (2004). Lysosomal glycosphingolipid recognition by NKT cells. Science *306*, 1786-1789.

Zhou, L., Seo, K.H., He, H.Z., Pacholczyk, R., Meng, D.M., Li, C.G., Xu, J., She, J.X., Dong, Z., and Mi, Q.S. (2009). Tie2cre-induced inactivation of the miRNA-processing enzyme Dicer disrupts invariant NKT cell development. Proc Natl Acad Sci U S A *106*, 10266-10271.

Zhou, T., Cheng, J., Yang, P., Wang, Z., Liu, C., Su, X., Bluethmann, H., and Mountz, J.D. (1996). Inhibition of Nur77/Nurr1 leads to inefficient clonal deletion of self-reactive T cells. J Exp Med *183*, 1879-1892.

Zhou, X., Yu, S., Zhao, D.M., Harty, J.T., Badovinac, V.P., and Xue, H.H. (2010). Differentiation and persistence of memory CD8(+) T cells depend on T cell factor 1. Immunity *33*, 229-240.

APPENDIX

LIST OF PUBLICATIONS

1. **Gordy, L.E**., Bezbradica, J.S., Dunkle, A.K., Stanic, A.K., Boothby, M.R., He, Y.W., Van Kaer, L., Joyce, S. (**2011**) IL-15 regulates homeostasis and terminal maturation of NKT cells. *J Immunol*; 187:6335-6345.

2. Boelte, KC, **Gordy, LE**, Joyce, S, Thompson, MA, Yang, L and Lin, PC. (**2011**) Rgs2 mediates pro-angiogenic function of myeloid derived suppressor cells in the tumor microenvironment via upregulation of MCP-1. *PloS One*; 6(4): e18534.

3. Hoek, K.L., **Gordy, L.E.**, Collins, P.L., Parekh, V.V., Aune, T.M., Joyce, S., Thomas, J.W., Van Kaer, L., Sebzda, E. (**2010**) Follicular B cell trafficking within the spleen actively restricts humoral immune responses. *Immunity*; 33(2):254- 265.

4. Joyce, S., **Gordy, LE.** (**2010**) Natural killer T cell-a cat o'nine lives! *EMBO;* 29(9):1475-6.

5. Florence, W.C., Xia, C.,**Gordy, L.E.**, Chen, W., Zhang, Y., Scott-Browne, J.K., Kinjo, Y., Yu, K.O., Keshipeddy, S., Pellicci, D.G., Patel, O., Kjer-Nielsen, L., McCluskey, J., Godfrey, D.I., Rossjohn, J., Richardson, S.K., Porcelli, S.A., Howell, A.R., Haykawa, K., Gapin, L., Zajonc, D.M. Wang, P.G., Joyce, S. (**2009**) Adaptability of the semi-invariant natural killer T-cell

receptor towards structurally diverse CD1d-restricted ligands. *EMBO*; 28(22):3579-3590.

6. Torres, V.J., Stauff, D.L., Pishchany, G., Bezbradica, J.S., **Gordy, L.E.**, Iturregui, J., Anderson, K.L., Duman, P.M., Joyce, S., Skaar, E.P. (**2007**) A *Staphylococcus aureus* regulatory system that responds to host heme and modulates virulence. *Cell Host & Microbe*; 1:109-119.

7. Bezbradica, J.S**.**, **Gordy, L.E**., Stanic, A.K., Dragovic, S., Hill, T., Hawiger, J., Unutmaz, D., Van Kaer, L., Joyce, S. (**2006**) Granulocyte-Macrophage Colony-Stimulating Factor Regulates Effector Differentiation of Invariant Natural Killer T Cells during Thymic Ontogeny. *Immunity*; 25(3):487-497.

IL-15 Regulates Homeostasis and Terminal Maturation of NKT Cells

Laura E. Gordy,* Jelena S. Bezbradica,*,[1] Andrew I. Flyak,* Charles T. Spencer,* Alexis Dunkle,[†] Jingchun Sun,[‡,§] Aleksandar K. Stanic,*,[2] Mark R. Boothby,* You-Wen He,[†] Zhongming Zhao,[‡,§] Luc Van Kaer,* and Sebastian Joyce*

Semi-invariant NKT cells are thymus-derived innate-like lymphocytes that modulate microbial and tumor immunity as well as autoimmune diseases. These immunoregulatory properties of NKT cells are acquired during their development. Much has been learned regarding the molecular and cellular cues that promote NKT cell development, yet how these cells are maintained in the thymus and the periphery and how they acquire functional competence are incompletely understood. We found that IL-15 induced several Bcl-2 family survival factors in thymic and splenic NKT cells in vitro. Yet, IL-15–mediated thymic and peripheral NKT cell survival critically depended on Bcl-x_L expression. Additionally, IL-15 regulated thymic developmental stage 2 to stage 3 lineage progression and terminal NKT cell differentiation. Global gene expression analyses and validation revealed that IL-15 regulated *Tbx21* (T-bet) expression in thymic NKT cells. The loss of IL-15 also resulted in poor expression of key effector molecules such as IFN-γ, granzyme A and C, as well as several NK cell receptors, which are also regulated by T-bet in NKT cells. Taken together, our findings reveal a critical role for IL-15 in NKT cell survival, which is mediated by Bcl-x_L, and effector differentiation, which is consistent with a role of T-bet in regulating terminal maturation. *The Journal of Immunology*, **2011, 187: 6335–6345.**

Natural killer T cells are thymus-derived lymphocytes whose functions are regulated by foreign or self-glycolipid ligands presented by CD1d molecules. Most NKT cells recognize Ag with a semi-invariant TCR consisting of an invariant mouse Vα14Jα18 (human Vα24Jα18) α-chain that pairs with a Vβ8.2 (human Vβ11), Vβ7, or Vβ2 β-chain. Upon agonistic ligand recognition, NKT cells rapidly secrete large amounts of immunoregulatory cytokines and upregulate costimulatory molecules to initiate and modulate the effector functions of myeloid and lymphoid cells. By doing so, NKT cells regulate microbial and tumor immunity as well as autoimmune diseases (1, 2). NKT cells acquire these immunoregulatory properties during ontogeny through poorly understood processes. NKT cell frequency varies both between mouse strains, the highest in BALB/c (1–2 million in thymus, liver, and spleen) and lowest in the autoimmune disease-predisposed strains NOD and SJL (0.1–0.3 million), and between healthy human individuals, ranging from 0.01–5.0% in peripheral blood (3). Hence, understanding how NKT cells develop, regulate their frequency, and acquire functional potential is critical for designing NKT cell-based therapies.

NKT cells develop in the thymus and acquire markers typical of NK and activated/memory T cells as they mature (3). NKT cell precursors ($CD24^{int}CD69^{+}CD44^{-}NK1^{-}$; stage [ST]0) emerge from CD4 and CD8 double-positive (DP) thymocytes soon after expression of the semi-invariant TCR in a process requiring three transcription factors: HEB, a basic helix-loop-helix E protein; retinoic acid-related orphan receptor γt; and c-Myb (4–7). Precursor ST0 cells proliferate extensively in a c-Myc–dependent manner (8, 9) and undergo positive selection through heterotypic interactions between the semi-invariant TCR and CD1d molecules expressed by DP thymocytes (1, 3). Further development and differentiation into ST1 ($CD24^{-}CD44^{-}NK1.1^{-}$), ST2 ($CD24^{-}CD44^{+}NK1.1^{-}$), and to fully functional ST3 ($CD24^{-}CD44^{+}NK1.1^{+}$) NKT cells require transcriptional regulation by promyelocytic leukemia zinc finger (PLZF) (10, 11), c-Myb (7), NF-κB/Rel-A (12–15), Egr-2 (16), Gata-3 (17–19), and T-bet (17, 20), as well as sustained homotypic interactions between the signaling lymphocyte activation molecule (SLAM) family members Slamf1 and Slamf6 (21) by a mechanism involving the SAP and Fyn signaling module (22–26). Furthermore, effector differentiation, which is ontogenetically coupled in NKT cells, is regulated by Itk (27), NF-κB (28), T-bet (20, 29), Egr-2 (16), Th-POK (30), and CSF-2 (31). Upon lineage commitment and the emergence of ST0 NKT precursors and through subsequent stages of differentiation and maturation, thymic and peripheral NKT cells are maintained by complex yet poorly understood homeostatic mechanisms involving NF-κB (28), RelA (15), CYLD (32), c-Myc (8, 9), CD122 (33), γc (34), IL-7Rα (34), IL-15 (35, 36), IL-15Rα (37, 38), IRF-1 (39), calcineurin (16), Egr-2 (16), and Id2 (40).

*Department of Pathology, Microbiology and Immunology, Vanderbilt University School of Medicine, Nashville, TN 37232; [†]Department of Immunology, Duke University, Durham, NC 27710; [‡]Department of Biomedical Informatics, Vanderbilt University School of Medicine, Nashville, TN 37232; and [§]Department of Cancer Biology, Vanderbilt University School of Medicine, Nashville, TN 37232

[1]Current address: Department of Immunobiology, Yale University School of Medicine, New Haven, CT.

[2]Current address: Vincent Center for Reproductive Biology, Massachusetts General Hospital, Harvard Medical School, Boston, MA.

Received for publication December 9, 2010. Accepted for publication October 18, 2011.

This work was supported by National Institutes of Health training (HL069765 and AI007611), research (AI042284, AI016721, AI070305, HL089667, AI068149, AI074754, and AI064639), and core (CA068485 and DK058404) grants.

The microarray data presented in this article have been submitted to the Gene Expression Omnibus (http://www.ncbi.nlm.nih.gov/geo/query/acc.cgi?token=dtgxpkoosiokmpm&acc=) under accession number GSE32568.

Address correspondence and reprint requests to Prof. Sebastian Joyce, Vanderbilt University Medical Center, A4223 Medical Center North, 1161 21st Avenue South, Nashville, TN 37232-2363. E-mail address: sebastian.joyce@vanderbilt.edu

The online version of this article contains supplemental material.

Abbreviations used in this article: CT, threshold cycle; DP, double-positive; αGalCer, α-galactosylceramide; IL-15^{0}, IL-15–deficient; PLZF, promyelocytic leukemia zinc finger; qPCR, quantitative PCR; rh, recombinant human; SLAM, signaling lymphocyte activation molecule; ST, stage; wt, wild-type.

www.jimmunol.org/cgi/doi/10.4049/jimmunol.1003965

During differentiation, NKT cells acquire the ability to produce IL-4 (ST1), IL-4 and IFN-γ (ST1 and ST2), or IL-4^{LO} and IFN-γ^{HI} (ST3) in response to TCR stimulation (27, 41), and secretion of these cytokines is regulated by CSF-2 (31). At ST2 and ST3, NKT cells also acquire memory T cell markers (CD44^{HI}, CD62L^{LO}) as well as NK cell markers (NKG2D, Ly49, and NK1.1) and cytolytic function (granzyme B and perforin) (1, 42). Although a substantial fraction of ST2 cells remains in the thymus and matures to ST3, a small fraction egresses from the thymus and immigrates into the spleen and liver, whereupon further maturation occurs (41, 43, 44). Migration to these peripheral sites depends on CXCR6 (45), whereas continued development and maintenance in the liver require LFA-1 (46) and Id2 (40). Even though mature thymic and splenic NKT cells are phenotypically similar, they behave as distinct functional populations at these sites because the developmental cues and perhaps the agonistic ligands are distinct at different sites (44, 47, 48). Thus, unlike conventional T lymphocytes, which undergo complete ontogenetic maturation in the thymus but commit to effector differentiation only upon Ag recognition in the periphery, NKT cells complete both these processes within and outside the thymus. The instructive signals that differentially regulate the maturation and acquisition of effector functions of NKT cells remain poorly understood.

IL-15 is a pleiotropic cytokine that regulates the development and maintenance of several subsets of innate-like lymphocytes, including γδ T, CD8αα T, NK, and NKT cells (49). Furthermore, IL-15 signals the ontogeny, effector differentiation, and Mcl-1–dependent survival of NK cells (50). Moreover, thymic and peripheral NKT cells develop poorly in IL-15–deficient (IL-15^0) mice (35, 36). In the periphery, this is due to impaired NKT cell homeostatic proliferation (36). In the thymus, NKT cell proliferation appears intact, yet IL-15^0 mice develop a severe blockade in NKT cell ontogeny at ST2, with leaky progression to ST3 (36). What role IL-15 signals play during thymic NKT cell ontogeny and whether IL-15 is essential for NKT cell functional maturation in the periphery remain unknown.

In this study, we provide evidence that thymic and peripheral NKT cell survival critically depends on IL-15. One important downstream target of IL-15 appears to be Bcl-x_L. Furthermore, we describe a new function for IL-15 by which it regulates ST2 to ST3 lineage progression and terminal NKT cell maturation, which is consistent with a role of T-bet in regulating ST2 to ST3 transition and terminal differentiation.

Materials and Methods

Mice

B6–IL-15^0, B6.129–IL-7α^0, B6.Jα18^0, and B6.129-CD1dTD mice (34, 35, 51–53) were generous gifts from J. Peschon (Immunex), M. Taniguchi (RIKEN), and A. Bendelac (University of Chicago), respectively. B6–IL-15^0 and B6.129–IL-7Rα^0 mice were bred with B6-Eμ36–Bcl-2^{tg} (54) and C-Lck–Bcl-x_L^{tg} (55) mice. B6.C–IL-15^0;Bcl-x_L^{tg} mice were backcrossed to B6–IL-15^0 mice for six generations. All mouse crosses and experiments were performed under approval by Institutional Animal Care and Use Committee protocols.

Abs and reagents

All Abs used for the identification of NKT cells were from BD Pharmingen as described (56). Anti-BrdU–Alexa 647 (PRB-1; Invitrogen); anti-human Bcl-x_L–PE and IgG3 isotype control-PE (7B25 and B10; Southern Biotechnology Associates); anti-mouse Bcl-2–PE (3F11) and Armenian hamster IgG1κ isotype control-PE (A19-3), anti-human Bcl-2–PE (6C8) and Armenian hamster IgG2λ isotype control-PE (Ha4/8), anti–Mcl-1 rabbit polyclonal (Rockland); chicken anti-rabbit–Alexa 647 (Invitrogen); anti–T-bet–Alexa 647 (eBio4B10) and mouse IgG1 isotype control-Alexa 647 (P3; eBioscience); anti–Gata-3–Alexa 647 (L50-823) and mouse IgG1κ isotype control-Alexa 647 (MOPC-21; Santa Cruz Biotechnology); and mouse IgG1 isotype control and anti-mouse IgG-FITC (eBioscience) Abs were purchased. α-galactosylceramide (αGalCer; KRN7000) was generously provided by Kirin Brewery Company (Gunma, Japan) or purchased from Funakoshi (Tokyo, Japan). Mouse αGalCer-loaded CD1d monomers were obtained from the National Institutes of Health Tetramer Facility (Emory University). Preparation of αGalCer-loaded CD1d tetramers from monomer and their use are described elsewhere (56).

Flow cytometry

Abs and staining procedures for the identification of NKT cells were as described elsewhere (56). NKT cells were identified as CD3ε$^+$tetramer$^+$ cells among B220^{LO} splenocytes and hepatic mononuclear cells or CD8^{LO} thymocytes. Four-color flow cytometry was performed with a FACSCalibur instrument (BD Biosciences), whereas seven-color flow cytometry was performed with an LSR II instrument (BD Biosciences). Data were analyzed with FlowJo software (Tree Star). Absolute NKT cell numbers were calculated from the percentage of tetramer$^+$ cells and total number of cells recovered from each organ.

Ex vivo stimulation of thymocytes and splenocytes with IL-15

Thymocytes and splenocytes were stimulated in vitro with 100 ng/ml recombinant human (rh)IL-15 (Miltenyi Biotec) for 5 d. Cells were then collected and stained with specific mAb for intracellular expression of Bcl-2, Bcl-x_L, and Mcl-1.

Cytokine responses

Individual age-matched (6–10-wk-old) mice were injected i.p. with 5 μg αGalCer or vehicle (0.1% Tween-20 in PBS) as controls. After 4 h, serum, splenocytes, and hepatic mononuclear cells were prepared. Cells were stained with anti-CD3ε mAb, tetramer, and anti–IFN-γ or –IL-4 mAb and analyzed by flow cytometry. Sandwich ELISA was performed as described (56) to monitor serum cytokine response.

Cells were fixed and permeabilized with Cytofix/Cytoperm solution for intracellular staining or with Cytofix/Cytoperm Plus (both from BD Pharmingen) for intranuclear BrdU staining according to the manufacturer's protocol. Staining for intracellular IFN-γ and IL-4 also used GolgiStop (BD Pharmingen). Staining for intracellular T-bet and Gata-3 used the Foxp3 staining buffer kit (eBioscience). Intracellular and intranuclear staining was performed according to the manufacturer's protocol.

Thymocyte sorting

Thymic NKT cells were enriched by magnetic sorting using a Pan-T cell isolation kit in combination with CD8 beads (Miltenyi Biotec) as instructed by the manufacturer. Enriched NKT cells from 5–10 mice were pooled and further purified by flow sorting CD3ε$^+$tetramer$^+$ cells (FACSAria; BD Biosciences). CD4 and CD8 DP thymocytes were flow sorted as above. Freshly purified NKT cells and DP thymocytes were >98% pure as judged by CD3ε$^+$tetramer$^+$ and CD4/CD8-specific staining (data not shown).

RNA preparation, microarray hybridization, and analyses

Freshly purified NKT cells were washed and lysed by passage through a Qiashedder column (Qiagen). Total RNA was extracted per the manufacturer's instructions (RNeasy; Qiagen). RNA yield was quantified spectrophotometrically (Nanodrop ND-1000; Nanodrop) and aliquots electrophoresed to determine sample purity and concentration (Agilent 2100 Bioanalyzer; Agilent Technologies). Microarray hybridizations were performed using one-color hybridization on a SurePrint G3 Mouse GE 60K Microarray (Agilent Technologies) by the Functional Genomics and Shared Resources Core (Vanderbilt University). Scanning was performed using a GenePix 4000B Microarray Scanner (Molecular Devices). The resulting images were processed with Agilent Feature Extraction software (Agilent Technologies) to generate raw probe intensity data, which was subsequently normalized by the quantile method (57). Differential expression analysis was carried out with an empirical Bayes approach on a linear model using the limma package (58, 59). In this study, we defined differentially expressed genes as those for which the $\log_2$ fold change values were ≥1.5 or ≤−1.5 and for which nominal p values were <0.001 (60). Next, we performed hierarchical clustering of the differentially expressed genes using the R AMAP Package (http://cran.r-project.org/web/packages/amap/). The microarray data are available at the Gene Expression Omnibus (http://www.ncbi.nlm.nih.gov/geo/query/acc.cgi?token=dtgxpkoosiokmpm&acc=) under accession number GSE32568.

Real-time quantitative PCR

RNA was reverse transcribed with MuLV RT Reverse Transcriptase (Applied Biosystems) according to the manufacturer's protocol. Quantitative PCR (qPCR) was performed in the presence of IQ RealTime Sybr Green PCR Supermix and target gene-specific primers (Supplemental Table I) in an iQ5 thermocycler (Bio-Rad). Results were analyzed using iQ5 software (Bio-Rad). Data were first normalized against β-actin control. As the threshold cycle (CT) values are obtained as $\log_2$ values, the normalized Δ CT values of wild-type (wt) samples were subtracted from normalized Δ CT values of IL-15^0 samples. The resulting $\log_2$ ΔΔ CT values were transformed yielding relative expression, which enabled comparison between NKT cells isolated from the two strains. For this, the IL-15^0 sample, called the Calibrator, was set to 1 and relative expression calculated as fold change in gene expression in wt NKT cells relative to the Calibrator.

TCRα rearrangement

cDNA was prepared from total RNA isolated from DP thymocytes. qPCR for *Vα14* to *Jα18* rearrangement was performed as described above using the following forward (^{F}) and reverse (^{R}) primers: $V\alpha14^F$ (5′-AGGTCTT GTGTCCCTGACAG-3′), $J\alpha18^R$ (5′-CAGGTATGACAATCAGCTGAGT-CC-3′), $V\alpha8^F$ (5′-TCACAGACAACAAGAGGACC-3′), and $J\alpha5^R$ (5′-AGTGAGCTGCCCCACAACCT-3′). PCR products were separated by agarose gel electrophoresis and visualized by ethidium bromide staining.

Statistics

Comparisons of normally distributed continuous data were performed by one-way ANOVA with Tukey's posttest to determine significance. The significance of gene expression analyzed by qPCR was determined by unpaired *t* test. Statistical significance of *Vα14-Jα18* rearrangement by

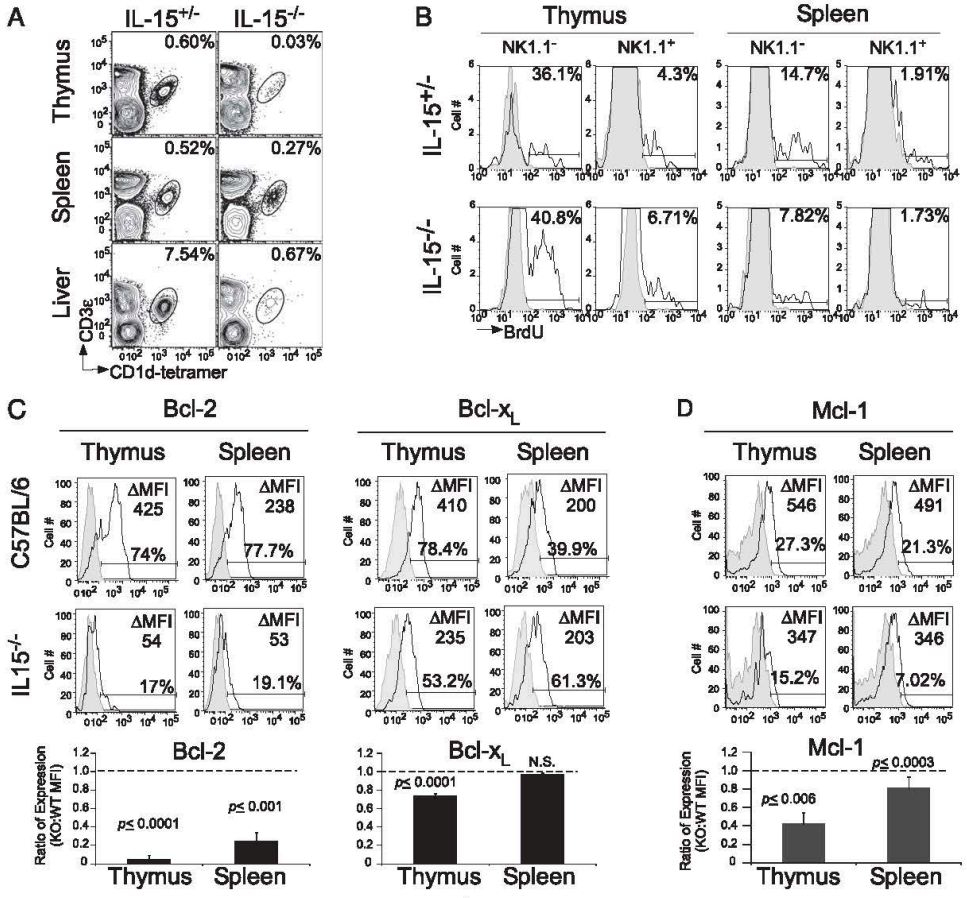

FIGURE 1. Defective NKT cell development and maintenance in IL-15^0 mice. *A*, Thymic, splenic, and hepatic NKT cells from B6 ($n = 13$) and B6–IL-15^0 ($n = 9$) mice were identified as $CD3\varepsilon^+$tetramer$^+$ cells within electronically gated $CD8^{LO}$ thymic, $B220^{LO}$ splenic, or liver mononuclear cells. Numbers are percent NKT cells among total leukocytes within each organ. Data are representative of nine independent experiments. *B*, B6 and B6–IL-15^0 mice were injected i.p. with 2 mg BrdU daily for 3 consecutive d and sacrificed 1 d later. BrdU incorporation was determined by flow cytometry after extracellular lineage-specific staining and intracellular labeling with anti-BrdU Alexa 647 mAb. Overlaid histograms are of NKT cells identified as in *A* from vehicle (shaded) or BrdU injected (open) mice. The histograms show the expression levels of BrdU within $NK1.1^{NEG}$ (*left panels*) and $NK1.1^+$ (*right panels*) NKT cells within the thymus and spleen. Data are representative of three independent experiments. $n = 6$. *C* and *D*, Thymic and splenic mononuclear cells from B6 and B6–IL-15^0 mice were assessed for intracellular expression of Bcl-2, Bcl-x_L (*C*), and Mcl-1 (*D*) detected with specific mAb within electronically gated $B220^{LO}CD3\varepsilon^+$tetramer$^+$ cells. Numbers refer to the difference in mean fluorescence intensity (ΔMFI) between isotype control (shaded) and specific mAb (open) staining. Data are representative of three independent experiments. $n = 5$. The flow data were acquired on two different instruments (FACSCalibur and LSR-II; BD Biosciences) in different experiments. Even though the actual MFI varied, the represented trend remained the same nonetheless. Therefore, we have chosen to represent the ratio of expression between wt and IL-15^0 NKT cells. The ratio of Bcl-2, Bcl-x_L, and Mcl-1 expression by IL-15^0 (KO) and wt NKT cells is shown. A ratio of ~1 indicates no difference in expression; a ratio <1 indicates lower expression in IL-15^0 NKT cells.

qPCR was calculated by two-tailed, unpaired *t* test. Comparisons were performed using Prism software (GraphPad).

Results

IL-15 induces Bcl-2 family survival factors within thymic but not peripheral NKT cells

Previous reports demonstrated that NKT cell frequency is significantly lower in mice lacking IL-15 compared with wt mice due to altered NKT cell homeostasis within the thymus and spleen (35, 36). Although IL-15 regulates proliferation of splenic NKT cells, its role in homeostasis of the thymic subset has remained unclear (36). A re-evaluation confirmed that NKT cell frequency was altered in the absence of IL-15, and, hence, their numbers were reduced in the thymus, spleen, and liver (Fig. 1*A*). Likewise, in vivo BrdU incorporation experiments revealed that splenic but not thymic NKT cell proliferation was impaired in IL-15^0 mice (Fig. 1*B*). These data indicate that, in addition to its role in cell proliferation, IL-15 plays another role(s) during thymic NKT cell ontogeny.

Previous studies have suggested that IL-15 induces antiapoptotic Bcl-2 family members, including Bcl-2, Bcl-x_L, and Mcl-1, to prevent apoptosis and regulate homeostasis in vivo (49). For example, IL-15 promotes the survival of NK cells by inducing the survival factor Mcl-1 (50). An examination of the expression of the Bcl-2 family of survival factors by flow cytometry revealed that intracellular Bcl-2 expression was dramatically reduced in IL-15^0 thymic and splenic NKT cells (Fig. 1*C*). Although not as dramatic, intracellular Bcl-x_L and Mcl-1 expression levels were also reduced either in thymic (Bcl-x_L) or in both thymic and splenic (Mcl-1) IL-15^0 NKT cells when compared with wt NKT cells (Fig. 1*C*, 1*D*).

To test whether IL-15 induces survival factors in NKT cells, wt thymocytes and splenocytes were cultivated in the absence or presence of exogenous rhIL-15 for 5 d. Bcl-2, Bcl-x_L, and Mcl-1 expression in fresh or cultivated NKT cells (with or without rhIL-15) was evaluated using flow cytometry. Both fresh NKT cells and those cultivated without rhIL-15 were included as controls because expression of these survival factors changes during the 5-d culture. The data revealed that IL-15 upregulated the expression of Bcl-2 and Bcl-x_L but not Mcl-1 in thymic NKT cells to levels above those expressed by freshly isolated NKT cells (Fig. 2*A*, 2*B*). Very few NKT cells cultivated without IL-15 expressed the three survival factors, and, hence, when compared with this control, IL-15 also appeared to induce Mcl-1 expression in thymic NKT cells (Fig. 2*B*). IL-15 also modestly induced Bcl-2 and Bcl-x_L expression within splenic NKT cells but not to the levels found in freshly isolated NKT cells; their expression was above control NKT cells cultured in medium without rhIL-15 (Fig. 2*A*). These data indicate that IL-15 has the potential to induce or maintain the expression of survival factors of the Bcl-2 family in thymic or splenic NKT cells, respectively, and, hence, to support NKT cell survival during development.

Bcl-x_L overexpression in IL-15^0 mice supports NKT cell survival

We took a genetic approach to further investigate the role of IL-15–induced genes in the survival of thymic and peripheral NKT cells.

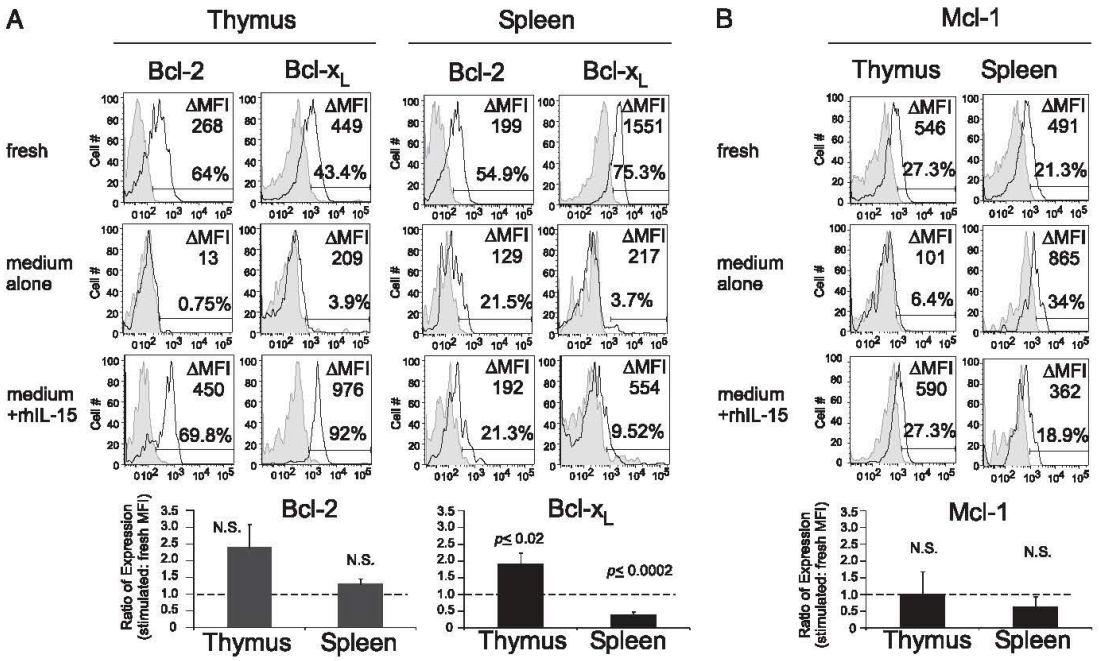

FIGURE 2. IL-15 upregulates expression of the survival factors Bcl-2, Bcl-x_L, and Mcl-1 within thymic and splenic NKT cells. Thymic and splenic mononuclear cells from B6 mice were cultivated in vitro in the absence or presence of 100 ng/ml of rhIL-15. After 5 d, intracellular expression of Bcl-2, Bcl-x_L (*A*), and Mcl-1 (*B*) was detected with specific mAb within electronically gated B220^{LO}CD3e$^+$tetramer$^+$ cells. Numbers refer to the ΔMFI between isotype control (shaded) and specific mAb (open). Data are representative of three independent experiments. $n = 5$. As for Fig. 1, the flow data were acquired on two different instruments in different experiments. Hence, the ratio of IL-15–induced Bcl-2, Bcl-x_L, and Mcl-1 expression within NKT cells in comparison with unstimulated, freshly isolated NKT cells is shown. A ratio of <1 indicates no induction; a ratio >1 indicates IL-15–induced expression.

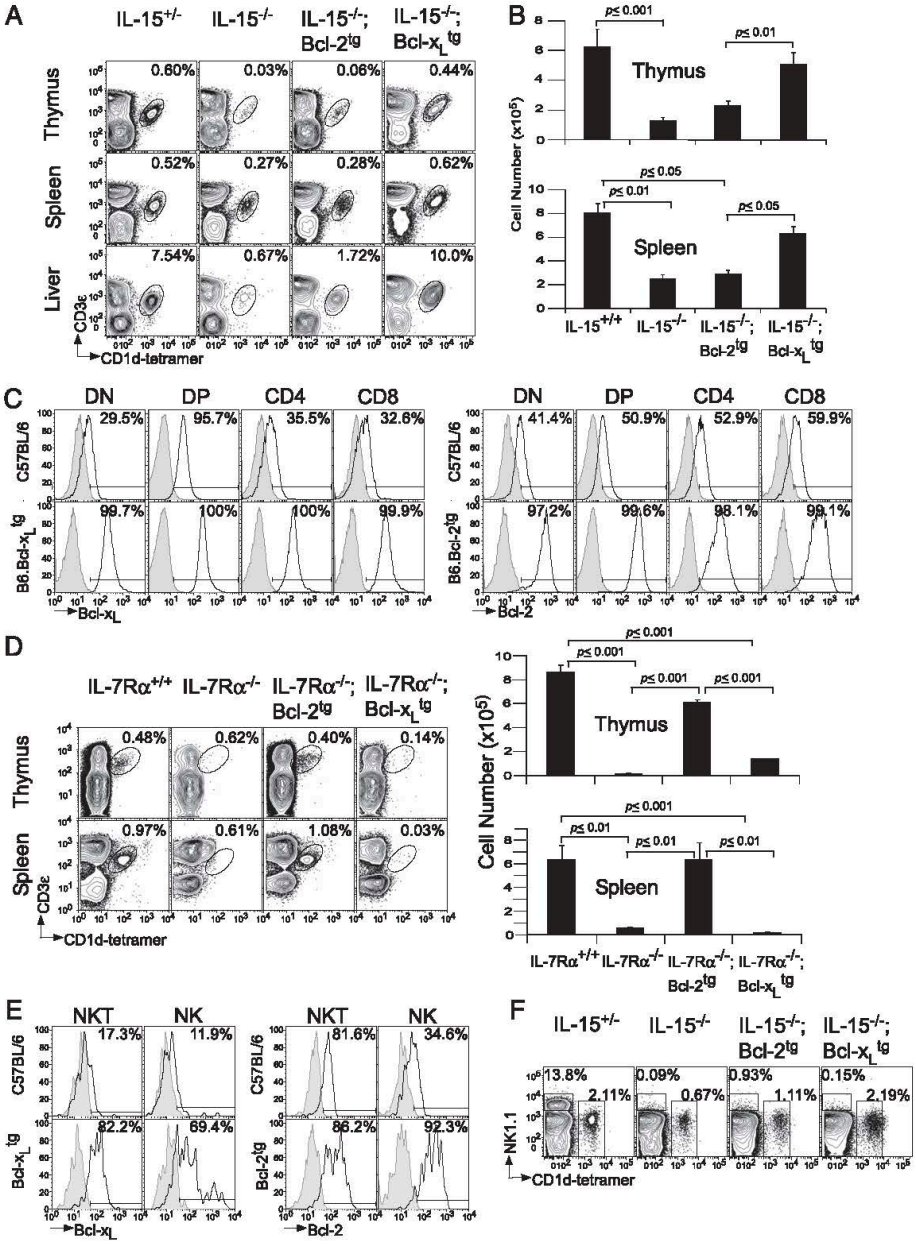

FIGURE 3. Bcl-x_L overexpression restores NKT cell development in IL-15^0 mice. *A*, Thymic, splenic, and hepatic NKT cells from B6 ($n = 8$), B6–IL-15^0 ($n = 10$), B6–IL-15^0;Bcl-2^{tg} ($n = 6$), and B6–IL-15^0;Bcl-x_L^{tg} ($n = 16$) mice were identified as CD3ε$^+$tetramer$^+$ cells within electronically gated $CD8^{LO}$ thymic, $B220^{LO}$ splenic, or liver mononuclear cells. Numbers are percent NKT cells among total leukocytes. *B*, Absolute numbers of NKT cells in the thymus and spleen of B6, B6–IL-15^0, B6–IL-15^0;Bcl-2^{tg}, and B6–IL-15^0;Bcl-x_L^{tg} mice were calculated from percent NKT cells in *A* and total cell count. Data are representative of six independent experiments showing mean + SEM; *n*, as in *A*. The *p* value was calculated by one-way ANOVA with Tukey's posttest. *C*, Intracellular expression of the hBcl-x_L and hBcl-2 transgene within double-negative, DP, $CD4^+CD8^{NEG}$, and $CD8^+CD4^-$ thymocytes of B6.C-Bcl-x_L^{tg} (*right panels*) and B6.Bcl-2^{tg} (*left panels*) mice. Overlaid histograms represent isotype control (shaded) and specific mAb (open). Data are representative of three independent experiments. $n = 5$. *D*, Thymic and splenic NKT cells from IL-7Rα$^{+/-}$ ($n = 3$), IL-7Rα^0 ($n = 3$), IL-7Rα^0;Bcl-2^{tg} ($n = 3$), and IL-7Rα^0;Bcl-x_L^{tg} ($n = 2$) mice were identified as CD3ε$^+$tetramer$^+$ cells within electronically gated $CD8^{LO}$ thymocytes or $B220^{LO}$ splenocytes and liver mononuclear cells. Numbers are percent NKT cells among total leukocytes. Absolute NKT cell number (mean + SEM) was calculated from percent NKT cells and total mononuclear cell number. Data are representative of two independent experiments. Note that because IL-7Rα^0 thymic size is small due to low cellularity, percent NKT cells appears artificially high despite extremely low NKT cell numbers. The *p* value was calculated by one-way ANOVA with Tukey's posttest. *E*, Intracellular expression of the hBcl-x_L and hBcl-2 transgenes within NKT and NK cells of B6.C-Bcl- (*Figure legend continues*)

Thus, *Bcl-2* and *Bcl-xl* transgenes were independently introgressed into IL-15^0 mice. Analysis of the resulting mice at age 6–8 wk, when thymic and splenic cellularity is similar between the different strains, revealed that enforced Bcl-x_L but not Bcl-2 overexpression rescued the frequency and absolute numbers of thymic, splenic, and hepatic NKT cells in IL-15^0 mice (Fig. 3*A*, 3*B*).

Because the *Bcl2* (*Ig*μ) and *Bclxl* (p*Lck*) transgenes are under the control of different promoters (54, 55), we assessed the expression patterns of both transgenes within different thymocyte subsets. The data revealed that both transgenes were expressed as early as the CD4$^-$CD8$^-$ double-negative stage of development, through the DP stage, and within CD4 and CD8 single-positive thymocytes (Fig. 3*C*). Consistent with Bcl-2 expression during early thymocyte development, *Bcl-2* transgene introgression into IL-7Rα null mice, which poorly if at all develop conventional T and NKT cells (34, 61), rescued the development of both lineages (Fig. 3*D*). Therefore, the failure of Bcl-2 overexpression to restore NKT cell numbers in IL-15^0 mice was not due to the lack of proper transgene expression or functionality, but most likely due to the fact that Bcl-2 plays a minor role when compared with Bcl-x_L in conveying IL-15 signals for NKT cell survival. Together, the above data indicate that IL-15 relays specific, Bcl-x_L–dependent survival signals during NKT cell ontogeny.

A previous study reported that IL-15–induced Mcl-1 specifically supported NK cell survival in vivo and in vitro (50) and that overexpression of Bcl-2 in mice lacking IL-2Rβ, the common β-chain of IL-2R and IL-15R, or in IL-15^0 mice repopulates NK cells in vivo (62, 63). Because NKT and NK cells are closely related innate-like lymphocyte lineages and because both lineages use IL-15 for survival, we ascertained whether IL-15 induces survival of the two cell types by similar mechanism(s). This question was addressed because *Bcl-2* and *Bcl-x_L* transgenes were expressed in NK cells from B6–Bcl-2^{tg} and C-Bcl-x_L^{tg} mice (Fig. 3*E*). We found that, as previously reported (62, 63), Bcl-2 partially rescued hepatic but not splenic NK cells. Nonetheless, Bcl-x_L overexpression rescued NKT but not hepatic or splenic NK cells in IL-15^0 mice (Fig. 3*F*), which is consistent with the reported model in which NK cells predominantly use Mcl-1 for IL-15–induced survival (50). Thus, IL-15 appears to regulate survival of distinct lineages in a unique, cell type-specific manner, with Bcl-x_L serving as an IL-15–induced survival factor for NKT cells.

Because Bcl-x_L is required for DP thymocyte survival and *Vα14* to *Jα18* rearrangement (4), it is possible that IL-15^0 DP thymocytes poorly rearrange these distal gene segments, thereby resulting in low NKT cell numbers. To test this, *Vα14* to *Jα18* rearrangement within DP thymocytes flow sorted from wt, IL-15^0, Jα18^0, and CD1dTD mice, which rearrange *Vα14* to *Jα18* gene segments but are deficient in positive selection of NKT cells (52), was quantified. No defect in the canonical *Vα14* to *Jα18* rearrangement was seen in IL-15^0 DP thymocytes (Fig. 4). Likewise, the more distal *Vα8* to *Jα5* rearrangement was also unaffected in IL-15^0 DP thymocytes as gauged by nonquantitative PCR (Fig. 4*B*). Interestingly, however, ~1.5-fold higher *Vα14* to *Jα18* rearrangement was observed in DP thymocytes of IL-15^0;Bcl-x_L^{tg} mice (Fig. 4*A*), which was statistically insignificant. This result suggests that any increase in the initial pool of NKT cell precursors in DP thymocytes of IL-15^0;Bcl-x_L^{tg} mice less likely led to increased numbers of NKT cells in these mice.

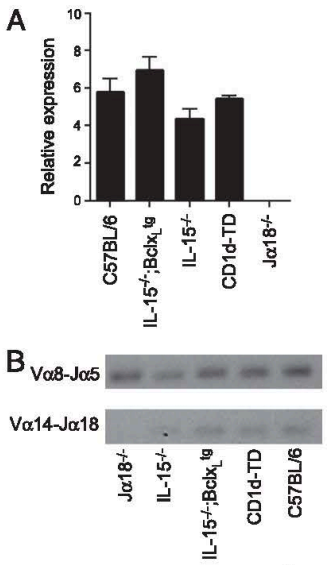

FIGURE 4. Normal TCRα rearrangement in IL-15^0 mice. *A*, *Vα14*-to-*Jα18* rearrangement within DP thymocytes flow sorted from the indicated strains was assessed by real-time qPCR and represented as mean + SD of two independent experiments. β-actin was used as the internal control for normalization. The p value calculated by two-tailed, unpaired t test indicated that *Vα14*-to-*Jα18* rearrangement in B6, B6–IL-15^0, and B6–IL-15^0; Bcl-x_L^{tg} DP thymocytes was significant only when compared with that in B6-Jα18^0 DP cells. The ~1.5-fold increased *Vα14*-to-*Jα18* rearrangement seen in B6–IL-15^0;Bcl-x_L^{tg} DP thymocytes compared with the others was statistically insignificant ($p < 0.0997$). *B*, RT-PCR assessment of *Vα8*-to-*Jα5* and *Vα14*-to-*Jα18* rearrangements. Data are representative of two experiments.

IL-15 regulates terminal maturation of NKT cells

Because IL-15 deficiency reduced the numbers of thymic CD44$^+$ NK1.1$^-$ ST2 and CD44$^+$NK1.1$^+$ ST3 NKT cells, and because forced Bcl-x_L overexpression in IL-15^0 mice rescued total thymic and peripheral NKT cell numbers (Fig. 3), whether IL-15 has additional roles in NKT cell ontogeny was ascertained. Therefore, we determined whether IL-15 regulates terminal maturation of developing NKT cells as well, particularly at ST3, in which NKT cells acquire most of their NK cell-like effector functions. Thus, the phenotype of IL-15^0;Bcl-x_L^{tg} NKT cells was compared with wt and IL-15^0 NKT cells. Surprisingly, akin to IL-15^0 NKT cells, phenotypic ST2 to ST3 transition, as measured by acquisition of the NK1.1 surface marker, was still partially impaired in IL-15^0;Bcl-x_L^{tg} mice (Fig. 5*A*, 5*B*), despite near wt numbers of NKT cells in these mice. Additional phenotypic analyses revealed that expression patterns of few other mature NKT cell markers, such as NKG2D, Ly6C, CD69, and Ly49C/I, reflected those of thymic NKT cells that were blocked at ST2 (Fig. 5*C*), as these markers are predominantly expressed by NK1.1$^+$ NKT cells (Fig. 6*A*). Of those markers, the expression of Ly6C was also altered in hepatic but not splenic NKT cells in IL-15^0 and IL-15^0;Bcl-x_L^{tg} mice (Fig. 5*C*). Thus, IL-15 is required not only for lineage sur-

x_L^{tg} and B6.Bcl-2^{tg} mice. Overlaid histograms represent isotype control (shaded) and specific mAb (open) staining. Data are representative of two independent experiments; n, as in *C*. *F*, Splenic and hepatic NK and NKT cells from B6 ($n = 6$), B6–IL-15^0 ($n = 7$), B6–IL-15^0;Bcl-2^{tg} ($n = 4$), and B6–IL-15^0; Bcl-x_L^{tg} ($n = 10$) mice were identified as NK1.1$^+$tetramer^{NEG} and NK1.1$^+$tetramer$^+$ cells, respectively, within electronically gated B220^{LO} splenic or hepatic mononuclear cells. Data are representative of four independent experiments.

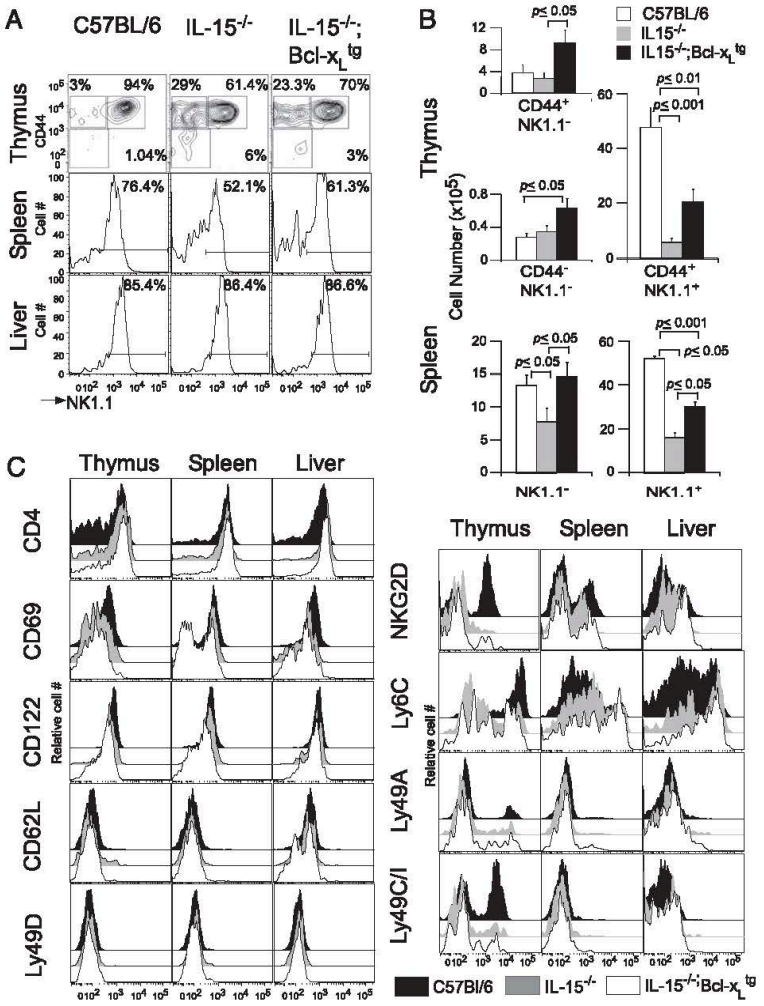

FIGURE 5. IL-15 regulates terminal maturation of NKT cells. *A*, NKT cell developmental stages in B6 (n = 9), B6–IL-15^0 (n = 6), and B6–IL-15^0;Bcl-x_L^{tg} (n = 13) mice were identified as CD44^{NEG} NK1.1^{NEG} ST1, CD44$^+$NK1.1^{NEG} ST2, or CD44$^+$NK1.1$^+$ ST3 in the thymus or as NK1.1^{NEG}tetramer$^+$ or NK1.1$^+$tetramer$^+$ within the splenic and hepatic mononuclear cells. Numbers are percentage of cells among total NKT cells. Data are representative of six independent experiments. *B*, Absolute numbers of thymic NKT cells within ST1, ST2, and ST3 were calculated as in Fig. 3*D*. Data are representative of six independent experiments showing the mean + SEM; n, same as in *A*. The p value was calculated by one-way ANOVA with Tukey's posttest. *C*, Expression of lineage-specific markers by thymic, splenic, and hepatic NKT cells from B6 (n = 6), B6–IL-15^0 (n = 6), and B6–IL-15^0;Bcl-x_L^{tg} (n = 6) mice as determined by flow cytometry after staining with specific mAb. Data are representative of three independent experiments.

vival but also for terminal maturation of NKT cells, especially of the thymic subset. Furthermore, the differential requirement for IL-15 in terminal differentiation (e.g., acquisition of Ly6C, NK1.1) of some (thymic and/or hepatic) but not all (splenic) NKT cells suggests that distinct signals instruct NKT cell maturation in distinct lymphoid organs.

IL-15 regulates multiple gene expression changes during ST2 to ST3 NKT cell transition

To define the mechanism by which IL-15 regulates terminal maturation of thymic NKT cells, microarray experiments were performed. For this, wt and IL-15^0 thymic NKT cells were flow sorted, and the derived RNA was subjected to hybridization to a mouse microarray chip containing 60,000 genes; hybridization was performed in duplicate (IL-15^0) or triplicate (wt). Select genes differentially expressed (minimally $\log_2$ fold change $\geq +1.5/\leq -1.5$ and nominal p value < 0.001) in wt and IL-15^0 NKT cells (Fig. 6*A*) were then validated by real-time qPCR. We found that *Tbx21* (T-bet) was upregulated in wt NKT cells compared with IL-15^0 NKT cells (Fig. 6*A*, 6*B*). This finding is consistent with the previously reported IL-15–induced *Tbx21*-encoded T-bet expression in NKT cells in vitro (20). Furthermore, multiple *Tbx21*-regulated genes, such as *Ifng*, *Gzma* (granzyme A), *Gzmc*, *Hopx*, and several NK cell receptor genes (*Klra3* [NKG2E], *Klrb1c* [NK1.1], *Klrc1* [NKG2A/B], and *Klrk1* [NKG2D]) (20, 29), were upregulated in wt thymic NKT cells, which predominantly consist of ST3 NKT cells (Fig. 6*B*). Consistent with the lack of intracellular Bcl-2 in IL-15^0 NKT cells (Fig. 1*C*), the *Bcl2* gene was poorly expressed in these cells (Fig. 6*B*). Conversely, *Zbtb16* (PLZF), *Tcf7* (T cell factor 1), and *Rorc* (retinoic acid-related orphan receptor γt) genes, all signatures of ST1 and ST2 NKT cells, were upregulated in IL-15^0 thymic NKT cells (Fig. 6*C*), consistent with developmental arrest at ST2. Because T-bet is a critical regulator of differentiation in other lineages with cytotoxic properties (CTL and NK cells), our results are consistent with a role of *Tbx21* in regulating ST2 to ST3 transition.

IL-15 regulates functional maturation of NKT cells

Terminally mature NKT cells produce the highest amounts of effector cytokines. Because phenotypically this subset of NKT cells appears impaired in IL-15^0 and IL-15^0;Bcl-x_L^{tg} mice, we determined whether they were functionally competent. For this purpose, the potent NKT cell ligand αGalCer (64) was administered

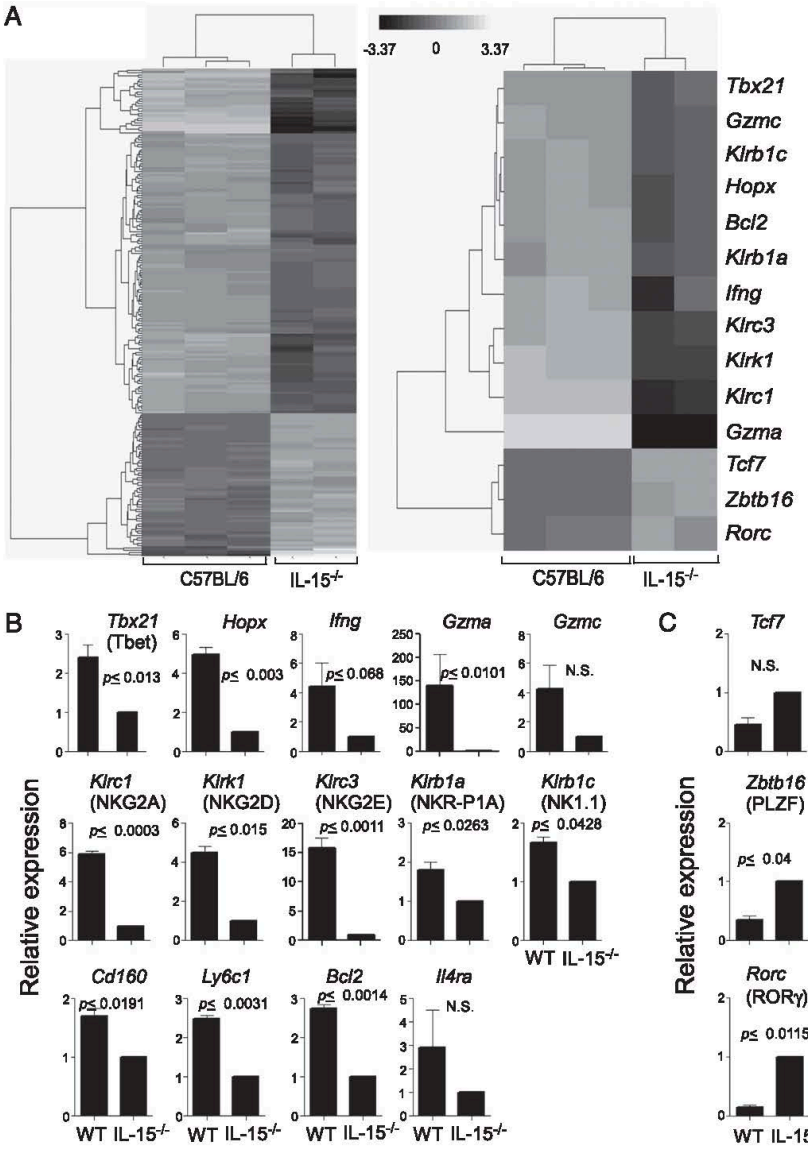

FIGURE 6. IL-15 induces *Tbx21*- and T-bet–regulated genes in developing NKT cells. *A*, Cluster analysis of all (*left panel*) or select genes (*right panel*) differentially expressed in B6 ($n = 3$) and IL-15^0 ($n = 2$) NKT cells from microarray experiments are shown. Differential expression was defined as those genes that showed $\log_2$ fold change $\geq 1.5 / \leq -1.5$ with a nominal p value <0.001. *B* and *C*, Select differentially expressed genes identified in *A* were validated by qPCR using RNA isolated from flow-sorted B6 and B6–IL-15^0 thymic NKT cells. Genes upregulated in B6-derived thymic NKT cells (*B*) and genes upregulated in B6–IL-15^0–derived NKT cells (*C*) are shown. β-actin was used to normalize expression levels. Data represent mean + SD of two independent experiments; each qPCR was performed in duplicate for an n value of 4 to calculate the p value by unpaired t test.

i.p. into IL-$15^{+/-}$, IL-15^0, and IL-15^0;Bcl-x_L^{tg} mice, and 4 h later, intracellular and serum IL-4 and IFN-γ responses were monitored. Compared to IL-$15^{+/-}$ mice, significantly fewer splenic and hepatic NKT cells from IL-15^0 and IL-15^0;Bcl-x_L^{tg} mice expressed intracellular IL-4 and IFN-γ in response to in vivo stimulation (Fig. 7*A*, 7*B*). Furthermore, NKT cells that expressed IL-4 (splenic) and IFN-γ (splenic and hepatic) in IL-15^0 and IL-15^0; Bcl-x_L^{tg} mice expressed these cytokines at significantly lower levels compared with those in IL-$15^{+/-}$ mice (Fig. 7*A*, 7*B*). Consistent with this expression pattern, the serum IFN-γ and IL-4 responses were also poor in IL-15^0 and IL-15^0;Bcl-x_L^{tg} mice compared with their IL-$15^{+/-}$ counterparts (Fig. 7*C*, 7*D*). Thus, IL-15 signaling is required for fully competent NKT cell responses in vivo.

IFN-γ and IL-4 responses by NKT cells require transcriptional regulation by T-bet and Gata-3 (17, 19). T-bet is also required for the terminal maturation of thymic NKT cells, as T-bet deficiency blocked NKT cell ontogeny at the ST2 to ST3 transition (20),

similar to that seen with IL-15 deficiency (Fig. 5). Because *Tbx21* expression is reduced in IL-15^0 NKT cells, and IL-15 induces *Tbx21* expression in NK cells in vitro (20), we investigated whether impaired NKT cell function in IL-15^0 and IL-15^0;Bcl-x_L^{tg} mice was due to altered levels of T-bet and Gata-3 expression. For this, thymic and splenic NK1.1$^-$ and NK1.1$^+$ NKT cells from wt and IL-15^0 mice were probed for intracellular expression of T-bet and Gata-3. We found that the level of T-bet expression was reduced by 30 (splenic) to 50% (thymic) in IL-15^0 compared with wt NKT cells (Fig. 7*E*, 7*G*). Additionally, a slightly reduced percentage of thymic, but not splenic, NKT cells expressed T-bet in IL-15^0 mice. Similarly, intracellular Gata-3 expression was ~15–20% lower in thymic and splenic NK1$^-$ NKT cells but about similar in NK1$^+$ NKT cells of IL-15^0 mice compared with their wt counterparts (Fig. 7*F*, 7*G*), consistent with somewhat more preserved IL-4 production in IL-15^0 NKT cells when compared with IFN-γ response. In wt NKT cells, Gata-3 expression level was constant, whereas T-bet levels increased with ST3 differentiation (Fig. 7*G*). Hence, the reduced T-bet expression (Fig. 7*E*) in IL-15^0 mice is consistent with reduced ST3 NKT cells in these mice. Thus, IL-15 signals are partially required for T-bet and Gata-3 expression in NKT cells and, possibly, for the robust IFN-γ and IL-4 cytokine responses seen in wt but not in IL-15^0 and IL-15^0; Bcl-x_L^{tg} mice.

Discussion

We describe three unique features of IL-15 that are essential for functional NKT cell development: 1) it induces survival of thymic and peripheral NKT cells by regulating Bcl-x_L and Bcl-2 expression; 2) IL-15 regulates T-bet expression and signals ST3 NKT cell induction and differentiation; and 3) it regulates effector differentiation that is consistent with the role of T-bet in this process. Thus, IL-15 plays a central role in NKT cell development and function.

It appears as though NKT cells narrowly escape death at each stage of their development: immediately after positive selection,

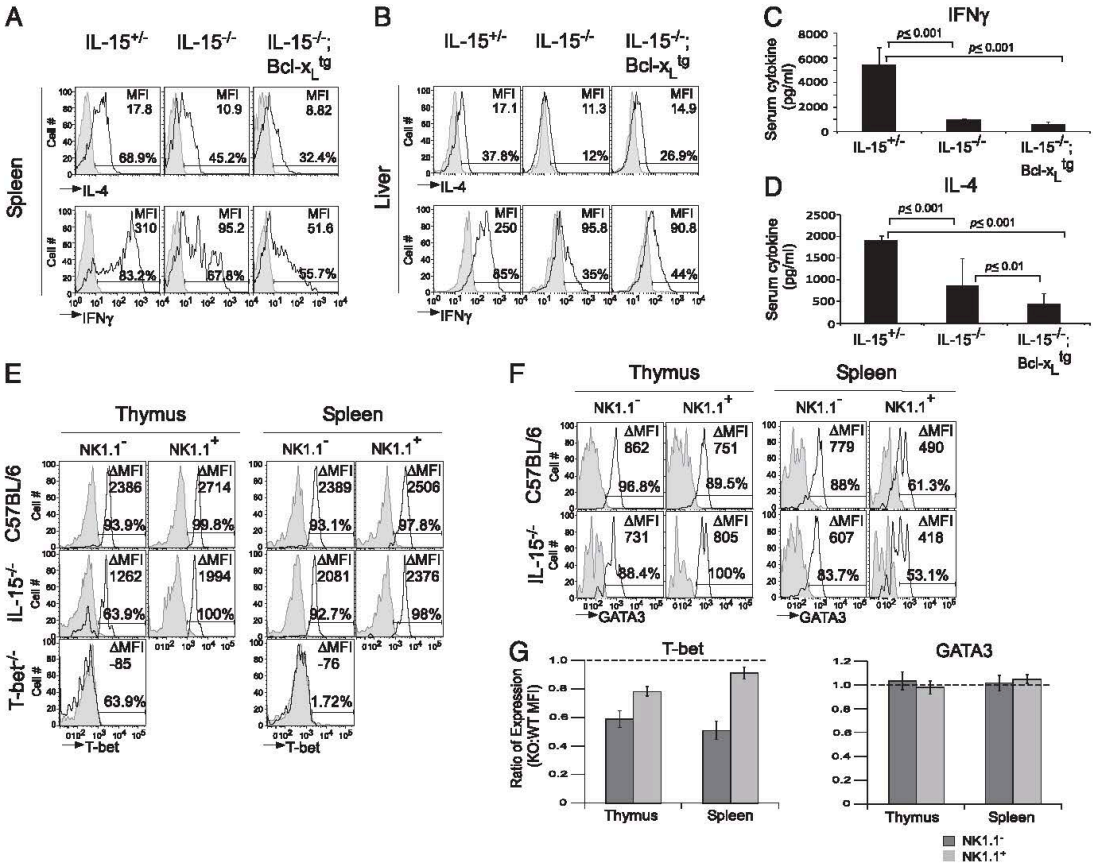

FIGURE 7. IL-15 regulates functional maturation of NKT cells. *A* and *B*, B6 (n = 6), B6–IL-15^0 (n = 6), and B6–IL-15^0;Bcl-x_L^{tg} (n = 12) mice were injected i.p. with 5 μg αGalCer (open) or vehicle (shaded). After 4 h, splenic (*A*) and hepatic (*B*) B220^{LO}CD3ε$^+$tetramer$^+$ cells were electronically gated, and intracellular IL-4 and IFN-γ expression was monitored. Numbers refer to ΔMFI. Data are representative of four independent experiments. *C* and *D*, Using ELISA, serum IFN-γ (*C*) and IL-4 (*D*) responses to in vivo NKT cell stimulation in the above experiment were measured. The p value was calculated by one-way ANOVA with Tukey's posttest. *E* and *F*, Thymic and splenic mononuclear cells from B6 and B6–IL-15^0 mice were analyzed for intracellular T-bet (*E*) and Gata-3 (*F*) expression within electronically gated CD8^{LO}CD3ε$^+$tetramer^{NEG} thymocytes or B220^{LO}CD3ε$^+$tetramer$^+$ splenocytes. Numbers refer to the ΔMFI between isotype control (shaded) and specific mAb (open). Data are representative of two independent experiments. n = 5. *G*, The ratio of T-bet and Gata-3 expression by IL-15^0 and wt NKT cells is shown. A ratio of ~1 (e.g., Gata-3) indicates no difference in expression; a ratio <1 (e.g., T-bet) indicates lower expression in IL-15^0 NKT cells.

they turn on Nur77 expression in ST0 NKT cells (65), perhaps owing to high-avidity interactions with their cognate ligand, namely, CD1d–self-lipid complexes. In T cells, the transcription factor Nur77, in addition to inducing an apoptotic program, when targeted to the mitochondrion binds to the otherwise antiapoptotic factor Bcl-2 and, by changing its conformation, converts it into a proapoptotic protein (66). Therefore, onward development of NKT cells perhaps requires survival signal(s) to protect the lineage from death. We have identified one such survival signal to be IL-15. It induces both Bcl-2 and Bcl-x_L within thymic NKT cells in vitro. Yet, only genetic overexpression of Bcl-x_L but not Bcl-2 confers survival potential to ST1 and ST2, but not ST3, NKT cells. These data are consistent with a previous report showing that enforced Bcl-2 expression does not rescue NKT cell development in IL-15Rβ–null mice (62). A recent report suggested that forced Bcl-2 overexpression or introgression of Bim deficiency modestly rescues NKT cell development in the IL-15–presenting IL-15Rα–null mice (38). The differences in survival mechanisms in these three animal models currently remain unknown.

The global gene expression analysis of wt and IL-15–deficient NKT cells, as well as our published data (14), indicate that ST3 but not ST0–2 NKT cells express high levels of Bcl-2. Hence, it is possible that Bcl-2 functions as an important survival factor only upon commitment and development into ST3 NKT cells. Because the ST3 NKT cells are absent in IL-15–, IL-15Rα–, and IL-15Rβ–null mice, another factor must be necessary to support NKT cell survival up to this stage. Our data suggest Bcl-x_L provides that function. The failure of transgenic Bcl-2 to do so in this study perhaps reflects the need for an IL-15–induced, ST3-specific accessory factor to execute its function.

Previous studies have demonstrated that thymic and peripheral NKT cells represent distinct functional subsets (44, 47, 48). The factor(s) that impacts differentiation of these two subsets remained incompletely defined. We found that most thymic NKT cells in IL-15^0;Bcl-x_L^{tg} mice were blocked at the ST2-to-ST3 ontogenetic transition and lacked activation/memory marker expression, as were IL-15^0 NKT cells. In striking contrast, splenic and hepatic NKT cells in IL-15^0 and IL-15^0;Bcl-x_L^{tg} mice underwent almost complete phenotypic maturation, suggesting that developmental cues in the thymus and periphery are somewhat distinct. In contrast, gene expression analyses indicated reduced T-bet expression in both thymic and splenic NKT cells of IL-15^0 mice. T-bet was previously shown to regulate the ST2-to-ST3 NKT ontogenetic transition (20, 29). Thus, reduced T-bet expression is consistent with the ST2-to-ST3 developmental block in IL-15^0 NKT cells. Furthermore, low levels of T-bet may in part explain the poor expression of NK cell receptors as well as the deficiency in ST3-specific IFN-γ response in IL-15^0 mice. Taken together, we conclude that IL-15 differentially impacts central and peripheral NKT cell maturation in vivo.

It is noteworthy that T-bet belongs to a group of transcription factors whose functions are regulated not only by their presence or absence but also by absolute levels. An example of such regulation is seen in effector CD8 T cell fate determination via graded expression of T-bet (67). Differentiation into effector and memory CD8 T cell fates was dictated by the levels of T-bet, in which high T-bet expression induced an effector cell fate, whereas lower T-bet level directed cells into the memory pool. Such a model would in principle be consistent with a past report (38) and ours suggesting that partially reduced levels of T-bet expression in IL-15^0 mice could indeed significantly impair the NKT cell differentiation program. Finally, because T-bet regulates expression of IL-15/IL-2Rβ (CD122) on NKT cells (this report and 29) and therefore IL-15 responsiveness, the two factors (IL-15 and T-bet) generate a positive-feedback regulatory loop. The property of all such loops is that small changes in gene expression are amplified by self-sustained and self-amplified system oscillation. Therefore, we predict that the reduced but not the complete absence of T-bet observed in IL-15^0 NKT cells may be sufficient to prevent complete effector differentiation.

The importance of NKT cell function(s) is implicated in multiple infectious diseases. Because NKT cells acquire most of their NK cell-like properties at ST3 of their differentiation, and because IL-15 seems to regulate acquisition of these properties, we speculate that IL-15–encoded NKT cell functions will be important in controlling in vivo responses to infections. This will be an exciting area for future investigations. In conclusion, IL-15 functions by supporting survival of developing NKT cells and perhaps by inducing *Tbx21* expression as an ST3-specific differentiation factor in NKT cells. NKT cells share this feature with NK cells and CD8 T cells and are expected to collaborate with these lineages in executing *Tbx21*-induced functions in vivo.

Acknowledgments

We thank Drs. J.J. Peschon (Immunex), M. Taniguchi (RIKEN, Yokohama, Japan), and A. Bendelac (University of Chicago) for sharing B6–IL-15^0, B6.129–IL-$7\alpha^0$, B6-J$\alpha18^0$, and B6.129-CD1dTD mice; the National Institutes of Health Tetramer Facility for unloaded and PBS57-loaded mouse CD1d monomers; the Kirin Brewery Company for KRN7000; and A.J. Joyce for technical assistance.

Disclosures

The authors have no financial conflicts of interest.

References

1. Bendelac, A., P. B. Savage, and L. Teyton. 2007. The biology of NKT cells. *Annu. Rev. Immunol.* 25: 297–336.
2. Van Kaer, L. 2005. α-Galactosylceramide therapy for autoimmune diseases: prospects and obstacles. *Nat. Rev. Immunol.* 5: 31–42.
3. Godfrey, D. I., S. Stankovic, and A. G. Baxter. 2010. Raising the NKT cell family. *Nat. Immunol.* 11: 197–206.
4. Bezbradica, J. S., T. Hill, A. K. Stanic, L. Van Kaer, and S. Joyce. 2005. Commitment toward the natural T (iNKT) cell lineage occurs at the CD4+8+ stage of thymic ontogeny. *Proc. Natl. Acad. Sci. USA* 102: 5114–5119.
5. D'Cruz, L. M., J. Knell, J. K. Fujimoto, and A. W. Goldrath. 2010. An essential role for the transcription factor HEB in thymocyte survival, Tcra rearrangement and the development of natural killer T cells. *Nat. Immunol.* 11: 240–249.
6. Egawa, T., G. Eberl, I. Taniuchi, K. Benlagha, F. Geissmann, L. Hennighausen, A. Bendelac, and D. R. Littman. 2005. Genetic evidence supporting selection of the Valpha14i NKT cell lineage from double-positive thymocyte precursors. *Immunity* 22: 705–716.
7. Hu, T., A. Simmons, J. Yuan, T. P. Bender, and J. Alberola-Ila. 2010. The transcription factor c-Myb primes CD4+CD8+ immature thymocytes for selection into the iNKT lineage. *Nat. Immunol.* 11: 435–441.
8. Dose, M., B. P. Sleckman, J. Han, A. L. Bredemeyer, A. Bendelac, and F. Gounari. 2009. Intrathymic proliferation wave essential for Valpha14+ natural killer T cell development depends on c-Myc. *Proc. Natl. Acad. Sci. USA* 106: 8641–8646.
9. Mycko, M. P., I. Ferrero, A. Wilson, W. Jiang, T. Bianchi, A. Trumpp, and H. R. MacDonald. 2009. Selective requirement for c-Myc at an early stage of V(α)14i NKT cell development. *J. Immunol.* 182: 4641–4648.
10. Kovalovsky, D., O. U. Uche, S. Eladad, R. M. Hobbs, W. Yi, E. Alonzo, K. Chua, M. Eidson, H. J. Kim, J. S. Im, et al. 2008. The BTB-zinc finger transcriptional regulator PLZF controls the development of invariant natural killer T cell effector functions. *Nat. Immunol.* 9: 1055–1064.
11. Savage, A. K., M. G. Constantinides, J. Han, D. Picard, E. Martin, B. Li, O. Lantz, and A. Bendelac. 2008. The transcription factor PLZF directs the effector program of the NKT cell lineage. *Immunity* 29: 391–403.
12. Schmidt-Supprian, M., J. Tian, E. P. Grant, M. Pasparakis, R. Maehr, H. Ovaa, H. L. Ploegh, A. J. Coyle, and K. Rajewsky. 2004. Differential dependence of CD4+CD25+ regulatory and natural killer-like T cells on signals leading to NF-kappaB activation. *Proc. Natl. Acad. Sci. USA* 101: 4566–4571.
13. Sivakumar, V., K. J. Hammond, N. Howells, K. Pfeffer, and F. Weih. 2003. Differential requirement for Rel/nuclear factor kappa B family members in natural killer T cell development. *J. Exp. Med.* 197: 1613–1621.
14. Stanic, A. K., J. S. Bezbradica, J. J. Park, N. Matsuki, A. L. Mora, L. Van Kaer, M. R. Boothby, and S. Joyce. 2004. NF-κ B controls cell fate specification, survival, and molecular differentiation of immunoregulatory natural T lymphocytes. *J. Immunol.* 172: 2265–2273.

15. Vallabhapurapu, S., I. Powolny-Budnicka, M. Riemann, R. M. Schmid, S. Paxian, K. Pfeffer, H. Körner, and F. Weih. 2008. Rel/NF-kappaB family member RelA regulates NK1.1- to NK1.1+ transition as well as IL-15-induced expansion of NKT cells. *Eur. J. Immunol.* 38: 3508–3519.
16. Lazarevic, V., A. J. Zullo, M. N. Schweitzer, T. L. Staton, E. M. Gallo, G. R. Crabtree, and L. H. Glimcher. 2009. The gene encoding early growth response 2, a target of the transcription factor NFAT, is required for the development and maturation of natural killer T cells. *Nat. Immunol.* 10: 306–313.
17. Cen, O., A. Ueda, L. Guzman, J. Jain, H. Bassiri, K. E. Nichols, and P. L. Stein. 2009. The adaptor molecule signaling lymphocytic activation molecule-associated protein (SAP) regulates IFN-gamma and IL-4 production in V alpha 14 transgenic NKT cells via effects on GATA-3 and T-bet expression. *J. Immunol.* 182: 1370–1378.
18. Kim, P. J., S. Y. Pai, M. Brigl, G. S. Besra, J. Gumperz, and I. C. Ho. 2006. GATA-3 regulates the development and function of invariant NKT cells. *J. Immunol.* 177: 6650–6659.
19. Wang, Z. Y., S. Kusam, V. Munugalavadla, R. Kapur, R. R. Brutkiewicz, and A. L. Dent. 2006. Regulation of Th2 cytokine expression in NKT cells: unconventional use of Stat6, GATA-3, and NFAT2. *J. Immunol.* 176: 880–888.
20. Townsend, M. J., A. S. Weinmann, J. L. Matsuda, R. Salomon, P. J. Farnham, C. A. Biron, L. Gapin, and L. H. Glimcher. 2004. T-bet regulates the terminal maturation and homeostasis of NK and Valpha14i NKT cells. *Immunity* 20: 477–494.
21. Griewank, K., C. Borowski, S. Rietdijk, N. Wang, A. Julien, D. G. Wei, A. A. Mamchak, C. Terhorst, and A. Bendelac. 2007. Homotypic interactions mediated by Slamf1 and Slamf6 receptors control NKT cell lineage development. *Immunity* 27: 751–762.
22. Eberl, G., B. Lowin-Kropf, and H. R. MacDonald. 1999. Cutting edge: NKT cell development is selectively impaired in Fyn- deficient mice. *J. Immunol.* 163: 4091–4094.
23. Gadue, P., N. Morton, and P. L. Stein. 1999. The Src family tyrosine kinase Fyn regulates natural killer T cell development. *J. Exp. Med.* 190: 1189–1196.
24. Nichols, K. E., J. Hom, S. Y. Gong, A. Ganguly, C. S. Ma, J. L. Cannons, S. G. Tangye, P. L. Schwartzberg, G. A. Koretzky, and P. L. Stein. 2005. Regulation of NKT cell development by SAP, the protein defective in XLP. *Nat. Med.* 11: 340–345.
25. Chung, B., A. Aoukaty, J. Dutz, C. Terhorst, and R. Tan. 2005. Signaling lymphocytic activation molecule-associated protein controls NKT cell functions. *J. Immunol.* 174: 3153–3157.
26. Pasquier, B., L. Yin, M. C. Fondanèche, F. Relouzat, C. Bloch-Queyrat, N. Lambert, A. Fischer, G. de Saint-Basile, and S. Latour. 2005. Defective NKT cell development in mice and humans lacking the adapter SAP, the X-linked lymphoproliferative syndrome gene product. *J. Exp. Med.* 201: 695–701.
27. Gadue, P., and P. L. Stein. 2002. NK T cell precursors exhibit differential cytokine regulation and require Itk for efficient maturation. *J. Immunol.* 169: 2397–2406.
28. Stanic, A. K., J. S. Bezbradica, J. J. Park, L. Van Kaer, M. R. Boothby, and S. Joyce. 2004. Cutting edge: the ontogeny and function of Va14Ja18 natural T lymphocytes require signal processing by protein kinase C θ and NF-κ B. *J. Immunol.* 172: 4667–4671.
29. Matsuda, J. L., Q. Zhang, R. Ndonye, S. K. Richardson, A. R. Howell, and L. Gapin. 2006. T-bet concomitantly controls migration, survival, and effector functions during the development of Valpha14i NKT cells. *Blood* 107: 2797–2805.
30. Engel, I., K. Hammond, B. A. Sullivan, X. He, I. Taniuchi, D. Kappes, and M. Kronenberg. 2010. Co-receptor choice by V alpha14i NKT cells is driven by Th-POK expression rather than avoidance of CD8-mediated negative selection. *J. Exp. Med.* 207: 1015–1029.
31. Bezbradica, J. S., L. E. Gordy, A. K. Stanic, S. Dragovic, T. Hill, J. Hawiger, D. Unutmaz, L. Van Kaer, and S. Joyce. 2006. Granulocyte-macrophage colony-stimulating factor regulates effector differentiation of invariant natural killer T cells during thymic ontogeny. *Immunity* 25: 487–497.
32. Lee, A. J., X. Zhou, M. Chang, J. Hunzeker, R. H. Bonneau, D. Zhou, and S. C. Sun. 2010. Regulation of natural killer T-cell development by deubiquitinase CYLD. *EMBO J.* 29: 1600–1612.
33. Ohteki, T., S. Ho, H. Suzuki, T. W. Mak, and P. S. Ohashi. 1997. Role for IL-15/IL-15 receptor β-chain in natural killer 1.1+ T cell receptor-α β+ cell development. *J. Immunol.* 159: 5931–5935.
34. Boesteanu, A., A. D. Silva, H. Nakajima, W. J. Leonard, J. J. Peschon, and S. Joyce. 1997. Distinct roles for signals relayed through the common cytokine receptor γ chain and interleukin 7 receptor α chain in natural T cell development. *J. Exp. Med.* 186: 331–336.
35. Kennedy, M. K., M. Glaccum, S. N. Brown, E. A. Butz, J. L. Viney, M. Embers, N. Matsuki, K. Charrier, L. Sedger, C. R. Willis, et al. 2000. Reversible defects in natural killer and memory CD8 T cell lineages in interleukin 15-deficient mice. *J. Exp. Med.* 191: 771–780.
36. Matsuda, J. L., L. Gapin, S. Sidobre, W. C. Kieper, J. T. Tan, R. Ceredig, C. D. Surh, and M. Kronenberg. 2002. Homeostasis of V α 14*i* NKT cells. *Nat. Immunol.* 3: 966–974.
37. Lodolce, J. P., D. L. Boone, S. Chai, R. E. Swain, T. Dassopoulos, S. Trettin, and A. Ma. 1998. IL-15 receptor maintains lymphoid homeostasis by supporting lymphocyte homing and proliferation. *Immunity* 9: 669–676.
38. Chang, C. L., Y. G. Lai, M. S. Hou, P. L. Huang, and N. S. Liao. 2011. IL-15Rα of radiation-resistant cells is necessary and sufficient for thymic invariant NKT cell survival and functional maturation. *J. Immunol.* 187: 1235–1242.
39. Ohteki, T., H. Yoshida, T. Matsuyama, G. S. Duncan, T. W. Mak, and P. S. Ohashi. 1998. The transcription factor interferon regulatory factor 1 (IRF-1) is important during the maturation of natural killer 1.1+ T cell receptor-α/β+ (NK1+ T) cells, natural killer cells, and intestinal intraepithelial T cells. *J. Exp. Med.* 187: 967–972.
40. Monticelli, L. A., Y. Yang, J. Knell, L. M. D'Cruz, M. A. Cannarile, I. Engel, M. Kronenberg, and A. W. Goldrath. 2009. Transcriptional regulator Id2 controls survival of hepatic NKT cells. *Proc. Natl. Acad. Sci. USA* 106: 19461–19466.
41. Benlagha, K., T. Kyin, A. Beavis, L. Teyton, and A. Bendelac. 2002. A thymic precursor to the NK T cell lineage. *Science* 296: 553–555.
42. Godfrey, D. I., and S. P. Berzins. 2007. Control points in NKT-cell development. *Nat. Rev. Immunol.* 7: 505–518.
43. Pellicci, D. G., K. J. Hammond, A. P. Uldrich, A. G. Baxter, M. J. Smyth, and D. I. Godfrey. 2002. A natural killer T (NKT) cell developmental pathway iInvolving a thymus-dependent NK1.1(-)CD4(+) CD1d-dependent precursor stage. *J. Exp. Med.* 195: 835–844.
44. Berzins, S. P., F. W. McNab, C. M. Jones, M. J. Smyth, and D. I. Godfrey. 2006. Long-term retention of mature NK1.1+ NKT cells in the thymus. *J. Immunol.* 176: 4059–4065.
45. Geissmann, F., T. O. Cameron, S. Sidobre, N. Manlongat, M. Kronenberg, M. J. Briskin, M. L. Dustin, and D. R. Littman. 2005. Intravascular immune surveillance by CXCR6+ NKT cells patrolling liver sinusoids. *PLoS Biol.* 3: e113.
46. Ohteki, T., C. Maki, S. Koyasu, T. W. Mak, and P. S. Ohashi. 1999. Cutting edge: LFA-1 is required for liver NK1.1+TCR alpha beta+ cell development: evidence that liver NK1.1+TCR alpha beta+ cells originate from multiple pathways. *J. Immunol.* 162: 3753–3756.
47. McNab, F. W., S. P. Berzins, D. G. Pellicci, K. Kyparissoudis, K. Field, M. J. Smyth, and D. I. Godfrey. 2005. The influence of CD1d in postselection NKT cell maturation and homeostasis. *J. Immunol.* 175: 3762–3768.
48. McNab, F. W., D. G. Pellicci, K. Field, G. Besra, M. J. Smyth, D. I. Godfrey, and S. P. Berzins. 2007. Peripheral NK1.1 NKT cells are mature and functionally distinct from their thymic counterparts. *J. Immunol.* 179: 6630–6637.
49. Ma, A., R. Koka, and P. Burkett. 2006. Diverse functions of IL-2, IL-15, and IL-7 in lymphoid homeostasis. *Annu. Rev. Immunol.* 24: 657–679.
50. Huntington, N. D., H. Puthalakath, P. Gunn, E. Naik, E. M. Michalak, M. J. Smyth, H. Tabarias, M. A. Degli-Esposti, G. Dewson, S. N. Willis, et al. 2007. Interleukin 15-mediated survival of natural killer cells is determined by interactions among Bim, Noxa and Mcl-1. *Nat. Immunol.* 8: 856–863.
51. Calnan, B. J., S. Szychowski, F. K. Chan, D. Cado, and A. Winoto. 1995. A role for the orphan steroid receptor Nur77 in apoptosis accompanying antigen-induced negative selection. *Immunity* 3: 273–282.
52. Chiu, Y. H., S. H. Park, K. Benlagha, C. Forestier, J. Jayawardena-Wolf, P. B. Savage, L. Teyton, and A. Bendelac. 2002. Multiple defects in antigen presentation and T cell development by mice expressing cytoplasmic tail-truncated CD1d. *Nat. Immunol.* 3: 55–60.
53. Cui, J., T. Shin, T. Kawano, H. Sato, E. Kondo, I. Toura, Y. Kaneko, H. Koseki, M. Kanno, and M. Taniguchi. 1997. Requirement for Valpha14 NKT cells in IL-12-mediated rejection of tumors. *Science* 278: 1623–1626.
54. Strasser, A., A. W. Harris, and S. Cory. 1991. bcl-2 transgene inhibits T cell death and perturbs thymic self-censorship. *Cell* 67: 889–899.
55. Chao, D. T., G. P. Linette, L. H. Boise, L. S. White, C. B. Thompson, and S. J. Korsmeyer. 1995. Bcl-XL and Bcl-2 repress a common pathway of cell death. *J. Exp. Med.* 182: 821–828.
56. Bezbradica, J. S., A. K. Stanic, and S. Joyce. 2006. Characterization and functional analysis of mouse invariant natural T (iNKT) cells. *Curr. Protoc. Immunol.* Chapter 14: Unit 14.13.
57. Bolstad, B. M., R. A. Irizarry, M. Astrand, and T. P. Speed. 2003. A comparison of normalization methods for high density oligonucleotide array data based on variance and bias. *Bioinformatics* 19: 185–193.
58. Smyth, G. K. 2004. Linear models and empirical bayes methods for assessing differential expression in microarray experiments. *Stat. Appl. Genet. Mol. Biol.* 3: Article3.
59. Smyth, G. K. 2005. *Limma: Linear models for Microarray Data*. Springer, New York.
60. Huang, H. C., S. Zheng, V. VanBuren, and Z. Zhao. 2010. Discovering disease-specific biomarker genes for cancer diagnosis and prognosis. *Technol. Cancer Res. Treat.* 9: 219–230.
61. Peschon, J. J., P. J. Morrissey, K. H. Grabstein, F. J. Ramsdell, E. Maraskovsky, B. C. Gliniak, L. S. Park, S. F. Ziegler, D. E. Williams, C. B. Ware, et al. 1994. Early lymphocyte expansion is severely impaired in interleukin 7 receptor-deficient mice. *J. Exp. Med.* 180: 1955–1960.
62. Minagawa, M., H. Watanabe, C. Miyaji, K. Tomiyama, H. Shimura, A. Ito, M. Ito, J. Domen, I. L. Weissman, and K. Kawai. 2002. Enforced expression of Bcl-2 restores the number of NK cells, but does not rescue the impaired development of NKT cells or intraepithelial lymphocytes, in IL-2/IL-15 receptor beta-chain-deficient mice. *J. Immunol.* 169: 4153–4160.
63. Nakazato, K., H. Yamada, T. Yajima, Y. Kagimoto, H. Kuwano, and Y. Yoshikai. 2007. Enforced expression of Bcl-2 partially restores cell numbers but not functions of TCRgammadelta intestinal intraepithelial T lymphocytes in IL-15-deficient mice. *J. Immunol.* 178: 757–764.
64. Kawano, T., J. Cui, Y. Koezuka, I. Toura, Y. Kaneko, K. Motoki, H. Ueno, R. Nakagawa, H. Sato, E. Kondo, et al. 1997. CD1d-restricted and TCR-mediated activation of valpha14 NKT cells by glycosylceramides. *Science* 278: 1626–1629.
65. Moran, A. E., K. L. Holzapfel, Y. Xing, N. R. Cunningham, J. S. Maltzman, J. Punt, and K. A. Hogquist. 2011. T cell receptor signal strength in Treg and iNKT cell development demonstrated by a novel fluorescent reporter mouse. *J. Exp. Med.* 208: 1279–1289.
66. Thompson, J., M. L. Burger, H. Whang, and A. Winoto. 2010. Protein kinase C regulates mitochondrial targeting of Nur77 and its family member Nor-1 in thymocytes undergoing apoptosis. *Eur. J. Immunol.* 40: 2041–2049.
67. Joshi, N. S., W. Cui, A. Chandele, H. K. Lee, D. R. Urso, J. Hagman, L. Gapin, and S. M. Kaech. 2007. Inflammation directs memory precursor and short-lived effector CD8(+) T cell fates via the graded expression of T-bet transcription factor. *Immunity* 27: 281–295.

OPEN ACCESS Freely available online

PLoS one

Rgs2 Mediates Pro-Angiogenic Function of Myeloid Derived Suppressor Cells in the Tumor Microenvironment via Upregulation of MCP-1

Kimberly C. Boelte[1], Laura E. Gordy[2], Sebastian Joyce[2], Mary Ann Thompson[3], Li Yang[4], P. Charles Lin[4]*

1 Department of Cancer Biology, Vanderbilt University Medical Center, Nashville, Tennessee, United States of America, **2** Department of Microbiology and Immunology, Vanderbilt University Medical Center, Nashville, Tennessee, United States of America, **3** Department of Pathology, Vanderbilt University Medical Center, Nashville, Tennessee, United States of America, **4** Center for Cancer Research, National Institutes of Health, Bethesda, Maryland, United States of America

Abstract

Background: Tumor growth is intimately linked with stromal interactions. Myeloid derived suppressor cells (MDSCs) are dramatically elevated in cancer patients and tumor bearing mice. MDSCs modulate the tumor microenvironment through attenuating host immune response and increasing vascularization.

Methodology/Principal Findings: In searching for molecular mediators responsible for pro-tumor functions, we found that regulator of G protein signaling-2 (Rgs2) is highly increased in tumor-derived MDSCs compared to control MDSCs. We further demonstrate that hypoxia, a common feature associated with solid tumors, upregulates the gene expression. Genetic deletion of Rgs2 in mice resulted in a significant retardation of tumor growth, and the tumors exhibit decreased vascular density and increased cell death. Interestingly, deletion of Rgs2 in MDSCs completely abolished their tumor promoting function, suggesting that Rgs2 signaling in MDSCs is responsible for the tumor promoting function. Cytokine array profiling identified that Rgs2−/− tumor MDSCs produce less MCP-1, leading to decreased angiogenesis, which could be restored with addition of recombinant MCP-1.

Conclusion: Our data reveal Rgs2 as a critical regulator of the pro-angiogenic function of MDSCs in the tumor microenvironment, through regulating MCP-1 production.

Citation: Boelte KC, Gordy LE, Joyce S, Thompson MA, Yang L, et al. (2011) Rgs2 Mediates Pro-Angiogenic Function of Myeloid Derived Suppressor Cells in the Tumor Microenvironment via Upregulation of MCP-1. PLoS ONE 6(4): e18534. doi:10.1371/journal.pone.0018534

Editor: Songtao Shi, University of Southern California, United States of America

Received January 13, 2011; **Accepted** March 2, 2011; **Published** April 11, 2011

Funding: This work was supported in part by grants from National Institutes of Health to PCL (CA108856, NS45888 and AR053718) and SJ (HL054977, AI061721 and AI042284) as well as training grants to KCB (T32CA009582) and LEG (T32HL069765 and T32AI007611). The funders had no role in study design, data collection and analysis, decision to publish, or preparation of the manuscript.

Competing Interests: The authors have declared that no competing interests exist.

* E-mail: p.lin@nih.gov

Introduction

It has become clear that the tumor microenvironment plays an important role in tumor progression. Tumors are comprised of several host derived cell types, including fibroblasts, smooth muscle cells, endothelial cells, immune cells, and epithelial cells, each contributing to the microenvironment in ways we are only beginning to understand [1]. In addition to the cells present, the tumor microenvironment contains extracellular matrix (ECM) and other factors secreted by the tumor and stromal cells that can greatly affect tumor progression.

Immune suppression and promotion of angiogenesis are essential for tumor growth and progression. Interestingly, MDSCs possess both properties, and create an environment to facilitate tumor progression. MDSCs increase in tumor bearing hosts, including cancer patients, and this accumulation is mediated by inflammatory and angiogenic factors [2]. MDSCs are also known to promote a shift to a type 2, tumor-promoting response in macrophages [3]. In addition, they infiltrate into tumors, and promote tumor vascularization, tumor growth, and metastasis through modulating VEGF bioavailability and protease activity in the tumor microenvironment [4,5,6,7]. The pro-angiogenic function of these myeloid cells is sufficient to confer tumor refractoriness to anti-VEGF treatment [8], a common target for anti-angiogenic therapy. This further illustrates the importance of MDSCs in tumor progression, as well as in molecular therapies for cancer.

Rgs2 (NM_009061) is a signaling molecule known to function downstream of G protein coupled receptors. Rgs2 contains a conserved Regulator of G protein Signaling domain, and functions as a GTPase-activating protein (GAP) for several Gα subunits of G proteins [9,10,11]. Rgs2 is widely expressed in a variety of cells, including myeloid cells [12,13]. A variety of stimuli can induce Rgs2 expression, most of which signal through G proteins. Therefore, Rgs2 functions in a negative feedback loop with regard to G protein coupled receptors (GPCRs). It enhances the intrinsic GTPase activity of the Gα subunit, and thereby decreases the time that the G protein subunits are dissociated, leading to decreased signaling [14,15]. In addition, cell stress, such as heat shock or DNA damage, can also increase Rgs2 levels [16,17]. Rgs2 inhibits cell proliferation, and is a known mediator of cell differentiation in several cell types, such as myeloid cells [18].

Monocyte chemoattractant protein 1 (MCP-1) is a chemokine important for cell migration [19,20]. It signals through CCR2, a

GPCR found on monocytes, endothelial cells, T cells, etc. [20,21,22]. In part due to a migratory effect on endothelial cells, MCP-1 is a potent angiogenic factor, promoting vascularization *ex vivo* and *in vivo* [22]. Blocking MCP-1 with a neutralizing antibody inhibited angiogenesis, and led to decreased tumor metastases and increased survival in a mouse tumor model [22].

Here, we report a novel role of Rgs2 in tumor growth and progression. Rgs2 expression is elevated in tumor derived MDSCs, and hypoxia, a condition commonly associated with tumors, upregulates its expression. Inactivation of Rgs2 in MDSCs leads to a significant reduction of MCP-1, and retards tumor angiogenesis and tumor progression. Thus, this study identifies Rgs2 as a critical mediator of pro-angiogenic function associated with MDSCs in the tumor microenvironment.

Materials and Methods

Ethics

All mouse studies have been conducted according to Animal Welfare Act and the Public Health Service Policy and approved by Vanderbilt University Institution Animal Care and Use Committee (IACUC) (M/05/083). The animals were housed in pathogen-free units at Vanderbilt University Medical Center, in compliance with IACUC regulations. Rgs2−/− mice in C57Bl/6 background were obtained from Dr. Josef Penninger at the Institute of Molecular Biotechnology GmbH, and were bred at Vanderbilt University Medical Center. Age and gender matched wild type control mice were purchased from Jackson Laboratories.

Cell culture

HL-60 and 3LL cell lines (purchased from ATCC) were cultured in RPMI 1640+10% FBS at 37°C, 5% CO_2. The 3LL cell line is a subclone of LLC (Lewis lung carcinoma) cell line. The B16 (purchased from ATCC) and MC26 [4] cell lines were grown in DMEM+10% FBS. Human umbilical vein endothelial cells (HUVECs) were obtained from Lonza, and cultured in EGM-2 Bulletkit medium, also from Lonza, at 37°C, 5% CO_2. HUVECs were used between passages 3 to 7.

Isolation of lung microvascular cells

Mice were sacrificed, and the chest cavity was opened. The right ventricle of the heart was punctured with a 25 gauge butterfly needle and syringe. The heart and lungs were flushed with PBS+2 mM EDTA until the lungs were white, followed by 0.25%

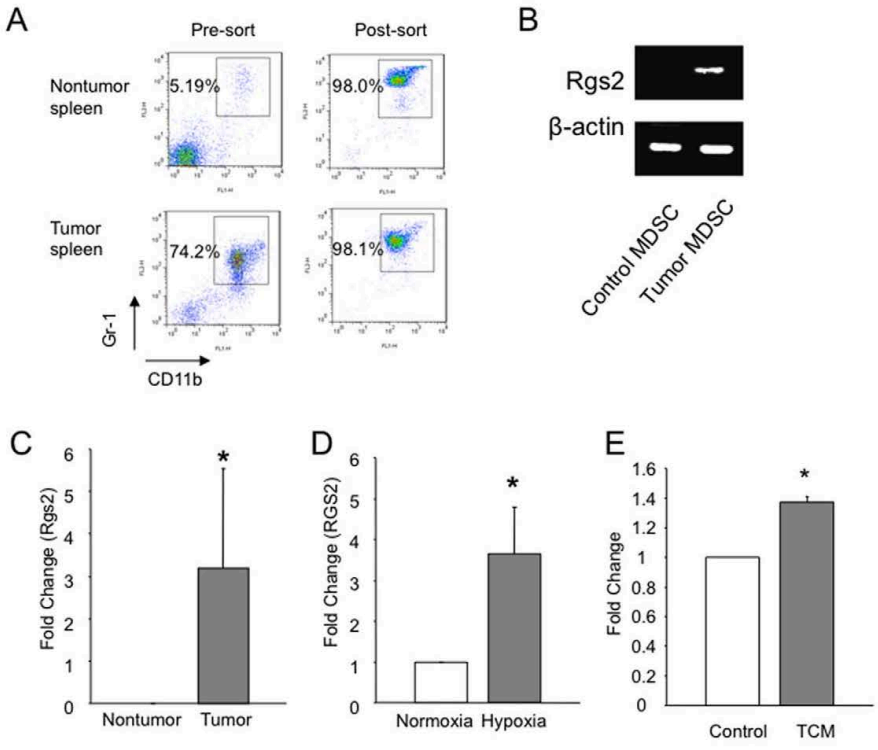

Figure 1. Induction of Rgs2 in tumor derived MDSCs. (A) Purity of cells from isolation of Gr-1+CD11b+ cells using MACS. Spleens from non-tumor bearing and MC26 tumor bearing BALB/c mice were isolated and processed into to single cell suspension, followed by sorting using MACS, as described in the Methods section. (B) and (C) Gr-1+CD11b+ cells were isolated from non tumor bearing and tumor bearing mice, MC26 tumors in BALB/c (B) and 3LL tumors in C57BL/6 (C), by magnetic sorting of pooled splenocytes from 5–10 mice, generating MDSCs of greater than 98% purity. Cells were then subjected to RNA isolation and RT-PCR (B) and real time PCR (C) for Rgs2 expression. These experiments were repeated 3 times. (D) HL-60 cells were incubated under normoxic (20% O_2) or hypoxic (1.0–2% O_2) conditions for an hour, and RNA was isolated, followed by real time PCR analysis. This experiment was performed 5 times. (E) HL-60 cells were treated with medium conditioned by 3LL tumor cells for one hour. RNA was isolated, followed by real time PCR analysis. The experiment was performed 3 times. * $p<0.05$.
doi:10.1371/journal.pone.0018534.g001

trypsin + 2 mM EDTA until the lungs were pink. Lungs were removed, pumped with more trypsin, and allowed to incubate at 37°C for 20 minutes. The lungs were then diced, and the tissue was pipetted several times in DMEM + 10% FBS. After centrifugation, the cell pellet was resuspended in EGM, and seeded into plates. Medium was changed the next day to remove cell debris and red blood cells.

RT-PCR

RNA was isolated from cells using the RNeasy kit from Qiagen. iScript cDNA synthesis kit (BioRad) was used to produce cDNA. For PCR, Hi-Fidelity PCR mix (Invitrogen) was used, and for Real Time PCR, SYBR green kit (BioRad) and an iCycler or MyiQ machine (BioRad) were used.

Tumor model

For tumor growth studies, 3LL or B16 cells were injected subcutaneously into the left hindlimbs of mice. For the reconstitution assay, 3LL cells were mixed with MDSCs isolated by fluorescence activated cell sorting (FACS) and injected as before. Tumor size was measured by caliper, and tumor volume was calculated as volume = length $\times$(width)$^2 \times 0.5$. Tumor samples taken at days 17 21 post-injection were flash frozen in OCT (Sakura) or fixed in formalin and embedded in paraffin, then sectioned. Sections were incubated with primary antibodies overnight, then either Texas Red-fluorescent or biotin-labeled secondary antibodies for immunofluorescent or immunohistochemical analysis, respectively. Slides were imaged on an Olympus BX51 microscope with an Olympus DP70 camera. Images were overlaid using Adobe Photoshop.

Flow cytometry, FACS, and MACS

Tissues were prepared into single cell suspensions and labeled with antibodies for markers of mature and immature blood cells (BD Biosciences). Cells were analyzed using a BD LSRII or BD FACScan. For FACS, spleen cells were labeled with Gr-1

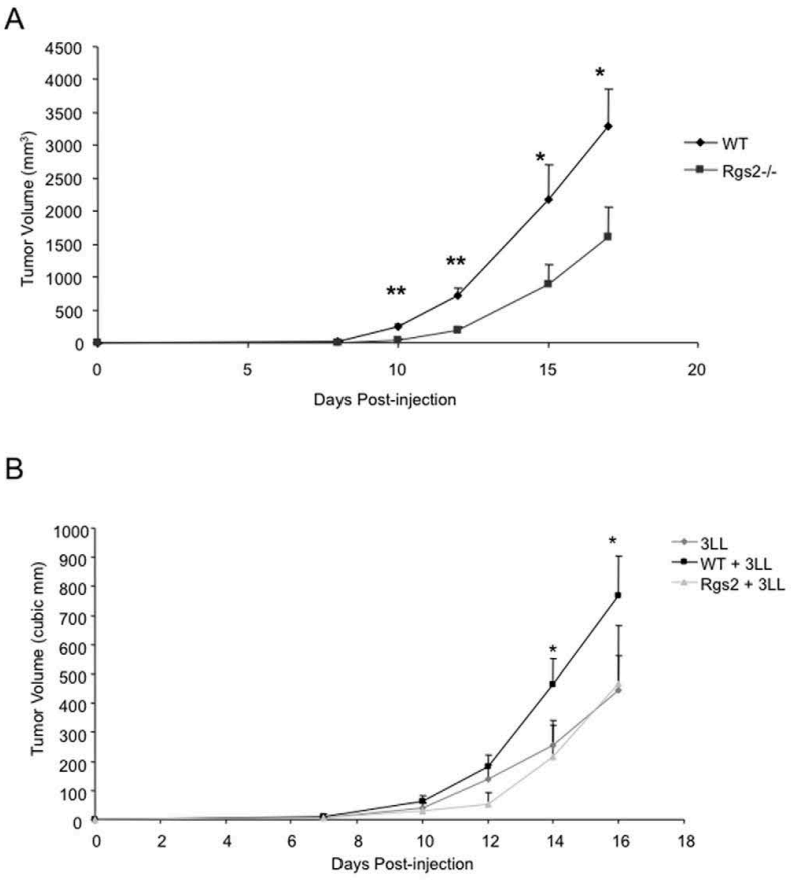

Figure 2. Deletion of Rgs2 in MDSCs retards tumor growth. (A) Rgs2−/− and C57BL/6 wild type mice were injected with 5×10^5 3LL tumor cells subcutaneously in the hindlimb, and tumor size was measured by caliper over time (n = 12 mice per group). This experiment was repeated 3 times. (B) Wild type mice were injected subcutaneously in the hindlimb with 1×10^5 3LL cells alone, or 3LL cells combined with 1×10^4 wild type or Rgs2−/− MDSCs sorted by flow cytometry (>95% purity; data not shown) from spleens of tumor-bearing mice. Tumor growth was measured by caliper over time. n = 8 mice per group. This experiment was performed twice. * $p<0.05$.
doi:10.1371/journal.pone.0018534.g002

(Miltenyi Biotec) and CD11b (BD Biosciences) and sorted in the VA Flow Cytometry Resource.

For magnetic activated cell sorting (MACS) of MDSCs, tumors were digested with collagenase A (Sigma) and hyaluronidase (Sigma). Tumor and spleen MDSCs were isolated by sequential labeling and column isolation with anti-Gr1-PE and anti-PE multisort beads, then CD11b beads (all from Miltenyi). We achieved equal to or greater than 98% purity of Gr-1+CD11b+ cells using MACS (Figure 1A).

BrdU incorporation

BrdU incorporation was performed using the BrdU Flow Kit from BD Biosciences per the manufacturer's instructions. Briefly, BrdU was added to endothelial cells at a final concentration of 10 uM. The cells were collected after 2 hours, fixed, and permeabilized. The cells were then subjected to DNase treatment at 37°C, followed by labeling with anti-BrdU and analysis by flow cytometry.

MDSC morphology

MDSCs were isolated from spleens of wild type and Rgs2−/− tumor bearing mice by MACS. The samples were placed on a slide using a cytospin centrifuge, stained with the Three Step Stain (Richard Allan Scientific), and analyzed for morphology by a hematopathologist (M.A. Thompson) in blind fashion.

In vitro angiogenic assays

Endothelial cell migration: Tumor MDSCs were isolated by MACS and cultured in RPMI with 1% FBS overnight. Transwells with 8 micron pores (Corning) were coated with fibronectin in 0.1% gelatin at 37°C one hour prior to addition of HUVECs. Transwells were placed over the cultured MDSCs, and HUVECs were added in basal RPMI at 1×10^5/well and allowed to migrate for 3.5 hours. Migrated HUVECs were fixed, stained with crystal violet, and counted in randomly selected fields under microscopy.

Vascular tube formation: MDSCs were isolated by MACS from tumor tissue, and cultured in EBM (Lonza) plus 1% FBS overnight. Wells of 48-well plates were coated with Matrigel (BD Bioscience). HUVECs were suspended in MDSC conditioned medium and plated over Matrigel at 80,000 cells/well. Tube formation was scored by counting branch points at 48 and 72 hours.

Cytokine array

MDSCs were isolated from tumor tissues using MACS, and the cytokine array was performed according to the manufacturer's protocol (RayBiotech). The data were analyzed by densitometry, with each band being normalized to internal controls.

Statistical analysis

Data were averaged and compared using Student's t test. Error bars on graphs represent standard error across experiments or mice.

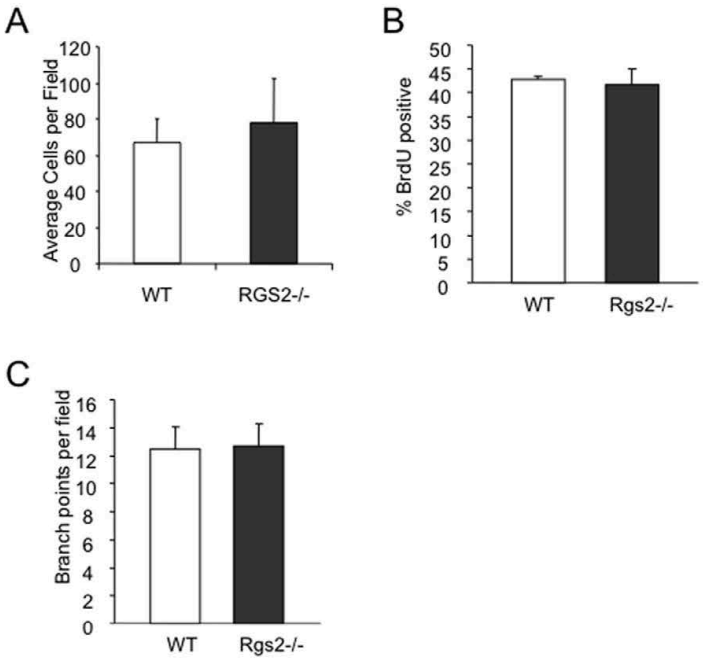

Figure 3. Lack of Rgs2 in endothelial cells does not affect migration, BrdU incorporation, or tube fomation. Lung microvascular endothelial cells were isolated from lungs of wild type and Rgs2−/− mice and cultured. (A) 1×10^5 cells were placed in the top chamber of a Transwell, and migrated to growth medium for 4 hours. Cells on the bottom of the Transwell (migrated cells) were fixed, stained with crystal violet, and counted. Experiment was performed 3 times in duplicate. (B) Cells were pulsed with 10 uM BrdU for 2 hours, then collected, processed, and analyzed by flow cytometry. The average percentages of BrdU positive cells was plotted. Experiment was performed 2 times in duplicate. (C) Cells were seeded on top of Matrigel in growth medium and allowed to form tube structures for 48 hours. Branch points were counted, and the average number per field was graphed.
doi:10.1371/journal.pone.0018534.g003

Results

Rgs2 is dramatically increased in tumor derived MDSCs

It is well documented that MDSCs from tumor bearing mice function differently from those from non-tumor bearing mice. In an effort to investigate the mechanism the tumor utilizes to condition the MDSCs, we examined gene expression on isolated MDSCs from spleens of BALB/c mice, either tumor bearing or non-tumor bearing. We achieved greater than 98% purity (Figure 1A). RT-PCR analysis showed a significant increase of Rgs2 mRNA in tumor derived MDSCs compared to cells from non-tumor hosts in both MC26 tumor model in BALB/c mice (Figure 1B) and 3LL tumor model in C57BL/6 mice (Figure 1C). Interestingly, we found a similar Rgs2 induction in MDSCs associated with MC26 and 3LL tumor conditions compared to non-tumor conditions by RT-PCR (Figure 1B C). Further analysis showed that hypoxia, a feature commonly associated with solid tumors, significantly increased Rgs2 RNA levels in a myeloid cell line *in vitro* (Figure 1D), consistent with published studies indicating that Rgs2 may be a stress response gene, increasing rapidly under conditions which are stressful for the cell. In addition, treatment with 3LL tumor conditioned medium led to a significant increase in Rgs2 mRNA levels in myeloid cells, suggesting that the tumor cells are secreting a factor capable of modulating Rgs2 expression (Figure 1E). The findings demonstrate that tumor conditions, such as hypoxia and secreted factors, upregulate Rgs2 expression in MDSCs.

Rgs2 signaling in MDSCs mediates tumor growth

Because MDSCs of tumor bearing mice upregulate Rgs2 expression, we sought to understand the role Rgs2 plays in

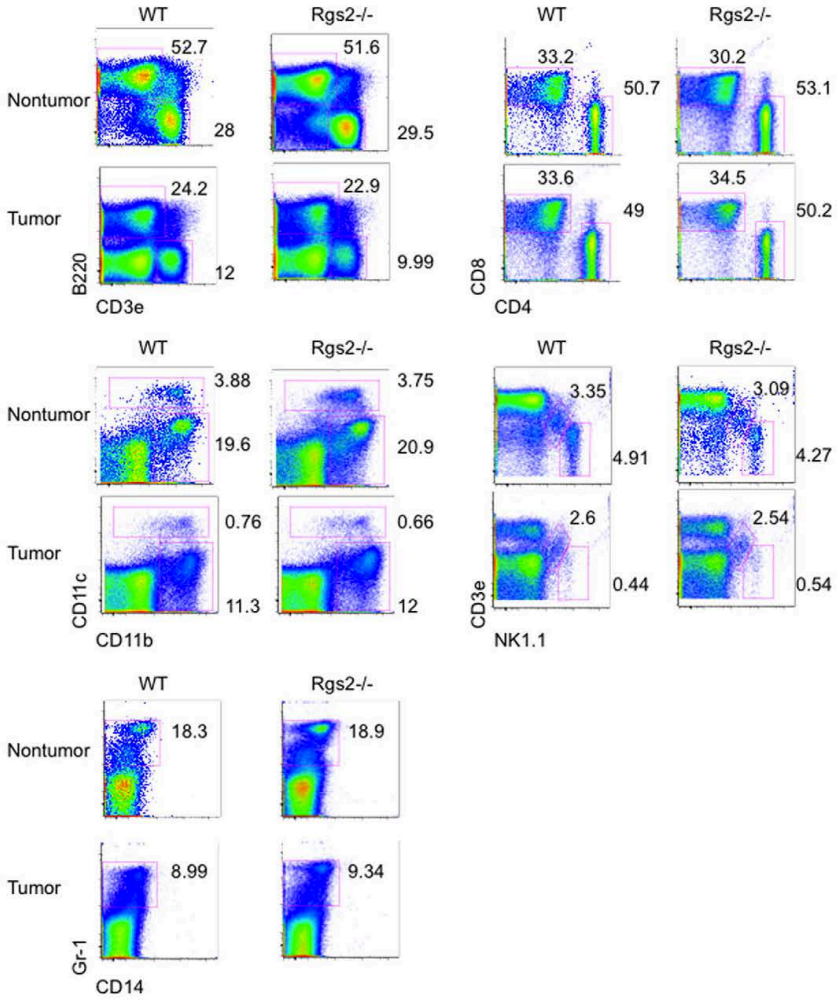

Figure 4. Lack of Rgs2 does not affect populations of mature leukocytes. Spleens were isolated from non-tumor bearing and 3LL tumor bearing WT and Rgs2−/− mice, processed into single cell suspensions, and labeled with the indicated antibodies, then analyzed by flow cytometry. Experiment was performed 3 times with 3–4 mice per group.
doi:10.1371/journal.pone.0018534.g004

MDSCs in tumor progression using Rgs2 knockout mice. Mice without Rgs2 are viable, healthy, and fertile, but have defects in hippocampal development [23]. Since the Rgs2 null mouse was developed in the C57Bl/6 background, we injected Rgs2−/− mice and C57BL/6 wild type controls with syngeneic 3LL cells subcutaneously in the hindlimb, and measured tumor growth over time. The null mice exhibited significantly retarded tumor growth compared to the wild type mice (Figure 2A). Similar results were achieved when the mice were injected with a syngeneic melanoma tumor line, B16 (data not shown). These results reveal a positive role of Rgs2 in tumor growth and progression.

To examine the specific role of Rgs2 in MDSCs, we performed a reconstitution experiment. MDSCs were isolated from spleens of tumor bearing wild type or null mice by fluorescence activated cell sorting using antibodies against Gr-1 and CD11b. We achieved greater than 95% purity (data not shown). These MDSCs were co-injected with 3LL cells subcutaneously in the hindlimb of wild type mice, and tumor growth was measured over time (Figure 2B). We found that while wild type MDSCs were able to promote tumor growth, Rgs2−/− MDSCs lost their tumor promoting function, when compared to growth of the tumor cells alone (Figure 2B). Furthermore, we evaluated lung microvascular endothelial cells isolated from WT and Rgs2−/− mice, and found no difference in

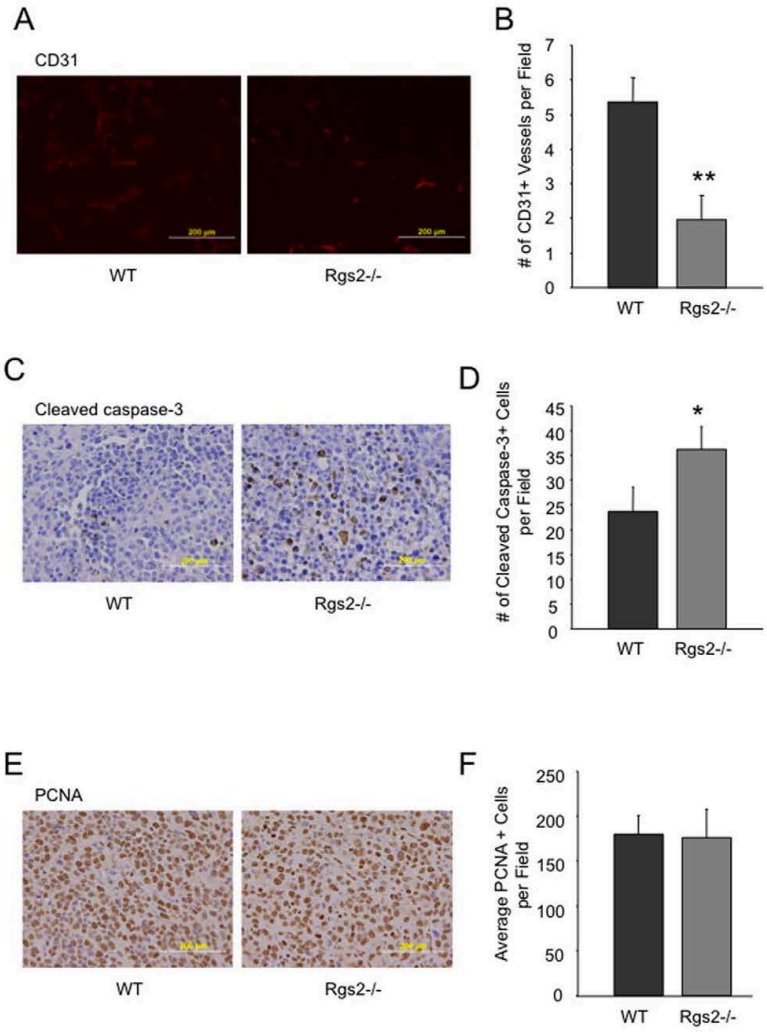

Figure 5. Tumors in Rgs2−/− mice exhibit decreased vascular density and increased cell death. (A), (C), (E) Sections from size matched 3LL tumors grown in wild type mice and Rgs2 null mice were stained for CD31, active caspase-3 and PCNA, respectively. Representative images are shown. (B), (D), (F) The numbers of CD31 positive vascular structures, active caspase-3 positive cells, and PCNA positive cells, respectively, were quantified in 10 randomly selected fields under microscopy. These experiments were repeated 3–4 times. ** $p<0.005$, * $p<0.05$.
doi:10.1371/journal.pone.0018534.g005

vascular tube formation, BrdU incorporation, or endothelial cell migration in response to serum stimulation between the two groups (Figure 3). In addition, Rgs2 deficiency did not affect the proportions of immature hematopoietic populations (data not shown) or mature hematopoietic populations (Figure 4). Together, these data support a specific role of Rgs2 signaling in MDSCs that is responsible for their tumor promoting activity.

Tumors from Rgs2−/− mice exhibit decreased vascularization and increased cell death

MDSCs are known to infiltrate into tumors and promote tumor angiogenesis. Histological analysis of size-matched 3LL tumors from wild type and Rgs2−/− mice revealed a significantly lower vascular density, as measured by CD31-positive vessel structures, in tumors harvested from null mice than from wild type controls (Figure 5A B). Similar results were observed when we used another vascular marker, von Willebrand factor (data not shown). Consistently, there is a significant increase in cell death, as indicated by cleaved caspase-3 staining in tumors from the null mice (Figure 5C D). We did not see any significant difference in cell proliferation, as measured by PCNA staining, between the two groups (Figure 5E F). These findings point to a pro-angiogenic function of Rgs2 in MDSCs in tumor growth and progression.

Rgs2 plays no significant role in MDSC expansion and differentiation

MDSCs are elevated in tumor bearing hosts, and display different differentiation profiles compared to cells from non-tumor bearing hosts [4,5,6,7]. Since Rgs2 is elevated in tumor derived MDSCs, we then determined whether Rgs2 has a role in MDSC expansion by analyzing spleens from 3LL tumor bearing wild type and null mice by flow cytometry. We found that spleens of both mice contained similar numbers of MDSCs (Figure 6A). Next, to determine if the lack of Rgs2 affects the proportions of the cells that comprise the heterogeneic Gr-1+CD11b+ fraction, we isolated Gr-1+CD11b+ cells from spleens of tumor bearing wild type and Rgs2−/− mice and scored them by morphology (Figure 6B). We observed a small decrease in the more monocytic MDSCs. However, no other cell types were different. Furthermore, we analyzed several cell surface molecules, such as Ly6C and Ly6G, on Gr-1+CD11b+ cells from wild type and Rgs2−/− mice by flow cytometry, and found no significant differences (Figure 7). These data indicate that it is less likely that Rgs2 plays a major role in expansion and differentiation of MDSC.

Rgs2 upregulates MCP-1 in MDSCs

A major function for MDSCs is secretion of growth factors, contributing to the cytokine milieu that promotes tumor growth. To determine if lack of Rgs2 affects cytokine production within

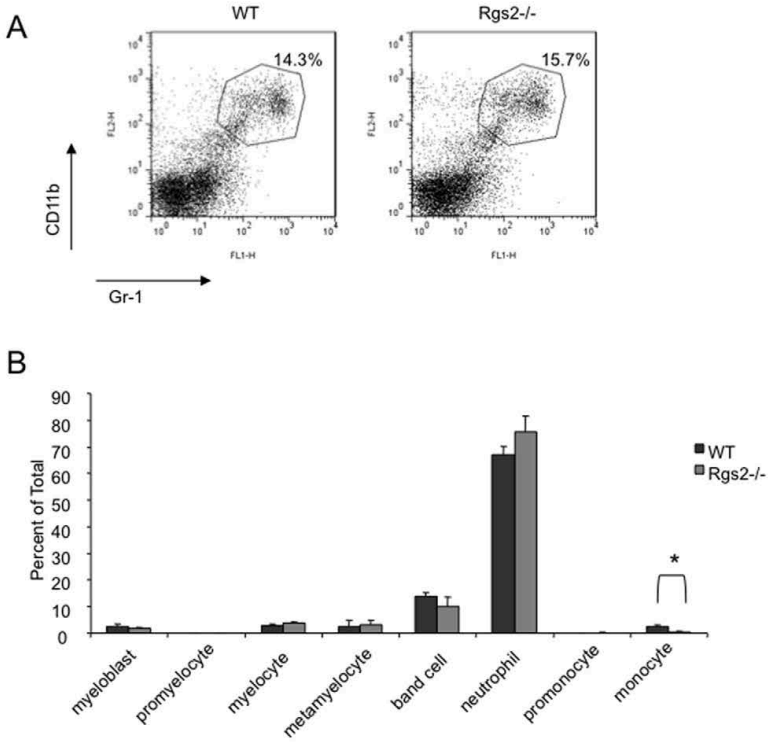

Figure 6. Rgs2 deficiency has minimal effects on MDSC expansion and differentiation. (A) Wild type and Rgs2−/− mice were injected with 1×10^5 3LL cells in the hindlimb, and 20 days later, spleens were isolated and analyzed by flow cytometry for Gr-1+CD11b+ MDSCs. This experiment was performed at least 3 times and the graphs shown are results from pooling of 3 mice per group. (B) MDSCs were isolated from spleens of tumor bearing Rgs2−/− and wild type mice using the MACS system, spun onto slides using a cytospin centrifuge, and stained. The slides were read by a hematopathologist in a blind fashion, and cells were categorized by morphology. This experiment was performed 4 times. * $p<0.01$.
doi:10.1371/journal.pone.0018534.g006

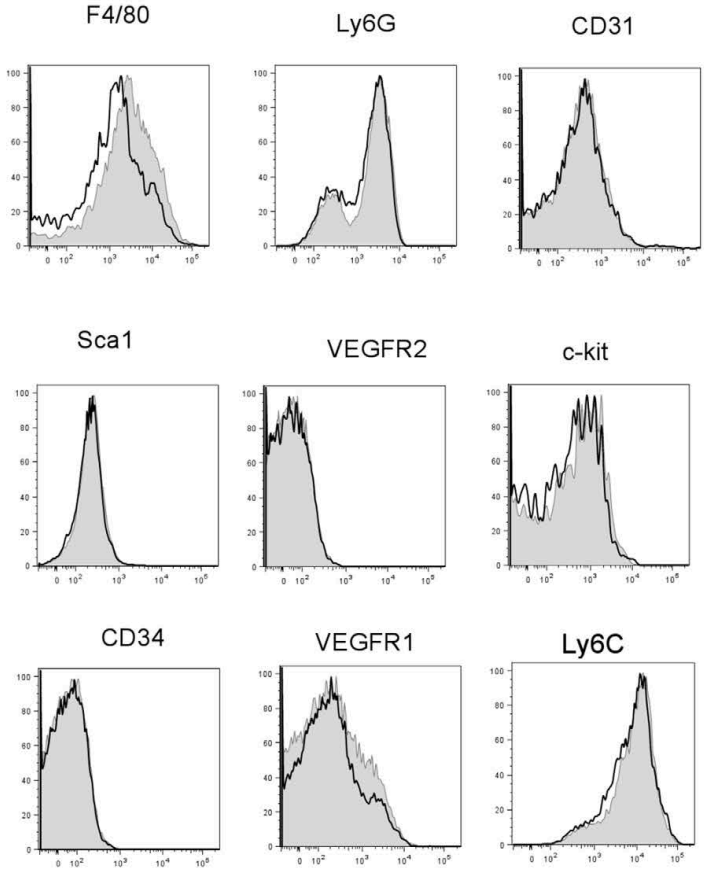

Figure 7. Analysis of cell surface molecules on Gr-1+CD11b+ MDSCs. Spleens were harvested from 3LL tumor bearing WT or Rgs2−/− mice between days 17–21 post-injection, processed into single cell suspensions, and labeled with antibodies against the indicated cell surface molecules. Representative plots are shown. Experiment was performed 3 times with 3–4 mice per group. Shaded = WT, open = Rgs2−/−.
doi:10.1371/journal.pone.0018534.g007

these cells, we performed a protein cytokine array on the lysates of wild type and null MDSCs isolated directly from 3LL tumor tissue. We found a dramatic reduction of MCP-1 (~9 10-fold) in Rgs2 null MDSCs compared to wild type MDSCs (Figure 8A). Using real time RT-PCR on RNA isolated from 3LL tumor tissue-derived MDSCs, we confirmed that, similar to the cytokine array, MCP-1 mRNA levels were significantly reduced in Rgs2 null MDSCs compared to wild type MDSCs (Figure 8B). Moreover, we measured MCP-1 protein levels by ELISA from media of cultured MDSCs purified from tumor tissues of wild type and Rgs2−/− mice for 48 hours. Consistently, we detected a dramatic reduction in the MCP-1 protein levels produced and secreted by Rgs2−/− MDSCs compared to wild type cells (Figure 8C).

In addition, we analyzed a potential correlation of Rgs2 and MCP-1 mRNA levels *in vivo* using freshly isolated MDSCs by real time RT-PCR. Consistent with an induction of Rgs2 in tumor derived MDSCs, there is a significant increase of MCP-1 levels in these cells compared to MDSCs isolated from non-tumor bearing mice (Figure 8D). These results support a positive role of Rgs2 in regulating MCP-1 expression in MDSCs. Together, the findings suggest that tumor conditions regulate Rgs2 expression, and Rgs2 regulates MCP-1 expression in MDSCs.

Rgs2 mediates pro-angiogenic function in MDSCs through MCP-1

MCP-1 is a potent angiogenic factor, and we found that tumors in Rgs2−/− mice have decreased vascular density compared to tumors in wild type mice (Figure 5A B). To determine whether decreased production of MCP-1 in the null MDSCs is responsible for defective angiogenesis associated with the Rgs2 null condition, we performed *in vitro* angiogenic assays. MDSCs isolated from tumor tissues of wild type or Rgs2−/− mice were cultivated overnight. Endothelial cells, (HUVECs) were then cultivated in the conditioned media from the MDSCs on Matrigel, which allowed vascular tube structures to form, and branch points were counted over time. There were significantly fewer vascular structures developed in the group treated with Rgs2−/− MDSC conditioned medium compared to those treated with wild type MDSC conditioned medium (Figure 9A and B).

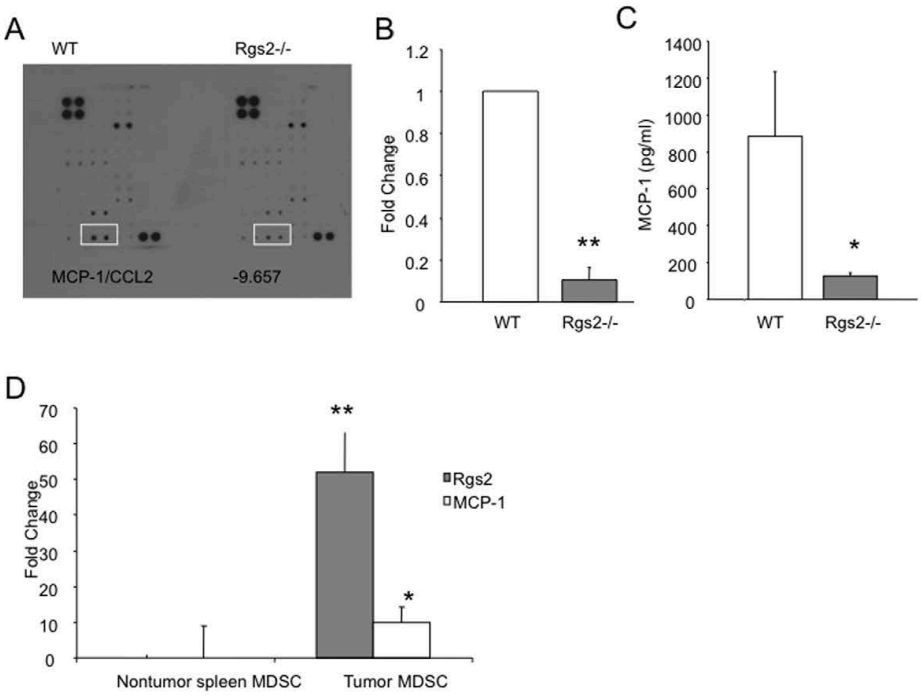

Figure 8. Rgs2 regulates MCP-1 expression in MDSCs. MDSCs were isolated from 3LL tumor tissues of wild type or Rgs2−/− mice by magnetic sorting after digestion of the tissues with hyaluronidase and collagenase. (A) Protein lysates from the isolated cells were analyzed using a cytokine array. Each cytokine is detected in duplicate, and intensity was determined using ImageJ software. Positive controls provided on the array were used for normalization. This experiment was performed twice. (B) RNA was extracted from the isolated MDSCs, and analyzed by real time PCR. Beta-actin was used as an internal control. This experiment was repeated 3 times. (C) MDSCs were isolated from tumors of wild type and Rgs2 null mice, and cultured for 48 hours. Culture medium was assayed for MCP-1 protein by ELISA. This experiment was performed in duplicate and repeated 3 times. * $p<0.05$, ** $p<0.00005$. (D) MDSCs were isolated from normal spleen and 3LL tumor tissues of wild type mice. Rgs2 and MCP-1 levels were measured by real time PCR. Beta-actin was used as an internal control. This experiment was repeated 2 times. * $p<0.05$, ** $p<0.005$.
doi:10.1371/journal.pone.0018534.g008

Next, we assessed the ability of endothelial cells to migrate toward MDSCs. MDSCs were isolated from the tumor tissues of wild type and Rgs2−/− mice and cultivated overnight. Then, HUVECs were seeded in the top Transwell chamber and allowed to migrate toward the bottom chamber containing the MDSCs. In agreement with poor vascular tube formation induced by Rgs2 null MDSC conditioned medium, a significant reduction was observed in endothelial cell migration toward the null MDSCs compared to wild type cells (Figure 9C). Interestingly, addition of neutralizing MCP-1 specific antibody significantly inhibited wild type MDSC mediated endothelial cell migration. The number of migrated endothelial cells is not statistically different from the retarded migration observed toward Rgs2 null MDSCs (Figure 9C). Conversely, addition of recombinant MCP-1 with the Rgs2−/− MDSCs rescued defective angiogenic function (Figure 9C). Collectively, these data indicate that MCP-1 is responsible for Rgs2-mediated pro-angiogenic function in MDSCs.

Discussion

MDSCs play a critical role in tumor progression through modulating the tumor microenvironment. They promote tumor growth at the primary site, as well as enhance metastasis [4,6]. They have been linked to resistance to anti- angiogenic therapy in cancer [8]. Efforts focused at differentiating or attenuating the function of MDSCs have been promising, leading to improved immune response against the tumor and a better prognosis for the patient [2]. Clearly, identifying molecular mediators important for MDSC function will enhance our ability to better target these cells for cancer treatment. In this study, we identified a new mediator, Rgs2, that regulates pro-angiogenic function of MDSCs. We found that tumor conditions upregulate Rgs2 expression in MDSCs, and MDSCs lacking Rgs2 were no longer capable of promoting tumor growth in tumor reconstitution assays. Tumors in Rgs2−/− mice grew more slowly, and had less vascular density and increased cell death.

Furthermore, we identified the downstream molecular mediator responsible for Rgs2 mediated pro-angiogenic function in MDSCs. We found that Rgs2−/− MDSCs isolated from tumors produce drastically reduced levels of MCP-1 compared to wild type. While MCP-1 has been reported to promote migration of MDSCs [24,25], production of MCP-1 by MDSCs has previously not been well studied. MCP-1 is a potent angiogenic factor. It promotes angiogenesis through indirect effects, such as through monocyte migration or induction of angiogenic factors such as VEGF and MMP9 [26,27,28], or by directly functioning on endothelial cells [22]. In this study, we show that wild type MDSCs secrete MCP-1,

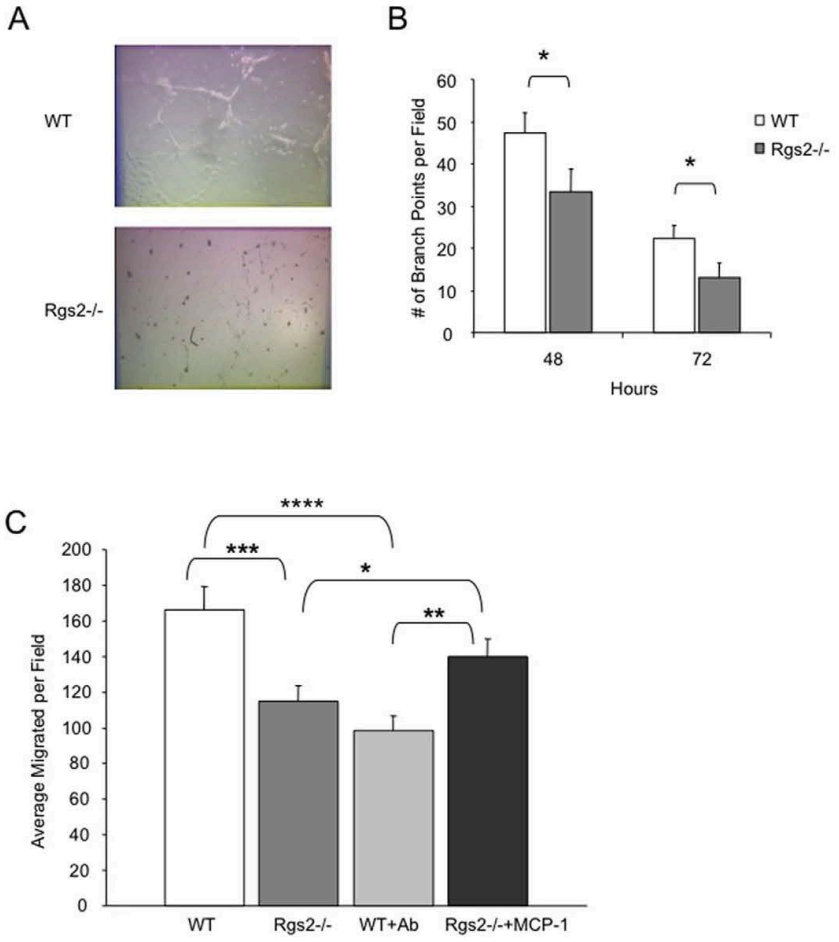

Figure 9. Angiogenic function of Rgs2 in MDSC is mediated through MCP-1. (A) and (B) Wild type and Rgs2−/− MDSCs were isolated from 3LL tumor tissues by magnetic sorting, and incubated overnight at 37°C. 80,000 HUVECs were plated in each well of a 48-well plate on top of Matrigel in the conditioned medium derived from the isolated MDSCs. Representative images are shown at 72 hours, and Vascular network branch points were scored at the times indicated. This experiment was performed in duplicate and repeated twice. (C) MDSCs were isolated from tumors of Rgs2−/− and wild type mice by magnetic sorting, and incubated overnight. Transwells containing 1×10^5 HUVECs in the top chamber were added and allowed to migrate for 3.5 hours. MCP-1 neutralizing antibody (Ab) (1 ug/ml) was added to wild type cells or 1 ng/ml of recombinant MCP-1 was added to Rgs2−/− cells. This experiment was performed 3 times in duplicate. * $p\leq0.05$, ** $p<0.005$, *** $p<0.001$, **** $p<0.00005$.
doi:10.1371/journal.pone.0018534.g009

which promotes endothelial cell migration and vascular tube formation. Rgs2−/− MDSCs secrete much lower levels of MCP-1, which leads to reduced angiogenesis in tumors from Rgs2−/− mice.

Together, this study links the tumor promoting roles of Rgs2 in MDSCs to a secreted molecule, MCP-1. We show that hypoxia, commonly associated with solid tumors, upregulates Rgs2 expression in MDSCs, which leads to increased production of MCP-1. The MCP-1 then mediates the angiogenic effects. MCP-1 is produced mainly under pathological conditions, and is expressed by several cancer types [28,29]. In a mouse model of breast cancer, treatment with neutralizing antibodies against MCP-1 enhanced survival and decreased metastasis [22], suggesting that targeting of this pathway in human cancer will likely prove beneficial. While it is uncertain how Rgs2 modulates MCP-1 levels, Rgs2 was predicted to encode a basic helix-loop-helix protein [30,31]. Nuclear expression of Rgs2 was reported in several studies [16,32,33] including our unpublished data. These findings point to a function of Rgs2 in gene transcription. Future studies will be necessary to elucidate the mechanism involved.

In summary, our studies indicate that Rgs2 and MCP-1 are important molecules for the effector functions of MDSCs. Lack of Rgs2 in MDSCs abolishes their tumor promoting function, and leads to decreased levels of MCP-1, along with slower tumor progression and decreased vascular density in tumors. Thus, targeting Rgs2 and MCP-1 signaling may have important clinical implications, and lead to a better prognosis for cancer patients.

Acknowledgments

We thank Dr. Laura DeBusk at Vanderbilt University Medical Center for stimulating discussion and critical comments on the manuscript.

Author Contributions

Conceived and designed the experiments: KCB LEG SJ PCL. Performed the experiments: KCB LEG MAT LY. Analyzed the data: KCB LEG MAT LY PCL. Contributed reagents/materials/analysis tools: KCB LEG SJ MAT LY PCL. Wrote the paper: KCB LEG SJ MAT LY PCL.

References

1. Tlsty TD, Coussens LM (2006) Tumor stroma and regulation of cancer development. Annu Rev Pathol 1: 119 150.
2. Gabrilovich DI, Nagaraj S (2009) Myeloid-derived suppressor cells as regulators of the immune system. Nat Rev Immunol 9: 162 174.
3. Sinha P, Clements VK, Bunt SK, Albelda SM, Ostrand-Rosenberg S (2007) Cross-talk between myeloid-derived suppressor cells and macrophages subverts tumor immunity toward a type 2 response. J Immunol 179: 977 983.
4. Yang L, DeBusk LM, Fukuda K, Fingleton B, Green-Jarvis B, et al. (2004) Expansion of myeloid immune suppressor Gr+CD11b+ cells in tumor-bearing host directly promotes tumor angiogenesis. Cancer Cell 6: 409 421.
5. Shojaei F, Wu X, Zhong C, Yu L, Liang XH, et al. (2007) Bv8 regulates myeloid-cell-dependent tumour angiogenesis. Nature 450: 825 831.
6. Yang L, Huang J, Ren X, Gorska AE, Chytil A, et al. (2008) Abrogation of TGF beta signaling in mammary carcinomas recruits Gr-1+CD11b+ myeloid cells that promote metastasis. Cancer Cell 13: 23 35.
7. Murdoch C, Muthana M, Coffelt SB, Lewis CE (2008) The role of myeloid cells in the promotion of tumour angiogenesis. Nat Rev Cancer 8: 618 631.
8. Shojaei F, Wu X, Malik AK, Zhong C, Baldwin ME, et al. (2007) Tumor refractoriness to anti-VEGF treatment is mediated by CD11b+Gr1+ myeloid cells. Nat Biotechnol 25: 911 920.
9. Druey KM, Blumer KJ, Kang VH, Kehrl JH (1996) Inhibition of G-protein-mediated MAP kinase activation by a new mammalian gene family. Nature 379: 742 746.
10. Koelle MR, Horvitz HR (1996) EGL-10 regulates G protein signaling in the C. elegans nervous system and shares a conserved domain with many mammalian proteins. Cell 84: 115 125.
11. Siderovski DP, Hessel A, Chung S, Mak TW, Tyers M (1996) A new family of regulators of G-protein-coupled receptors? Curr Biol 6: 211 212.
12. Reif K, Cyster JG (2000) RGS molecule expression in murine B lymphocytes and ability to down-regulate chemotaxis to lymphoid chemokines. J Immunol 164: 4720 4729.
13. Shi GX, Harrison K, Han SB, Moratz C, Kehrl JH (2004) Toll-like receptor signaling alters the expression of regulator of G protein signaling proteins in dendritic cells: implications for G protein-coupled receptor signaling. J Immunol 172: 5175 5184.
14. De Vries L, Zheng B, Fischer T, Elenko E, Farquhar MG (2000) The regulator of G protein signaling family. Annu Rev Pharmacol Toxicol 40: 235 271.
15. Ross EM, Wilkie TM (2000) GTPase-activating proteins for heterotrimeric G proteins: regulators of G protein signaling (RGS) and RGS-like proteins. Annu Rev Biochem 69: 795 827.
16. Zmijewski JW, Song L, Harkins L, Cobbs CS, Jope RS (2001) Oxidative stress and heat shock stimulate RGS2 expression in 1321N1 astrocytoma cells. Arch Biochem Biophys 392: 192 196.
17. Song L, Jope RS (2006) Cellular stress increases RGS2 mRNA and decreases RGS4 mRNA levels in SH-SY5Y cells. Neurosci Lett 402: 205 209.
18. Schwable J, Choudhary C, Thiede C, Tickenbrock L, Sargin B, et al. (2005) RGS2 is an important target gene of Flt3-ITD mutations in AML and functions in myeloid differentiation and leukemic transformation. Blood 105: 2107 2114.
19. Rollins BJ, Walz A, Baggiolini M (1991) Recombinant human MCP-1/JE induces chemotaxis, calcium flux, and the respiratory burst in human monocytes. Blood 78: 1112 1116.
20. Melgarejo E, Medina MA, Sanchez-Jimenez F, Urdiales JL (2009) Monocyte chemoattractant protein-1: a key mediator in inflammatory processes. Int J Biochem Cell Biol 41: 998 1001.
21. Loetscher P, Seitz M, Baggiolini M, Moser B (1996) Interleukin-2 regulates CC chemokine receptor expression and chemotactic responsiveness in T lymphocytes. J Exp Med 184: 569 577.
22. Salcedo R, Ponce ML, Young HA, Wasserman K, Ward JM, et al. (2000) Human endothelial cells express CCR2 and respond to MCP-1: direct role of MCP-1 in angiogenesis and tumor progression. Blood 96: 34 40.
23. Oliveira-Dos-Santos AJ, Matsumoto G, Snow BE, Bai D, Houston FP, et al. (2000) Regulation of T cell activation, anxiety, and male aggression by RGS2. Proc Natl Acad Sci U S A 97: 12272 12277.
24. Huang Y, Chen X, Dikov MM, Novitskiy SV, Mosse CA, et al. (2007) Distinct roles of VEGFR-1 and VEGFR-2 in the aberrant hematopoiesis associated with elevated levels of VEGF. Blood 110: 624 631.
25. Sawanobori Y, Ueha S, Kurachi M, Shimaoka T, Talmadge JE, et al. (2008) Chemokine-mediated rapid turnover of myeloid-derived suppressor cells in tumor-bearing mice. Blood 111: 5457 5466.
26. Goede V, Brogelli L, Ziche M, Augustin HG (1999) Induction of inflammatory angiogenesis by monocyte chemoattractant protein-1. Int J Cancer 82: 765 770.
27. Varney ML, Olsen KJ, Mosley RL, Singh RK (2005) Paracrine regulation of vascular endothelial growth factor a expression during macrophage-melanoma cell interaction: role of monocyte chemotactic protein-1 and macrophage colony-stimulating factor. J Interferon Cytokine Res 25: 674 683.
28. Raman D, Baugher PJ, Thu YM, Richmond A (2007) Role of chemokines in tumor growth. Cancer Lett 256: 137 165.
29. Conti I, Rollins BJ (2004) CCL2 (monocyte chemoattractant protein-1) and cancer. Semin Cancer Biol 14: 149 154.
30. Siderovski DP, Blum S, Forsdyke RE, Forsdyke DR (1990) A set of human putative lymphocyte G0/G1 switch genes includes genes homologous to rodent cytokine and zinc finger protein-encoding genes. DNA Cell Biol 9: 579 587.
31. Siderovski DP, Heximer SP, Forsdyke DR (1994) A human gene encoding a putative basic helix-loop-helix phosphoprotein whose mRNA increases rapidly in cycloheximide-treated blood mononuclear cells. DNA Cell Biol 13: 125 147.
32. Chatterjee TK, Fisher RA (2000) Cytoplasmic, nuclear, and golgi localization of RGS proteins. Evidence for N-terminal and RGS domain sequences as intracellular targeting motifs. J Biol Chem 275: 24013 24021.
33. Song L, Zmijewski JW, Jope RS (2001) RGS2: regulation of expression and nuclear localization. Biochem Biophys Res Commun 283: 102 106.

Immunity
Article

Follicular B Cell Trafficking within the Spleen Actively Restricts Humoral Immune Responses

Kristen L. Hoek,[1] Laura E. Gordy,[1] Patrick L. Collins,[1] Vrajesh V. Parekh,[1] Thomas M. Aune,[1,2] Sebastian Joyce,[1] James W. Thomas,[1,2] Luc Van Kaer,[1] and Eric Sebzda[1,*]
[1]Department of Microbiology and Immunology
[2]Department of Medicine
Vanderbilt University, Nashville, TN 37232-2363, USA
*Correspondence: eric.sebzda@vanderbilt.edu
DOI 10.1016/j.immuni.2010.07.016

SUMMARY

Follicular (FO) and marginal zone (MZ) B cells are maintained in distinct locations within the spleen, but the genetic basis for this separation is still enigmatic. We now report that B cell sequestration requires lineage-specific regulation of migratory receptors by the transcription factor *Klf2*. Moreover, using gene-targeted mice we show that altered splenic B cell migration confers a significant in vivo gain-of-function phenotype to FO B cells, including the ability to quickly respond to MZ-associated antigens and pathogens in a T cell-dependent manner. This work demonstrates that in wild-type animals, naive FO B cells are actively removed from the MZ, thus restricting their capacity to respond to blood-borne pathogens.

INTRODUCTION

The B cell compartment is composed of three mature lymphocyte lineages: B1 B cells (Fagarasan et al., 2000), B2 marginal zone (MZ) B cells (Lopes-Carvalho and Kearney, 2004; Martin and Kearney, 2002), and B2 follicular (FO) B cells (Okada and Cyster, 2006). All three lineages are located in distinct anatomical sites that contribute to their unique humoral functions. B1 B cells are found in the pleural and peritoneal cavities and respond to invading bacteria within the gut. Mature MZ B cells reside within the splenic white pulp, directly adjacent to the marginal sinus in the MZ. These cells come in direct contact with slow-flowing blood and typically respond to blood-borne pathogens. In adult mice, B1 B cells and MZ B cells act to mediate the initial wave of humoral immunity against invading pathogens by quickly producing antigen-specific antibodies in a thymus-independent (TI) fashion. In sharp contrast, FO B cells circulate between the blood and spleen and comprise the majority of B cells found in peripheral lymph nodes. These cells rely on thymus dependent (TD) signals to respond to antigen and are located adjacent to T cell-rich areas in secondary lymphoid organs. How these B cell lineages remain compartmentalized is the subject of intense research.

A major challenge is to determine the mechanisms by which B cell migration is transcriptionally controlled. Quiescent B cells express Kruppel-like factor 2 (Klf2), a transcription factor previously implicated in naive T cell cycling (Buckley et al., 2001; Kuo et al., 1997b) and trafficking (Carlson et al., 2006; Sebzda et al., 2008). To determine whether this factor was similarly required within the B cell lineage, we excised *Klf2* in a B cell-specific manner. We discovered that Klf2 differentially regulates FO and MZ B cell migratory receptors and that loss of Klf2 causes a blurring of MZ and FO B cell separation within the spleen. As a result of this migratory defect, Klf2-deficient FO B cells gain the ability to respond to MZ-associated antigens and pathogens. This study indicates that Klf2 supports lineage-specific B cell homeostatic trafficking patterns and, in the case of FO B cells, restricts antigen recognition within the spleen.

RESULTS

Klf2-Deficient B Cells Prematurely Exit the Bone Marrow

Klf2 expression is first detected in the B cell compartment after productive pre-B cell receptor signaling in small resting pre-B lymphocytes (Schuh et al., 2008). This transcription factor is preferentially expressed in quiescent B cells (Bhattacharya et al., 2007; Fruman et al., 2002; Glynne et al., 2000), and we found that several factors that induce B cell activation quickly downregulated Klf2 expression (Figure S1A available online). Although transcription varied between B cell lineages (e.g., naive FO B cell express 2.5× more Klf2 than MZ B cells, $p = 0.004$), all three cell types efficiently extinguished Klf2 expression following B cell-receptor stimulation (Figure S1B). To better understand the role of Klf2 within the B cell compartment, we crossed *loxP*-flanked *Klf2* mice with gene-targeted animals expressing Cre under the CD19 promoter (*Klf2*$^{fl/fl}$; *Cd19-Cre*$^{+/}$). As expected, efficient Klf2 excision was observed exclusively in B cells, both at the transcriptional (Figure S1C) and translational level (Figure S1D). Flow cytometric analysis of bone marrow cells indicated that Klf2-deficient B cell development up to the immature B cell stage was normal, both in terms of surface receptors and absolute cell numbers (Figure 1A). In contrast, fewer transitional or recirculating Klf2-deficient B cells were detected. Both T1 (AA4$^+$IgM$^+$CD23) and T2 (AA4$^+$IgM$^+$CD23$^+$) transitional B cell numbers were increased in spleens from genetically targeted animals (Figure 1B), suggesting that *Klf2* excision did not block late stages of B cell development but instead played a role in immature B cell retention within the bone marrow.

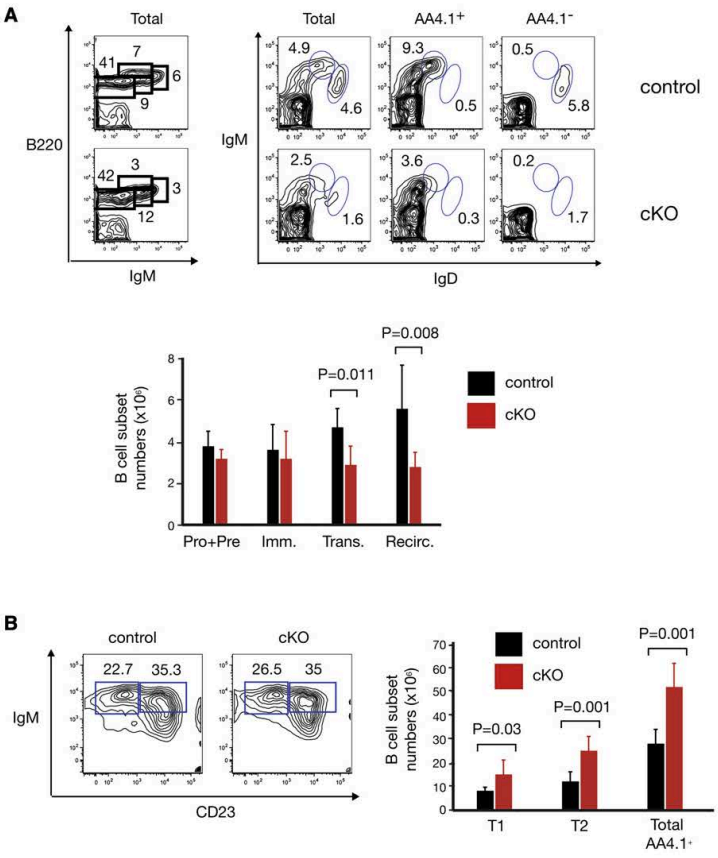

Figure 1. *Klf2*$^{fl/fl}$; CD19-cre$^{+/-}$ Mice Have Decreased Numbers of Mature B Cells in the Bone Marrow but Increased Numbers of Transitional B Cells in the Spleen

(A) Transitional and mature B cell numbers are reduced in bone marrow of genetically targeted mice. The left panels show B cell differentiation within the bone marrow of *Klf2*$^{fl/fl}$; *Cd19-Cre*$^{+/}$ (cKO = genetically targeted) and *Klf2*$^{+/+}$; *Cd19-Cre*$^{+/}$ (control) mice, which was analyzed by flow cytometry with surface markers that distinguish between Pro-B + Pre-B cells (B220^{low}IgM^{low}), immature B cells (B220^{int-hi}IgM^{int}), transitional B cells (B220^{int}IgM^{hi}), and mature + recirculating B cells (B220^{hi}IgM^{int}). The right panels show transitional (AA4.1^{+} IgM^{hi}IgD^{int}) and mature + recirculating (AA4.1 IgM^{int}IgD^{hi}) B cells, which were reanalyzed with an alternative staining technique. Numbers are B cell percentages within each compartment; absolute cell numbers are displayed in the corresponding bar graph. (Pro + Pre, Pro-B and Pre-B cells; Imm., immature B cells; Trans., transitional B cells; and Recirc., recirculating B cells) Note that Pro+Pre B cell numbers are displayed on a different scale (×10^{7}). n = 4 animals per group. $p > 0.05$ for Pro + Pre and Imm. B cell stages. Error bars indicate the standard deviation.

(B) Transitional B cell stages (B220^{+}AA4.1^{+}) within the spleen of cKO and control mice were examined by flow cytometry and corresponding absolute cell numbers, and p values are listed in the adjoining bar graph. Percentages of T1 (AA4.1^{+}B220^{+}IgM^{hi}CD23^{low}) and T2 (AA4.1^{+} B220^{+}IgM^{hi}CD23^{hi}) B cells are displayed in the contour plots. n = 8 animals per group. Error bars indicate the standard deviation.

Genetically Targeted Mice Have Increased Numbers of Splenic B Cells

The mature splenic B cell compartment is composed of circulating FO B cells and noncirculating MZ B cells. As shown in Figure 2A, genetically targeted mice had an increased proportion of MZ B cells (AA4.1 CD21^{hi}IgM^{hi}) relative to control littermates (*Klf2*$^{+/+}$; *Cd19-Cre*-cre$^{+/}$ or *Klf2*$^{fl/+}$; *Cd19-Cre*$^{+/}$). In fact, both FO and MZ B cell numbers were significantly increased in the spleens of genetically targeted animals (Figure 2B). To ensure that lymphocytes were correctly identified, we reanalyzed the B cell compartment using additional staining techniques. First, circulating FO B cells were identified in mesenteric lymph nodes of control animals, which are known to lack MZ B cells (Allman and Pillai, 2008), with antibodies directed against CD21, CD23, and IgM (Figure S2A). A similar cell population, which expresses slightly higher levels of CD21, was then identified in lymph nodes of genetically targeted mice. These gating parameters were transferred to the splenic B cell compartment to demarcate FO B cells. MZ B cell populations were then gated in relation to the FO B cell compartment (Figure S2B). To ensure that CD23^{+} MZ B cell precursors were not mistakenly identified as FO B cells, splenocytes were stained with a combination of antibodies to distinguish MZ B cell precursors from MZ and FO B cells (Srivastava et al., 2005). Similar to transitional B cell stages, genetically targeted mice had relatively normal frequencies of MZ B cell precursors (Figure S2C), which translated into significantly increased cell numbers (control = 2.8 ± 1.7 × 10^{6}, genetically targeted mice = 13.1 ± 5.8 × 10^{6}, p = 0.005). FO-II B cells (AA4.1^{+} CD19^{+} IgM^{hi} IgD^{hi} CD21^{int} CD23^{+}), which are speculated to act as a reservoir for MZ precursors (Cariappa et al., 2007), were not affected by the loss of Klf2 (control = 3.1 ± 1.4 × 10^{6}, genetically targeted mice = 3.9 ± 2.2 × 10^{6}, p = 0.56). Both Klf2^{+} and Klf2-deficient FO B cells (FO-I cells) displayed similar staining patterns for IgD, CD1d, and CD9 (Figure S2D), which were distinct from Klf2^{+} and Klf2-deficient MZ B cell precursors. These conserved surface markers (Figure S2E) confirmed that FO B cells were distinct from MZ B cell precursors in genetically targeted animals, and that despite elevated surface expression of CD21 in Klf2-deficient B cells, this receptor could be used to properly identify FO B cells (Figure S2F). It should be noted that a small number of AA4.1 CD21^{hi}IgM^{hi} cells were detected in the blood and lymph nodes of *Klf2*$^{fl/fl}$; *Cd19-Cre*$^{+/}$ mice

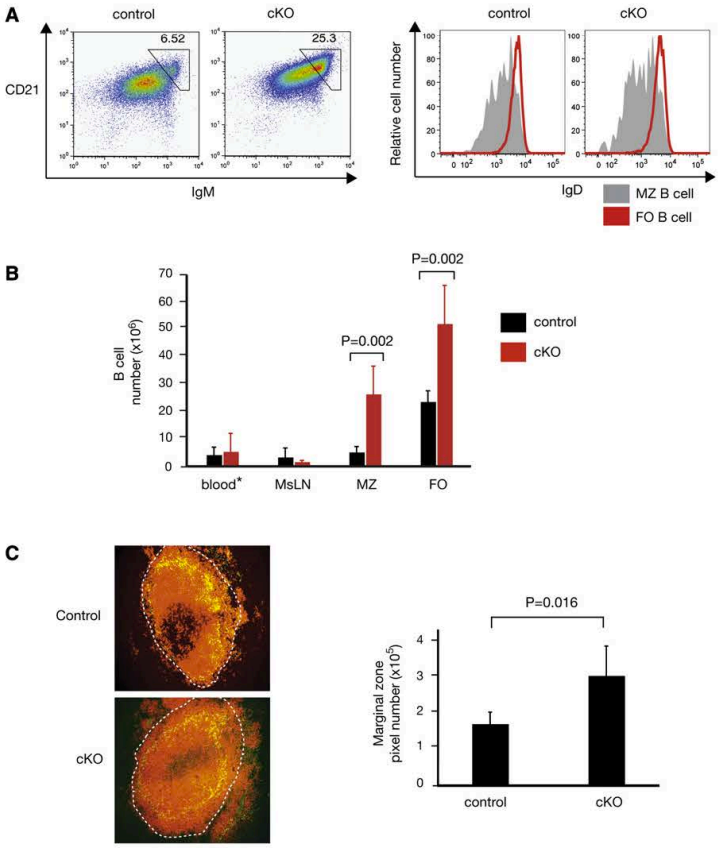

Figure 2. Genetically Targeted Animals Have Increased Numbers of Splenic B Cells

(A) Mature splenic B cells ($B220^+$ $AA4.1^-$) from *Klf2*$^{fl/fl}$; *Cd19-Cre*$^{+/-}$ (genetically targeted = cKO) and *Klf2*$^{fl/+}$; *Cd19-Cre*$^{+/-}$ (control) mice are displayed in terms of the lineage-defining markers CD21, IgD, and IgM. The inner quadrant demarcates MZ B cells and their relative frequency. n > 20 animals per group.

(B) Absolute $AA4.1^-$ B cell numbers from *Klf2*$^{+/+}$; *Cd19-Cre*$^{+/-}$ (black bars) and *Klf2*$^{fl/fl}$; *Cd19-Cre*$^{+/-}$ (red bars) animals are shown along with significant p values. Error bars indicate the standard deviation. Note that blood is measured in terms of volume instead of total tissue and is displayed on an alternative scale ($\times 10^5$ per ml). (MsLN, mesenteric lymph nodes; MZ, splenic MZ B cells; and FO, splenic follicular B cells) n = 6 animals per group. p > 0.05 for blood and MsLN.

(C) Immunohistochemistry of spleens from control and cKO mice, stained for $B220^+$ (red) and $MOMA\text{-}1^+$ (green). The $MOMA1^+$ metallophilic macrophages appear yellow in the overlay. A white dashed line highlights the outer edge of the MZ. MZ area was enumerated from ten separate images and displayed as a bar graph with an arbitrary scale (number of pixels). Error bars indicate the standard deviation. n = 4 animals per group.

(2%–3% of $AA4.1^-$ B cells); however, these cells costained for CD23 and IgD but not CD1d or CD9 (Figure S2G), indicating that these were FO B lymphocytes and not aberrantly migrating MZ B cells.

Immunohistochemistry confirmed that the MZ area was increased in *Klf2*$^{fl/fl}$; *Cd19-Cre*$^{+/-}$ animals relative to littermate controls (Figure 2C). Using the MOMA1 antibody to identify metallophilic macrophages that border the marginal sinus, we found increased numbers of cells expressing the pan-B cell marker, B220, within the MZ. On the contrary, the follicular area was not significantly altered (control = $1.4 \pm 0.7 \times 10^5$, genetically targeted mice = $2.0 \pm 0.3 \times 10^5$ pixels, p = 0.16). Therefore, we conclude that *Klf2*$^{fl/fl}$; *Cd19-Cre*$^{+/-}$ mice had increased numbers of splenic B cells and that this correlated with a significantly larger B cell-filled MZ.

Klf2 Differentially Regulates Chemokine Receptor Expression on FO and MZ B Cells

Premature exit from bone marrow was suggestive of a Klf2-deficient migratory defect. Moreover, it has been reported that Klf2-deficient T cells aberrantly traffic because of inappropriately expressed migratory receptors (Bai et al., 2007; Carlson et al., 2006; Sebzda et al., 2008). When we examined B cell homing receptors, we noted that Klf2-deficient MZ B cells had reduced mRNA expression of C-X-C chemokine receptor 5 (CXCR5) and sphingosine-1-phosphate receptor 1 ($S1P_1$) (Figure 3A). In contrast, Klf2-deficient FO B cells upregulated expression of these receptors. To determine whether Klf2 was directly influencing CXCR5 and $S1P_1$ transcription, we conducted chromatin immunoprecipitation (ChIP) assays. Highly conserved, noncoding sequences that contained the consensus Klf2 binding motif CACCC (Anderson et al., 1995), proximal to CXCR5 and $S1P_1$ transcriptional initiation sites, were chosen as regulatory targets. Klf2 protein directly bound to regulatory regions of CXCR5 and $S1P_1$ in MZ B cells but not FO B cells (Figure 3B), which suggested that Klf2 directly promoted CXCR5 and $S1P_1$ transcription in MZ B cells and indirectly repressed these receptors in FO B cells. To confirm that altered transcription resulted in modified protein expression, we examined receptor intensity by flow cytometry (Figure 3C). Consistent with real-time polymerase chain reaction (PCR) results, Klf2-deficient FO B cells expressed increased amounts of CXCR5, whereas no changes were detected with antibodies specific for CCR7 or CXCR4. Antibodies that recognize an extracellular portion of $S1P_1$ were not available so this receptor was not examined with this technique. No consistent differences in CXCR5 intensity were detected on Klf2-deficient MZ B cells by flow cytometry, despite significant differences in mRNA expression. To address this apparent discrepancy, we conducted

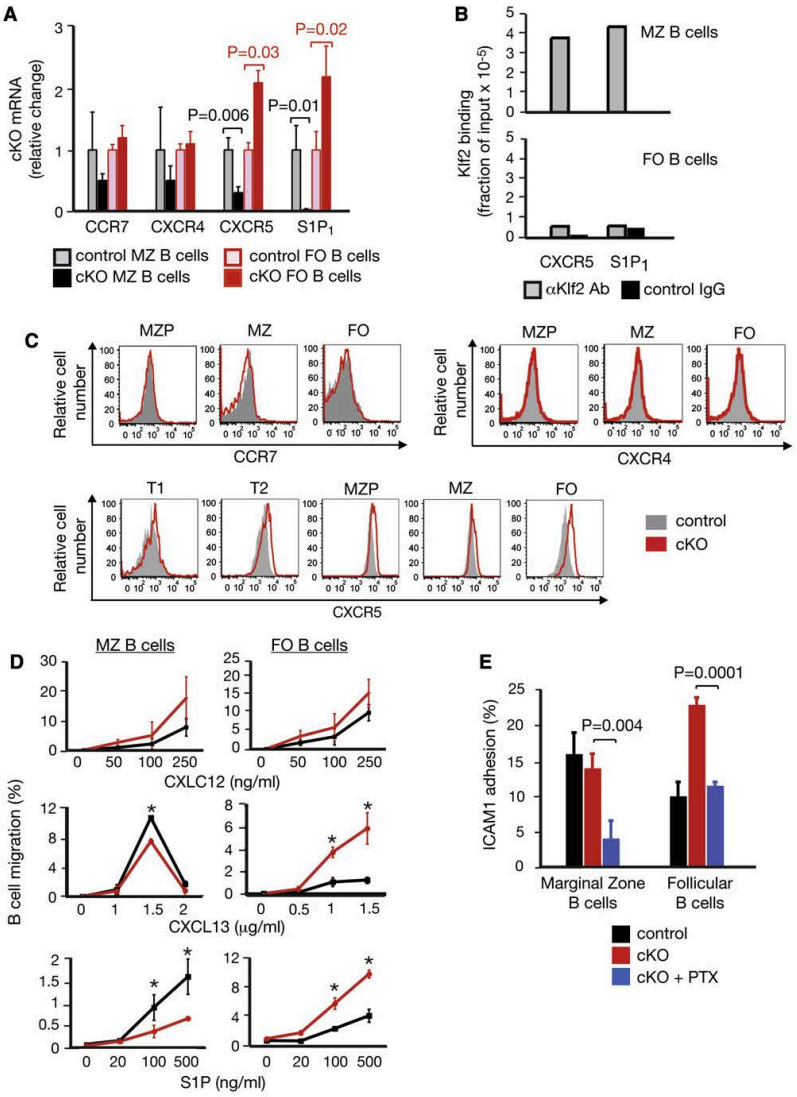

Figure 3. Klf2 Regulates MZ and FO B Cell Homing Receptors

(A) MZ and FO B cells from *Klf2*$^{+/+}$; *Cd19-Cre*$^{+/}$ (control) and *Klf2*$^{fl/fl}$; *Cd19-Cre*$^{+/}$ (genetically targeted = cKO) mice were analyzed for B cell homing receptor mRNA expression levels by real time PCR. Results are graphed as the fold change relative to control. $p > 0.05$ unless otherwise stated. This experiment was repeated twice. Error bars indicate the standard deviation.

(B) Chromatin immunoprecipitation (ChIP) assays were performed on quiescent MZ (top panel) or FO B cells (lower panel) with primers specific for the regulatory regions of CXCR5 and S1P$_1$. ChIP assays with Klf2 antibody are shown in gray; assays with isotype control antibody are shown in black. Klf2 binding to the regulatory regions of CXCR5 or S1P$_1$ is graphed relative to input amounts of these two sequences, respectively. This experiment was repeated twice.

(C) Surface expression of chemokine receptors on B cell populations are displayed as overlaid histograms. Results are representative of three independent experiments.

(D) Chemokine or sphingolipid-mediated ex vivo B cell migration. Control (black) and cKO (red) B cells were placed in common transwell chambers and migration toward CXCL12 (CXCR4 ligand), CXCR13 (CXCR5 ligand), or S1P (S1P$_1$ ligand) was measured. Asterisks (*) denote P values < 0.05. Migration assays using CXCL12 were conducted twice; the other assays were done three times.

(E) B cell adhesion was measured by culturing unstimulated or pertussis toxin (PTX)-treated B cells in ICAM1-coated plates and analyzing adherent cells by flow cytometry. Error bars indicate the standard deviation. This experiment was performed twice.

ex vivo migration assays to determine the functional state of chemokine receptors on Klf2-deficient B cells. FO B cells from genetically targeted mice displayed enhanced migration toward the chemokine CXCL13 (Figure 3D). In contrast, Klf2-deficient MZ B cell responses to this chemokine were diminished, indicating that real-time PCR results correctly reflected homing receptor expression. A similar dichotomy occurred with the sphingolipid, S1P; Klf2-deficient FO B cells migrated more robustly than control FO B cells, whereas Klf2-deficient MZ B cells had a decreased response to this ligand relative to control MZ B cells. These data suggest that Klf2 promotes or suppresses chemokine-specific migration in MZ and FO B cells, respectively.

Chemokine receptors activate integrins through a $G\alpha_i$ receptor-coupled signaling process (Kinashi, 2005), so B cell adhesion was examined as an indirect measure of chemokine receptor engagement. One of the primary integrins used by both FO and MZ B cells is LFA-1 ($\alpha L+\beta 2$). With the LFA-1 ligand ICAM1, ex vivo adhesion assays demonstrated enhanced binding by Klf2-deficient FO, but not MZ, B cells (Figure 3E). MZ B cells are particularly sensitive to the $G\alpha_i$ inhibitor pertussis toxin (Guinamard et al., 2000), and pretreatment with this drug reduced MZ B cell adhesion. Consistent with $G\alpha_i$ receptor-coupled signaling promoting integrin activation, pretreated Klf2-deficient FO B cells no longer expressed elevated adhesive properties. Together with gene expression data and functional migration studies, these experiments indicate that Klf2 differentially regulates migratory receptors on FO and MZ B cells.

Klf2-Deficient FO and MZ B Cells Are Anatomically Displaced within the Spleen

Differential regulation of chemokine receptors by Klf2 suggested that FO and MZ B cell homing was disrupted in genetically targeted mice. Therefore, splenic architecture was assessed with antibodies that preferentially recognize MZ B cells (IgM) and a subset of FO B cells (IgD). Gross examination showed that Klf2-deficient MZ B cells were present in the MZ (Figure 4A). However, closer inspection revealed that this IgM^+ area was discontinuous and often included overlap with $MOMA1^+$ or IgD^+ cells. Together with functional migration studies, these results suggest that Klf2 is required for efficient retention of MZ B cells in the MZ. To determine whether these cells were utilizing known homing receptors, we treated animals with FTY720, an agonistic peptide that removes surface expression of $S1P_1$ (Chiba et al., 2006). Under these conditions, Klf2-deficient MZ B cells completely vacated the MZ (Figure 4A, right panel) yet remained within the spleen (Figure 4B). These data suggested that Klf2-deficient MZ B cells still retained some homeostatic homing receptors, but that these cells were more inclined to enter B cell follicles than $Klf2^+$ MZ B cells.

Despite subtle defects in MZ B cell migration, $B220^+$ MZ areas were increased in genetically targeted animals, suggesting the presence of alternative B cell lineages within this zone. To test this hypothesis, we costained splenic tissue sections for IgD and MOMA1; anti-IgM antibody was excluded from this stain to increase detection of FO B cells. Analysis of $Klf2^{fl/+}$; $Cd19\text{-}Cre^{+/}$ control spleen showed a distinct separation between FO B cells (green) and MZ specific macrophages (red) (Figure 4C). In contrast, Klf2-deficient FO B cells converged

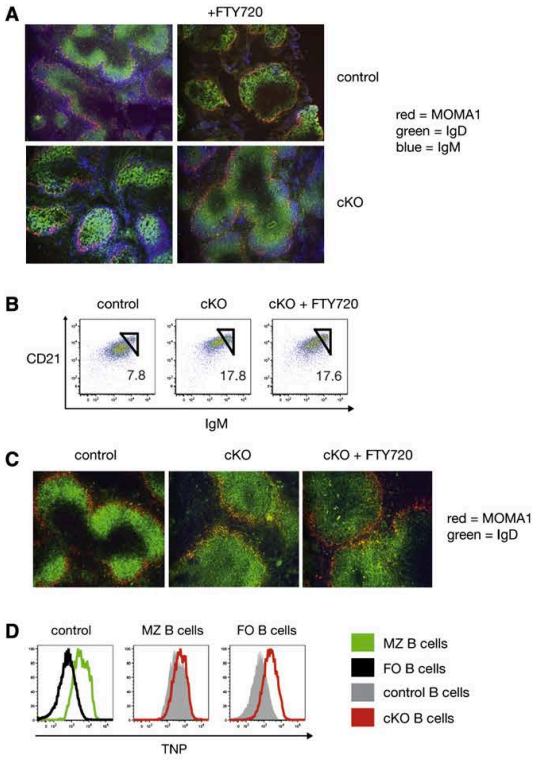

Figure 4. Klf2-Deficient FO and MZ B Cells Are Subtly Repositioned within the Spleen

(A) Immunohistochemistry of spleens from $Klf2^{+/+}$; $Cd19\text{-}Cre^{+/}$ (control) and $Klf2^{fl/fl}$; $Cd19\text{-}Cre^{+/}$ (genetically targeted = cKO) animals that were previously treated ± FTY720. A magnification that is 20× the original image is shown. MZ B cells are detected with IgM antibody, FO B cells are detected using IgD antibody, and metallophilic macrophages are highlighted with MOMA-1 antibody. These experiments were conducted twice.

(B) Flow cytometric analysis of splenic B cell lineages from control and cKO mice ± FTY720 treatment. Triangles identify MZ B cells and their corresponding frequencies (%). These data are representative of three experiments.

(C) FO B cell location relative to the MZ was analyzed by immunohistochemistry with tissue sections from control, cKO, and FTY720-treated cKO mice. A magnification that is 40× the original image is shown. FO B cells are IgD^+ and metallophilic macrophages are $MOMA\text{-}1^+$. This experiment was performed twice.

(D) Splenic B cell exposure to blood-borne antigen. Thirty minutes after intravenous injection of TNP-Ficoll, antigen surface binding was examined by flow cytometry with a TNP-specific antibody. Histograms display TNP levels on mature B cell lineages from control (solid gray) and cKO (red line) mice. TNP-binding on $Klf2^+$ MZ B cells (green line) and $Klf2^+$ FO B cells (black line) are shown in the left panel.

with MZ macrophages, as evidenced by an orange hue in the staining pattern. Treatment with FTY720 led to a clear separation of FO B cells and MZ macrophages, suggesting that Klf2-deficient FO B cells used $S1P_1$ to enter and/or remain within the MZ. To analyze dynamic FO B cell migration, we transferred FO B cells from $Klf2^{+/+}$; $Cd19\text{-}Cre^{+/}$ or $Klf2^{fl/fl}$; $Cd19\text{-}Cre^{+/}$

mice into C57Bl/6 recipient animals. As reported previously (van Ewijk and van der Kwast, 1980), newly transferred Klf2^{+} FO B cells efficiently entered splenic B cell follicles within 24 hr (Figure S3A). In contrast, Klf2-deficient FO B cells were found both within the B cell follicle and the surrounding MZ area. When Klf2^{+} and Klf2-deficient FO B cells were cotransferred into C57Bl/6 recipients (Figure S3B), these distinct migration patterns became more apparent; Klf2^{+} FO B cells migrated directly into splenic follicles, whereas the majority of transferred Klf2-deficient cells remained within the MZ. In addition, FO B cells from *Klf2*$^{fl/fl}$; *Cd19-Cre*$^{+/}$ donors were preferentially retained within the spleen following transfer (Figure S3C), indicating that this organ contains distinct anatomical properties that favor Klf2-deficient B cell retention.

To functionally test whether Klf2-deficient FO B cells were in the MZ, and thus in direct contact with blood-borne molecules, we examined splenic B cell compartments after a 30 min exposure to intravenously injected trinitrophenol (TNP)-coupled Ficoll. Flow cytometric analysis showed that in control mice, MZ B cells preferentially bound the hapten-carrier conjugate, whereas both FO and MZ B cells quickly bound TNP-Ficoll in genetically targeted animals (Figure 4D). Therefore, we conclude that Klf2-deficient B cell migration was modified within the spleen, allowing FO B cell encroachment into the MZ and access to MZ-associated antigens.

Klf2 Is Not Required for Ex Vivo Humoral Immune Responses

Such unusual B cell trafficking patterns raised the possibility that humoral immunity was compromised in *Klf2*$^{fl/fl}$; *Cd19-Cre*$^{+/}$ mice. To address this issue, we first needed to determine whether cell-intrinsic effector functions were intact in Klf2-deficient B cells. Neither FO B cells nor MZ B cells harvested from genetically targeted mice displayed variations in activation markers (Figure S4A), suggesting B cell quiescence was not disrupted. No significant differences in cell cycling were detected when MZ and FO B cells were stimulated with various regimens (Figure S4B). Moreover, titration curves of BCR-stimulation demonstrated that Klf2^{+} and Klf2-deficient B cells had identical activation thresholds (Figure S4C). In terms of ex vivo immunoglobulin (Ig) isotype production, both control and Klf2-deficient B cells responded to the TD antigen, ovalbumin peptide, by class switching to IgG1 in a T cell-dependent manner (Figure S5A). Likewise, type 1 TI (TI-1) antigenic responses, induced either by LPS + IL4 or LPS alone, promoted class switching to IgG1 or IgG3 in both cell populations (Figure S5B). Klf2-deficient B cells also responded normally when stimulated under type 2 (TI-2) antigenic conditions (Figure S5C) by preferentially class switching to the IgG3 isotype. Enzyme-linked immunosorbent assay (ELISA) measurements of Ig production further confirmed that control and Klf2-deficient B cells responded similarly to TI and TD ex vivo stimulation (Figure S5D). These results led us to conclude that Klf2-deficient B cells had normal cell-intrinsic effector functions.

Enhanced In Vivo Responses to TI-2 Antigens in Genetically Targeted Mice

Having established that cell-intrinsic effector functions were intact, we conducted experiments to determine whether Klf2-deficient B cell trafficking patterns affected in vivo humoral responses. Total Ig levels were normal; however, sera IgM was significantly increased in genetically targeted animals (Figure 5A), which may reflect increased Klf2-deficient splenic B cells numbers. As well, genetically targeted mice had decreased amounts of serum IgA, an Ig isotype that is primarily produced by B1 B cells under disease-free conditions (Kaminski and Stavnezer, 2006; Kroese et al., 1989; Kunisawa et al., 2007; Macpherson et al., 2000). Genetically targeted animals had very few B1 B cells in the peritoneal cavity (Figures S6A and S6B), which probably contributed to reduced amounts of serum IgA. Mechanisms responsible for this B1 B cell defect are currently being investigated. In this regard, limited numbers of B1 B cells were found in the blood and spleen of genetically targeted mice (Figure S6C) and Klf2-deficient B1 B cells could be generated from bone marrow precursors with defined ex vivo techniques (Montecino-Rodriguez and Dorshkind, 2006; Montecino-Rodriguez et al., 2006) (Figure S6D), suggesting that the defect was migratory in nature. *Cxcl13* $^{/}$ mice exhibit a similar defect in peritoneal B1 B cells (Ansel et al., 2002), raising the possibility that this lineage is particularly sensitive to trafficking defects. Importantly, all other Ig isotypes were maintained at normal levels, indicating that Klf2-deficient B cells did not undergo excessive antigen-independent in vivo class switching.

The presence of Klf2-deficient FO B cells within the MZ raised the possibility that TD antigen responses were compromised in genetically targeted mice. However, when animals were challenged with ovalbumin peptide coupled to TNP, similar amounts of total TNP-specific Ig were detected (Figure 5B). Likewise, the preferential Ig isotype utilized during a TD immune response, IgG1, was comparable between control and genetically targeted animals. Statistical differences in IgM and IgA levels were observed, which mirrored the previously noted differences in basal serum antibody concentrations. Thus aberrant Klf2-deficient B cell migration did not adversely affect B-T cell interactions or TD immune reactions.

Given that Klf2-deficient MZ B cells exhibited a limited migratory defect, we wanted to determine whether this affected TI immune responses in vivo. No differences were detected when mice were challenged with TNP-LPS (Figure 5C), indicating that aberrant Klf2-deficient B cell migration did not inhibit TI-1 antigenic reactions. With regards to TI-2 antigen, mice were challenged with TNP-Ficoll, a compound that preferentially activates MZ B cells and induces isotype class switching to IgG3 and to a lesser extent, IgG2a (Guinamard et al., 2000; Oliver et al., 1997). *Klf2*$^{fl/fl}$; *Cd19-Cre*$^{+/}$ mice responded more robustly to TNP-Ficoll than control littermates, as measured by total TNP-specific Ig levels (Figure 5D). ELISPOT experiments indicated that elevated antibody concentrations were due to increased frequencies of responding B cells (control = 58 ± 12 spot forming cells/10^6 splenocytes, genetically targeted mice = 106 ± 21 spot forming cells/10^6 splenocytes, $p = 0.004$) rather than more Ig production per cell (control = 11 ± 2 × 10^3 mm^2, genetically targeted mice = 10 ± 1 × 10^3 mm^2 mean spot size, $p = 0.19$). Increased Ig levels resulted from enhanced production of IgM and, unexpectedly, IgG1. Both FO and MZ B cells produce IgM during an immune response; however, IgG1 is typically restricted to Th cell-mediated reactions. TNP-specific IgG2a and IgG3 levels were comparable between control and

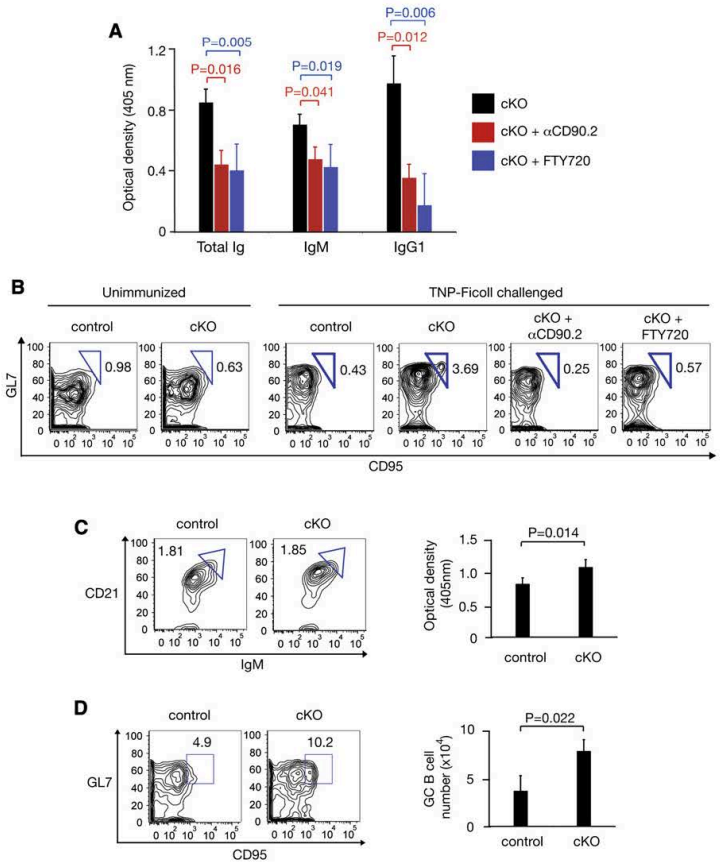

Figure 6. Characterization of Enhanced Klf2-Deficient B Cell Responses toward TI-2 Antigen

(A) Serum Ig levels from *Klf2*$^{fl/fl}$; *Cd19-Cre*$^{+/}$ (genetically targeted = cKO) (black), T cell-depleted cKO (red), and FTY720-treated cKO (blue) mice challenged with TNP-Ficoll. This experiment was repeated twice.

(B) Germinal center formation in the draining lymph nodes of TNP-Ficoll challenged mice. Mesenteric lymph nodes from control, cKO, T cell-depleted cKO, and FTY720-treated cKO mice were analyzed for germinal center surface markers (GL7$^+$ and CD95$^+$) 1 week after challenge. Percentages of B220$^+$AA4.1$^-$GL7$^+$CD95$^+$ B cells are shown. This experiment was performed twice in triplicate; representative figures are shown.

(C) Humoral responses were measured in day 12 neonates challenged with TNP-Ficoll. The left panels show the relative abundance of MZ B cells (triangles) in control and cKO mice at the time of analysis (day 19). This figure is representative of six neonatal spleens, with three per group. The right bar graph displays the amount of TNP-specific IgM from control and cKO mouse sera.

(D) Germinal center formation was examined in day 19 neonates after a 7 day challenge with TNP-Ficoll. Mesenteric lymph nodes were examined for the germinal center surface markers GL7 and CD95 (percentages shown). Absolute germinal center B cell (B220$^+$AA4.1 GL7$^+$CD95$^+$) numbers are shown in the right bar graph. n = 3 per group. In all cases, error bars indicate the standard deviation.

confirmed that 7 days after TNP-Ficoll challenge, clusters of proliferating cells could be identified within the follicles of genetically targeted mice (Figure S7D). GC B cells were located interior to the MZ, adjacent to the T cell-rich periarteriolar lymphoid sheath (PALS) (Figure S7E), suggesting that GC formation was anatomically correct in *Klf2*$^{fl/fl}$; *Cd19-Cre*$^{+/}$ mice. T cell-depleted genetically targeted animals challenged with TNP-Ficoll did not produce GCs (Figure 6B), confirming this process was T cell dependent. To ensure that Klf2 excision within the B cell compartment did not indirectly affect T cell-intrinsic effector functions, we examined various elements of T cell homeostasis in genetically targeted animals. Normal proportions of CD4$^+$ and CD8$^+$ T cells were found in secondary lymphoid organs (Figure S7F) and splenic T cells correctly homed to PALS in *Klf2*$^{fl/fl}$; *Cd19-Cre*$^{+/}$ mice (Figure S7G). Relative proportions of regulatory T cells were also intact (Figure S7H), indicating that B cell-specific Klf2-deficiency did not confer an overt hyperresponsive phenotype to the T cell compartment. Instead, GC formation was dependent upon B cell trafficking, as evidenced by the absence of GC B cells in FTY720-treated animals challenged with TNP-Ficoll (Figure 6B). These traits—a requirement for T cell interactions and access to the MZ to generate GCs after TNP-Ficoll challenge—were most consistent with a homing defect in Klf2-deficient FO B cells.

To directly test whether FO B cells underpin the gain-of-function phenotype in genetically targeted mice, TI-2 reactivity was examined in the absence of MZ B cells. Humoral responses were examined in 12-day-old neonates given that it takes approximately 3–4 weeks for MZ B cells to populate the spleen (Martin and Kearney, 2002; Pillai et al., 2005). After a one-week exposure to TNP-Ficoll, both control and genetically targeted mice had very few MZ B cells present in the spleen (Figure 6C); nevertheless, Klf2-deficient FO B cells still displayed significantly enhanced TNP-specific humoral responses. It should be noted that robust class switching did not occur at this early time point in either control or genetically targeted mice (data not shown), which may have reflected the still-developing architecture of the spleen (Pihlgren et al., 2003). However, GC formation was more pronounced in genetically targeted neonates (Figure 6D), suggestive of imminent class switching. To prove that Klf2-deficient FO B cells directly interacted with T cells during a TI-2 antigenic response, we cotransferred Klf2$^+$ and Klf2-deficient FO B cells into adult C57Bl/6 recipient mice and challenged them with TNP-Ficoll 24 hr later. Klf2$^+$ FO B cells did not form T cell conjugates, either spontaneously or after

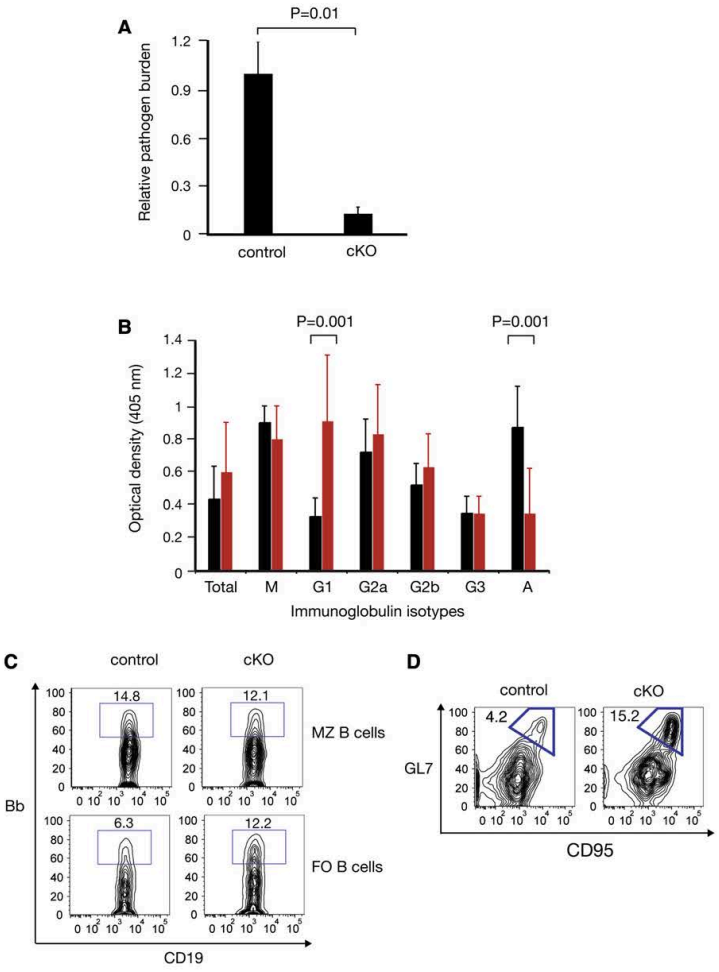

Figure 7. Genetically Targeted Mice Have Enhanced Responsiveness against *Borrelia burgdorferi*

(A) Bacterial titers in the bladders of *Klf2*$^{+/+}$; *Cd19-Cre*$^{+/}$ (control) and *Klf2*$^{fl/fl}$; *Cd19-Cre*$^{+/}$ (cKO = genetically targeted) mice were measured by real-time PCR one week after *B. burgdorferi* infection. For comparison purposes, the relative pathogen burden was set as 1.0 for the control mice. n = 3 mice per group. Similar results were obtained when this experiment was repeated. Error bars indicate the standard deviation.

(B) ELISA measurements of Borrelia-specific antibody from the sera of infected control and cKO animals. n = 5 mice per group. $p > 0.05$ except where stated. This experiment was repeated once, yielding similar results. Error bars indicate the standard deviation.

(C) Ex vivo B cell recognition of *B. burgdorferi* was examined with MZ and FO B cells from the spleens of infected animals. After a brief incubation with *B. burgdorferi* lysate, Klf2^{+} and Klf2-deficient B cells were examined by flow cytometry with *B. burgdorferi* antibody. Quadrants show the relative frequency of Borrelia-binding B cells. These contour blots are representative of eight mice, with four per group.

(D) Analysis of germinal center formation in draining lymph nodes of infected control and cKO animals. Germinal center B cells (CD19^{+}AA4.1 GL7^{+}CD95^{+}) are outlined with corresponding frequencies. These figures are representative of eight mice, with four per group. This experiment was repeated twice.

antigen challenge, whereas Klf2-deficient FO B cells formed CD4^{+} T cell conjugates in a TNP-Ficoll-responsive manner (Figure S7I). These data demonstrate that subsequent to TNP-Ficoll exposure in the MZ, Klf2-deficient FO B cells are able to interact with CD4^{+} T cells in the spleen. Thus, a mechanistic link can be made between the homing properties of Klf2-deficient FO B cell and the ability of *Klf2*$^{fl/fl}$; *Cd19-Cre*$^{+/}$ mice to respond to TI-2 antigens in a TD manner.

Klf2-Deficient FO B Cells Respond to MZ-Associated Pathogens

The biological importance of this phenotype was examined by challenging genetically targeted mice with *Borrelia burgdorferi*, an infectious spirochete bacterium responsible for Lyme disease in humans (Barbour and Hayes, 1986; Steere, 1989). Mouse studies have revealed that MZ B cells play a critical role in the initial humoral response to this pathogen (Belperron et al., 2007; McKisic and Barthold, 2000). Seven days after infection, genetically targeted mice displayed enhanced clearance of *B. burgdorferi* relative to littermate controls (Figure 7A). Analysis of *B. burgdorferi*-specific antibody showed increased amounts of IgG1 in experimental sera, whereas IgG2a and IgG3 concentrations were comparable between control and genetically targeted mice (Figure 7B). IgA levels were decreased in *Klf2*$^{fl/fl}$; *Cd19-Cre*$^{+/}$ mice, which we attributed to a lack of B1 B cells. To demonstrate that this gain of function was due to increased Klf2-deficient FO B cell recognition of the pathogen, we incubated infected splenic B cells from control and genetically targeted animals ex vivo with *B. burgdorferi* lysate, then stained them with Borrelia-specific antibody (Figure 7C). Both Klf2^{+} and Klf2-deficient MZ B cells displayed equivalent staining patterns. In contrast, Klf2-deficient FO B cells had an increased frequency of pathogen recognition relative to Klf2^{+} FO B cells, indicative of privileged access to MZ-associated pathogens. Moreover, analysis of draining lymph nodes from infected animals revealed that genetically targeted mice produced more GC B cells than littermate controls (Figure 7D), suggesting that enhanced pathogen clearance utilized a T cell-dependent mechanism. These results confirmed that in the absence of Klf2, FO B cells have enhanced responsiveness toward MZ-associated pathogens.

DISCUSSION

Klf2 is involved in numerous biological processes including vascular development (Kuo et al., 1997a; Lee et al., 2006; Wani et al., 1998), primitive erythropoiesis (Basu et al., 2007), monocyte activation (Das et al., 2006), and T cell homeostasis (Bai et al., 2007; Carlson et al., 2006; Kuo et al., 1997b; Sebzda et al., 2008). Robust expression of this transcription factor in B lymphocytes has suggested a critical role for Klf2 in B cells as well; however, genetic evidence has been lacking. Here, we report that *Klf2* excision in the B cell compartment leads to defects in homeostasis, cellular trafficking, and humoral immunity. Together, this work furthers our knowledge of chemokine receptor regulation and reveals how B cell migration imposes constraints on pathogen recognition.

Although Klf2 expression is first detected in pre-B cells, it does not appear to be required for early B cell development. Instead, Klf2-deficient B cell phenotypes are consistent with a late-stage defect in retention and recirculation to the bone marrow. Moreover, mature splenic B cell lineages are expanded in genetically targeted mice. Increased Klf2-deficient MZ B cell numbers may result from selective pressure to maintain normal serum antibody levels (Lopes-Carvalho and Kearney, 2004). Severely reduced B1 B cell numbers and the accompanying reduction in natural Abs produced by this lineage (Ansel et al., 2002; Hayakawa et al., 1984) may stimulate additional MZ B cell generation. Alternatively, premature egress from the bone marrow may disproportionately induce a surge in MZ B cell generation (Martin and Kearney, 2002). Unlike MZ B cells, FO B cells circulate throughout secondary lymphoid organs. Despite this, increased FO B cell numbers are limited to the spleen, suggesting that tissue-restricted factors normally utilized by $Klf2^{+}$ MZ B cells are involved in Klf2-deficient FO B cell retention.

Klf2 excision results in differential regulation of homing receptors in closely related lymphocyte lineages. However, Klf2-deficient MZ B cells still responded ex vivo to S1P and in vivo to FTY720, indicating that these cells retain some functional S1P-sensitive homing receptors. Klf2-deficient MZ B cells also express less CXCR5, a chemokine receptor used to shuttle activated MZ B cells into follicles (Cinamon et al., 2008), which may partially negate the effects of decreased $S1P_1$ expression. With regard to FO B cells, a considerable number of Klf2-deficient cells are able to remain within the MZ, possibly due to increased expression of $S1P_1$ and enhanced integrin activation. At the same time, increased CXCR5 levels on Klf2-deficient FO B cells probably allows these cells to eventually recirculate. Therefore, we conclude that dysregulated expression of migratory receptors disrupts the well-defined anatomical separation of MZ and FO B cells in $Klf2^{fl/fl}$; $Cd19\text{-}Cre^{+/}$ mice.

Hypothetically, merging B cell populations might have impaired humoral activities. Instead, in vivo TI-2 antigenic responses were enhanced in genetically targeted mice. This was not simply a reflection of increased splenic B cell numbers because TI-1 antigenic reactions were unaffected. With regards to TI-2 antigenic reactivity, Klf2-deficient FO B cells were probably causal, as evidenced by: (1) in vivo gain-of-function phenotypes included recognition of MZ-associated antigens; (2) enhanced responsiveness was T cell dependent and required B cell access to MZs; (3) these events were associated with GC formation; and (4) GC formation and increased production of TI-2-specific Ig occurred in genetically targeted neonates that lacked MZ B cells. These experiments also suggest that unlike MZ B cells, FO B cells are "hardwired" to require Th cell signals during a TI-2 response, regardless of anatomical location.

Klf2 excision results in increased surface expression of CD21 on MZ and FO B cells. Because this molecule acts as a coreceptor that can potently lower activation thresholds (Fearon and Carroll, 2000), there is the formal possibility that CD21 contributes to some of the gain-of-function phenotypes seen in genetically targeted mice. However, multiple independent assays indicate that cell-intrinsic properties (excluding homing receptor expression) are normal in Klf2-deficient B cells, including proliferation, isotype class switching, and immunoglobulin production. Moreover, gain-of-function phenotypes are restricted to TI-2 antigens, confined to the FO B cell lineage, and depend upon anatomical location. All of these attributes are best described in terms of aberrant migration patterns exhibited by Klf2-deficient FO B cells.

$Klf2^{fl/fl}$; $Cd19\text{-}Cre^{+/}$ mice clear *B. burgdorferi* more efficiently than control littermates, demonstrating the physiological advantage of allowing FO B cell access to the MZ. Given that blood-borne bacteria are widely prevalent and in some cases life threatening, why are $Klf2^{+}$ FO B cells removed from MZs? FO B cell retention within the MZ may increase the risk of T cell-mediated autoimmunity. Autoreactive BCR-transgenic B cells have been shown to quickly (2–3 days) prime self-reactive T cells following in vivo antigen challenge (Yan et al., 2006), suggesting a role for MZ B cells in breaking peripheral tolerance to blood-borne particles. In this regard, the BCR repertoire of MZ B cells is limited relative to FO B cells (Carey et al., 2008; Dammers et al., 2000). Therefore, it is possible that FO B cell trafficking into the MZ is restricted to reduce self-antigen recognition and autoreactive T cell induction. Because B cell malignancy and autoreactivity are associated with the MZ (Ferreri and Zucca, 2007; Lopes-Carvalho and Kearney, 2005; Viau and Zouali, 2005), studies examining B cell retention within this compartment may offer new clinical insights. This is especially relevant in light of the gain-of-function phenotypes exhibited by MZ-associated FO B cells in genetically targeted animals.

EXPERIMENTAL PROCEDURES

Mice

$Klf2^{fl/fl}$; $Cd19Cre^{+/}$ mice were generated by mating $Klf2^{fl/fl}$ mice (Lee et al., 2006) with $Cd19\text{-}Cre^{+}$ mice (The Jackson Laboratory). OTII transgenic mice were obtained from Taconic. Mice were housed in pathogen-free conditions at Vanderbilt University Medical Center according to National Institutes of Health guidelines and approved institutional animal committee protocols.

Flow Cytometry

B cell populations were identified as previously described (Hoek et al., 2009). Additional antibodies used for characterizing B cell populations include: CD1d, CD9, CD25, CD44, CD45RB, CD62L, CD69, CD80, CD86, CD95, GL7, α4+β7 integrin, CXCR4, CXCR5 (BD Biosciences), and CCR7 (eBioscience). Intracellular Klf2 was measured with polyclonal rabbit anti-Klf2 (Schuh et al., 2008). Data were acquired on a five-laser BD Bioscences Life Science Research II flow cytometer and analyzed with the FlowJo software package (TreeStar).

Real-Time PCR

RNA was extracted from sorted B cells with an RNeasy Micro Kit (QIAGEN). cDNA was generated with a SuperScript VILO cDNA synthesis kit (Invitrogen),

and real-time reactions were performed in triplicate with SYBR Green master mix (Applied Biosystems). Data were acquired on an iCycler iQ Real-Time PCR Detection System (BioRad). Primers used (forward + reverse) are as follows:

Klf2: 5′-CACCAACTGCGGCAAGACCTAC-3′ + 5′-TCTGTGACCTGTGTG CTTTCGG-3′
CXCR4: 5′-AGCTAAGGAGCATGACGGACAAGT-3′ + 5′-AACGTGCTGTA GAGGTTGACAGT-3′
CXCR5: 5′-AAGCGGAAACTAGAGCCTGGTTCA-3′ + 5′-ACCATCCCATC ACAAGCATCGGTA-3′
CCR7: 5′-CCAGACCGTGGCAATTTCAACAT-3′ + 5′-ACAAGAAAGGGT TGACACAGCAGC-3′
$S1P_1$: 5′-GTGTAGACCCAGAGTCCTGCG-3′ + 5′-AGCTTTTCCTTGGCTG GAGAG-3′

Data is expressed as:2^[(CT for Klf2-deficient experimental gene – CT for Klf2-deficient *Gapdh*) – (CT for control experimental gene – CT for control *Gapdh*)]. Burden levels of *B. burgdorferi* were measured in a similar manner, with the bacterial *recA* gene and the eukaryotic *tubulin* gene.

ChIP Assay

MZ and FO B cells (6×10^6) were sorted from C57Bl/6 mice, and chromatin immunoprecipitation (ChIP) assays were performed with the EZ-ChIP kit (Millipore) according to the manufacturer's protocol. Immunoprecipitations were performed with anti-Klf2 (Santa Cruz) or rabbit IgG control antibody. The following primer sets amplified DNA from Klf2 pulldowns: CXCR5 5′: GCTTGCCTCTCGACTCATCT, CXCR5 3′: GCACTGAAATGCTTGCGTAG, $S1P_1$ 5′: TGAAGAGGCCTTGGTCAGAT, and $S1P_1$ 3′: TTGAAACTGCACAGC AGAGG.

Immunofluorescent Microscopy

Spleen sections were prepared and analyzed as previously described (Acevedo-Suarez et al., 2005). B cells were identified with B220, IgD, and IgM antibodies (BD Biosciences), and MZ was delineated with MOMA1 antibody (Cedar Lane Labs).

In Vitro Migration Assays

Migration assays were conducted as previous described (Sebzda et al., 2008). Input and migrated cells were identified with IgM, CD21, CD23, AA4.1, and CD19 antibodies. The percentage of migration = 100% × ((experimental number – background number)/total input).

In Vitro Adhesion Assay

Splenocytes from control or genetically targeted mice were placed in ICAM1-coated six-well plates (10^7/well) and allowed to settle at 37°C for 90 min. Wells were filled, sealed, inverted, and left at room temperature for 30 min. Media was removed, wells rinsed, and remaining cells analyzed by flow cytometry. Alternatively, splenocytes from genetically targeted mice were pretreated with pertussis toxin (20 ng/ml; Sigma) for 1 hr at 37°C. The percentage of adhesion = 100% × (ICAM1-coated well – uncoated well)/total input. Wells were performed in triplicate.

Immunizations

For TI immune responses, mice were immunized intraperitoneally (i.p.) with 1 mg/kg TNP-LPS or 10 μg/kg TNP-Ficoll in 100 μl PBS, and bled 7 days after immunization for measurement of primary immune responses. In some experiments, mice were treated with FTY720 (Cayman Chemical Company; 2 μg/ml in drinking water) or anti-CD90.2 (BioLegend; 2 doses, 250 μg i.p. on consecutive days) prior to immunization. For TD immune responses, mice were immunized i.p. with 10 mg/kg TNP-Ovalbumin (TNP-Ova) in Alum (1:1, Alum:PBS; 100 μl per mouse) and bled 14 days after immunization. For *B. burgdorferi*, mice were intradermally inoculated with 1×10^4 spirochetes from a low-passage clinical isolate and bled 7 days after immunization for measurement of primary immune responses.

ELISA

ELISA was performed as previously described (Hoek et al., 2009). For *B. burgdorferi*-specific ELISA, plates were coated with *B. burgdorferi* lysate (3 μg in 50 μl of 100% ethanol per well), and serum was diluted 1:25–1:1000.

ELISPOT

Millipore Immobilon-P 96-well plates were coated with 10 μg/ml TNP-BSA, blocked with 10% FCS, and total splenocytes (1×10^5 cells per well) from mice immunized for 7 days with TNP-Ficoll were cultured in the absence of additional stimulation. Cells were removed and bound TNP-specific Ig was quantified with horseradish peroxidase-conjugated goat anti-mouse Ig.

Statistical Analysis

Data were analyzed with a two-tailed Student's t test. Values $p \leq 0.05$ were considered statistically significant.

SUPPLEMENTAL INFORMATION

Supplemental Information includes Supplemental Experimental Procedures and seven figures and can be found with this article online at doi:10.1016/j.immuni.2010.07.016.

ACKNOWLEDGMENTS

We thank F. Gherardini and E.P. Skaar for supplying *B. burgdorferi* stocks, H.M. Jäck for supplying rabbit polyclonal Klf2 antibody, and J. Hawiger, M. Boothby, and D. Ballard for helpful comments. The VMC Immunohistochemistry Core Laboratory and the VMC SDRC Molecular Genetics Core provided technical assistance. Flow cytometry and cell sorting was performed in the VMC Flow Cytometry Shared Resource. This research was supported by a postdoctoral fellowship from the National Multiple Sclerosis Society (V.V.P.), NIH training grant HL069765 (L.E.G.), NIH grant AI44924 (T.M.A.), NIH grant AI042284 and AI061721 (S.J.), NIH grant AI051448 (J.W.T), NIH grant HL089667 (L.V.K.), and NIH grant HL094773 and an Edward Mallinckrodt, Jr. Foundation award (E.S.).

Received: October 8, 2009
Revised: June 18, 2010
Accepted: July 26, 2010
Published online: August 5, 2010

REFERENCES

Acevedo-Suarez, C.A., Hulbert, C., Woodward, E.J., and Thomas, J.W. (2005). Uncoupling of anergy from developmental arrest in anti-insulin B cells supports the development of autoimmune diabetes. J. Immunol. *174*, 827–833.

Allman, D., and Pillai, S. (2008). Peripheral B cell subsets. Curr. Opin. Immunol. *20*, 149–157.

Anderson, K.P., Kern, C.B., Crable, S.C., and Lingrel, J.B. (1995). Isolation of a gene encoding a functional zinc finger protein homologous to erythroid Kruppel-like factor: Identification of a new multigene family. Mol. Cell. Biol. *15*, 5957–5965.

Ansel, K.M., Harris, R.B., and Cyster, J.G. (2002). CXCL13 is required for B1 cell homing, natural antibody production, and body cavity immunity. Immunity *16*, 67–76.

Bai, A., Hu, H., Yeung, M., and Chen, J. (2007). Kruppel-like factor 2 controls T cell trafficking by activating L-selectin (CD62L) and sphingosine-1-phosphate receptor 1 transcription. J. Immunol. *178*, 7632–7639.

Barbour, A.G., and Hayes, S.F. (1986). Biology of Borrelia species. Microbiol. Rev. *50*, 381–400.

Basu, P., Lung, T.K., Lemsaddek, W., Sargent, T.G., Williams, D.C., Jr., Basu, M., Redmond, L.C., Lingrel, J.B., Haar, J.L., and Lloyd, J.A. (2007). EKLF and KLF2 have compensatory roles in embryonic beta-globin gene expression and primitive erythropoiesis. Blood *110*, 3417–3425.

Belperron, A.A., Dailey, C.M., Booth, C.J., and Bockenstedt, L.K. (2007). Marginal zone B-cell depletion impairs murine host defense against Borrelia burgdorferi infection. Infect. Immun. *75*, 3354–3360.

Bhattacharya, D., Cheah, M.T., Franco, C.B., Hosen, N., Pin, C.L., Sha, W.C., and Weissman, I.L. (2007). Transcriptional profiling of antigen-dependent murine B cell differentiation and memory formation. J. Immunol. *179*, 6808–6819.

Buckley, A.F., Kuo, C.T., and Leiden, J.M. (2001). Transcription factor LKLF is sufficient to program T cell quiescence via a c-Myc–dependent pathway. Nat. Immunol. *2*, 698–704.

Carey, J.B., Moffatt-Blue, C.S., Watson, L.C., Gavin, A.L., and Feeney, A.J. (2008). Repertoire-based selection into the marginal zone compartment during B cell development. J. Exp. Med. *205*, 2043–2052.

Cariappa, A., Boboila, C., Moran, S.T., Liu, H., Shi, H.N., and Pillai, S. (2007). The recirculating B cell pool contains two functionally distinct, long-lived, post-transitional, follicular B cell populations. J. Immunol. *179*, 2270–2281.

Carlson, C.M., Endrizzi, B.T., Wu, J., Ding, X., Weinreich, M.A., Walsh, E.R., Wani, M.A., Lingrel, J.B., Hogquist, K.A., and Jameson, S.C. (2006). Kruppel-like factor 2 regulates thymocyte and T-cell migration. Nature *442*, 299–302.

Chiba, K., Matsuyuki, H., Maeda, Y., and Sugahara, K. (2006). Role of sphingosine 1-phosphate receptor type 1 in lymphocyte egress from secondary lymphoid tissues and thymus. Cell. Mol. Immunol. *3*, 11–19.

Cinamon, G., Zachariah, M.A., Lam, O.M., Foss, F.W., Jr., and Cyster, J.G. (2008). Follicular shuttling of marginal zone B cells facilitates antigen transport. Nat. Immunol. *9*, 54–62.

Dammers, P.M., Visser, A., Popa, E.R., Nieuwenhuis, P., and Kroese, F.G. (2000). Most marginal zone B cells in rat express germline encoded Ig VH genes and are ligand selected. J. Immunol. *165*, 6156–6169.

Das, H., Kumar, A., Lin, Z., Patino, W.D., Hwang, P.M., Feinberg, M.W., Majumder, P.K., and Jain, M.K. (2006). Kruppel-like factor 2 (KLF2) regulates proinflammatory activation of monocytes. Proc. Natl. Acad. Sci. USA *103*, 6653–6658.

Fagarasan, S., Watanabe, N., and Honjo, T. (2000). Generation, expansion, migration and activation of mouse B1 cells. Immunol. Rev. *176*, 205–215.

Fearon, D.T., and Carroll, M.C. (2000). Regulation of B lymphocyte responses to foreign and self-antigens by the CD19/CD21 complex. Annu. Rev. Immunol. *18*, 393–422.

Ferreri, A.J., and Zucca, E. (2007). Marginal-zone lymphoma. Crit. Rev. Oncol. Hematol. *63*, 245–256.

Fruman, D.A., Ferl, G.Z., An, S.S., Donahue, A.C., Satterthwaite, A.B., and Witte, O.N. (2002). Phosphoinositide 3-kinase and Bruton's tyrosine kinase regulate overlapping sets of genes in B lymphocytes. Proc. Natl. Acad. Sci. USA *99*, 359–364.

Glynne, R., Ghandour, G., Rayner, J., Mack, D.H., and Goodnow, C.C. (2000). B-lymphocyte quiescence, tolerance and activation as viewed by global gene expression profiling on microarrays. Immunol. Rev. *176*, 216–246.

Guinamard, R., Okigaki, M., Schlessinger, J., and Ravetch, J.V. (2000). Absence of marginal zone B cells in Pyk-2-deficient mice defines their role in the humoral response. Nat. Immunol. *1*, 31–36.

Hayakawa, K., Hardy, R.R., Honda, M., Herzenberg, L.A., and Steinberg, A.D. (1984). Ly-1 B cells: Functionally distinct lymphocytes that secrete IgM autoantibodies. Proc. Natl. Acad. Sci. USA *81*, 2494–2498.

Hoek, K.L., Carlesso, G., Clark, E.S., and Khan, W.N. (2009). Absence of mature peripheral B cell populations in mice with concomitant defects in B cell receptor and BAFF-R signaling. J. Immunol. *183*, 5630–5643.

Kaminski, D.A., and Stavnezer, J. (2006). Enhanced IgA class switching in marginal zone and B1 B cells relative to follicular/B2 B cells. J. Immunol. *177*, 6025–6029.

Kinashi, T. (2005). Intracellular signalling controlling integrin activation in lymphocytes. Nat. Rev. Immunol. *5*, 546–559.

Kroese, F.G., Butcher, E.C., Stall, A.M., Lalor, P.A., Adams, S., and Herzenberg, L.A. (1989). Many of the IgA producing plasma cells in murine gut are derived from self-replenishing precursors in the peritoneal cavity. Int. Immunol. *1*, 75–84.

Kunisawa, J., Kurashima, Y., Gohda, M., Higuchi, M., Ishikawa, I., Miura, F., Ogahara, I., and Kiyono, H. (2007). Sphingosine 1-phosphate regulates peritoneal B-cell trafficking for subsequent intestinal IgA production. Blood *109*, 3749–3756.

Kuo, C.T., Veselits, M.L., Barton, K.P., Lu, M.M., Clendenin, C., and Leiden, J.M. (1997a). The LKLF transcription factor is required for normal tunica media formation and blood vessel stabilization during murine embryogenesis. Genes Dev. *11*, 2996–3006.

Kuo, C.T., Veselits, M.L., and Leiden, J.M. (1997b). LKLF: A transcriptional regulator of single-positive T cell quiescence and survival. Science *277*, 1986–1990.

Lee, J.S., Yu, Q., Shin, J.T., Sebzda, E., Bertozzi, C., Chen, M., Mericko, P., Stadtfeld, M., Zhou, D., Cheng, L., et al. (2006). Klf2 is an essential regulator of vascular hemodynamic forces in vivo. Dev. Cell *11*, 845–857.

Lopes-Carvalho, T., and Kearney, J.F. (2004). Development and selection of marginal zone B cells. Immunol. Rev. *197*, 192–205.

Lopes-Carvalho, T., and Kearney, J.F. (2005). Marginal zone B cell physiology and disease. Curr. Dir. Autoimmun. *8*, 91–123.

Macpherson, A.J., Gatto, D., Sainsbury, E., Harriman, G.R., Hengartner, H., and Zinkernagel, R.M. (2000). A primitive T cell-independent mechanism of intestinal mucosal IgA responses to commensal bacteria. Science *288*, 2222–2226.

Martin, F., and Kearney, J.F. (2002). Marginal-zone B cells. Nat. Rev. Immunol. *2*, 323–335.

McKisic, M.D., and Barthold, S.W. (2000). T-cell-independent responses to Borrelia burgdorferi are critical for protective immunity and resolution of lyme disease. Infect. Immun. *68*, 5190–5197.

Montecino-Rodriguez, E., and Dorshkind, K. (2006). Stromal cell-dependent growth of B-1 B cell progenitors in the absence of direct contact. Nat. Protoc. *1*, 1140–1144.

Montecino-Rodriguez, E., Leathers, H., and Dorshkind, K. (2006). Identification of a B-1 B cell-specified progenitor. Nat. Immunol. *7*, 293–301.

Okada, T., and Cyster, J.G. (2006). B cell migration and interactions in the early phase of antibody responses. Curr. Opin. Immunol. *18*, 278–285.

Oliver, A.M., Martin, F., Gartland, G.L., Carter, R.H., and Kearney, J.F. (1997). Marginal zone B cells exhibit unique activation, proliferative and immunoglobulin secretory responses. Eur. J. Immunol. *27*, 2366–2374.

Pihlgren, M., Tougne, C., Bozzotti, P., Fulurija, A., Duchosal, M.A., Lambert, P.H., and Siegrist, C.A. (2003). Unresponsiveness to lymphoid-mediated signals at the neonatal follicular dendritic cell precursor level contributes to delayed germinal center induction and limitations of neonatal antibody responses to T-dependent antigens. J. Immunol. *170*, 2824–2832.

Pillai, S., Cariappa, A., and Moran, S.T. (2005). Marginal zone B cells. Annu. Rev. Immunol. *23*, 161–196.

Schuh, W., Meister, S., Herrmann, K., Bradl, H., and Jack, H.M. (2008). Transcriptome analysis in primary B lymphoid precursors following induction of the pre-B cell receptor. Mol. Immunol. *45*, 362–375.

Sebzda, E., Zou, Z., Lee, J.S., Wang, T., and Kahn, M.L. (2008). Transcription factor KLF2 regulates the migration of naive T cells by restricting chemokine receptor expression patterns. Nat. Immunol. *9*, 292–300.

Srivastava, B., Quinn, W.J., 3rd, Hazard, K., Erikson, J., and Allman, D. (2005). Characterization of marginal zone B cell precursors. J. Exp. Med. *202*, 1225–1234.

Steere, A.C. (1989). Lyme disease. N. Engl. J. Med. *321*, 586–596.

van Ewijk, W., and van der Kwast, T.H. (1980). Migration of B lymphocytes in lymphoid organs of lethally irradiated, thymocyte-reconstituted mice. Cell Tissue Res. *212*, 497–508.

Viau, M., and Zouali, M. (2005). B-lymphocytes, innate immunity, and autoimmunity. Clin. Immunol. *114*, 17–26.

Wani, M.A., Means, R.T., Jr., and Lingrel, J.B. (1998). Loss of LKLF function results in embryonic lethality in mice. Transgenic Res. *7*, 229–238.

Yan, J., Harvey, B.P., Gee, R.J., Shlomchik, M.J., and Mamula, M.J. (2006). B cells drive early T cell autoimmunity in vivo prior to dendritic cell-mediated autoantigen presentation. J. Immunol. *177*, 4481–4487.

THE EMBO JOURNAL

Have you seen ...?

The EMBO Journal (2010) 29, 1475–1476 | © 2010 European Molecular Biology Organization | All Rights Reserved 0261-4189/10
www.embojournal.org

Natural killer T cell–a cat o' nine lives!

Sebastian Joyce* and Laura E Gordy

Department of Microbiology and Immunology, Vanderbilt University School of Medicine, Nashville, TN, USA
*Correspondence to: sebastian.joyce@vanderbilt.edu

The EMBO Journal (2010) **29,** 1475–1476. doi:10.1038/emboj.2010.66

The cylindromatous gene *Cyld* encodes a deubiquitylase (DUB), which regulates NF-κB activation. CYLD deficiency results in faulty innate and adaptive immune systems in mice, the basis for which remains incompletely understood. In this issue of *The EMBO Journal*, Sun and colleagues report that CYLD-deficient mice develop the innate-like lymphocyte called natural killer T (NKT) cells but lose them to death, which resulted from overactivation of NF-κB and low interleukin-7 receptor (IL-7R) expression. Consequently, CYLD-deficient NKT cells poorly respond to IL-7 and do not upregulate inducible costimulatory (ICOS) receptor, molecules that serve as survival signals in other cellular contexts. These findings integrate disparate prior knowledge revealing the molecular basis for NKT cell homeostasis and have implications for understanding why human NKT cell frequency varies between individuals.

The tumour suppressor gene ***Cyld*** encodes a DUB that belongs to the ubiquitin-specific protease class. CYLD regulates a multitude of fundamental biologic processes including innate and adaptive immune responses. Its constitutive DUB activity regulates nuclear NF-κB function by acting on multiple components within the pattern recognition receptor-NF-κB and the T-cell receptor (TCR)-NF-κB signalling axes whose activation depend on ubiquitylation. Uniquely, CYLD also acts on the lymphoid-specific kinase Lck to regulate the activation of its target Zap70. Thus, CYLD deficiency results in impaired thymocyte development as well as in faulty innate and adaptive immune functions (Sun, 2008). As NKT cells—a thymus-derived lymphocyte known to regulate antitumour and antimicrobial immunity as well as autoimmunity—require NF-κB signalling for their ontogeny, homeostasis and function, Sun and colleagues now assessed the function of CYLD in these processes (Lee *et al*, 2010).

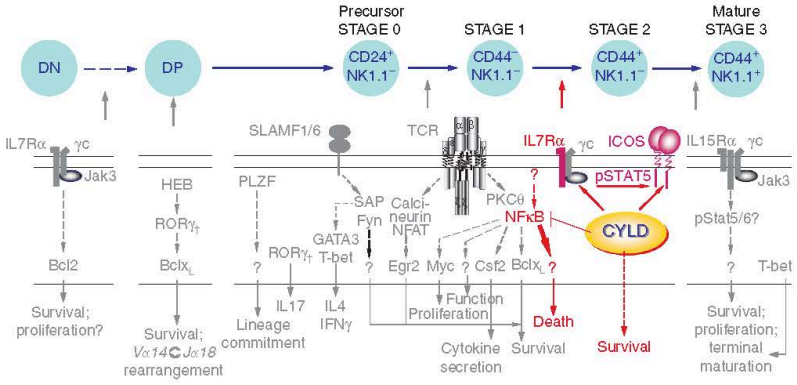

Figure 1 CYLD regulates multiple survival signals within developing NKT cells. The function of CYLD (shown in red) in NKT cell ontogeny and maintenance (see text) is diagrammed against the backdrop of currently known factors (shown in grey) that regulate these processes within this lineage (Godfrey *et al*, 2010). T-cell development begins with CD4CD8 double-negative (DN) thymocytes, which progress through four stages (not shown) to beget CD4CD8 double-positive (DP) cells. NKT cell lineage commitment occurs with HEB (an E2A family transcription factor)-RORγt-dependent expression of the semi-invariant TCR at the DP stage. Hence, both NKT cells and conventional CD4 and CD8 T cells require the same factors to progress from the DN to DP thymocyte stage. Positive selection by DP thymocytes displaying CD1d-self-lipid complexes at stage 0/1 induces the expression of promyelocytic zinc finger protein (PLZF), and perhaps NF-κB. Ontogenetic progression at this stage is further regulated by signalling lymphocyte activation molecule family member (SLAMF)-SLAM-associated protein (SAP)-Fyn (a Src kinase) signalling axes culminating in GATA3 and T-bet expression, which are transcription factors essential for the elaboration of IL-4 and interferon-γ for which this lineage is best known (stages 1 and 2). At these stages, TCR-induced calcineurin-NFAT-Egr2 and PKCθ-NF-κB signalling axes have critical functions in lineage proliferation (e.g. Myc), maintenance (e.g. Bcl-x_L) and effector differentiation (e.g. Csf2). Finally, terminal maturation to stage 3 requires T-bet and IL-15 signalling. Dashed arrows, intermediates not known; thick arrow, over activation.

Although NKT cells have critical immunoregulatory functions *in vivo*, their frequency varies among different mouse strains as well as between individuals, especially among those that are predisposed to autoimmune diseases (Godfrey *et al*, 2010). Yet, the molecular basis for this variation remains an enigma. Over the years, a number of receptors, cytokines, signalling molecules and transcription factors were independently identified as regulates of NKT cell ontogeny, homeostasis and function (Figure 1; Godfrey *et al*, 2010). Although several essential pathways for NKT cell ontogeny and maintenance have been identified, how these diverse pathways are integrated in one well-orchestrated regulatory network remained unknown.

Lee *et al* found that CYLD-deficient mice develop NKT cells, which progress from progenitors (stage 0) of this lineage through the entire ontogenetic programme to give rise to mature NKT cells (stage 3; Figure 1). Yet, the overall frequency of these cells was very low in CYLD-deficient mice. On dissecting the basis of this deficiency, Lee *et al* found overt apoptosis at all developmental stages of this lineage. Moreover, CYLD deficiency resulted in unbridled classical NF-κB activation within NKT cells, which was tempered by T cell-specific overexpression of a mutant incapable of signal-dependent phosphorylation of IκBα (Lee *et al*, 2010). This is consistent with the earlier findings that (1) among other pathways, CYLD regulates the TCR-NF-κB signalosome (Sun, 2008); (2) the TCR-PKCθ-NF-κB axis regulates NKT cell homeostasis through the induction of the pro-survival factor Bcl-x_L (Stanic *et al*, 2004a, b) and (3) the overexpression of the constitutively active IκB kinase-2 mutant results in the development of all stages of NKT cells yet maintains them only at low frequency (Cen *et al*, 2009). Together, these findings suggest that NF-κB functions as a rheostat within developing NKT cells requiring an optimal threshold of NF-κB activity for lineage survival.

Further mechanistic studies by Lee *et al* revealed that *Cyld*-null NKT cells express lower levels of IL-7R when compared with their wild-type counterpart. Hence, *Cyld*-null NKT cells poorly responded to IL-7 and phosphorylated STAT5 at tyrosine-694 and failed to induce ICOS (Lee *et al*, 2010). This phenotype is consistent with earlier studies, which showed that IL-7R-deficient mice developed low numbers of mature NKT cells (Boesteanu *et al*, 1997). As IL-7R signalling is also critical for the first two stages (DN1–DN2) of thymocyte development, the function of IL-7R signalling in NKT cell ontogeny—which bifurcates at the DP stage (Figure 1; Godfrey *et al*, 2010)—went unnoticed. As IL-7R and Bcl2 are developmentally expressed within NKT cells (Godfrey *et al*, 2010), it is possible that IL-7 signalling induces Bcl2 to further regulate NKT cell survival.

ICOS was previously shown to regulate NKT cell development and homeostasis (Godfrey *et al*, 2010). As shown by Lee *et al*, IL-7 induced *Icos* expression in NKT cells that was interrupted in CYLD-deficient mice. Together, these data for the first time provide an integrated picture of how multiple signalling pathways cross-talk to aid the narrow escape of NKT cells from death (Lee *et al*, 2010). Perhaps such an integrated regulation is essential for the maintenance of a lineage that was designed to be self-reactive. So, the question becomes, what death signals are these cells escaping from? Clearly, it is not Fas–Fas ligand mediated (Lee *et al*, 2010). So, is it a signal emanating from the NKT cell receptor for antigen? If it is, is it because this TCR is constantly exposed to its ligand, CD1d displaying endogenous lipids, thereby over stimulating NF-κB in the absence of CYLD's reign? If so, the function of CYLD in regulating the NF-κB rheostat seems to be an important one for NKT cell development and homeostasis. Such a function raises the intriguing possibility that some of the known mutations/polymorphisms in human *CYLD* (Courtois, 2008) that temper its DUB activity and those within CYLD-regulated proteins (e.g. NEMO; Sun, 2008) could underlie varied (ranging from 0.01 to 3%) NKT cell frequencies within our population.

Acknowledgements

Supported by RO1 (AI061721 and AI042284 to S Joyce) as well as T32 (HL069765 and AI007611 to LE Gordy) grants from the NIH.

Conflict of interest

The authors declare that they have no conflict of interest.

References

Boesteanu A, Silva AD, Nakajima H, Leonard WJ, Peschon JJ, Joyce S (1997) Distinct roles for signals relayed through the common cytokine receptor gamma chain and interleukin 7 receptor alpha chain in natural T cell development. *J Exp Med* **186**: 331–336

Cen O, Ueda A, Guzman L, Jain J, Bassiri H, Nichols KE, Stein PL (2009) The adaptor molecule signaling lymphocytic activation molecule-associated protein (SAP) regulates IFN-gamma and IL-4 production in V alpha 14 transgenic NKT cells via effects on GATA-3 and T-bet expression. *J Immunol* **182**: 1370–1378

Courtois G (2008) Tumor suppressor CYLD: negative regulation of NF-kappaB signaling and more. *Cell Mol Life Sci* **65**: 1123–1132

Godfrey DI, Stankovic S, Baxter AG (2010) Raising the NKT cell family. *Nat Immunol* 11: 197–206

Lee A, Zhou X, Chang M, Hunzeker J, Bonneau R, Zhou D, Sun S-C (2010) Regulation of natural killer T-cell development by deubiquitinase CYLD. *EMBO J* **29**: 1600–1612

Stanic AK, Bezbradica JS, Park JJ, Matsuki N, Mora AL, Van Kaer L, Boothby MR, Joyce S (2004a) NF-kappa B controls cell fate specification, survival, and molecular differentiation of immunoregulatory natural T lymphocytes. *J Immunol* **172**: 2265–2273

Stanic AK, Bezbradica JS, Park JJ, Van Kaer L, Boothby MR, Joyce S (2004b) Cutting edge: the ontogeny and function of Va14Ja18 natural T lymphocytes require signal processing by protein kinase C theta and NF-kappa B. *J Immunol* **172**: 4667–4671

Sun SC (2008) Deubiquitylation and regulation of the immune response. *Nat Rev Immunol* **8**: 501–511

The EMBO Journal (2009) 28, 3579–3590 | © 2009 European Molecular Biology Organization | All Rights Reserved 0261-4189/09
www.embojournal.org

THE EMBO JOURNAL

Adaptability of the semi-invariant natural killer T-cell receptor towards structurally diverse CD1d-restricted ligands

William C Florence[1,11], Chengfeng Xia[2,11], Laura E Gordy[1], Wenlan Chen[2], Yalong Zhang[2], James Scott-Browne[3], Yuki Kinjo[4], Karl OA Yu[5], Santosh Keshipeddy[6], Daniel G Pellicci[7], Onisha Patel[8], Lars Kjer-Nielsen[7], James McCluskey[8], Dale I Godfrey[7], Jamie Rossjohn[8], Stewart K Richardson[6], Steven A Porcelli[5], Amy R Howell[6], Kyoko Hayakawa[9], Laurent Gapin[3], Dirk M Zajonc[10,*], Peng George Wang[2,*] and Sebastian Joyce[1,*]

[1]Department of Microbiology and Immunology, Vanderbilt University School of Medicine, Nashville, TN, USA, [2]Department of Chemistry and Biochemistry, Ohio State University, Columbus, OH, USA, [3]National Jewish Centre for Allergy and Immunology Research, Denver, CO, USA, [4]Division of Developmental Immunology, La Jolla Institute for Allergy and Immunology, La Jolla, CA, USA, [5]Department of Microbiology and Immunology, Albert Einstein College of Medicine, Bronx, NY, USA, [6]Department of Chemistry, University of Connecticut, Storrs, CT, USA, [7]Department of Microbiology and Immunology, University of Melbourne, Melbourne, Victoria, Australia, [8]Department of Biochemistry and Molecular Biology, Monash University, Melbourne, Victoria, Australia, [9]Fox Chase Cancer Centre, Philadelphia, PA, USA and [10]Division of Cell Biology, La Jolla Institute for Allergy and Immunology, La Jolla, CA, USA

The semi-invariant natural killer (NK) T-cell receptor (NKTcr) recognises structurally diverse glycolipid antigens presented by the monomorphic CD1d molecule. While the α-chain of the NKTcr is invariant, the β-chain is more diverse, but how this diversity enables the NKTcr to recognise diverse antigens, such as an α-linked monosaccharide (α-galactosylceramide and α-galactosyldiacylglycerol) and the β-linked trisaccharide (isoglobotriaosylceramide), is unclear. We demonstrate here that NKTcrs, which varied in their β-chain usage, recognised diverse glycolipid antigens with a similar binding mode on CD1d. Nevertheless, the NKTcrs recognised distinct epitopic sites within these antigens, including α-galactosylceramide, the structurally similar α-galactosyldiacylglycerol and the very distinct isoglobotriaosylceramide. We also show that the relative roles of the CDR loops within the NKTcr β-chain varied as a function of the antigen. Thus, while NKTcrs characteristically use a conserved docking mode, the NKTcr β-chain allows these cells to recognise unique aspects of structurally diverse CD1d-restricted ligands.

The EMBO Journal (2009) **28,** 3579–3590. doi:10.1038/emboj.2009.286; Published online 8 October 2009
Subject Categories: immunology
Keywords: antigen recognition; glycolipid antigens; NKT cells; recognition logic; semi-invariant T-cell receptor

Introduction

The antigen receptor of αβ T cells faces a daunting recognition problem because each T-cell receptor (TCR) interfaces multiple ligands during its lifetime and yet maintains specificity. They recognise self-ligand (peptide or lipid) in the context of a self-antigen-presenting molecule (major histocompatibility complex (MHC) class I, class II or CD1) in the thymus; foreign ligand in the context of a self-MHC/CD1 molecule in the periphery; and in some cases, non-self-ligands in the context of non-self-MHC molecules. This recognition conundrum is much more daunting for the semi-invariant natural killer (NK) T-cell receptor (NKTcr) because its recognition landscape is predominantly germline-encoded and, hence, highly conserved (Borg *et al*, 2007; Scott-Browne *et al*, 2007; Wun *et al*, 2008), while the antigenic landscapes of CD1d–lipid complexes are highly diverse (Koch *et al*, 2005; Zajonc *et al*, 2005, 2008; Kinjo *et al*, 2006). Understanding how NKT cells see extremely diverse lipid antigens is important because this innate T lymphocyte regulates early immune responses to pathogens and tumours, and is a target for immunotherapy against some autoimmune diseases (Van Kaer, 2005).

The TCR α and β-chains each comprise variable (V) and constant (C) domains, in which the V domains contain the complementarity determining region-1 (CDR1), CDR2 and CDR3, that interact with the peptide-laden MHC (pMHC) molecules. While variations within *V*-gene segments confer diversity to CDR1 and CDR2, imprecise joining and non-templated nucleotide additions during V(D)J recombination generate the much more diverse CDR3 (Rudolph *et al*, 2006). TCR specificity is not limited to peptidic antigens. NKT cells express a semi-invariant TCR that recognises lipid-based antigens presented by the monomorphic CD1d molecule. The NKTcr is made up of an invariant TCR α-chain, which is generated by TRAV11*02 (mouse and rat *Vα14*) to TRAJ18 (*Jα18*) or orthologous TRAV10 (human *Vα24*) to TRAJ18 rearrangement. Despite the stochastic nature of V(D)J recombination, stringent intrathymic selection steps permit only one CDR3α for NKT cells. Thus, NKT cells express a completely invariant TCR α-chain that is highly conserved across

*Corresponding authors. S Joyce, Department of Microbiology and Immunology, Vanderbilt University School of Medicine, A4223 Medical Centre North, 1161 21st Avenue South, Nashville, TN 37232, USA. Tel.: +1 615 322 1472; Fax: +1 615 343 7392; E-mail: sebastian.joyce@vanderbilt.edu or
DM Zajonc, Division of Cell Biology, La Jolla Institute for Allergy and Immunology, La Jolla, CA 92037, USA. Tel.: +1 858 752 6605; Fax: +1 858 752 6994; E-mail: dzajonc@liai.org or
PG Wang, Department of Chemistry and Biochemistry, Ohio State University, Columbus, OH 43210, USA. Tel.: +1 614 292 9884; Fax: +1 614 688 3106; E-mail: wang.892@osu.edu
[11]These authors contributed equally to this work

Received: 17 June 2009; accepted: 3 September 2009; published online: 8 October 2009

species (Koseki *et al*, 1990; Porcelli *et al*, 1993; Dellabona *et al*, 1994; Lantz and Bendelac, 1994). In contrast, CDR3β of TRBV13-2*01 (mouse Vβ8.2) and the orthologous TRBV25-1 (human Vβ11), which pair with the invariant Vα14 and Vα24 α-chains, respectively, are highly diverse (Porcelli *et al*, 1993; Lantz and Bendelac, 1994). So too are the CDR3β of TRBV29*02 (Vβ7) and TRBV1 (Vβ2) β-chains, which also pair with Vα14 and Vα24 α-chains in mice (Lantz and Bendelac, 1994; Capone *et al*, 2003). Thus, NKT cells have an invariant TCR α-chain, but maintain some diversity in their TCR β-chain, which is why they are referred to as semi-invariant.

The NKTcr binds structurally diverse CD1d-restricted ligands that range from α-linked monohexosylceramides such as the prototypic NKT-cell antigen α-galactosylceramide (αGalCer; Kawano *et al*, 1997; Burdin *et al*, 1998) and the closely related α-galacturonosylceramide (αGalACer; *Sphingomonas* spp.; Kinjo *et al*, 2005; Mattner *et al*, 2005; Sriram *et al*, 2005); α-galactosyldiacylglycerol (αGalDAG; *Borrelia burgdorferi*) (Kinjo *et al*, 2006), to the trihexosylceramide isoglobotriaosylceramide (iGb3) Zhou *et al*, 2004). Despite this apparent diversity, most mammalian glycolipids are not recognised by the NKTcr, including lactosylceramide (LacCer), globotriaosylceramide (Gb3; α1,4Gal-LacCer), which is closely related to iGb3 (α1,3Gal-LacCer), monosialylganglioside GM1 (α2,3sialyl-LacCer) or isoglobotetraosylceramide (iGb4) (Zhou *et al*, 2004). A small subset of NKTcrs also recognise phosphatidylethanolamine (Rauch *et al*, 2003), phosphatidylinositol (Gumperz *et al*, 2000), β-galactosylceramide (Ortaldo *et al*, 2004; Parekh *et al*, 2004), the disialylganglioside GD3 (Wu *et al*, 2003) and microbial phosphatidylinositol-mannoside (PIM_4; *Mycobacterium tuberculosis* (Fischer *et al*, 2004). Crystal structures of several CD1d–antigen complexes showed that these lipids bind to CD1d through their long-chain base (LCB) and/or fatty acyl chain(s) so that the polar head groups protrude out of the CD1d antigen-binding site (ABS). Furthermore, the disposition of the head group depends on the unique pattern of hydrogen-bond network formed by residues of CD1d α1 and α2-helices with the polar aspects of the bound ligand (Giabbai *et al*, 2005; Koch *et al*, 2005; Zajonc *et al*, 2005, 2006). Thus, the α-linked galactose of αGalCer lies just above the entrance, flat and parallel to the plain of CD1d's ABS (Koch *et al*, 2005; Zajonc *et al*, 2005). In striking contrast, the β-anomeric linkage of the first sugar orients the glycan α1,3Gal–β1, 4Gal–β1,1′Glc of iGb3 perpendicular to the ABS (Zajonc *et al*, 2008). How the semi-invariant NKTcr recognises multiple diverse ligands in the context of CD1d remains an enigma.

A major advance in understanding how the NKTcr recognises its cognate antigen came from the crystal structure of the human NKTcr/CD1d–αGalCer co-complex (Borg *et al*, 2007). It showed that the Vα24 NKTcr interfaces CD1d–αGalCer in an unusual parallel docking mode by engaging germline-encoded CDR1α, CDR3α and CDR2β residues above the F′ pocket (Borg *et al*, 2007; Wun *et al*, 2008). Further, alanine-scanning mutagenesis of mouse and human NKTcrs revealed that they interact with CD1d–αGalCer similarly by using germline-encoded hotspots within CDR1α, CDR3α and CDR2β (Scott-Browne *et al*, 2007; Wun *et al*, 2008). One of these studies also revealed that the Vα14 NKTcr bound to CD1d–αGalCer and the very different CD1d–iGb3 landscapes in a conserved manner, using similar germline-encoded hotspots (Scott-Browne *et al*, 2007). The NKTcr showed very little conformational change upon ligation (Gadola *et al*, 2006; Kjer-Nielsen *et al*, 2006; Borg *et al*, 2007; Zajonc *et al*, 2008), consistent with a 'lock and key' recognition model where neither temperature nor ionic strength affected the CD1d–αGalCer interaction (Cantu *et al*, 2003). These findings suggest that the NKTcr acts like a pattern-recognition receptor and also explain why the NKTcr ligand recognition is CD1d-restricted. Yet, these studies provide little insight into ligand specificity and the molecular features of the diverse epitopes recognised, and do not explain the basis for distinct TCR β-chain usage for antigen recognition by the NKTcr.

As an approach to understand the role of β-chain in CD1d-restricted antigen recognition, we probed a panel of NKT-cell-derived hybridomas that express different TCR β-chains, as well as a panel of NKTcr point mutants that have altered CDR, with a variety of CD1d-restricted glycolipid ligands and variants with modifications of their sugar moieties. From the recognition patterns that emerged, we concluded that the NKTcr was highly adaptable, depending on the β-chain used, to recognise unique aspects of structurally diverse ligands within a conserved binding footprint on CD1d molecules.

Results

TCR β-chain usage dictates diverse glycolipid antigen recognition by the NKTcr

Unlike the CDR3α of the NKTcr, the CDR3β is highly diverse, both in length and primary structure (e.g., Supplementary Table S1). Additionally, CDR1β and CDR2β of distinct β-chains differ from each other. Because mouse NKTcr use multiple different β-chains (Vβ8.2, Vβ7 and Vβ2, as well as Vβ14 and Vβ6; Porcelli *et al*, 1993; Lantz and Bendelac, 1994), we hypothesised that differences within CDR1β, CDR2β and CDR3β account for the ability of NKTcr to recognise diverse lipid antigens. Using a panel of NKT hybridomas expressing identical Vα14 α-chain paired with four commonly used β-chains (Vβ8.2, Vβ14, Vβ7 and Vβ6; Lantz and Bendelac, 1994; Gui *et al*, 2001), we determined whether TCR β-chain usage influences recognition of diverse glycolipid ligands (Supplementary Figure S1A). Note that Vβ8.2, Vβ14, Vβ7 and Vβ6 have diverse CDR1β, but partly conserved, CDR2β sequences (e.g., Y46 and/or Y48 residues that were critical for interaction with the α1-helix of CD1d; Borg *et al*, 2007; Scott-Browne *et al*, 2007; Wun *et al*, 2008; Mallevaey *et al*, 2009; Pellicci *et al*, 2009). Additionally, the NKT hybridomas expressed diverse CDR3β regions in association with the same Vβ-region and, hence, the same CDR1β and CDR2β (Supplementary Table S1).

Bone marrow-derived dendritic cells (BMDCs) pulsed with αGalCer, iGb3 or αGalDAG were co-cultivated with the above NKT hybridoma panel and IL-2 secretion was assessed as a measure of activation. The data showed that the Vβ8.2+, Vβ14+ and Vβ7+ hybridomas recognised αGalCer whereas the Vβ6+ hybridoma did not (Figure 1A), despite the fact that these hybridomas showed comparable response to antigen-independent stimulation through CD3ε (Figure 1D). These data are consistent with previous reports, which demonstrated that several NKTcr β-chains are permissive to αGalCer recognition (Mallevaey *et al*, 2009). The Vβ8.2Jβ2.6+ hybridoma was autoreactive (i.e., in the

absence of exogenously added lipid) to BMDCs and was included as a positive control for the assay (Figure 1C).

Compared with the αGalCer recognition pattern, the recognition of iGb3 and αGalDAG by this hybridoma panel was clearly distinct (Figure 1). With the exception of the Vβ8.2Jβ2.2+ hybridoma, most Vβ8.2+ NKT hybridomas recognised iGb3 (Figure 1B). While the Vβ7+ hybridoma also recognised iGb3, the Vβ14+ and Vβ6+ hybridomas did not (Figure 1B). Note that a titration experiment showed that the hybridoma panel required a minimum of 10 μg of iGb3 and 20 μg of αGalDAG for recognition (data not shown). Therefore, because micelle formation and bioavailability influence lipid antigen presentation at higher concentrations, the functional avidity of the different Vβ-expressing NKTcrs for iGb3 and αGalDAG could not be determined.

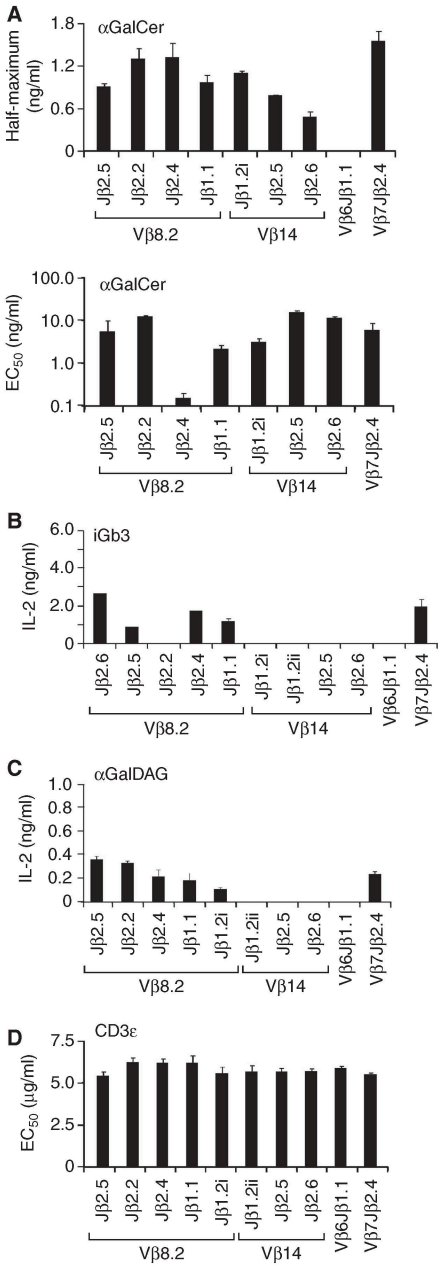

Figure 1 TCRβ usage impacts Vα14 TCR antigen recognition. (**A**) BMDCs pulsed with 0.1–100 ng/ml αGalCer overnight were co-cultivated with a panel of NKT hybridomas expressing Vα14 α-chain paired with unique TCR Vβ-chains (Supplementary Table S1). After 24 h, ELISA measured IL-2 secreted into the culture medium in response to NKT hybridoma activation. The data are represented as the half-maximal response (top panel) or half-maximal stimulatory concentration (EC_{50}; bottom panel) of αGalCer. (**B**, **C**) BMDCs pulsed with 10 μg/ml iGb3 (B) or 20 μg/ml αGalDAG (C) overnight were co-cultivated with the hybridoma panel and activation was measured by ELISA after 24 h stimulation. (**D**) NKT hybridomas expressing different β-chains were stimulated with 0.1–27 μg (in three-fold dilution) plate-bound anti-CD3ε mAb. After ~24 h, IL-2 ELISA was performed on culture supernatants to determine the sensitivity of each hybridoma to direct TCR stimulation. The data are represented as the EC_{50} of anti-CD3ε mAb. Data are representative of duplicate (B–D) or triplicate (A) experiments, each performed in triplicate.

As the aforementioned experiment used phytosphingosine-containing iGb3 (Supplementary Figure S1A), we determined whether the chemical make-up of the LCB influenced the recognition pattern. iGb3 made up of sphingosine-, sphinganine (4,5-dihydro)- and 4,5-dibromosphinganine-containing LCB were recognised just as well as phytosphingosine-based iGb3 (data not shown), suggesting that the chemical composition of the sphingoid backbone had very little influence on iGb3 recognition. Finally, all Vβ8.2+, the Vβ7+ and only the Vβ14Jβ1.2i+ hybridomas recognised αGalDAG (Figure 1C), whereas the remaining three Vβ14+ and the Vβ6+ hybridomas were unresponsive to this antigen (Figure 1C).

The varied antigen-recognition pattern could have resulted from variation in TCR expression and differences in the activation threshold of the different NKT hybridomas. Therefore, we determined the IL-2 response of each NKT hybridoma to antigen-independent stimulation using anti-CD3ε monoclonal antibody (mAb). All hybridomas responded similarly to this stimulation (Figure 1D). This result suggests that the recognition pattern of NKT hybridomas was intrinsic to the NKTcr and not due to variation in TCR expression levels or activation threshold. Taken together, the above data suggest that CDR3β together with CDR1β and CDR2β dictate NKTcr's ability to recognise structurally diverse ligands. Alternatively, although less likely, other cell-surface molecules differentially expressed by the hybridomas could result in the observed differences in responses.

Vβ usage impacts the recognition of 3′ and 4′ αGalCer analogues

To gain insight into how the NKTcr recognises αGalCer, we used αGalCer analogues, which contain modifications at the 3′- and 4′-hydroxyls of galactose (Supplementary Figure S1B). Note that the αGalCer analogues contained C_8 acyl chain, which does not alter the conformation of CD1d upon binding

(Zajonc *et al*, 2005; Pellicci *et al*, 2009). The 3′- and 4′-hydroxyls of αGalCer interact with NKTcr's CDR1α and/or CDR3α residues (Supplementary Figure S2) (Pellicci *et al*, 2009) yet their deoxy forms were reported not to affect recognition (Wun *et al*, 2008). Therefore, we determined whether chemical modifications at the 3′ (-amino, -azido and -*N*-acetyl) and 4′ (-*O*-methyl, -*O*-ethanol and -*N*-acetyl) of galactose are recognised by NKTcr, and whether Vβ usage influences this recognition using the approach described above. Replacement of the 3′-hydroxyl with an -amino, -azido or -*N*-acetyl group prevented recognition by the NKT hybridoma panel regardless of the NKTcr's β-chain composition (Figure 2A). Therefore, although the 3′-hydroxyl itself is dispensable (Wun *et al*, 2008), chemical substitutions at this position are detrimental for NKTcr recognition.

On the other hand, the recognition of the 4′ α-GalCer analogues was quite varied. All Vβ8.2+ hybridomas recognised these αGalCer variants, but to different degrees, indicating that CDR3β sequences might influence this recognition (Figure 2B, top row panel 1). The Vβ8.2+ hybridomas recognised 4′-*O*-methyl and 4′-*O*-ethanol αGalCer analogues to a similar extent (Figure 2B, top row panels 2 and 3), whereas the 4′-*N*-acetyl variant was less antigenic when compared with the recognition of αGalCer (Figure 2B, top row panel 4). All Vβ14+ NKT hybridomas recognised αGalCer but not to the same extent as the Vβ8.2+ hybridomas (Figure 2B, middle row panel 1). Recognition of the 4′ analogues by Vβ14+ NKT hybridomas was Jβ-dependent, such that only the Vβ14Jβ2.6+ hybridoma recognised both 4′-*O*-methyl and 4′-*O*-ethanol analogues, whereas the Vβ14Jβ1.2i+ hybridoma recognised only the 4′-*O*-ethanol variant (Figure 2B, middle row panels 2 and 3). The 4′-*N*-acetyl variant was not recognised by any of the Vβ14+ hybridomas (Figure 2B, middle row panel 4). Furthermore, the Vβ7+ NKT hybridoma recognised αGalCer and each of the 4′ variants to similar extent, whereas the Vβ6+ hybridoma failed to respond to any of these lipid antigens (Figure 2B, bottom row). These data suggest that the 4′-*N*-acetyl variant is a less potent antigen than the 4′-*O*-methyl and -*O*-ethanol analogues, thereby revealing an agonistic hierarchy in NKTcr ligands: αGalCer > 4′-*O*-methyl ∼ 4′-*O*-ethanol ≫ 4′-*N*-acetyl. As the 4′-*N*-acetyl analogue is not recognised by Vβ14+ hybridomas (Figure 3B), we conclude that the recognition of weak NKTcr ligands is influenced not only by CDR3β but also by CDR1β and CDR2β loops.

Vβ usage also impacts iGb3 recognition

Low affinity of the CD1d–iGb3/NKTcr interaction has complicated structural, biochemical and functional studies of this ligand–receptor complex (Zhou *et al*, 2004; Zajonc *et al*, 2008). We approached the structural analyses of this complex using a combination of iGb3 variants and the aforementioned hybridoma panel expressing Vα14 α-chain paired with Vβ8.2, Vβ14, Vβ7 or Vβ6 β-chain. For this, 2‴′, 3‴, 4‴′ or 6‴′ deoxy variants of the terminal galactose were incorporated into the phytosphingosine-based ceramide backbone during syntheses (Supplementary Figure S1C).

As described above, we found that only Vβ7+ and Vβ8.2+, with the exception of Vβ8.2Jβ2.2+, NKT hybridomas recognised iGb3 (Figure 1A), a pattern similar to 4′-*N*-acetyl-αGalCer recognition (Figure 2B). This recognition required the 2‴′-hydroxyl group within the terminal galactose by most (Vβ8.2Jβ2.5, Vβ8.2Jβ2.2, Vβ8.2Jβ2.4 and Vβ8.2Jβ2.2), and the 3‴′-hydroxyl by some (Vβ8.2Jβ2.5 and Vβ8.2Jβ2.2 only), Vβ8.2 NKT hybridomas (Figure 3). None of the Vβ14+ hybridomas recognised iGb3 or its deoxy variants (Figure 3). Therefore, despite their obvious structural differences, the three CDRβ loops impact iGb3 recognition in a manner similar to 4′-*N*-acetyl αGalCer recognition.

CDR1β and CDR3β residues, in addition to previously identified 'hotspots' influence the recognition of αGalCer variants

The crystal structure of human CD1d–αGalCer/Vα24–Vβ11 NKTcr (Borg *et al*, 2007), as well as mouse CD1d–αGalCer/Vα14–Vβ8.2 and CD1d–αGalCer/Vα14–Vβ7 NKTcrs (Pellicci *et al*, 2009), combined with mutagenesis studies (Scott-Browne *et al*, 2007; Wun *et al*, 2008; Mallevaey *et al*, 2009), have shown that CDR1α, CDR3α and CDR2β residues are critical for CD1d–αGalCer recognition. As the 4′-αGalCer analogues were differentially recognised by different hybridomas (Figure 2), these variants were used in combination with a panel of Vα14Jα18/Vβ8.2Jβ1.1-derived mutants with individual amino-acid alteration within their CDRs to determine the CDRβ residues that influence recognition of the variant part of the antigen. The rationale behind this approach was that some of the Vα14 NKTcr mutants may gain recognition and reveal the CDR residues that influence recognition either directly or indirectly. From the Vα14-Vβ8.2 NKTcr/CD1d–αGalCer crystal structure (Pellicci *et al*, 2009), we were able to precisely gauge whether the effect of the alanine-scan mutants were likely a result of adverse affect on the conformation of the NKTcr (indirect effects, namely CDR1α: V26A, P28A, H31A, L32A, R33A; CDR1β: H27A, N29A and CDR2β: S47A, G49A) or on CD1d-antigen recognition (direct effects). Also note that none of the mutants become autoreactive to BMDCs, the APC used for antigen presentation (data not shown).

As reported previously (Borg *et al*, 2007; Scott-Browne *et al*, 2007; Wun *et al*, 2008), our results revealed that CDR1α, CDR3α and CDR2β residues were critical for αGalCer recognition (Figure 4). For the most part, residues critical for αGalCer recognition were also critical for 4′-*O*-methyl- and 4′-*O*-ethanol-αGalCer recognition (Figure 4), suggesting that the footprint of the NKTcr binding to CD1d molecules remains essentially the same for these two variants. Exceptions were CDR1α mutants R33A, which did not recognise 4′-*O*-methyl or 4′-*O*-ethanol-αGalCer, and H31A, which did not recognise 4′-*O*-methyl-αGalCer, but partially recognised 4′-*O*-ethanol-αGalCer (Figure 4). The effects of H31A and R33A are perhaps indirect because they are thought to alter the fold of the NKTcr (Borg *et al*, 2007; Scott-Browne *et al*, 2007; Wun *et al*, 2008; Pellicci *et al*, 2009).

The 4′-*N*-acetyl variant was poorly (∼20%) recognised by Vα14Jα18/Vβ8.2Jβ1.1 TCR compared with recognition of αGalCer (Figures 2B and 4), but alteration of residues within CDR1α, CDR2α, CDR1β and CDR3β restored recognition of this variant (Figure 4). Specifically, CDR1α mutants D29A and N30A, as well as CDR2α mutants V50A, D51A and D54A, overcame poor recognition of the 4′-*N*-acetyl variant (Figure 4). Similarly, CDR1β mutants N26A and N29A and CDR3β mutant G94A also rescued defective recognition of the 4′-*N*-acetyl analogue (Figure 4). Note that the differential recognition pattern of the mutant NKT hybridomas was not

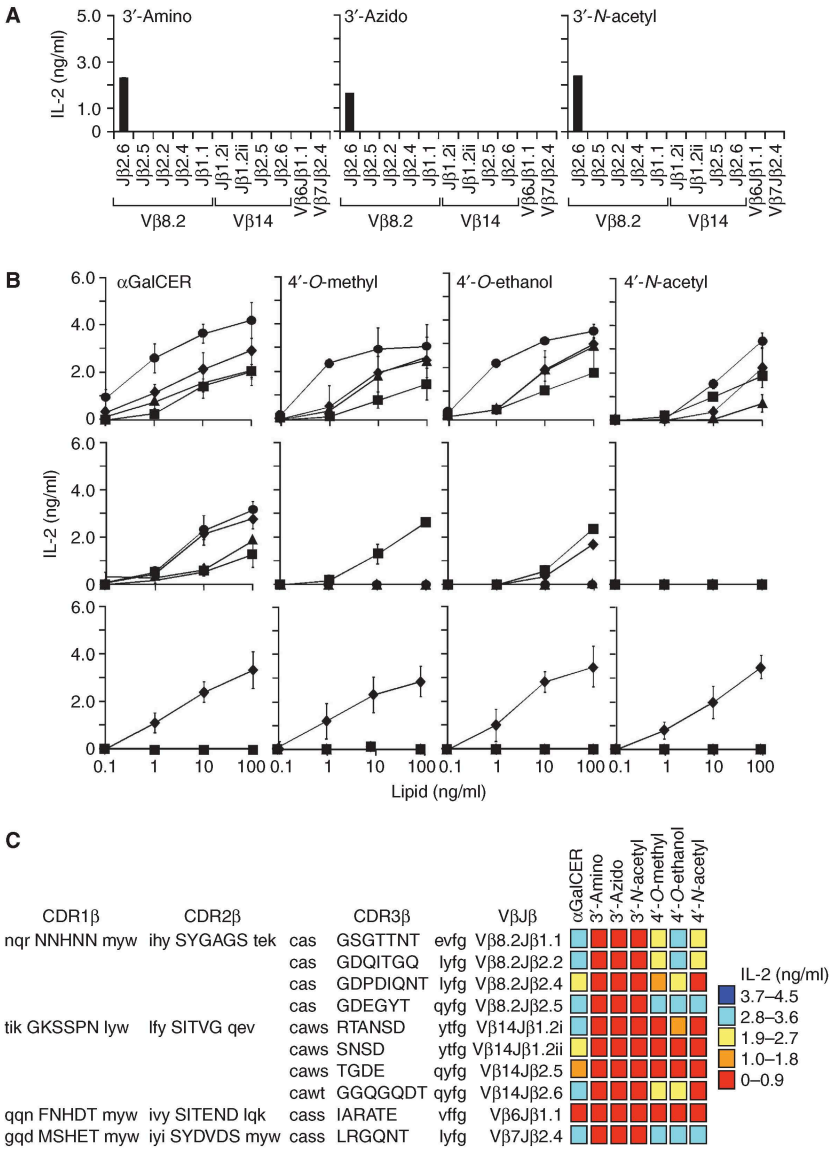

Figure 2 NKTcrs recognise 4′-hydroxy variants in a distinct manner. (**A**) BMDCs pulsed with 500 ng/ml of 3′-hydroxy variants (Supplementary Figure S1B) overnight were co-cultivated with the same panel of NKT hybridomas described in Figure 1. After 24 h, ELISA measured IL-2 secreted into the culture medium in response to NKT hybridoma activation. (**B**) BMDCs were pulsed with the indicated concentrations of αGalCer or its 4′-hydroxy variants and used to stimulate NKT hybridomas. Top row: Vβ8.2Jβ1.1 (circles); Vβ8.2Jβ2.1 (diamonds); Vβ8.2Jβ2.5 (triangles) and Vβ8.2Jβ2.6 (squares); middle row: Vβ14Jβ1.2i (circles); Vβ14Jβ1.2ii (diamonds); Vβ14Jβ2.5 (triangles) and Vβ14Jβ2.6 (squares); bottom row: Vβ7 (diamonds) and Vβ6 (squares). ELISA measured IL-2 secreted into the culture medium in response to NKT hybridoma activation. (**C**) Schematic rendition of NKTcr recognition pattern. Amino-acid sequence of CDR1β, CDR2β and CDR3β (upper case) of each Vα14 TCR is indicated on the left; lowercase indicates residues flanking each CDR. Vβ sequences were obtained from IMGT (http://www.imgt.org/textes/IMGTrepertoire/). Data in panels A and B are representative of two independent experiments performed in triplicate.

due to differences in TCR expression levels or activation thresholds because they were similar for all hybridomas as previously reported (Scott-Browne *et al*, 2007). Together, these data suggest that the family of NKTcrs is afforded plasticity through different TCR β-chains, which, therefore, permit binding of structurally variant glycolipid ligands. Furthermore, in addition to the CDR1α, CDR3α and CDR2β residues that form a common NKTcr footprint (Scott-Browne *et al*, 2007; Wun *et al*, 2008; Mallevaey *et al*, 2009; Pellicci *et al*, 2009), recognition of weak agonists such as 4′-*N*-acetyl-

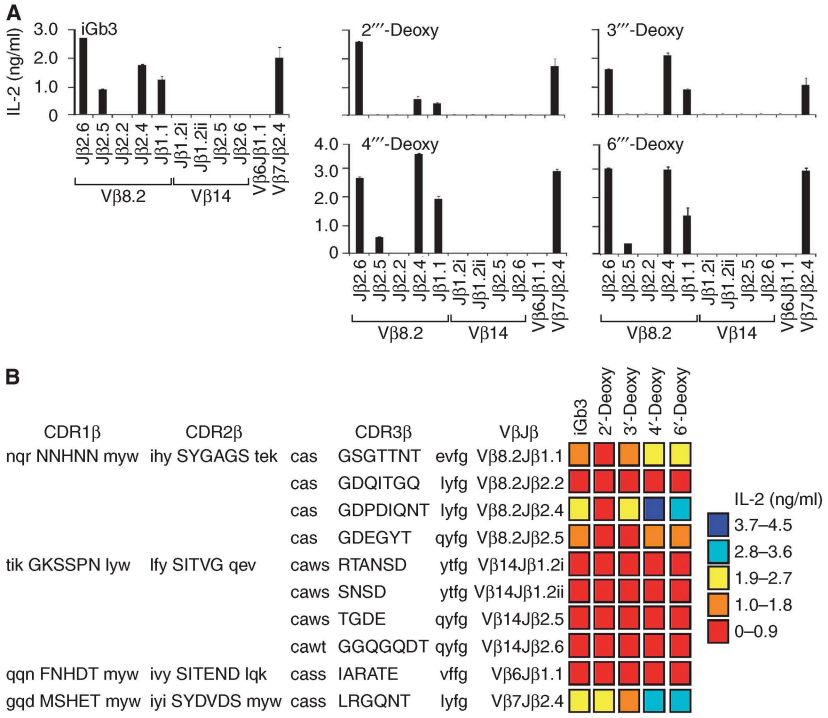

Figure 3 NKTcr interfaces CD1d–iGb3 with a distinct recognition logic. (**A**) BMDCs pulsed with 10 μg/ml iGb3, 2‴-deoxy-iGb3, 3‴-deoxy-iGb3, 4‴-deoxy-iGb3 or 6‴-deoxy-iGb3 were used to stimulate a panel of NKT hybridomas described in Figure 1. After 24 h, ELISA measured IL-2 secreted into the culture medium in response to NKT hybridoma activation. Data are representative of two independent experiments performed in triplicate. (**B**) Schematic rendition of NKTcr recognition pattern. Amino-acid sequence of CDR1β, CDR2β and CDR3β (upper case) of each Vα14 TCR is indicated on the left; lowercase indicates residues flanking each CDR (for sequences see http://www.imgt.org/textes/IMGTrepertoire/).

αGalCer may be influenced by CDR residues outside these 'hotspots'. Consistent with this, the β-chain of the Vβ7+ and Vβ6+ NKTcrs was shown to have a greater role in interacting with CD1d–αGalCer in comparison with the Vβ8.2+ NKTcr (Mallevaey *et al*, 2009; Pellicci *et al*, 2009).

CDR2α, CDR1β and CDR3β residues impact on iGb3 recognition

The NKTcr mutant hybridomas were probed with iGb3 and its four deoxy analogues (Supplementary Figure S1C), focusing on the 2‴- and 3‴-deoxy variants that were poorly recognised by the Vα14Jα18/Vβ8.2Jβ1.1 NKTcrs (Figure 5). In agreement with a previous study (Scott-Browne *et al*, 2007), we also observed that iGb3 recognition involved the same germline-encoded 'hotspots', which include residues within CDR1α, CDR3α and CDR2β (Figure 5). Furthermore, mutations within all three β-chain CDRs also affected recognition of iGb3, none of which, except CDR3β G94A, were rescued by the 2‴- and 3‴-deoxy variants (Figure 5). Most interestingly, alanine mutations either partially (CDR2α V50A) or fully (CDR2α K53A and CDR3β G94A) rescued the recognition of 2‴-deoxy-iGb3 and 3‴-deoxy-iGb3, which were poorly recognised by the wt NKTcr (Figure 5). From these data we conclude that iGb3 recognition by the NKTcr is distinct from αGalCer but shares some characteristics with that of 4′-*N*-acetyl-αGalCer. Furthermore, the data suggest a potential role of CDR1β and CDR3β, in addition to the CDR2α, loop in the recognition of iGb3.

CDR2α and CDR1β residues impact on αGalDAG recognition

Having determined that the αGalDAG recognition pattern by naturally occurring Vα14+ hybridomas was distinct from that of αGalCer and iGb3 (Figure 1), we tested how the Vα14 NKTcr mutants recognise this antigen. The responses of the mutant hybridomas again revealed that αGalDAG recognition involved the germline-encoded 'hotspots' within CDR1α, CDR3α and CDR2β (Figure 6). While none of the CDR3α mutants recognised αGalCer or iGb3, we found that CDR3α D93A uniquely recognised αGalDAG (Figures 4–6). Further, although Y48A mutant does not recognise the three ligands, the remainder of CDR2β residues were differentially required for recognition: none were required for αGalCer, but S47, G51 and S52 were required for iGb3 while S47 and S52 were required for αGalDAG recognition (Figures 4–6). A similar discordance was also observed with CDR3β mutants: none were critical for αGalCer and αGalDAG recognition (Figures 4 and 6), but many (S93, T95, T96 and T98) were critical for

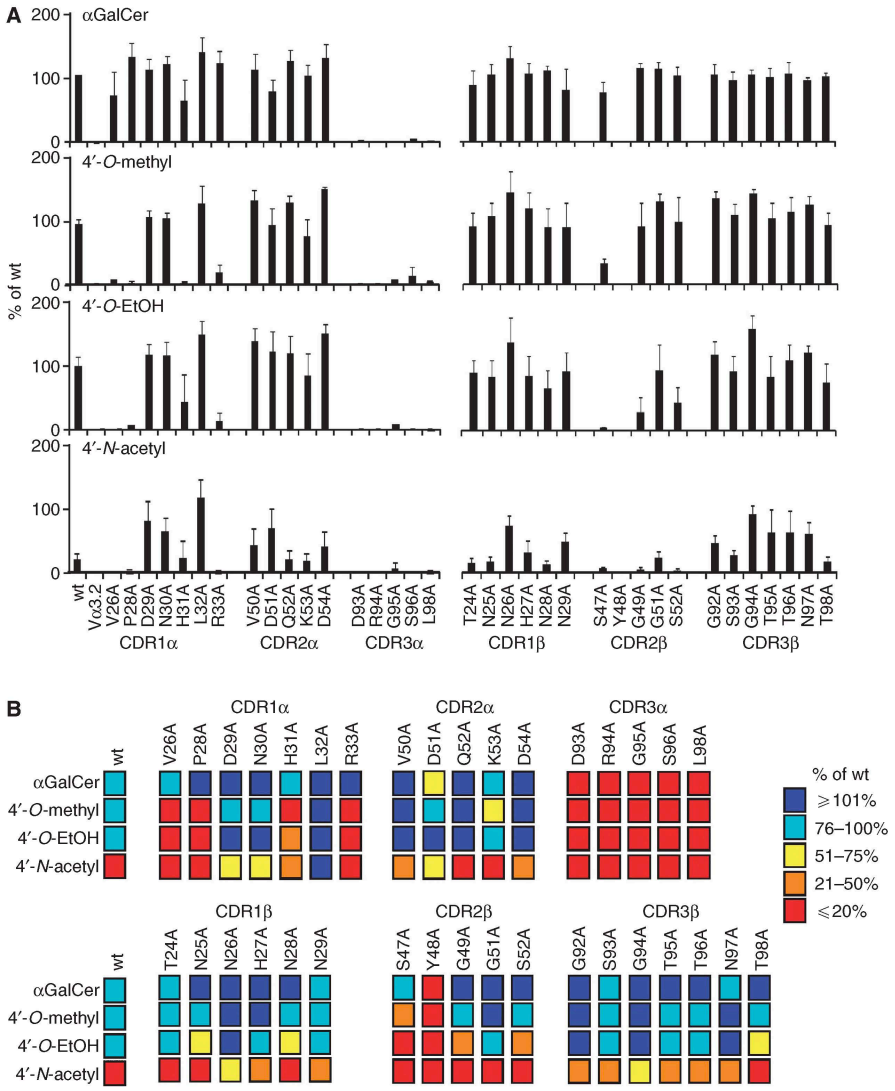

Figure 4 The 4′-*N*-acetyl αGalCer variant interacts with Vα14 TCR with a unique register. (**A**) BMDCs pulsed with 500 ng/ml αGalCer, 4′-*O*-methyl, 4′-*O*-ethanol or 4′-*N*-acetyl variants were used to stimulate a panel of NKTcr mutants consisting of a single point mutation within CDR1, CDR2 and CDR3 of both TCR α- and β-chains. The Vα3.2+ NKT hybridoma was used as the negative control. After 24 h, ELISA measured IL-2 secreted into the culture medium in response to NKT hybridoma activation. As the wt hybridoma and the derived mutants were equally sensitive to antigen-independent stimulation (Scott-Browne *et al*, 2007), the data were normalised to wt IL-2 response to αGalCer-pulsed BMDCs and represented as mean ± s.e.m. of three independent experiments performed in triplicate. (**B**) Schematic rendition of NKTcr recognition pattern.

iGb3 recognition (Figure 5). Moreover, CDR2α residues V50 and K53, which were required for 2‴-deoxy iGb3 recognition, along with D54, were critical for αGalDAG recognition, but were irrelevant for αGalCer recognition (Figures 4–6). These data indicate that the galactose head group of αGalDAG when bound to CD1d is disposed differently from the galactose of αGalCer. Thus, while maintaining a common NKTcr footprint mediated by the 'hotspots', effective recognition of αGalDAG involves different contact residues within these hotspots, and additionally requires CDR2α and CDR1β residues.

Discussion

Our current knowledge of how NKTcr recognises its cognate ligands is based on the crystal structure of Vα24–Vβ11 NKTcr/CD1d–αGalCer (Borg *et al*, 2007) as well as the recently solved crystal structures of Vα14–Vβ8.2 and Vα14–Vβ7 NKTcr/CD1d–αGalCer (Pellicci *et al*, 2009) complexes. Moreover these structures have been complemented by mutational studies on the Vα14 and Vα24 NKTcrs (Borg *et al*, 2007; Scott-Browne *et al*, 2007; Wun *et al*, 2008; Mallevaey

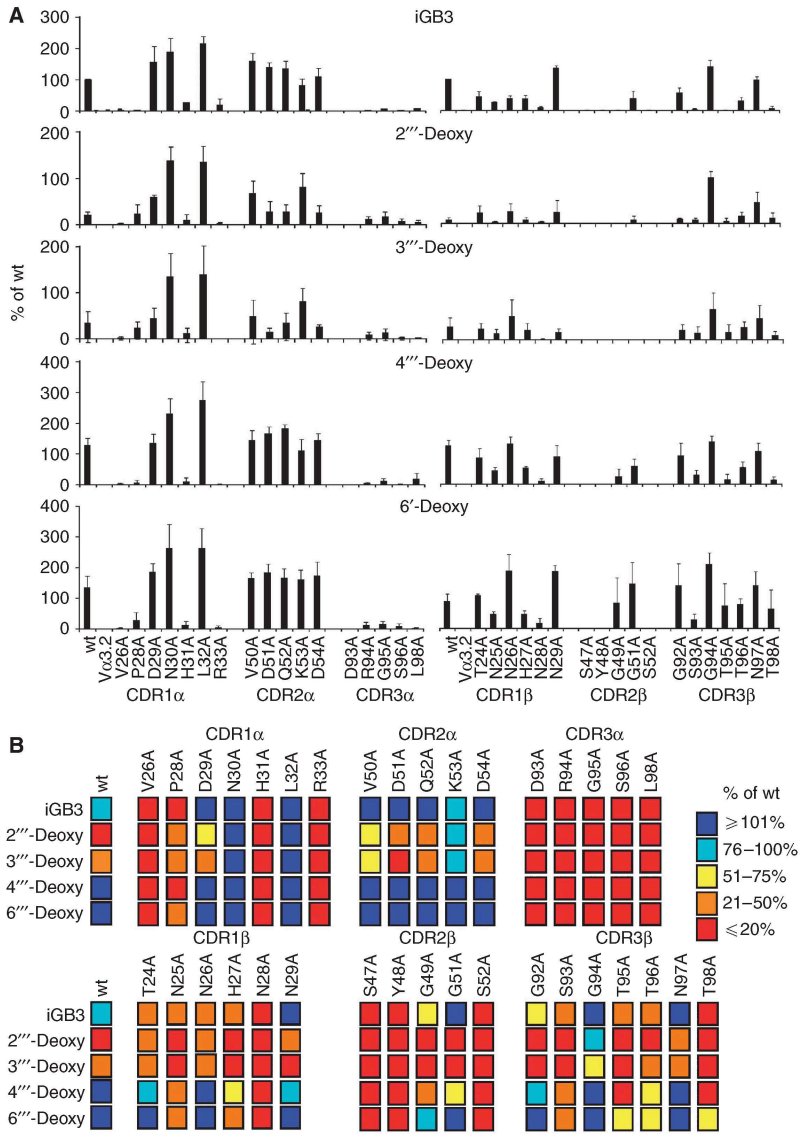

Figure 5 NKTcr recognises CD1d–iGb3 with a distinct recognition logic. (**A**) BMDCs were pulsed with iGb3 or its variants (as described in Figure 3A) and used to stimulate a panel of NKTcr mutants, and activation was monitored (as described in Figure 3A). Data were normalised as in Figure 4A and represented as mean ± s.e.m. of at least three independent experiments performed in triplicate. (**B**) Schematic rendition of NKTcr recognition pattern.

et al, 2009). Collectively, these structures have revealed a similar docking mode between the Vα14–Vβ8.2, Vα14–Vβ7 and Vα24–Vβ11 NKTcrs. These structures also revealed that differences in Vβ-chain usage nevertheless impacted on CD1d–αGalCer recognition. How differing Vβ usage would impact on recognising CD1d-restricted antigens other than αGalCer was less clear. In the absence of the crystal structures of NKTcr/CD1d–iGb3 and NKTcr/CD1d–αGalDAG, we have used an approach based on functional recognition to delineate how semi-invariant NKTcrs recognise diverse ligands. The approach involved probing a panel of naturally occurring Vα14 TCRs and derived point mutants that have altered CDRs with a panel of CD1d-restricted glycolipids and their sugar variants. Importantly, the recently solved crystal structure of the Vα14–Vβ8.2 NKTcr/CD1d–αGalCer structure enabled us to ascertain the mutations that are likely to exert indirect effects (e.g., CDR1α: V26A, P28A, H31A, L32A, R33A; CDR1β: H27A, N29A; CDR2β: S47A; G49A (Pellicci *et al*, 2009) versus mutations that would impact directly on recognition.

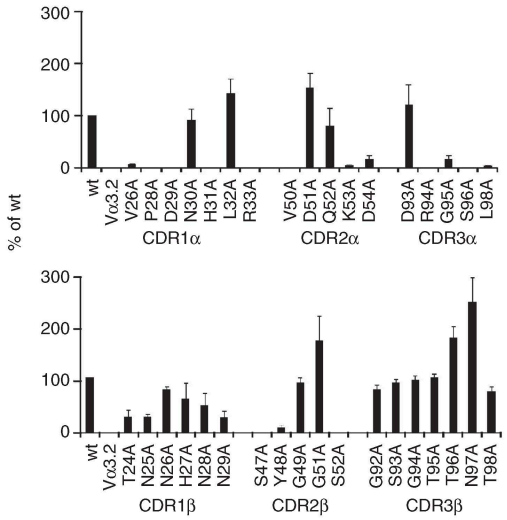

Figure 6 The αGalDAG recognition logic is distinct from that of αGalCer or iGb3 recognition by NKTcr. BMDCs pulsed with 20 μg/ml αGalDAG were used to stimulate a panel of NKTcr mutants and activation was measured as described in Figure 4A. Data were normalised as described in Figure 4A and represent the mean ± s.e.m. of at least three independent experiments performed in triplicate.

Our results revealed several hitherto unknown key features of diverse ligand recognition by NKTcr: first, we found that distinct epitopic sites in αGalCer and iGb3 were critical for recognition. Second, recognition of weak CD1d-restricted NKTcr agonists critically depended on the β-chain that paired with the Vα14 α-chain. Third, we discovered that while the NKTcrs dock on CD1d with a conserved footprint, they are malleable enough to recognise αGalDAG, which is structurally related to αGalCer, and the structurally most divergent iGb3 (Figure 7B). Fourth, as we will discuss below, our data best fit the 'squash' model for iGb3 recognition by the NKTcr (Figure 7A).

We found that the Vα14 NKTcr is intolerant to chemical modifications at the 3′ position of αGalCer even though the 3′-hydroxyl is dispensable for NKTcr recognition (Wun *et al*, 2008). On the other hand, the Vα14 NKTcr was tolerant to multiple 4′ modifications, consistent with the previous finding that the 4′-hydroxyl is dispensable for recognition (Wun *et al*, 2008). Nonetheless, a unique modification of αGalCer with 4′-*N*-acetyl was very poorly recognised by Vα14Jα18–Vβ8.2Jβ1.1 TCR. Its recognition was rescued by several mutations within CDR1α, CDR2α, CDR1β and CDR3β, many of which are surprisingly outside the common binding footprint. Thus, the CDRβ loops appear to complement the recognition landscape formed by the α-chain CDRs.

The 2‴- and 3‴-hydroxyls of the terminal α1,3Gal of iGb3 were essential for Vα14Jα18–Vβ8.2Jβ1.1 recognition. As with the 4′-*N*-acetyl-αGalCer variant, mutations within CDR1α, CDR2α and CDR3β rescued recognition of both the deoxy-iGb3 variants. Because this and previous mutagenesis studies revealed germline-encoded CDR1α, CDR3α and CDR2β 'hotspots' in αGalCer and iGb3 recognition (Scott-Browne *et al*, 2007), we assume that the Vα14 NKTcr docks on both CD1d–αGalCer and CD1d–iGb3 complexes in a similar mode. The perpendicular disposition of the trihexoses of iGb3 in an unliganded state (Zajonc *et al*, 2008) as compared with the parallel orientation of the monohexose in CD1d–αGalCer (Zajonc *et al*, 2005) structure poses a serious recognition problem, and would result in steric clashes with the NKTcr (Figure 7A) if one assumed a docking mode similar with respect to CD1d–αGalCer recognition. Thus, we suggest that the glycan moiety of iGb3 is flattened upon NKTcr engagement, which is analogous to the TCR-induced flattening of extremely bulged pMHC class-I ligands (Tynan *et al*, 2007). However, with our current data, it is not possible to speculate on precisely how iGb3 might be flattened to fit into an NKTcr/CD1d–antigen complex. Notwithstanding, because LacCer and Gb3, which are related to iGb3, are not recognised by the NKTcr (Zhou *et al*, 2004), it appears as though the terminal α1-3Gal in iGb3, in its squashed position, provides critical new contact(s) that are required for binding to CD1d, NKTcr or both.

CD1d–αGalDAG recognition by the Vα14 NKTcr also involves the previously reported germline-encoded 'hotspots' made up of residues within CDR1α, CDR3α and CDR2β. In addition, it involves additional unique residues contributed by other CDR many of which are dispensable for αGalCer and iGb3 recognition. Most importantly, CDR2α V50, K53 and D54 were critical for αGalDAG recognition. These results suggest that the positioning of the galactosyl group in αGalDAG differs from that of αGalCer. In the recently reported model, the diacylglycerol backbone of αGalDAG is predicted not to form the critical hydrogen bond network with CD1d R79 and D80. Hence, it is expected that the galactose in αGalDAG is raised above the plane of the galactose in αGalCer and is moved away from the α2-helix (Kinjo *et al*, 2006). A similar disposition of the galactose is observed when human CD1d displays αGalCer that is caused by a species variation (human W153, which is equivalent to mouse G155; Koch *et al*, 2005; Zajonc *et al*, 2005). The putative differences in the disposition between the galactoses of αGalDAG and αGalCer when displayed by CD1d might explain the distinct logic used by the NKTcr for αGalDAG and αGalCer recognition.

We found that the β-chain played a significant role in 4′-*N*-acetyl-αGalCer, iGb3, iGb3 analogues and αGalDAG recognition because none of the Vβ14+ NKTcr recognised these ligands. This could partly be because Vβ14 lacks the CDR2β Y48 residue, which is critically important for the binding of Vβ8.2-containing NKTcr to CD1d (Borg *et al*, 2007; Scott-Browne *et al*, 2007; Wun *et al*, 2008; Mallevaey *et al*, 2009). Equally intriguing was the finding that despite the lack of Y48, Vβ14+ NKTcr recognised αGalCer. This is perhaps because Y46 present in Vβ14 compensates for the absence of Y48. Notwithstanding, Vβ14+ NKTcr did not recognise iGb3 or αGalDAG. As well as because CDR2β Y46-containing Vβ6+ NKTcr does not recognise any of the ligands tested, we predict that CDR3β contributes significantly to the energetic landscape for low-affinity ligand recognition (4′*N*-acetyl-αGalCer, αGalDAG and iGb3), perhaps by influencing the structure of the closely disposed CDRα loops. A recent report identified an I/LxxPI/L (I, L and P are isoleucine, leucine and proline; x is any amino acid) motif within CDR3β as a potential contributor for Vβ6+ NKTcr antigen recognition (Mallevaey *et al*, 2009). Such a recognition logic would then

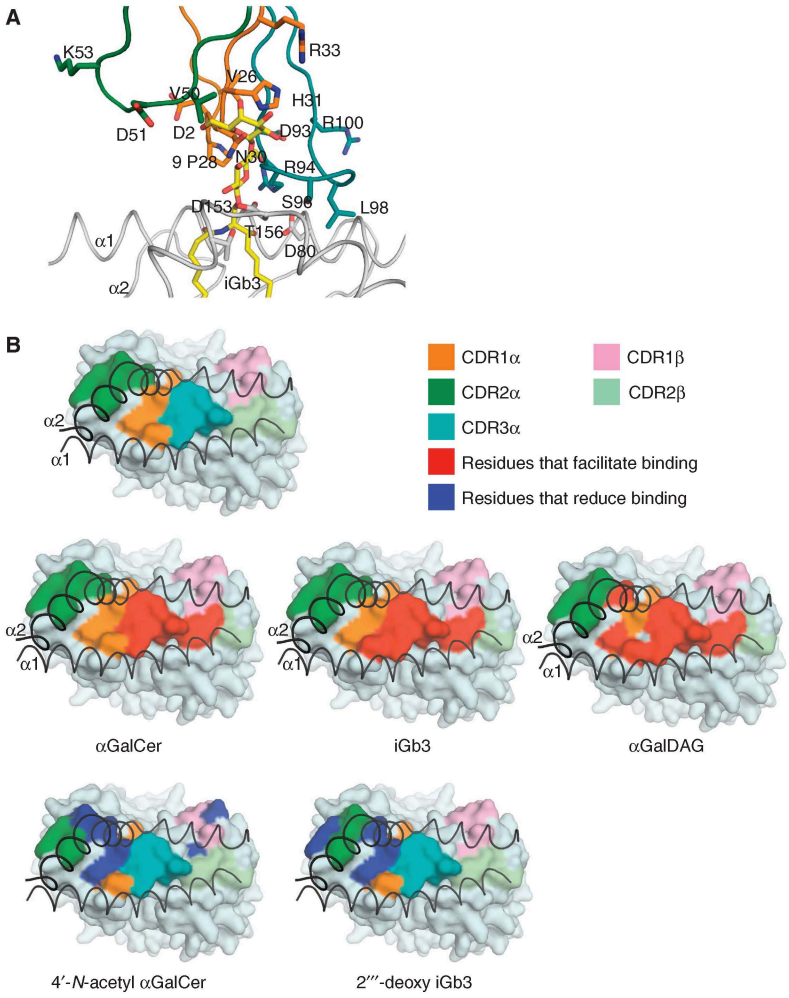

Figure 7 The recognition logic. (**A**) iGb3 modelled onto the Vα14Vβ8.2/CD1d–αGalCer crystal structure shows clashes with the CDR1α and CDR3α loops. CDR1α (orange); CDR2α (green); CDR3α (blue); CD1d (grey) and iGb3 (yellow). (**B**) The Vα14Vβ8.2 NKTcr surface showing CDR loops (top panel). Mutations that decreased ligand binding are shown in red (middle panel). The NKTcr surface with αGalCer (left), iGb3 (middle) and αGalDAG (right). Mutations that increased ligand binding are shown in dark blue (bottom panel). The NKTcr surface with 4′-*N*-acetyl analogue of αGalCer (left) and 2‴-deoxy analogue of iGb3 (right). TCR surface (pale cyan); CDR1α (orange); CDR2α (green); CDR3α (blue); CDR1β (pale green); CDR2β (pink) and CD1d helices (dark grey); CDR3β is not shown.

explain the exclusion of the majority of the β-chains from the NKTcr repertoire during positive selection (Mallevaey *et al*, 2009), which is presumably mediated by low-affinity self-ligands. Thus, we conclude that the β-chain CDRs fine-tune the affinity threshold for NKTcr ligand recognition.

While CDR3β did not appear to play a key role in recognition of αGalCer, variations in its length and composition did impact on the recognition of analogues of αGalCer and iGb3, as well as αGalDAG. Existing structural data (Borg *et al*, 2007; Pellicci *et al*, 2009) have not supported a key role for CDR3β in direct recognition of CD1d–αGalCer; however, some CDR3β conformations appear to be more permissive than others for CD1d–glycolipid-antigen recognition (Kjer-Nielsen *et al*, 2006; Scott-Browne *et al*, 2007; Mallevaey *et al*, 2009). Taken together, the impact of CDR3β conformation seems to vary as a function of the glycolipid antigen. It is difficult to speculate on precisely how CDR3β is contributing to recognition in these instances, although some CDR3β conformations might inhibit binding through steric hindrance, as suggested for the human NKT-15 TCR (Kjer-Nielsen *et al*, 2006), and some may indirectly affect recognition by altering the juxtaposition of other CDR regions that are involved in direct binding as has been observed in the structure of Vα14–Vβ7 NKTcr/CD1d–αGalCer complex in comparison to that of Vα14–Vβ8.2 NKTcr/CD1d–αGalCer complex (Pellicci *et al*, 2009).

In sum, the second site-suppression strategy allowed us to gain new insight into how the NKTcr recognises multiple

ligands, especially of CD1d–iGb3 and CD1d–αGalDAG complexes for which crystal structures of the receptor/antigen co-complexes are yet to be solved. Our data reinforce the previously reported common docking footprint, but extend the recognition logic significantly further for the recognition of weak/low-affinity agonists. Such weak agonists require other areas of the recognition landscape (e.g., CDR2α, CDR1β and CDR3β) to achieve the energy necessary for NKT-cell activation. Therefore, we conclude that there is a consistent logic with which the NKTcr positions its 'hotspot' to find the epitope. The malleable nature of NKTcrs described herein then determines whether the orientation with which they 'perch' on the antigens, especially weak agonists, can be stabilised sufficiently to generate an activation signal. These new insights can be used to design altered glycolipid ligands that will have the potential to steer downstream immune responses in a desired manner.

Materials and methods

Mice

C57BL/6 mice were purchased from the Jackson Laboratory and used in compliance with Vanderbilt Institutional Animal Care and Use Committee-approved regulations.

Glycolipids

The syntheses and structure validation of all αGalCer and iGb3 and their variants are described elsewhere (Chen *et al*, 2007; Xia *et al*, 2009). αGalCer and iGb3 and their sugar variants were dissolved in DMSO at 1 mg/ml and used at the indicated concentrations. αGalDAG preparation and use has been reported (Kinjo *et al*, 2006).

Preparation of BMDC

BM cells were harvested from the femurs of 8 to 10-week-old C57BL/6 mice and differentiated into DC by cultivating precursors in petridishes for 7 days in RPMI+ (RPMI-1640 supplemented with 10% fetal calf serum (FCS), 1% L-glutamine, 1 mM penicillin/streptomycin; CellGrow) containing 20 ng/ml recombinant murine colony-stimulating factor-2 (rCsf-2; PeproTech). On days 3 and 5 of culture, 70% of the medium containing non-adherent cells was removed and replaced with fresh medium containing 20 ng/ml of rCsf-2. On day 7, the loosely adherent and non-adherent cells largely containing BMDCs and some granulocytes were harvested and used immediately for antigen loading.

NKT hybridoma stimulation and ELISA

All Vα14+ mouse NKT hybridomas N38-3C3, DN32.D3, N37-1H5a, N38-2C12, N57-2C12, N57-2B6, H41-2C9, H41-3C5, H41-2D9, N38-2H4, Vα14-DOβ and its alanine mutants have been described (Lantz and Bendelac, 1994; Gui *et al*, 2001; Scott-Browne *et al*, 2007). TCR α- and β-chain usage and CDR sequences are shown in Supplementary Table S1. They were maintained in RPMI+ containing 55 μM 2-mercaptoethanol. BMDCs were dispensed into round-bottomed microtitre plates at a density of 3×10^4 cells/well and incubated with increasing concentrations of αGalCer and its 3′ and 4′ variants, (0.1–500 ng/ml), iGb3 and its deoxy variants (10 μg/ml) or αGalDAG (20 μg/ml) for 18–24 h at 37°C. Lipid-loaded BMDCs were washed twice with warm PBS and co-cultivated with 6×10^4 NKT hybridoma cells per well for 24 h at 37°C. Cell-free supernatant was harvested and IL-2 secreted during co-culture was determined by ELISA.

TCR modelling

The NKTcr/CD1d–iGb3 model was prepared based on the previously reported crystal structure of CD1d–iGb3 complex (Zajonc *et al*, 2008) and the Vα14Vβ8.2 crystal structure (Pellicci *et al*, 2009). All NKTcr–CD1d models were prepared in an identical docking orientation as observed in the Vα14Vβ8.2/CD1d–αGalCer crystal structure (Pellicci *et al*, 2009).

Supplementary data

Supplementary data are available at *The EMBO Journal* Online (http://www.embojournal.org).

Acknowledgements

We thank L Van Kaer for critical evaluation of the data and helpful suggestions on the writing of this paper. This work was supported by grants from the NIH HL069765 (WCF, LEG) AI007611 (LEG), AI45889 (SAP), AI057519 (ARH), AI074952 (DMZ), AI048224 and AI061721 (SJ), as well as by the Medical Scientist Training Program of the Albert Einstein College of Medicine (KAOY), the Cancer Research Institute's Investigator Award (DMZ) and an endowment from the Ohio State University (PGW).

Author contributions: WCF, LEG and SJ designed experiments. WCF and LEG performed experiments. CX, WC, and YZ synthesised glycolipids; OP, LK-N and RJ provided modelled structures based on mutagenesis data; JS-B, YK, KOAY, SK, SKR, SAP, ARH, KH, and LG provided critical reagents; WCF, CX, JR, DIG, DMZ, PGW and SJ wrote and WCF, DGP, DIG, JR, LG, SAP, ARH, DMZ, PGW and SJ edited the paper.

Conflict of interest

SA Porcelli serves as a paid consultant for Vaccinex Inc., Rochester, NY. The remaining authors have no conflicting financial interests.

References

Borg NA, Wun KS, Kjer-Nielsen L, Wilce MC, Pellicci DG, Koh R, Besra GS, Bharadwaj M, Godfrey DI, McCluskey J, Rossjohn J (2007) CD1d-lipid-antigen recognition by the semi-invariant NKT T-cell receptor. *Nature* **448:** 44–49

Burdin N, Brossay L, Koezuka Y, Smiley ST, Grusby MJ, Gui M, Taniguchi M, Hayakawa K, Kronenberg M (1998) Selective ability of mouse CD1 to present glycolipids: alpha-galactosylceramide specifically stimulates Valpha14+ NK T lymphocytes. *J Immunol* **161:** 3271–3281

Cantu III C, Benlagha K, Savage PB, Bendelac A, Teyton L (2003) The paradox of immune molecular recognition of alpha-galactosylceramide: low affinity, low specificity for CD1d, high affinity for alpha beta TCRs. *J Immunol* **170:** 4673–4682

Capone M, Cantarella D, Schumann J, Naidenko OV, Garavaglia C, Beermann F, Kronenberg M, Dellabona P, MacDonald HR, Casorati G (2003) Human invariant Valpha24–JalphaQ TCR supports the development of CD1d-dependent NK1.1+ and NK1.1− T cells in transgenic mice. *J Immunol* **170:** 2390–2398

Chen W, Xia C, Wang J, Thapa P, Li Y, Nadas J, Zhang W, Zhou D, Wang PG (2007) Synthesis and structure–activity relationship study of isoglobotrihexosylceramide analogues. *J Org Chem* **72:** 9914–9923

Dellabona P, Padovan E, Casorati G, Brockhaus M, Lanzavecchia A (1994) An invariant V alpha 24–JalphaQ/Vbeta 11 T cell receptor is expressed in all individuals by clonally expanded CD4-8− T cells. *J Exp Med* **180:** 1171–1176

Fischer K, Scotet E, Niemeyer M, Koebernick H, Zerrahn J, Maillet S, Hurwitz R, Kursar M, Bonneville M, Kaufmann SH, Schaible UE (2004) Mycobacterial phosphatidylinositol mannoside is a natural antigen for CD1d-restricted T cells. *Proc Natl Acad Sci USA* **101:** 10685–10690

Gadola SD, Koch M, Marles-Wright J, Lissin NM, Shepherd D, Matulis G, Harlos K, Villiger PM, Stuart DI, Jakobsen BK, Cerundolo V, Jones EY (2006) Structure and binding kinetics of three different human CD1d–alpha-galactosylceramide-specific T cell receptors. *J Exp Med* **203:** 699–710

Giabbai B, Sidobre S, Crispin MD, Sanchez-Ruiz Y, Bachi A, Kronenberg M, Wilson IA, Degano M (2005) Crystal structure of mouse CD1d bound to the self ligand phosphatidylcholine: a molecular basis for NKT cell activation. *J Immunol* **175:** 977–984

Gui M, Li J, Wen LJ, Hardy RR, Hayakawa K (2001) TCR beta chain influences but does not solely control autoreactivity of Vα14Jα281T cells. *J Immunol* **167:** 6239–6246

Gumperz JE, Roy C, Makowska A, Lum D, Sugita M, Podrebarac T, Koezuka Y, Porcelli SA, Cardell S, Brenner MB, Behar SM (2000) Murine CD1d-restricted T cell recognition of cellular lipids. *Immunity* **12:** 211–221

Kawano T, Cui J, Koezuka Y, Toura I, Kaneko Y, Motoki K, Ueno H, Nakagawa R, Sato H, Kondo E, Koseki H, Taniguchi M (1997) CD1d-restricted and TCR-mediated activation of Valpha14 NKT cells by glycosylceramides. *Science* **278:** 1626–1629

Kinjo Y, Tupin E, Wu D, Fujio M, Garcia-Navarro R, Benhnia MR, Zajonc DM, Ben-Menachem G, Ainge GD, Painter GF, Khurana A, Hoebe K, Behar SM, Beutler B, Wilson IA, Tsuji M, Sellati TJ, Wong CH, Kronenberg M (2006) Natural killer T cells recognize diacylglycerol antigens from pathogenic bacteria. *Nat Immunol* **7:** 978–986

Kinjo Y, Wu D, Kim G, Xing GW, Poles MA, Ho DD, Tsuji M, Kawahara K, Wong CH, Kronenberg M (2005) Recognition of bacterial glycosphingolipids by natural killer T cells. *Nature* **434:** 520–525

Kjer-Nielsen L, Borg NA, Pellicci DG, Beddoe T, Kostenko L, Clements CS, Williamson NA, Smyth MJ, Besra GS, Reid HH, Bharadwaj M, Godfrey DI, Rossjohn J, McCluskey J (2006) A structural basis for selection and cross-species reactivity of the semi-invariant NKT cell receptor in CD1d/glycolipid recognition. *J Exp Med* **203:** 661–673

Koch M, Stronge VS, Shepherd D, Gadola SD, Mathew B, Ritter G, Fersht AR, Besra GS, Schmidt RR, Jones EY, Cerundolo V (2005) The crystal structure of human CD1d with and without alpha-galactosylceramide. *Nat Immunol* **6:** 819–826

Koseki H, Imai K, Nakayama F, Sado T, Moriwaki K, Taniguchi M (1990) Homogenous junctional sequence of the V14+ T-cell antigen receptor alpha chain expanded in unprimed mice. *Proc Natl Acad Sci USA* **87:** 5248–5252

Lantz O, Bendelac A (1994) An invariant T cell receptor alpha chain is used by a unique subset of major histocompatibility complex class I-specific CD4+ and CD4-8− T cells in mice and humans. *J Exp Med* **180:** 1097–1106

Mallevaey T, Scott-Browne JP, Matsuda JL, Young MH, Pellicci DG, Patel O, Thakur M, Kjer-Nielsen L, Richardson SK, Cerundolo V, Howell AR, McCluskey J, Godfrey DI, Rossjohn J, Marrack P, Gapin L (2009) T cell receptor CDR2β and CDR3β loops collaborate functionally to shape the iNKT cell repertoire. *Immunity* **31:** 60–71

Mattner J, Debord KL, Ismail N, Goff RD, Cantu III C, Zhou D, Saint-Mezard P, Wang V, Gao Y, Yin N, Hoebe K, Schneewind O, Walker D, Beutler B, Teyton L, Savage PB, Bendelac A (2005) Exogenous and endogenous glycolipid antigens activate NKT cells during microbial infections. *Nature* **434:** 525–529

Ortaldo JR, Young HA, Winkler-Pickett RT, Bere Jr EW, Murphy WJ, Wiltrout RH (2004) Dissociation of NKT stimulation, cytokine induction, and NK activation *in vivo* by the use of distinct TCR-binding ceramides. *J Immunol* **172:** 943–953

Parekh VV, Singh AK, Wilson MT, Olivares-Villagomez D, Bezbradica JS, Inazawa H, Ehara H, Sakai T, Serizawa I, Wu L, Wang CR, Joyce S, Van Kaer L (2004) Quantitative and qualitative differences in the *in vivo* response of NKT cells to distinct alpha- and beta-anomeric glycolipids. *J Immunol* **173:** 3693–3706

Pellicci DG, Patel O, Kjer-Nielsen L, Pang SS, Sullivan LC, Kyparissoudis K, Brooks AG, Reid HH, Gras S, Lucet I, Koh R, Smyth MJ, Mallevaey T, Matsuda JL, Gapin L, McCluskey J, Godfrey DI, Rossjohn J (2009) Differential recognition of CD1d–α-galactosyl ceramide by the Vβ8.2 and Vβ7 semi-invariant NKT T-cell receptors. *Immunity* **31:** 47–59

Porcelli S, Yockey CE, Brenner MB, Balk SP (1993) Analysis of T cell antigen receptor (TCR) expression by human peripheral blood CD4-8− alpha/beta T cells demonstrates preferential use of several V beta genes and an invariant TCR alpha chain. *J Exp Med* **178:** 1–16

Rauch J, Gumperz J, Robinson C, Skold M, Roy C, Young DC, Lafleur M, Moody DB, Brenner MB, Costello CE, Behar SM (2003) Structural features of the acyl chain determine self-phospholipid antigen recognition by a CD1d-restricted invariant NKT (iNKT) cell. *J Biol Chem* **278:** 47508–47515

Rudolph MG, Stanfield RL, Wilson IA (2006) How TCRs bind MHCs, peptides, and coreceptors. *Annu Rev Immunol* **24:** 419–466

Scott-Browne JP, Matsuda JL, Mallevaey T, White J, Borg NA, McCluskey J, Rossjohn J, Kappler J, Marrack P, Gapin L (2007) Germline-encoded recognition of diverse glycolipids by natural killer T cells. *Nat Immunol* **8:** 1105–1113

Sriram V, Du W, Gervay-Hague J, Brutkiewicz RR (2005) Cell wall glycosphingolipids of *Sphingomonas paucimobilis* are CD1d-specific ligands for NKT cells. *Eur J Immunol* **35:** 1692–1701

Tynan FE, Reid HH, Kjer-Nielsen L, Miles JJ, Wilce MC, Kostenko L, Borg NA, Williamson NA, Beddoe T, Purcell AW, Burrows SR, McCluskey J, Rossjohn J (2007) A T cell receptor flattens a bulged antigenic peptide presented by a major histocompatibility complex class I molecule. *Nat Immunol* **8:** 268–276

Van Kaer L (2005) Alpha-galactosylceramide therapy for autoimmune diseases: prospects and obstacles. *Nat Rev Immunol* **5:** 31–42

Wu DY, Segal NH, Sidobre S, Kronenberg M, Chapman PB (2003) Cross-presentation of disialoganglioside GD3 to natural killer T cells. *J Exp Med* **198:** 173–181

Wun KS, Borg NA, Kjer-Nielsen L, Beddoe T, Koh R, Richardson SK, Thakur M, Howell AR, Scott-Browne JP, Gapin L, Godfrey DI, McCluskey J, Rossjohn J (2008) A minimal binding footprint on CD1d-glycolipid is a basis for selection of the unique human NKT TCR. *J Exp Med* **205:** 939–949

Xia C, Zhang W, Zhang Y, Chen W, Nadas J, Woodward R, Wang B, Wang X, Kronenberg M, Wang PG (2009) Roles of 3′ and 4′ hydroxyls in α-galactosylceramide stimulation of invariant natural killer T cells. *Chem Med Chem* (doi:10.1002/cmdc.200900350)

Zajonc DM, Ainge GD, Painter GF, Severn WB, Wilson IA (2006) Structural characterization of mycobacterial phosphatidylinositol mannoside binding to mouse CD1d. *J Immunol* **177:** 4577–4583

Zajonc DM, Cantu III C, Mattner J, Zhou D, Savage PB, Bendelac A, Wilson IA, Teyton L (2005) Structure and function of a potent agonist for the semi-invariant natural killer T cell receptor. *Nat Immunol* **6:** 810–818

Zajonc DM, Savage PB, Bendelac A, Wilson IA, Teyton L (2008) Crystal structures of mouse CD1d-iGb3 complex and its cognate Valpha14 T cell receptor suggest a model for dual recognition of foreign and self glycolipids. *J Mol Biol* **377:** 1104–1116

Zhou D, Mattner J, Cantu III C, Schrantz N, Yin N, Gao Y, Sagiv Y, Hudspeth K, Wu YP, Yamashita T, Teneberg S, Wang D, Proia RL, Levery SB, Savage PB, Teyton L, Bendelac A (2004) Lysosomal glycosphingolipid recognition by NKT cells. *Science* **306:** 1786–1789

Cell Host & Microbe
Article

A *Staphylococcus aureus* Regulatory System that Responds to Host Heme and Modulates Virulence

Victor J. Torres,[1] Devin L. Stauff,[1] Gleb Pishchany,[1] Jelena S. Bezbradica,[1] Laura E. Gordy,[1] Juan Iturregui,[2] Kelsi L. Anderson,[3] Paul M. Dunman,[3] Sebastian Joyce,[1] and Eric P. Skaar[1,*]
[1] Department of Microbiology and Immunology
[2] Department of Pathology
Vanderbilt University Medical Center, Nashville, TN 37232, USA
[3] Department of Pathology and Microbiology
University of Nebraska Medical Center, Omaha, NE 68198-6495, USA
*Correspondence: eric.skaar@vanderbilt.edu
DOI 10.1016/j.chom.2007.03.001

SUMMARY

Staphylococcus aureus, a bacterium responsible for tremendous morbidity and mortality, exists as a harmless commensal in approximately 25% of humans. Identifying the molecular machinery activated upon infection is central to understanding staphylococcal pathogenesis. We describe the *h*eme *s*ensor system (HssRS) that responds to heme exposure and activates expression of the *h*eme-*r*egulated *t*ransporter (HrtAB). Inactivation of the Hss or Hrt systems leads to increased virulence in a vertebrate infection model, a phenotype that is associated with an inhibited innate immune response. We suggest that the coordinated activity of Hss and Hrt allows *S. aureus* to sense internal host tissues, resulting in tempered virulence to avoid excessive host tissue damage. Further, genomic analyses have identified orthologous Hss and Hrt systems in *Bacillus anthracis*, *Listeria monocytogenes*, and *Enterococcus faecalis*, suggesting a conserved regulatory system by which Gram-positive pathogens sense heme as a molecular marker of internal host tissue and modulate virulence.

INTRODUCTION

Staphylococcus aureus is one of the most significant infectious threats to global public health (Fridkin et al., 2005). Infections with *S. aureus* result in diverse human diseases ranging from skin and soft tissue infections to endocarditis, septicemia, and toxic shock syndrome (Brook, 2002; Fowler et al., 2005). Paradoxically, 25% of the human population is harmlessly colonized by *S. aureus* residing as normal flora of the skin and anterior nares (Wertheim et al., 2004). In order for *S. aureus* to initiate invasive infection, it must gain access to internal tissues or vasculature of its host. Once inside the host, *S. aureus* likely undergoes a shift in gene expression resulting in the controlled production of virulence determinants that facilitate infection. Although virulence gene regulation is one of the most well-studied aspects of staphylococcal pathogenesis (Bronner et al., 2004), the environmental cues and corresponding staphylococcal regulatory systems that are active during invasive infection have not been defined.

S. aureus pathogenesis is dependent on the secretion of an array of virulence factors and the surface exposure of multiple cell-wall-anchored proteins (Foster, 2005). The expression of these effectors in vivo is presumably coordinated by a network of two-component systems (TCS) and transcriptional regulators. Although the contributions of a subset of TCS (*agr*, *saeRS*, *srrAB*, *arlSR*, and *lytRS*) to virulence gene expression have been studied extensively (Bronner et al., 2004; Cheung et al., 2004; Novick, 2003), genomic analyses reveal that the majority of staphylococcal TCS remain unassigned. In this regard, environmental cues such as high salt, cell density, glucose, energy availability, pH, and subinhibitory antibiotics have been found to affect *S. aureus* virulence gene expression in laboratory conditions (Bronner et al., 2004; Cheung et al., 2004; Novick, 2003). However, the specific host molecules recognized by staphylococcal regulatory systems remain elusive. Decoding the signals sensed by *S. aureus* inside the host will set the stage to identify the molecular machinery that is activated during invasive infection.

One of the most significant obstacles that bacterial pathogens encounter when infecting vertebrates is iron limitation. Iron is an essential cofactor for many biochemical processes, and thus it is required by virtually all pathogenic bacteria to establish infection. The majority of vertebrate iron is in the form of the metalloporphyrin heme, the functional cofactor of hemoglobin and myoglobin, the oxygen transport and storage proteins of blood and muscle, respectively (Deiss, 1983). *S. aureus* acquire heme through the elaboration of transport systems that rapidly transport host-derived heme into the staphylococcal cytoplasm for use as a nutrient source (Mazmanian et al., 2003; Skaar et al., 2004; Torres et al., 2006; Vermeiren et al., 2006). Staphylococci likely facilitate this process through the hemolysin-mediated rupture of erythrocytes

upon entry into the blood stream (Bernheimer et al., 1968; Skaar and Schneewind, 2004).

Although heme is a valuable nutrient source to invading pathogens, the intracellular accumulation of heme is toxic due to the molecule's reactivity. Therefore, organisms that acquire exogenous heme to satisfy nutrient iron needs must have adaptable mechanisms to avoid surplus heme accumulation. In this regard, we have recently reported the identification of a subset of staphylococcal proteins that are affected by changes in environmental hemin (the oxidized form of heme) concentration (Friedman et al., 2006). In particular, exposure to exogenous hemin results in the 45-fold upregulation of the heme-regulated transporter HrtAB (Friedman et al., 2006). The dramatic upregulation of HrtAB upon exposure to hemin suggests that *S. aureus* possess systems capable of sensing heme and subsequently altering protein expression. The association of heme with the major protein constituents of blood and muscle establishes heme as a molecular marker that can potentially be exploited by infecting bacteria to distinguish internal host tissue from surface colonization sites. Hence, heme-sensing systems may represent a mechanism by which bacterial pathogens sense when the surface tissues of the host have been breached.

In this study, we identified a *S. aureus* TCS that we have called the *h*eme *s*ensor *s*ystem (HssRS). HssRS responds to heme exposure and activates the expression of HrtAB, an efflux pump that plays a pivotal role in intracellular heme homeostasis. Inactivation of the Hss or Hrt systems results in enhanced liver-specific *S. aureus* virulence, which correlates with a reduced innate immune response to infection. Staphylococcal strains unable to sense and excrete surplus heme exhibit increased virulence factor expression and secretion, providing a mechanistic explanation for the observed immunomodulation. Importantly, Hss and Hrt systems are present in *Bacillus anthracis*, *Listeria monocytogenes*, *Staphylococcus epidermidis*, and *Enterococcus faecalis*, suggesting a conserved mechanism by which these important human pathogens sense their vertebrate hosts to modulate virulence.

RESULTS

Staphylococcus aureus Adapt to Avoid Heme Toxicity

Heme-iron acquisition is vital to staphylococcal pathogenesis (Skaar et al., 2004; Torres et al., 2006). However, the value of heme as an iron source must be balanced against its toxicity at high concentrations (Everse and Hsia, 1997). In this regard, we found that *S. aureus* growth is slightly inhibited when bacteria are cultured in iron-replete medium supplemented with 5 μM hemin (Figure 1A). Exposure to concentrations of hemin at or above 10 μM severely inhibited staphylococcal growth in these same culture conditions (Figure 1A), highlighting the acute sensitivity of *S. aureus* to excess hemin.

The initial interaction between staphylococci and host heme sources is mediated by bacterial receptors that are covalently anchored to the cell wall by the action of

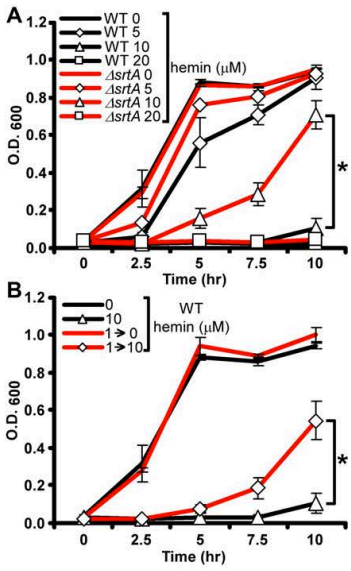

Figure 1. *S. aureus* Adapt to Avoid the Toxic Effects of Hemin

(A) *S. aureus* wild-type and *ΔsrtA* were grown overnight in TSB and then subcultured into TSB supplemented with 0, 5, 10, or 20 μM hemin. Growth rates were determined by measuring the absorbance ($O.D._{600}$) at the indicated time points.

(B) *S. aureus* wild-type was grown overnight in TSB supplemented with 0 or 1 μM hemin (1→) and then subcultured into TSB supplemented with 0 or 10 μM hemin (→0 or →10). The results represent the mean ± SD from triplicate experiments. Asterisks denote statistically significant differences as determined by Student's t test ($p \leq 0.05$).

the transpeptidase sortase A (SrtA) (Mazmanian et al., 2003; Torres et al., 2006; Vermeiren et al., 2006). To investigate the contribution of staphylococcal heme and hemoglobin receptors to heme toxicity, we compared wild-type *S. aureus* and a mutant lacking *srtA* (*ΔsrtA*) for their sensitivity to hemin toxicity. Growth curve analyses demonstrate that *ΔsrtA* proliferates in medium containing up to 10 μM hemin (Figure 1A), presumably due to the absence of surface linked heme receptors leading to a decreased ability to internalize free hemin. These data show that hemin-mediated growth inhibition is reliant on the same SrtA-dependent pathways required for the utilization of heme as a nutrient source.

S. aureus heme acquisition is a highly efficient process that results in the rapid cytoplasmic accumulation of heme (Mazmanian et al., 2000; Skaar et al., 2004). The strict requirement for heme uptake systems in staphylococcal virulence (Skaar et al., 2004; Torres et al., 2006) implies that *S. aureus* contain adaptable mechanisms that exploit heme as a nutrient iron source while avoiding heme-mediated toxicity. To explore this adaptation mechanism in more detail, we investigated whether pre-exposing *S. aureus* to subinhibitory concentrations of hemin increases

hemin tolerance. Staphylococcal cultures grown in sub-inhibitory hemin concentrations (1 μM) exhibited a pronounced resistance to hemin toxicity when subcultured at concentrations up to 10 μM (Figure 1B). These findings demonstrate that *S. aureus* undergo an adaptive response to exogenous hemin resulting in increased resistance to hemin toxicity.

S. aureus Adaptation to Hemin Toxicity Is Dependent on HrtAB

The ability of *S. aureus* to adapt to hemin toxicity is likely the result of coordinated changes in protein expression that occur upon hemin exposure. In this regard, we have recently identified the heme-regulated transport system (HrtAB), which increases expression by approximately 45-fold upon exposure to hemin (Friedman et al., 2006). HrtAB is composed of an ATP-binding protein (HrtA) and permease (HrtB) making up a canonical ABC-type transporter system. Genomic analyses suggest that HrtAB is a member of the MacAB family of ABC-type efflux carriers, which have been implicated in the export of small molecules (Kobayashi et al., 2001). Based on these facts, we predicted that HrtAB contributes to *S. aureus* avoidance of hemin toxicity by exporting surplus hemin from the bacterial cytoplasm. To facilitate experiments aimed at testing this prediction, we created a *S. aureus* strain in which *hrtA* was deleted (*ΔhrtA*). *S. aureus* wild-type and *ΔhrtA* proliferated at comparable rates in hemin-free medium; however, the *ΔhrtA* strain was significantly more susceptible to hemin toxicity (Figures 2A and 2B). The ability of staphylococci to adapt and avoid hemin toxicity was fully dependent on the presence of a functional HrtAB system (Figure 2C). The increased sensitivity to hemin toxicity exhibited by *ΔhrtA* was restored by providing a wild-type copy of the *hrtA* gene in *trans* (Figure 2D). These findings are in accordance with a model whereby *S. aureus* sense heme, resulting in the elaboration of a transport system (HrtAB) dedicated to the excretion of surplus heme to protect against toxicity.

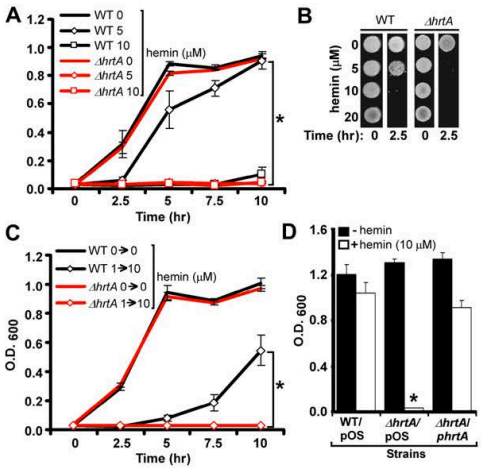

Figure 2. The HrtAB System Is Required for Staphylococcal Heme Adaptation

(A) *S. aureus* wild-type and *ΔhrtA* were grown overnight in TSB and then subcultured into TSB supplemented with 0, 5, or 10 μM hemin. Growth rates were determined by measuring the absorbance (O.D. $_{600}$) at the indicated time points.

(B) *S. aureus* wild-type and *ΔhrtA* were grown overnight in TSB and then subcultured for 2.5 hr into TSB supplemented with 0, 5, 10 or 20 μM hemin. The cultures were then serially diluted and plated on TSA plates.

(C) *S. aureus* wild-type and *ΔhrtA* were grown overnight in TSB and TSB supplemented with 1 μM hemin (1→) and then subcultured into TSB supplemented with 0 or 10 μM hemin (→0 or →10). Growth rates were determined by measuring the absorbance (O.D. $_{600}$) at the indicated time points (hr).

(D) *S. aureus* wild-type and *ΔhrtA* transformed with vector alone (WT/pOS and ΔhrtA/pOS) and *ΔhrtA* transformed with vector containing a wild-type copy of *hrtA* (*ΔhrtA/phrtA*) were grown in TSB supplemented with 1 μM hemin and then subcultured into TSB that either lacked hemin or contained 10 μM hemin and grown for 15 hr. The results represent the mean ± SD from triplicate experiments. Asterisks denote statistically significant differences as determined by Student's t test ($p \leq 0.05$).

HssRS Regulates *hrtAB* Expression

Examination of the genomic context immediately adjacent to the *hrtAB* locus revealed the presence of two genes predicted to encode for a TCS (Figure 3A). This TCS designation is based on BLAST analyses, which revealed that the closest annotated matches to these genes are the response regulator *ompR* (e value 6×10^{-55}) and histidine kinase *baeS* (e value 8×10^{-32}) of *Escherichia coli* (Nagasawa et al., 1993; Taylor et al., 1981). TCS sense environmental stimuli and regulate gene expression (Beier and Gross, 2006). On the basis of studies described below, we have named this newly identified TCS the *h*eme *s*ensor *s*ystem *r*egulator and *s*ensor (HssRS) (HssR-response regulator, HssS-histidine kinase). The predicted protein product of HssS contains two transmembrane regions flanking an extracytoplasmic ligand-sensing domain. The cytoplasmic portion of HssS is predicted to be comprised of a HisKA dimerization/phosphoacceptor region linked to an ATPase domain (Figure S1A in the Supplemental Data available with this article online). BLAST analyses of full-length HssS as well as the predicted sensor domain demonstrate that the protein is conserved across many Gram-positive bacteria; however, this sensing domain is distinct from all previously described ligand-binding domains of histidine kinases (Figure S1B). To evaluate the possibility that the heme-dependent expression of *hrtAB* is mediated by HssRS, we generated isogenic mutant strains in which either *hssR* or *hssS* was deleted (*ΔhssR*, *ΔhssS*). Growth curve analyses indicated that both HssR and HssS are required for *S. aureus* adaptation to heme toxicity (Figure 3B), a phenotype that was complemented by introducing a wild-type copy of *hssR* in *trans* into *ΔhssR* (Figure 3C). These data demonstrate that both HrtAB and HssRS are vital to staphylococcal heme adaptation.

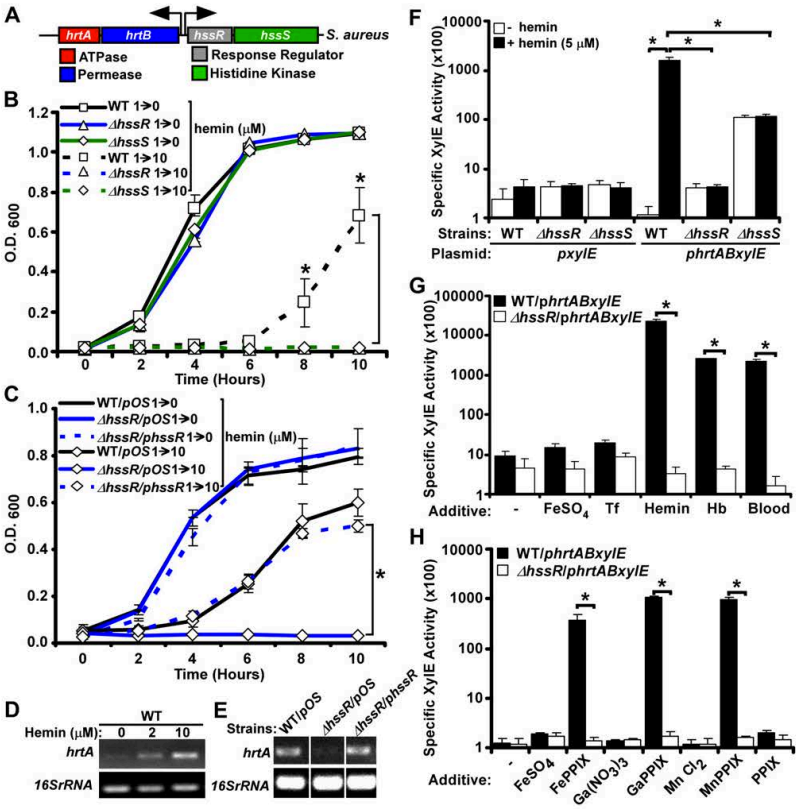

Figure 3. HssRS Is Required for *hrtA* Expression upon Exposure to Hemin

(A) Schematic representation of the *hrtAB* and *hssRS* loci in *S. aureus*.

(B and C) Listed staphylococcal strains were grown overnight in TSB supplemented with 1 μM heme (1→) and then subcultured into TSB supplemented with 0 or 10 μM heme (→0 or →10). Growth rates were determined by measuring the absorbance ($O.D._{600}$) at the indicated time points (hr).

(D and E) RT-PCR analyses. (D) Total RNA was extracted from overnight cultures of *S. aureus* wild-type grown in TSB supplemented with 0, 2, or 10 μM hemin. cDNA was synthesized as described in the Experimental Procedures, and transcription of the *hrtA* gene and the 16sRNA (loading control) was assessed by PCR. (E) Total RNA was extracted from overnight cultures of wild-type (WT/pOS), Δ*hssR*/pOS, and the complemented Δ*hssR* strain (Δ*hssR*/p*hssR*) grown in TSB supplemented with 2 μM hemin. The cDNA was synthesized as described above, and transcription of the *hrtA* gene and the 16sRNA (loading control) was determined as in (D). Differences in the relative level of RT-PCR product between (D) and (E) are likely a result of the required inclusion of chloramphenicol to the growth media in experiments shown in (E).

(F–H) XylE fusion reporter assay. (F) WT, Δ*hssR*, and Δ*hssS* transformed with the p*hrtABxylE* or the p*xylE* plasmid were grown 2 hr in TSB supplemented with 0 or 5 μM hemin, and XylE activity was determined as described in the Experimental Procedures. (G) Wild-type and Δ*hssR* harboring the p*hrtABxylE* reporter plasmid were grown 2 hr in TSB supplemented with $FeSO_4$ (8 μM), transferrin (Tf; 8 μM), hemin (8 μM), hemoglobin (Hb; 2 μM), or mouse blood, and XlyE activity was determined as in (F). (H) Wild-type and Δ*hssR* harboring the p*hrtABxylE* reporter plasmid were grown 2 hr in TSB supplemented with 1 μM of the indicated additives, and the XylE activity was determined as in (F). The results represent the mean ± SD from at least triplicate experiments. Asterisks denote statistically significant differences as determined by Student's t test ($p < 0.05$).

In wild-type staphylococci, *hrtA* expression is induced by exogenous hemin (Figure 3D). This heme-dependent increase in expression is presumably responsible for the ability of wild-type staphylococci to grow in 10 μM hemin after a prolonged overnight incubation (data not shown). Considering the critical role HssRS plays in staphylococcal heme adaptation, we investigated whether HssRS is responsible for the heme-dependent upregulation of *hrtA* transcript. We were unable to detect *hrtA* transcript in Δ*hssR* upon hemin exposure, a defect that was complemented by providing a wild-type copy of *hssR* in *trans* (Figure 3E). To confirm these data, we generated a reporter construct in which the predicted *hrtAB* promoter was fused to a *xylE* reporter gene (Chien et al., 1999). Wild-type and Δ*hssR* displayed background levels of reporter activity when the strains were grown in the absence of

hemin (Figure 3F). In contrast, *ΔhssS* exhibited appreciable *hrtAB* expression in the absence of inducer. This result is consistent with the idea that, as with many histidine kinases, HssS is responsible for maintaining its cognate response regulator (HssR) in an unphosphorylated state in the absence of inducer (Mascher et al., 2006). When the strains harboring the *phrtABxylE* reporter were grown in media containing hemin, only the wild-type strain displayed a heme-dependent increase in reporter activity (Figure 3F). These data establish an absolute requirement for both HssR and HssS in the heme-dependent upregulation of *hrtAB*. Notably, synthesis of endogenous heme by *S. aureus* is not sufficient for activation of *hrtAB* (Figure 3F), providing evidence that HssRS is triggered by exposure to exogenous heme.

In vertebrates, heme is predominantly bound to hemoglobin within erythrocytes. In this regard, hemoglobin exposure potently activates *hrtAB* expression (Figure 3G). Importantly, HssRS-dependent induction of *hrtAB* also occurs when staphylococci are exposed to blood (Figure 3G). Strains grown in medium supplemented with excess iron sulfate or the iron-sequestering protein transferrin did not activate reporter expression, eliminating a role for iron in *hrtAB* activation (Figure 3G). Together, these results suggest that HssRS responds to heme as a component of vertebrate blood, resulting in the induction of *hrtAB* expression.

It is possible that HssRS senses heme through direct binding to HssS. Alternatively, HssRS may sense cellular stress mediated by excess heme exposure. Analyses of available genomic and proteomic screens of staphylococcal regulatory circuits that respond to environmental cues reveals that *hrtAB* is not induced upon iron starvation (Friedman et al., 2006), exposure to mild acid (Weinrick et al., 2004), or treatment with nitric oxide (Richardson et al., 2006). In addition, *hrtA* expression is not affected by cold shock, heat shock, the stringent response, or activation of the SOS response (Anderson et al., 2006). Moreover, *hrtAB* expression is not regulated by the global regulators of staphylococcal virulence MgrA (Luong et al., 2006), SigB, Agr, or SarA (Bischoff et al., 2004; Dunman et al., 2001). Proteins that directly complex heme typically recognize the encircled metal atom of the metalloporphyrin through coordination with an axial ligand. To test if *S. aureus* requires metal complexed porphyrins for HssRS-dependent *hrtAB* expression, we exposed staphylococci to a variety of protoporphyrin IX (PPIX) analogs. These emerging data revealed that HssRS upregulates *hrtAB* expression upon exposure to Fe-PPIX (heme), Ga-PPIX, and Mn-PPIX. In contrast, exposure of *S. aureus* to metal-free PPIX does not result in activation of *hrtAB*. Furthermore, exposure of *S. aureus* to excess $FeSO_4$, $Ga(NO_3)_3$, or $MnCl_2$ does not result in *hrtAB* activation (Figure 3H). We conclude that metal-coordinated porphyrins are required for HssRS-dependent *hrtAB* activation and that HssRS does not indirectly recognize cellular stress associated with excess metal or porphyrin exposure. Moreover, although we cannot rule out the possibility that an as yet unidentified factor is transferring a signal from heme to HssRS, these data strongly support the model that HssRS senses heme to activate *hrtA* expression.

Inactivation of *hssRS* or *hrtAB* Increases Staphylococcal Virulence

To test the role of HssRS heme sensing and concomitant HrtAB expression in *S. aureus* pathogenesis, mice were infected intravenously with *S. aureus* wild-type, *ΔhrtA*, or *ΔhssR*. Animals infected with wild-type *S. aureus* exhibited overt signs of disease characteristic of staphylococcal infection. Surprisingly, all animals infected with *S. aureus ΔhrtA* or *ΔhssR* appeared more moribund than those infected with wild-type, as evidenced by a complete absence of mobility, a pronounced hunched posture, and extensive tremors. Autopsies conducted 96 hr postinfection revealed abscess formation in the kidneys of mice infected with any of the three staphylococcal strains (data not shown). In contrast, only mice infected with *S. aureus ΔhrtA* or *ΔhssR* developed abscesses in the liver (Figure 4). Enumeration of bacterial loads in the livers of infected animals revealed a 2 to 3 log increase in the number of mutant staphylococci as compared with wild-type (Figure 4B). This increase in virulence was liver specific, since no difference was detected in the ability of the mutant strains to colonize the spleen or kidney compared to wild-type (Figure 4B). The increased liver-specific hypervirulence of *S. aureus ΔhrtA* and *ΔhssR* is not due to intrinsically faster growth rates, because mutant strains exhibit similar growth kinetics to wild-type in laboratory growth conditions (Figures 2 and 3). Histological examination of livers infected with the mutant staphylococci revealed that hepatic hypervirulence occurs despite the recruitment of polymorphonuclear (PMN) cells (Figure 4D). More specifically, the *ΔhrtA* or *ΔhssR*-induced abscesses were characterized by collections of purulent material containing PMNs, injured hepatocytes, and dense fibrous tissue (Figure 4D). Together, these findings demonstrate that *S. aureus* strains lacking HssRS or HrtAB exhibit increased hepatic virulence.

The Liver-Specific Immune Response Is Inhibited against Staphylococci Inactivated for *hssRS* or *hrtAB*

The hepatic hypervirulence exhibited by *S. aureus ΔhrtA* or *ΔhssR* could be the consequence of (1) a defective immune response to mutant staphylococci, (2) an increase in the expression of staphylococcal virulence factors, (3) enhanced bacterial resistance to immune clearance, or (4) increased tissue tropism of *S. aureus ΔhssR* and *ΔhrtA*. To begin distinguishing between these possibilities, we characterized the immune cell profiles in organs from mice infected with *S. aureus* wild-type, *ΔhrtA*, or *ΔhssR* via multiparametric flow cytometric analyses. We did not detect changes in the adaptive immune response to these strains, as measured by equivalent numbers of resident or infiltrating B cells, $CD4^+$ T cells, or $CD8^+$ T cells between tissues from infected or uninfected mice (data not shown).

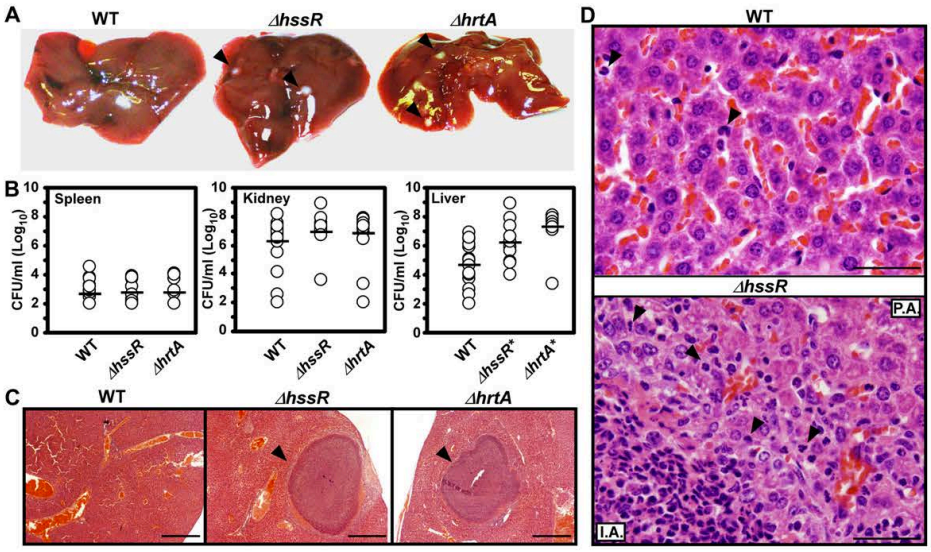

Figure 4. *S. aureus ΔhssR* and *ΔhrtA* Exhibit Liver-Specific Hypervirulence

(A) Photographs of livers dissected from BALB/c mice infected with wild-type and *ΔhssR* or *ΔhrtA* (1×10^6 CFUs for all strains) 96 hr postinfection. Arrowheads mark *ΔhssR*- and *ΔhrtA*-induced hepatic abscesses. Photographs are representative of all livers analyzed. Abscesses were visible in virtually all livers from *ΔhssR*- and *ΔhrtA*-infected mice, while none were found in wild-type-infected mice.

(B) *S. aureus* multiplication in infected mouse organs as measured by tissue homogenization, dilution, and colony formation on agar media 96 hr postinfection. Each symbol represents data from one infected animal. The limit of detection in these experiments is 100 CFUs. The horizontal line denotes the mean of the log, and the asterisks denote statistically significant differences from wild-type as determined by Student's t test ($p \leq 0.05$).

(C) Representative hematoxylin and eosin (H&E) staining of liver sections infected with WT, *ΔhrtA*, or *ΔhssR* strains at 40× magnification. Arrowheads mark *ΔhssR*- and *ΔhrtA*-induced hepatic abscesses.

(D) Representative H&E staining of liver sections infected with WT or *ΔhssR* strains at 1,000× magnification. Arrowheads mark PMNs in the tissues. P.A, proximal to the abscess; I.A, inside the abscess.

The organ-specific innate immune response to staphylococcal infection is not well defined. Therefore, we initially analyzed the innate immune cell populations in infected versus uninfected tissues. We found increased numbers of phagocytes ($CD11b^+/CD11c$) in the spleens of infected animals relative to uninfected controls (Figure 5A). We did not detect significant infiltration of dendritic cells, natural killer (NK) cells, or invariant-natural killer T (iNKT) cells into this organ (Figures 5B–5D). In contrast, we were able to detect infiltration of NK cells, iNKT cells, phagocytes, and granulocytes into the kidneys and livers of infected animals (Figures 5A–5D), organs containing a higher bacterial load than the spleen (Figure 4B). Importantly, the NK and iNKT cells detected in the livers and kidneys expressed activation markers (i.e., CD69), suggesting that these lymphocytes were activated and proliferated in response to staphylococcal infection (data not shown). Together, these results imply that differences in bacterial loads across organs influence the degree to which innate immune cells are recruited and activated in staphylococcal infected tissue.

Comparison of the immune cell profiles in the spleens and kidneys of animals infected with wild-type, *ΔhrtA*, or *ΔhssR* staphylococci revealed minimal differences, with the exception of NK cells (Figures 5A–5D). Indeed, there was a significant increase in the number of NK cells detected in the kidneys of wild-type-infected animals compared to those infected with *ΔhrtA* or *ΔhssR* (Figure 5D). Although this finding was interesting, we did not investigate it further, as the effect on NK cells was specific to the kidney and therefore not likely to play a role in the observed liver hypervirulence. Importantly, livers from *ΔhrtA*- or *ΔhssR*-infected mice contained approximately half the number of $CD11b^+/CD11c$ phagocytes found in livers from mice infected with wild-type *S. aureus* (Figure 5A). More rigorous analysis at 48 hr postinfection revealed that this decreased population is comprised primarily of $CD11b^+/Ly6G^+$ granulocytes (Figures 5E and 5F). Based on our visualization of PMNs in histological preparations of abscessed livers from mice infected with Δ*hssR*, it is possible that this quantitative decrease is due to increased granulocyte death in these organs. Alternatively, the nonquantitative nature of our histological analyses (Figure 4D) does not rule out the possibility that there is a decreased recruitment of granulocytes to the livers of Δ*hssR*/Δ*hrtA*-infected mice. Thus, we conclude that

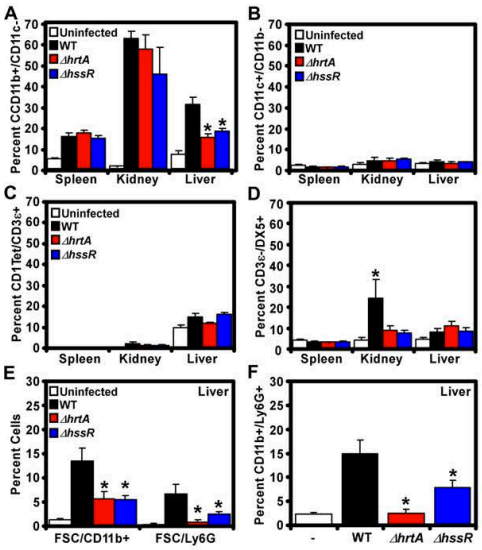

Figure 5. Infection with *S. aureus ΔhssR* or *ΔhrtA* Inhibits Innate Immune Responses

BALB/c animals were left uninfected or infected with wild-type, Δ*hssR*, or Δ*hrtA*. Four days postinfection (A–D) or two days postinfection (E–F), organs were dissected and homogenized, and the infiltration of the indicated immune cells was determined by multiparametric FACS analysis as described in the Experimental Procedures. Isolated cells were stained for the detection of phagocytes (B220 /CD11b$^+$/CD11c) (A), dendritic cells (CD11c$^+$/CD11b) (B), invariant natural killer T cells [iNKT: CD1 Tetramer (tet)$^+$/B220 /CD3ε$^+$] (C), natural killer cells (DX5$^+$/B220 /CD3ε) (D), large CD11b$^+$ and Ly6G$^+$ cells (FSC/CD11b$^+$ and FSC/Ly6G$^+$) (E), and granulocytes (B220 /CD11b$^+$/Ly6G$^+$) (F). Results represent the mean ± SE from at least three independent animals. Asterisks denote a statistically significant reduction in the detected cells compared to animals infected with the wild-type strain as determined by Student's t test ($p < 0.05$).

infection with *ΔhssR* or *ΔhrtA* inhibits the innate immune response to *S. aureus* infection.

Inactivation of HrtAB Alters Expression and Secretion of *S. aureus* Virulence Factors

The hepatic hypervirulence of *S. aureus ΔhrtA* and *ΔhssR* suggests a tip in the balance of the bacteria-phagocyte interaction to favor *S. aureus*. *S. aureus* pathogenesis is characterized by the secretion of numerous virulence factors that defend against immune cell killing (Foster, 2005). Thus, we investigated whether *ΔhrtA* differs from wild-type in its secreted protein profile following growth in medium with or without hemin. As shown in Figure 6, exposure to hemin induced changes in the abundance of multiple secreted proteins in *ΔhrtA* compared to wild-type. In contrast, the complemented *ΔhrtA* mutant strain (*ΔhrtA/phrtA*) displayed a secreted protein profile similar to the wild-type strain (Figure 6). Mass spectrometry-based identification of the proteins overrepresented in the supernatants of *ΔhrtA* grown in hemin revealed the increased expression and/or secretion of at least eight staphylococcal proteins. All proteins identified in this analysis are secreted or contain putative N-terminal secretion signals, eliminating the possibility that the integrity of the bacterial membrane is compromised upon inactivation of *hrtA*. The seven proteins found more abundantly in the supernatant of hemin-exposed *S. aureus ΔhrtA* were proteins with known roles in immunomodulation (exotoxin, exotoxin-3, -5, and -8) (Williams et al., 2000), inhibition of phagocyte recruitment (Map-w) (Chavakis et al., 2002), inhibition of opsonophagocytosis (fibrinogen-binding protein) (Foster, 2005; Lee et al., 2004), and inhibition of neutrophil activation and chemotaxis (FLIPr) (Prat et al., 2006). Transcriptional analyses demonstrated that the increased presence of the majority of these virulence factors in the supernatants of heme-exposed *ΔhrtA* is due to increased transcription of the corresponding genes (Figure 6C). Together, these data provide a potential mechanistic explanation for the decrease in phagocytes at hepatic sites of infection with *ΔhrtA* staphylococci. It is compelling to speculate that an increased expression of genes encoding for secreted proteins with known immunomodulatory functions is responsible for the hypervirulence of staphylococcal strains unable to sense and excrete surplus internalized heme.

HrtAB and HssRS Are Conserved across Gram-Positive Pathogens

Genomic analyses of the *hrt* and *hss* loci indicate that these systems are highly conserved across Gram-positive bacteria, including the important human pathogens *Staphylococcus epidermidis*, *Bacillus anthracis*, *Listeria monocytogenes*, and *Enterococcus faecalis* (Figure 7A). As an indirect measure of the functional conservation of these systems, we investigated whether *S. epidermidis* and *B. anthracis* adapt to hemin toxicity. Similar to *S. aureus*, *S. epidermidis* and *B. anthracis* adapt and avoid hemin toxicity when pre-exposed to subinhibitory concentrations of hemin (Figure S2). These functional data suggest that orthologous Hss and Hrt systems act across genera to coordinate a response to excess hemin exposure.

DISCUSSION

During commensal colonization of the skin, *S. aureus* is exposed to host tissues that are low in heme and heme-binding proteins. However, once the initial colonization sites are breached, *S. aureus* encounters elevated levels of hemoglobin-containing erythrocytes and myoglobin-containing myocytes in the vasculature and musculature, respectively. Herein we describe the identification of HssRS, a staphylococcal two-component system responsible for sensing heme as a component of these abundant host proteins and modulating virulence. One model to explain the data described in this manuscript is presented in Figure 7. Upon erythrocyte and myocyte lysis, *S. aureus* encounters high concentrations of hemoglobin and

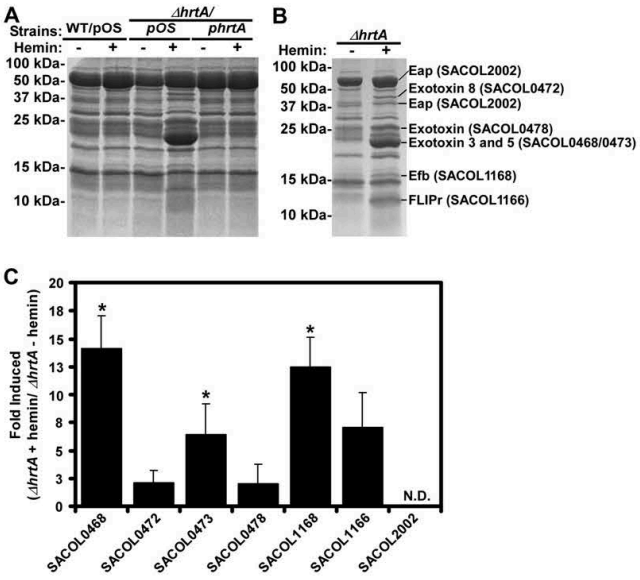

Figure 6. Inactivation of the HrtAB System Results in Increased Expression of Secreted Virulence Factors

(A) *S. aureus* wild-type (WT/pOS1), Δ*hrtA* mutant (Δ*hrtA*/pOS1), or Δ*hrtA*-complemented strain (Δ*hrtA*/*phrtA*) were grown overnight at 37°C with aeration for 15 hr in RPMI supplemented with 0 or 1 μM hemin. Culture supernatants were collected, filtered, precipitated, and separated on 15% SDS-PAGE gels. Proteins were stained with colloidal blue.

(B) Indicated proteins were excised from the gel and subjected to mass spectrometry-based identification. The identities of the proteins are indicated with corresponding gene numbers from *S. aureus* strain COL shown in parentheses.

(C) Fold induction of the indicated genes as determined by transcriptional analyses comparing changes between Δ*hrtA* grown in the presence or absence of 1 μM hemin. Transcript levels not determined due to saturating levels of expression are marked "N.D." Experiments were performed in triplicate, and asterisks denote statistical significance as determined by Student's t test ($p < 0.05$).

myoglobin at the infection site. Due to the efficiency of the staphylococcal heme uptake systems (Mazmanian et al., 2003; Skaar et al., 2004), heme is removed from these proteins and rapidly transported into the bacterial cytoplasm. Upon transport into the bacterium, heme is recognized by the HssS histidine kinase, resulting in the activation of HssR. Alternatively, HssS may indirectly sense heme through an as yet unidentified intermediary and subsequently activate HssR. Activated HssR then binds to the *hrtAB* promoter, inducing the expression of HrtAB. Heme that is not mobilized for cellular iron or porphyrin needs is excreted via HrtAB, resulting in the avoidance of heme toxicity. Our model envisions that *S. aureus* strains unable to elaborate HrtAB accumulate intracellular heme due to a block in heme excretion. In turn, the accumulation of intracellular heme activates staphylococcal stress-sensing systems responsible for increasing the transcription of genes encoding for virulence factors with potent immunomodulatory functions. In all, the coordinated activity of Hss and Hrt allow *S. aureus* to sense internal host tissues, resulting in the tempering of virulence to avoid excessive host tissue damage.

The enhanced virulence exhibited by *S. aureus* Δ*hrtA* or Δ*hssR* could be due to a combination of factors. However, the observed hypervirulence correlates with a profound decrease in viable granulocytes in the infected liver. This decrease is potentially caused by the increased expression and secretion of Map-w, fibrinogen-binding protein, FLIPr, and exotoxin-3, -5, and -8. Map-w is a staphylococcal factor that inhibits the interaction of ICAM-1 with integrins required for functional leukocyte adhesion systems, resulting in reduced phagocyte recruitment to the site of infection (Chavakis et al., 2005). Fibrinogen-binding protein binds complement factor C3 and blocks its deposition on the bacterial cell surface, thereby inhibiting opsonization (Lee et al., 2004). FLIPr inhibits the neutrophil response to formyl peptide receptor, inhibiting neutrophil activation and chemotaxis (Prat et al., 2006). Moreover, the staphylococcal exotoxins identified here belong to a family of cytotoxins with potent cytokine-modulating characteristics (Williams et al., 2000). It is possible that the combined effect of the increased secretion of these virulence factors inhibits phagocyte migration to infected livers. The liver-specific nature of the increased virulence is potentially due to the abundance of heme in this organ.

The contribution of phagocytes to the avoidance of staphylococcal infections is exemplified in humans with chronic granulomatous disease (CGD), a rare inherited immunodeficiency that results in a defective nicotinamide dinucleotide phosphate (NADPH) oxidase complex (Segal et al., 2000). Phagocytes from CGD patients are defective in the generation of an effective oxidative burst (Segal et al., 2000). Hence, patients with CGD suffer from recurrent, life-threatening infections by catalase-positive microorganisms (Segal et al., 2000). A common infectious complication experienced by CGD patients is the development of hepatic abscesses, which are most frequently caused by *S. aureus* (Lublin et al., 2002). These clinical data support our model that an impaired phagocytic response to the livers of animals infected with *S. aureus* Δ*hrtA* or Δ*hssR* is responsible for the observed hypervirulence and hepatic abscess formation reported here.

Numerous molecules that have been described as TCS activators can be found in vertebrates; however, very few of these molecules are associated specifically with internal tissues of the host. Some examples of host-specific

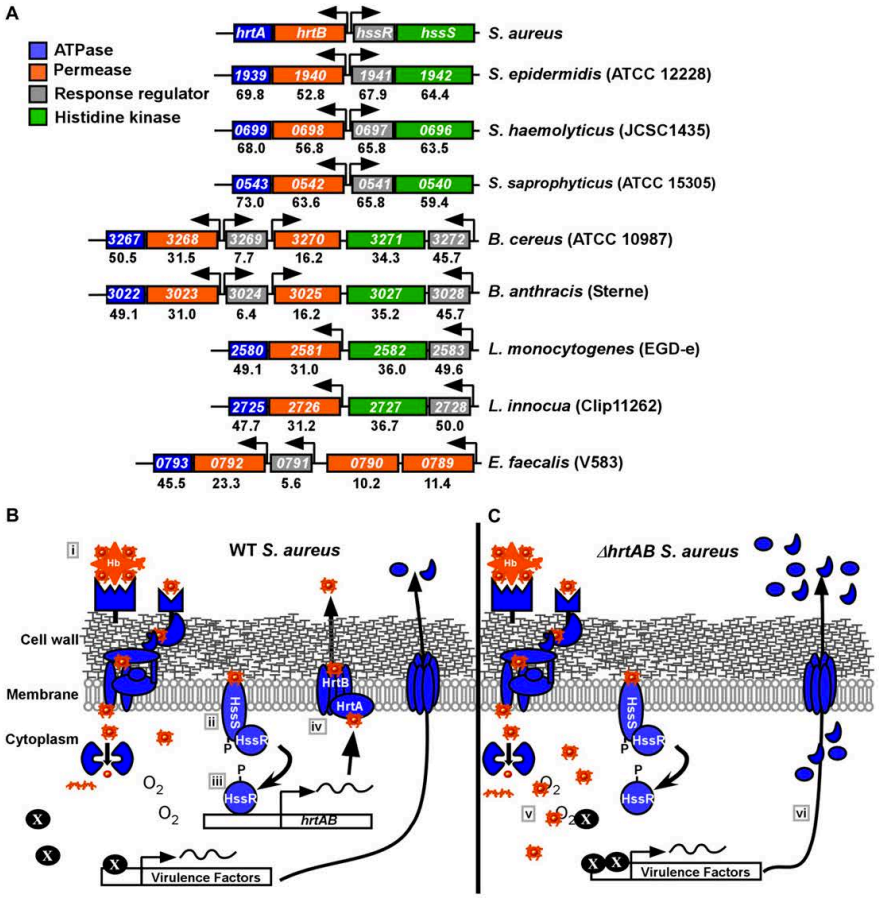

Figure 7. Model for the Role of HrtAB and HssRS in *S. aureus* Pathogenesis

(A) The Hrt and Hss systems are conserved across several Gram-positive bacteria. Alignment of genomic sequences among Gram-positive bacteria that contain orthologous *hrtAB* and *hssRS* systems. The numbers within each box represent corresponding gene numbers in the listed annotation. The numbers underneath each gene correspond to the percent amino acid identity to the representative *S. aureus* genes. Arrows denote the predicted direction of transcription.

(B) In *S. aureus*, heme internalized through cell-wall-anchored proteins (i), is sensed by HssS, which subsequently activates HssR (ii). HssR then binds the promoter region upstream of *hrtAB* (iii), leading to increased expression and elaboration of the HrtAB efflux pump (iv). HrtAB then pumps surplus cytoplasmic heme out of the bacterium.

(C) Inactivation of *hrtAB* leads to the cytoplasmic accumulation of heme, which increases cellular stress (v). Staphylococcal stress-sensing systems are activated, leading to an increase in the expression and/or secretion of virulence factors, including exotoxin-3, -5, and -8, Map-w, fibronectin-binding protein, and FLIPr (vi), which increase liver-specific hypervirulence through inhibiting immune cell recruitment.

molecules that activate TCS include antimicrobial peptides, which activate PhoPQ of *Salmonella typhimurium* (Bader et al., 2005), and epinephrine and norepinephrine, which activate QseCB of *E. coli* O157:H7 (Clarke et al., 2006). Staphylococcal regulatory systems that alter virulence gene expression may be the most well-studied area of staphylococcal pathogenesis; however, host molecules that activate these systems are not well defined. The identification and functional characterization of HssRS as a heme-sensing system fills a gap in our knowledge of the host molecule-sensing systems of *S. aureus*. Although *S. aureus* is capable of endogenous heme production, HssRS is not activated in the absence of extracellular heme, suggesting that this system specifically recognizes host-derived heme. The identification of systems that contribute to *S. aureus* virulence factor production and immune cell modulation in the host could lead to the development of novel therapeutics targeting

staphylococcal gene regulation. In light of the increased prevalence of *S. aureus* strains resistant to virtually all relevant antimicrobials, the design of novel therapeutics is paramount toward combating the inevitable increase in severe staphylococcal infections.

EXPERIMENTAL PROCEDURES

Bacterial Strains

S. aureus Newman, a human clinical isolate, was used in this study (Duthie and Lorenz, 1952). The *ΔsrtA* mutant strain has been previously described (Mazmanian et al., 1999, 2000). Erythromycin cassette insertion mutants of the *hrtA*, *hrtB*, and *hssS* genes were obtained from the Phoenix (N) library, clones PhiNE 03177 (SAV2359), PhiNE 01762 (SAV2360), PhiNE 01562 (SAV2362), and PhiNE 07744 (SAV2362) (Bae et al., 2004). All the Phoenix (N) library mutants were transduced into Newman. The *ΔhrtA* and *ΔhssR* isogenic mutant strains were generated by deletion of the genes following a protocol described by Bae and Schneewind (2005). To create a complementation vector coding for wild-type *hrtA*, the *hrtAB* intergenic region containing the predicted promoter sequence for *hrtAB* was fused to the *hrtA* coding sequence by polymerase chain reaction sequence overlap extension (PCR-SOE) (Horton et al., 1990). Details for the creation of these strains are available in the Supplemental Data.

Analyses of Secreted Proteins

S. aureus cultures were grown overnight at 37°C with shaking in 5 ml of RPMI containing 1% casamino acids with or without 1 μM hemin. Cultures were then sedimented, and the supernatant was collected. 1.2 ml of each supernatant was then precipitated by adding 10% TCA (v/v) and incubating the samples for ~15 hr at 4°C. The precipitated proteins were then sedimented and washed twice with 100% ethanol. Proteins were dried and then resuspended with 30 μl of a SDS-loading buffer and boiled at 95°C for 10 min. Protein samples were separated on 15% SDS-PAGE gels and stained with colloidal blue (Invitrogen). Gel slices containing proteins of interest were removed from the gel and subjected to in-gel digestion with trypsin, and the peptides were analyzed by matrix-assisted laser desorption/ionization, time-of-flight mass spectrometry (MALDI-TOF MS), and data-dependent TOF/TOF tandem MS/MS as described previously (Friedman et al., 2006). The resulting peptide mass maps and the associated fragmentation spectra were collectively used to interrogate *S. aureus* Mu50 sequences as described previously (Friedman et al., 2006).

Hemin Cytotoxicity Assays

S. aureus cultures were grown overnight at 37°C with shaking in TSB with or without hemin. Cultures were then diluted 1:75 and inoculated into round-bottom 96-well plates in a final volume of 150 μl of medium supplemented with different concentrations of hemin. Cultures were grown at 37°C with aeration for 2–3 hr. Bacterial viability was determined by serial dilution and plating on solid agar.

XylE Reporter Assay

Details on the construction of the reporter vectors are available in the Supplemental Data. *S. aureus* strains harboring the appropriate reporter construct were inoculated into 500 μl of TSB containing 10 μg/ml chloramphenicol in 1.5 ml tubes. Cultures were grown overnight at 37°C with shaking. Bacteria were pelleted by centrifugation, and spent medium was aspirated. The pellet was washed once with 500 μl of 20 mM potassium phosphate (pH 7.6) and resuspended in 150 μl of 100 mM potassium phosphate buffer (pH 8.0), 10% (v/v) acetone, and 25 μg/ml lysostaphin. After 20 min incubation at 37°C and 5 min incubation on ice, samples were centrifuged at 20,000 g for 30 min at 4°C. Supernatant (1–10 μl) was added to a 96-well plate, and 200 μl of 100 mM potassium phosphate (pH 8.0) and 0.2 mM pyrocatechol was added to each well. Formation of 2-hydroxymuconic semialdehyde was tracked by measuring the absorbance at 375 nm every minute for 30 min on a Varian MP 50 microplate reader. Protein concentration in samples was determined by BCA (Pierce). One unit of specific activity of XylE in a sample is defined as the formation of 1 nmol of 2-hydroxymuconic semialdehyde per minute per milligram of cellular protein at 30°C (Chien et al., 1999). Metalloporphyrins were purchased from Frontier Biosciences.

Histological Tissue Analysis

Paraffin-embedded mouse tissues were stained with H&E. Sections were evaluated by a single pathologist (J.I.).

Supplemental Data

The Supplemental Data include Supplemental Experimental Procedures and two supplemental figures and can be found with this article online at http://www.cellhostandmicrobe.com/cgi/content/full/1/2/109/DC1/.

ACKNOWLEDGMENTS

We thank members of the Skaar lab and Drs. David G. Russell, Timothy L. Cover, Hank S. Seifert, Dean W. Ballard, and Clarence B. Creech for critical reading of this manuscript. We would also like to thank the Vanderbilt pathology core and Dr. David Friedman for technical assistance, Dr. Ambrose Cheung for the gift of pALC1639, Dr. Olaf Schneewind for the gift of the *ΔsrtA* strain and the pOS-1 plasmid, and Dr. Dominique Missiakas for Phoenix Library Derivatives. This research was supported by Vanderbilt University Medical Center Development funds, the Searle Scholars Program, and United States Public Health Service Grant AI69233 (E.P.S.) and AI042284 (S.J.) from the National Institute of Allergy and Infectious Diseases. E.P.S. holds an Investigator in Pathogenesis of Infectious Disease Award from the Burroughs Wellcome Fund. V.J.T. was supported by Ruth L. Kirschstein NRSA AI071487 postdoctoral fellowship, and D.L.S. was supported by T32 HL069765 from the National Institute of Allergy and Infectious Diseases. P.M.D. and K.L.A. were supported by American Heart Association grant #0535037N.

Received: November 15, 2006
Revised: January 24, 2007
Accepted: March 12, 2007
Published: April 18, 2007

REFERENCES

Anderson, K.L., Roberts, C., Disz, T., Vonstein, V., Hwang, K., Overbeek, R., Olson, P.D., Projan, S.J., and Dunman, P.M. (2006). Characterization of the *Staphylococcus aureus* heat shock, cold shock, stringent, and SOS responses and their effects on log-phase mRNA turnover. J. Bacteriol. *188*, 6739–6756.

Bader, M.W., Sanowar, S., Daley, M.E., Schneider, A.R., Cho, U., Xu, W., Klevit, R.E., Le Moual, H., and Miller, S.I. (2005). Recognition of antimicrobial peptides by a bacterial sensor kinase. Cell *122*, 461–472.

Bae, T., and Schneewind, O. (2005). Allelic replacement in *Staphylococcus aureus* with inducible counter-selection. Plasmid *55*, 58–63.

Bae, T., Banger, A.K., Wallace, A., Glass, E.M., Aslund, F., Schneewind, O., and Missiakas, D.M. (2004). *Staphylococcus aureus* virulence genes identified by bursa aurealis mutagenesis and nematode killing. Proc. Natl. Acad. Sci. USA *101*, 12312–12317.

Beier, D., and Gross, R. (2006). Regulation of bacterial virulence by two-component systems. Curr. Opin. Microbiol. *9*, 143–152.

Bernheimer, A.W., Avigad, L.S., and Grushoff, P. (1968). Lytic effects of staphylococcal alpha-toxin and delta-hemolysin. J. Bacteriol. *96*, 487–491.

Bischoff, M., Dunman, P., Kormanec, J., Macapagal, D., Murphy, E., Mounts, W., Berger-Bachi, B., and Projan, S. (2004). Microarray-based analysis of the *Staphylococcus aureus sigmaB* regulon. J. Bacteriol. *186*, 4085–4099.

Bronner, S., Monteil, H., and Prevost, G. (2004). Regulation of virulence determinants in *Staphylococcus aureus*: Complexity and applications. FEMS Microbiol. Rev. *28*, 183–200.

Brook, I. (2002). Secondary bacterial infections complicating skin lesions. J. Med. Microbiol. *51*, 808–812.

Chavakis, T., Hussain, M., Kanse, S.M., Peters, G., Bretzel, R.G., Flock, J.I., Herrmann, M., and Preissner, K.T. (2002). *Staphylococcus aureus* extracellular adherence protein serves as anti-inflammatory factor by inhibiting the recruitment of host leukocytes. Nat. Med. *8*, 687–693.

Chavakis, T., Wiechmann, K., Preissner, K.T., and Herrmann, M. (2005). *Staphylococcus aureus* interactions with the endothelium: The role of bacterial "secretable expanded repertoire adhesive molecules" (SERAM) in disturbing host defense systems. Thromb. Haemost. *94*, 278–285.

Cheung, A.L., Bayer, A.S., Zhang, G., Gresham, H., and Xiong, Y.Q. (2004). Regulation of virulence determinants *in vitro* and *in vivo* in *Staphylococcus aureus*. FEMS Immunol. Med. Microbiol. *40*, 1–9.

Chien, Y., Manna, A.C., Projan, S.J., and Cheung, A.L. (1999). SarA, a global regulator of virulence determinants in *Staphylococcus aureus*, binds to a conserved motif essential for sar-dependent gene regulation. J. Biol. Chem. *274*, 37169–37176.

Clarke, M.B., Hughes, D.T., Zhu, C., Boedeker, E.C., and Sperandio, V. (2006). The QseC sensor kinase: A bacterial adrenergic receptor. Proc. Natl. Acad. Sci. USA *103*, 10420–10425.

Deiss, A. (1983). Iron metabolism in reticuloendothelial cells. Semin. Hematol. *20*, 81–90.

Dunman, P.M., Murphy, E., Haney, S., Palacios, D., Tucker-Kellogg, G., Wu, S., Brown, E.L., Zagursky, R.J., Shlaes, D., and Projan, S.J. (2001). Transcription profiling-based identification of *Staphylococcus aureus* genes regulated by the *agr* and/or *sarA* loci. J. Bacteriol. *183*, 7341–7353.

Duthie, E.S., and Lorenz, L.L. (1952). Staphylococcal coagulase; Mode of action and antigenicity. J. Gen. Microbiol. *6*, 95–107.

Everse, J., and Hsia, N. (1997). The toxicities of native and modified hemoglobins. Free Radic. Biol. Med. *22*, 1075–1099.

Foster, T.J. (2005). Immune evasion by staphylococci. Nat. Rev. Microbiol. *3*, 948–958.

Fowler, V.G., Jr., Miro, J.M., Hoen, B., Cabell, C.H., Abrutyn, E., Rubinstein, E., Corey, G.R., Spelman, D., Bradley, S.F., Barsic, B., et al. (2005). *Staphylococcus aureus* endocarditis: A consequence of medical progress. JAMA *293*, 3012–3021.

Fridkin, S.K., Hageman, J.C., Morrison, M., Sanza, L.T., Como-Sabetti, K., Jernigan, J.A., Harriman, K., Harrison, L.H., Lynfield, R., and Farley, M.M. (2005). Methicillin-resistant *Staphylococcus aureus* disease in three communities. N. Engl. J. Med. *352*, 1436–1444.

Friedman, D.B., Stauff, D.L., Pishchany, G., Whitwell, C.W., Torres, V.J., and Skaar, E.P. (2006). *Staphylococcus aureus* redirects central metabolism to increase iron availability. PLoS Pathog. *2*, e87. 10.1371/journal.ppat.0020087.

Horton, R.M., Cai, Z.L., Ho, S.N., and Pease, L.R. (1990). Gene splicing by overlap extension: Tailor-made genes using the polymerase chain reaction. Biotechniques *8*, 528–535.

Kobayashi, N., Nishino, K., and Yamaguchi, A. (2001). Novel macrolide-specific ABC-type efflux transporter in *Escherichia coli*. J. Bacteriol. *183*, 5639–5644.

Lee, L.Y., Hook, M., Haviland, D., Wetsel, R.A., Yonter, E.O., Syribeys, P., Vernachio, J., and Brown, E.L. (2004). Inhibition of complement activation by a secreted *Staphylococcus aureus* protein. J. Infect. Dis. *190*, 571–579.

Lublin, M., Bartlett, D.L., Danforth, D.N., Kauffman, H., Gallin, J.I., Malech, H.L., Shawker, T., Choyke, P., Kleiner, D.E., Schwartzentruber, D.J., et al. (2002). Hepatic abscess in patients with chronic granulomatous disease. Ann. Surg. *235*, 383–391.

Luong, T.T., Dunman, P.M., Murphy, E., Projan, S.J., and Lee, C.Y. (2006). Transcription profiling of the *mgrA* regulon in *Staphylococcus aureus*. J. Bacteriol. *188*, 1899–1910.

Mascher, T., Helmann, J.D., and Unden, G. (2006). Stimulus perception in bacterial signal-transducing histidine kinases. Microbiol. Mol. Biol. Rev. *70*, 910–938.

Mazmanian, S.K., Liu, G., Ton-That, H., and Schneewind, O. (1999). *Staphylococcus aureus* sortase, an enzyme that anchors surface proteins to the cell wall. Science *285*, 760–763.

Mazmanian, S.K., Liu, G., Jensen, E.R., Lenoy, E., and Schneewind, O. (2000). *Staphylococcus aureus* sortase mutants defective in the display of surface proteins and in the pathogenesis of animal infections. Proc. Natl. Acad. Sci. USA *97*, 5510–5515.

Mazmanian, S.K., Skaar, E.P., Gaspar, A.H., Humayun, M., Gornicki, P., Jelenska, J., Joachmiak, A., Missiakas, D.M., and Schneewind, O. (2003). Passage of heme-iron across the envelope of *Staphylococcus aureus*. Science *299*, 906–909.

Nagasawa, S., Ishige, K., and Mizuno, T. (1993). Novel members of the two-component signal transduction genes in *Escherichia coli*. J. Biochem. (Tokyo) *114*, 350–357.

Novick, R.P. (2003). Autoinduction and signal transduction in the regulation of staphylococcal virulence. Mol. Microbiol. *48*, 1429–1449.

Prat, C., Bestebroer, J., de Haas, C.J., van Strijp, J.A., and van Kessel, K.P. (2006). A new staphylococcal anti-inflammatory protein that antagonizes the formyl peptide receptor-like 1. J. Immunol. *177*, 8017–8026.

Richardson, A.R., Dunman, P.M., and Fang, F.C. (2006). The nitrosative stress response of *Staphylococcus aureus* is required for resistance to innate immunity. Mol. Microbiol. *61*, 927–939.

Segal, B.H., Leto, T.L., Gallin, J.I., Malech, H.L., and Holland, S.M. (2000). Genetic, biochemical, and clinical features of chronic granulomatous disease. Medicine (Baltimore) *79*, 170–200.

Skaar, E.P., and Schneewind, O. (2004). Iron-regulated surface determinants (Isd) of *Staphylococcus aureus*: Stealing iron from heme. Microbes Infect. *6*, 390–397.

Skaar, E.P., Humayun, M., Bae, T., DeBord, K.L., and Schneewind, O. (2004). Iron-source preference of *Staphylococcus aureus* infections. Science *305*, 1626–1628.

Taylor, R.K., Hall, M.N., Enquist, L., and Silhavy, T.J. (1981). Identification of OmpR: A positive regulatory protein controlling expression of the major outer membrane matrix porin proteins of Escherichia coli K-12. J. Bacteriol. *147*, 255–258.

Torres, V.J., Pishchany, G., Humayun, M., Schneewind, O., and Skaar, E.P. (2006). IsdB is a staphylococcal hemoglobin receptor required for heme-iron utilization. J. Bacteriol. *188*, 8421–8429.

Vermeiren, C.L., Pluym, M., Mack, J., Heinrichs, D.E., and Stillman, M.J. (2006). Characterization of the heme binding properties of *Staphylococcus aureus* IsdA. Biochemistry *45*, 12867–12875.

Weinrick, B., Dunman, P.M., McAleese, F., Murphy, E., Projan, S.J., Fang, Y., and Novick, R.P. (2004). Effect of mild acid on gene expression in *Staphylococcus aureus*. J. Bacteriol. *186*, 8407–8423.

Wertheim, H.F., Vos, M.C., Ott, A., van Belkum, A., Voss, A., Kluytmans, J.A., van Keulen, P.H., Vandenbroucke-Grauls, C.M., Meester, M.H., and Verbrugh, H.A. (2004). Risk and outcome of nosocomial *Staphylococcus aureus* bacteraemia in nasal carriers versus non-carriers. Lancet *364*, 703–705.

Williams, R.J., Ward, J.M., Henderson, B., Poole, S., O'Hara, B.P., Wilson, M., and Nair, S.P. (2000). Identification of a novel gene cluster encoding staphylococcal exotoxin-like proteins: Characterization of the prototypic gene and its protein product, SET1. Infect. Immun. *68*, 4407–4415.

Immunity 25, 487–497, September 2006 ©2006 Elsevier Inc. DOI 10.1016/j.immuni.2006.06.017

Granulocyte-Macrophage Colony-Stimulating Factor Regulates Effector Differentiation of Invariant Natural Killer T Cells during Thymic Ontogeny

Jelena S. Bezbradica,[1] Laura E. Gordy,[1] Aleksandar K. Stanic,[1] Srdjan Dragovic,[1] Timothy Hill,[1] Jacek Hawiger,[1] Derya Unutmaz,[1] Luc Van Kaer,[1] and Sebastian Joyce[1,*]
[1] Department of Microbiology and Immunology Vanderbilt University School of Medicine Nashville, Tennessee 37232

Summary

Invariant natural killer T (iNKT) cell-derived cytokines have important functions in inflammation, host defense, and immunoregulation. Yet, when and how iNKT cells undergo effector differentiation, which endows them with the capacity to rapidly secrete cytokines upon activation, remains unknown. We discovered that granulocyte-macrophage colony-stimulating factor (Csf-2)-deficient mice developed iNKT cells that failed to respond to the model antigen α-galactosylceramide because of an intrinsic defect in the fusion of secretory vesicles with the plasma membrane. Exogenous Csf-2 corrected the functional defect only when supplied during the development of thymic, but not mature, splenic Csf-2-deficient iNKT cells. Thus, we ascribe a unique function to Csf-2, which regulates iNKT cell effector differentiation during development by a mechanism that renders them competent for cytokine secretion.

Introduction

Commitment and differentiation to the T cell lineage occur in the thymus from a pluripotent lymphocyte progenitor. T lineage consists predominantly of αβ T cells and a minor population of γδ cells. Among the αβ T cells are the conventional $CD4^+$ and $CD8^+$ lymphocytes as well as several minor subsets, including $CD4^+CD25^+$ T_{reg} and $NK1.1^+$ natural killer T (NKT) cells. After commitment at the $CD4^+CD8^+$ double-positive stage, the conventional $CD4^+$ and $CD8^+$ lymphocytes mature and emigrate to peripheral lymphoid organs. Here, upon antigen recognition, they undergo further maturation by a process termed effector differentiation or functional maturation. In conventional T cells, effector differentiation requires chromatin remodeling and transcriptional regulation of cytokine gene loci. Thus, effector differentiation of conventional T cells is a postdevelopmental event that occurs in peripheral lymphoid organs. However, very little is known regarding effector differentiation of the remaining T cell subsets. Therefore, we have focused the current study on the mechanism(s) underlying effector differentiation of NKT cells.

Invariant NKT (iNKT) cells are unique T lineage cells whose immunoregulatory functions depend on rapid cytokine secretion (Van Kaer, 2005). Phenotypically, iNKT cells represent an unusual hybrid between conventional T and natural killer (NK) cells, expressing both an invariant $V_\alpha14J_\alpha18$ T cell receptor (TCR) and several NK cell-specific receptors (Van Kaer, 2005). Functionally, however, iNKT cells are distinct from these two lymphocyte lineages. They recognize pathogen-induced, endogenous (Brigl et al., 2003; Zhou et al., 2004) and pathogen-derived, exogenous (Kinjo et al., 2005; Mattner et al., 2005; Sriram et al., 2005) glycolipid antigens when presented in the context of CD1d molecules. Our current understanding of iNKT cell function in vivo has emerged from probing with a marine sponge-derived synthetic glycolipid antigen, α-galactosylceramide (αGC), that closely resembles a pathogen-derived antigen, α-galacturonosylceramide (Kinjo et al., 2005; Mattner et al., 2005; Sriram et al., 2005). These studies revealed that iNKT cells might detect glycolipids generated during infection or tumorigenesis and rapidly relay this information to other effector leukocytes. To accomplish this task, iNKT cells secrete copious amounts of effector cytokines as quickly as 30–60 min after activation in vivo (Carnaud et al., 1999; Yoshimoto and Paul, 1994). Interferon-γ (IFN-γ) secreted by activated iNKT cells promotes antitumor immunity and immune responses to pathogens or acts as a catalyst to facilitate T helper 1 (Th1) responses to peptide antigens (Fujii et al., 2003; Hermans et al., 2003; Silk et al., 2004; Smyth et al., 2002). Conversely, interleukin-4 (IL-4) secreted by in vivo activated iNKT cells promotes Th2 responses to peptide antigens and together with IL-10 prevents the onset of autoimmune disease in various animal models (Burdin et al., 1999; Singh et al., 1999; Van Kaer, 2005). Thus, a thorough appreciation of the immunoregulatory roles of iNKT cells requires an in-depth understanding of when and how this T subset acquires its unique effector functions.

Unlike conventional T cells, naive thymic, splenic, and hepatic iNKT cells have transcriptionally active *Il4* and *Ifng* gene loci (Matsuda et al., 2003; Stetson et al., 2003). Even the $NK1.1^-$ thymic iNKT cells, which are precursors of all iNKT cells, transcribe and translate their *Il4* locus (Benlagha et al., 2002; Gadue and Stein, 2002; Matsuda et al., 2003; Pellicci et al., 2002; Stetson et al., 2003). Therefore, we hypothesized that iNKT cells acquire effector properties during thymic development at the stage when they diverge into a distinct lineage from conventional T lymphocytes. iNKT cell precursors share the same early developmental stages with conventional T cells. It is only after the assembly of their unique TCR ($V_\alpha14J_\alpha18$ paired with $V_\beta8.2$, $V_\beta7$, or $V_\beta2$) and its positive selection by CD1d-expressing cortical thymocytes that commitment toward this distinct lineage occurs (Benlagha et al., 2005; Bezbradica et al., 2005a; Egawa et al., 2005; Gapin et al., 2001). At this time, a transcriptional program unique to iNKT cells is initiated. Thus, deficiencies in several signaling molecules and transcription factors (Ets, MEF, T-bet, SAP, Fyn, Itk, PKC-θ, Bcl-10, IKKβ, and NF-κB) profoundly impair iNKT cell ontogeny (Chung et al., 2005; Eberl et al., 1999; Gadue et al., 1999; Gadue and Stein, 2002; Lacorazza et al., 2002; Pasquier et al., 2005;

*Correspondence: sebastian.joyce@vanderbilt.edu

Schmidt-Supprian et al., 2004; Sivakumar et al., 2003; Stanic et al., 2004a, 2004b; Townsend et al., 2004; Walunas et al., 2000). We recently discovered that iNKT cells with a block in NF-κB signaling (IκBΔN) failed to complete their maturation program in the thymus, a defect that can be fully corrected by overexpression of the anti-apoptotic protein Bcl-x_L (Stanic et al., 2004a). However, we found that, despite full reconstitution of what appears to be phenotypically and molecularly mature iNKT cells, Bcl-x_L transgenesis did not restore iNKT cell function (Stanic et al., 2004b). This finding suggests that NF-κB signaling regulates not only survival but also functional maturation of iNKT cells during ontogeny and, hence, raises the question as to which NF-κB-regulated gene(s) is responsible for functional maturation of iNKT cells.

Previous studies have implicated granulocyte-macrophage colony-stimulating factor (Csf-2), an NF-κB-induced protein (Thomas et al., 1997), in iNKT cell ontogeny. Csf-2 was shown to promote maturation of iNKT cell precursors by enhancing $V_\alpha 14$ to $J_\alpha 18$ recombination in an in vitro cell-culture system. Further, mice deficient in the common β-chain (βc) receptor, which Csf-2 shares with IL-3 and IL-5, poorly develop iNKT cells (Sato et al., 1999). Moreover, the cytokine-specific, Csf-2 receptor-α (Csf-2Rα) chain signals through NF-κB in human umbilical cord endothelial cells (Ebner et al., 2003). For these reasons, we analyzed iNKT cell development and function in Csf-2-deficient mice. Our data highlight a previously unrecognized, instructive role for Csf-2 in functional maturation of iNKT cells. Further, they indicate that the acquisition of regulated secretory function is a unique differentiation step toward the generation of immunocompetent iNKT cells.

Results

iNKT Cells Express Functional Csf-2R, which Signals through NF-κB

Current evidence suggests that only myeloid cells express Csf-2R (Enzler and Dranoff, 2003). If Csf-2 regulates iNKT cell ontogeny and effector differentiation, this T subset should express functional Csf-2R and the thymus should have a source for Csf-2. We found that most thymic, splenic, and hepatic iNKT cells expressed the Csf-2R, as did some conventional T cells, albeit at a lower amount (Figure 1A). Further, thymocytes secreted modest amounts of Csf-2 when activated ex vivo via either αGC or by crosslinking CD3+CD28 molecules (Figure 1B).

To determine whether the expressed Csf-2R is functional, highly purified, unactivated primary iNKT cells were required. Therefore, we developed a strategy for sorting primary mouse iNKT cells without ligating any of their stimulatory or inhibitory receptors. In brief, we took advantage of 4get mouse in which the gene encoding enhanced green fluorescent protein (eGFP) preceded by an internal ribosome entry sequence was knocked in downstream of the *Il4* locus (Stetson et al., 2003). In naive 4get mice, the *Il4-eGFP* bicistronic transcript is highly restricted to $NK1.1^-$ and $NK1.1^+$ iNKT cells (Matsuda et al., 2003; Stetson et al., 2003; see Figure S1A in the Supplemental Data available online). Taking advantage of strong green fluorescence, naive iNKT cells were isolated by fluorescence-activated cell sorting (FACS). The iNKT cells isolated by this strategy were >95% pure as determined by CD3ε and αGC-loaded tetrameric mouse CD1d1 (tetramer) staining. They displayed all phenotypic properties of nonactivated iNKT cells (Figure S1B). Further, they did not secrete any cytokines or show other hallmarks of activation (TCR downmodulation, data not shown) unless stimulated through their TCR (Figure S1C). Thus, the iNKT cells isolated in this manner were viable, functional, and remained quiescent through the entire purification process.

Recent studies show that Csf-2Rα chain signals through NF-κB (Ebner et al., 2003). Because functional maturation of iNKT cells requires signaling through NF-κB (Stanic et al., 2004b), we determined whether Csf-2R ligation with recombinant mouse (rm) Csf-2 activates NF-κB in purified iNKT cells. The data revealed that Csf-2R ligation induced IκBα phosphorylation, which could not be attributed to lipopolysaccharide (LPS) contamination (Figure 1C). Thus, iNKT cells expressed functional Csf-2R in terms of its signaling through NF-κB pathway. Hence, Csf-2 may play a role in functional iNKT cell ontogeny.

Csf-2-Deficient iNKT Cells Are Functionally Impaired

We next determined whether Csf-2 signaling through its cognate receptor is essential for the development of functional iNKT cells. We found that Csf-2-deficient mice developed mature iNKT cells. Their numbers were ~85%–95% of those observed in wild-type (wt) thymus, spleen, and liver (Figures 2A and 2B). Detailed characterization revealed that Csf-2 was not essential for phenotypic (NK1.1, DX5, HSA, CD5, CD44, CD69, CD122, CD127, Ly49A) or molecular (Bcl-2, IL-4, IFN-γ) maturation of developing iNKT cells (data not shown). It was also not required for their survival and proliferation (data not shown). Thus, in contrast to the previous report (Sato et al., 1999), Csf-2 appears to be dispensable for the generation of iNKT cells.

We found that Csf-2-deficient mice elicited unusually small amounts of cytokines upon stimulation in vivo with αGC (Figure 2C) or in vitro with anti-CD3ε+CD28 Abs (Figure S2A). Delayed kinetics of cytokine secretion by Csf-2-deficient iNKT cells was unlikely, because Csf-2-deficient splenocytes did not respond to αGC even after 4 days of in vitro stimulation (Figure 2D). Further, the lack of cytokine response in vivo was not due to the lack of antigen recognition and stable cell-cell interaction with antigen-presenting cells (APCs), because early features of glycolipid presentation and recognition, such as TCR downmodulation on iNKT cells (Figure S2B) and CD86 upregulation on APCs (Figure S2C), were intact. Importantly, late, cytokine-dependent functions of iNKT cells, such as transactivation of B, $CD8^+$ T, and NK cells (Figures S2D and S2E), were severely impaired.

In additional experiments, we found that Csf-2-deficient NK but not iNKT cells secreted IFN-γ in response to phorbol myristate acetate (PMA)+ionomycin as well as IL-12, IL-18, and IL-12+IL-18 (Figures S2A and S2F). Similarly, Csf-2-deficient $CD8^+$ T cells secreted IFN-γ in response to minor histocompatibility (minor H) antigens (Figure S2G), MHC alloantigens, TCR+CD28 ligation, and PMA+ionomycin (Wada et al., 1997). Moreover, as described later, Csf-2-deficient dendritic cell (DC)

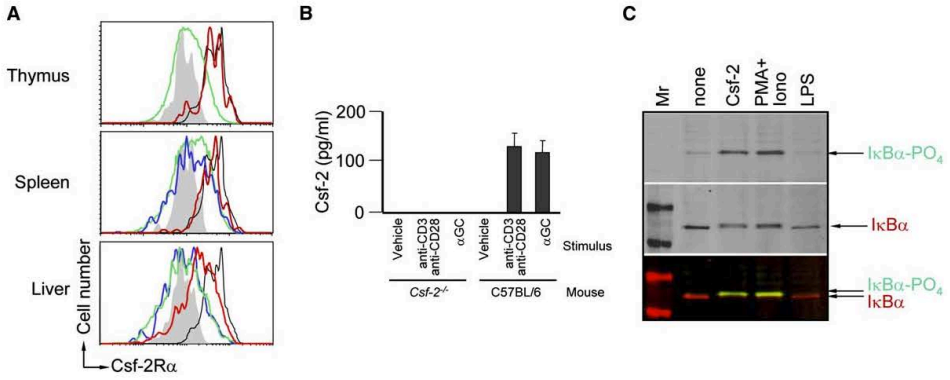

Figure 1. iNKT Cells Express Functional Csf-2R

(A) Cells were permeabilized and reacted with Csf-2Rα cytoplasmic tail-specific Ab (open histograms) or isotype control (gray histograms) and detected with anti-rabbit Ig-FITC. iNKT cells (red), T cells (green), NK cells (blue), and splenic DCs (black) were identified as $CD3^+tetramer^+$, $CD3^+tetramer^-$, $CD3^-NK1.1^+$, and $CD11c^+$ cells, respectively, within electronically gated $CD8^{lo}$ thymocytes, $B220^{lo}$ spleen, or liver cells.

(B) Thymocytes from C57BL/6 and Csf-2-deficient mice were stimulated for 30 hr with either αGC or anti-CD3ε+CD28 Abs. Secreted Csf-2 was measured by ELISA. Representative of two independent experiments; bars indicate mean ± standard error of mean (SEM).

(C) Purified thymic 4get iNKT cells were activated with 100 ng/ml PMA and 2 μM ionomycin, 100 ng/ml rmCsf-2, or 100 ng/ml LPS. After 15 min, total and phosphorylated IκBα were determined by immunoblot. Representative of three independent experiments.

function also appeared normal with respect to glycolipid antigen presentation. Together, these data indicate that defective cytokine secretion is a hallmark of Csf-2-deficient iNKT but not other cell lineages.

The Functional Defect in Csf-2-Deficient iNKT Cells Is Cell Intrinsic

Csf-2 is a myeloid growth and differentiation factor (Enzler and Dranoff, 2003). Because DCs are myeloid cells

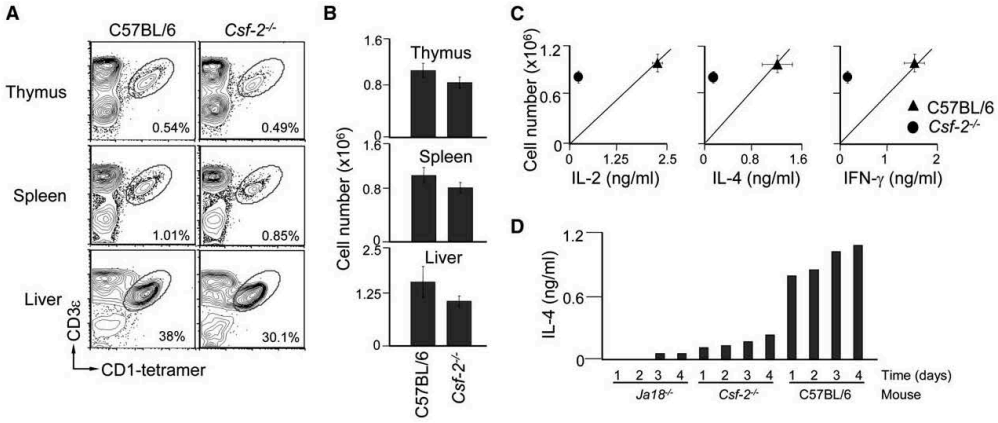

Figure 2. Csf-2-Deficient Mice Develop Functionally Impaired iNKT Cells

(A) Thymic, splenic, and hepatic iNKT cells from C57BL/6 and Csf-2-deficient mice were identified as $CD3^+tetramer^+$ cells within electronically gated $CD8^{lo}$ thymic or $B220^{lo}$ spleen and liver cells. Numbers are % iNKT cells among total leukocytes. Representative of five independent experiments.

(B) Absolute numbers of iNKT cells in thymus, spleen, and liver from C57BL/6 and Csf-2-deficient mice were calculated from % iNKT cells in (A) and total cell count. Representative of five independent experiments; bars indicate mean ± SEM.

(C) Serum cytokine response to in vivo activation of iNKT cells was measured after 2 (IL-2 and IL-4) and 6 (IFN-γ) hours of 5 μg αGC or vehicle injection. Cytokine response is plotted against average number of splenic iNKT cells determined in (B). To account for difference in absolute cell number in C57BL/6 and Csf-2-deficient mice, a diagonal was arbitrarily set from zero at the origin to C57BL/6 cytokine response. It represents what would be equal to wt response per cell basis. Values on the left and right of it represent responses lower or higher than wt, respectively. Background induced by vehicle was subtracted from specific αGC-induced responses. Data show mean of four independent experiments ± SEM.

(D) Splenocytes from $Ja18^{-/-}$, $Csf\text{-}2^{-/-}$, or C57BL/6 mice were activated in vitro with 100 ng/ml αGC for 4 days. IL-4 secreted into the culture supernatant after 1, 2, 3, or 4 days was measured by ELISA. Background was subtracted as in (C). One representative experiment of three independent ones is shown; bars indicate mean of triplicate measurement for each condition.

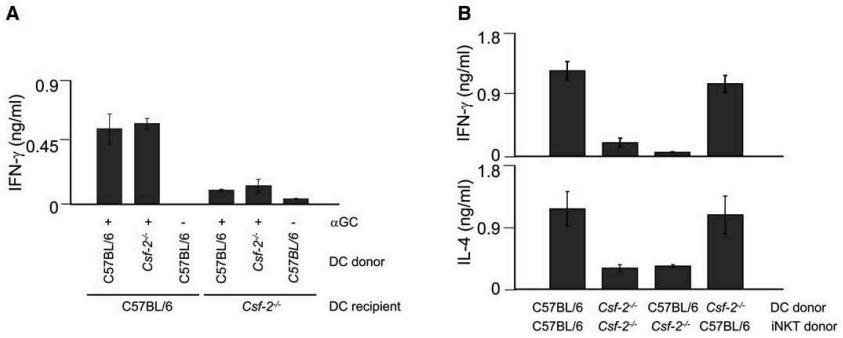

Figure 3. Functional Block within Csf-2-Deficient iNKT Cells Is Cell Intrinsic

(A) Freshly purified, vehicle- or αGC-pulsed splenic DCs from C57BL/6 and Csf-2-deficient mice were adoptively transferred into C57BL/6 or Csf-2-deficient mice, and serum IFN-γ response was measured 6 hr later by ELISA. Representative of two independent experiments; bars indicate mean ± SEM.

(B) Purified (~95% purity) DCs from C57BL/6 and Csf-2-deficient mice were incubated in vitro with iNKT cell-enriched splenic fraction from C57BL/6 or Csf-2-deficient mice at a ratio of 1:100 in the presence of αGC for 4 days. IFN-γ and IL-4 responses from iNKT cells were measured after 4 days. Background was subtracted as in Figure 2C. Representative of three independent experiments; bars indicate mean ± SEM.

critical for iNKT cell activation in vivo (Bezbradica et al., 2005b; Schmieg et al., 2005), iNKT cell unresponsiveness could be the result of altered growth and/or differentiation of Csf-2-deficient DCs. However, Csf-2-deficient mice developed wt numbers of DCs, expressed wt amounts of CD1d1 (Figure S3), and upregulated costimulatory molecules upon initial interaction with activated iNKT cells (Figure S2C). Thus, Csf-2-deficient DCs appear phenotypically mature. Next, we purified Csf-2-deficient and wt DCs, pulsed them with αGC, and transferred them into Csf-2-deficient and wt recipients to test their functional maturity. Both Csf-2-deficient and wt αGC-pulsed DCs activated wt iNKT cells, but neither reconstituted robust cytokine secretion when transferred into Csf-2-deficient recipients (Figure 3A). Further, we fully recapitulated the above results in more controlled, in vitro conditions, where purified Csf-2-deficient or wt DCs were cocultivated with iNKT cell-enriched Csf-2-deficient or wt splenocytes in the presence of antigen (Figure 3B). Thus, the functional defect in Csf-2-deficient mice is intrinsic to iNKT cells but not DCs.

Effector Differentiation of iNKT Cells Is Developmentally Regulated by Csf-2

The functional response to αGC in vivo is the result of complex interactions between DCs and iNKT cells, involving direct cell-cell communications and release of soluble factors (Van Kaer, 2005). Thus, the lack of robust cytokine response in Csf-2-deficient mice could reflect the absence of peripheral Csf-2 essential for DC-iNKT cell communication. However, provision of exogenous rmCsf-2 at the time of αGC delivery did not reconstitute the iNKT cell response in vivo (Figure 4A). Similarly, provision of rmCsf-2 during the entire course of in vitro stimulation with αGC did not rescue defective Csf-2-deficient iNKT cell function (Figure 4B). Note that 50, 100, 500, and 1000 ng Csf-2/mouse were tested and 100 ng of Csf-2 appeared optimal for this response (data not shown). The lack of cytokines in the culture medium was not due to rapid utilization or degradation because surface cytokine capture assay did not detect IFN-γ after Csf-2-deficient iNKT cell activation (Figure 4C).

From the above data, we speculated that Csf-2 promotes functional maturation of iNKT cells during ontogeny. Development of this lineage begins in postnatal thymus (Benlagha et al., 2005). Thus, we developed an ex vivo culture system with thymocytes derived from 3- to 21-day-old wt and Csf-2-deficient mice that were supplemented with recombinant human (rh) IL-7 and/or rhIL-15. We found that IL-7, IL-15, and IL-7+IL-15 expanded iNKT cells in this assay (Figures S4A–S4C). Supplementation of thymocyte cultures derived from 3- to 8-day-old but not 21-day-old or older mice with rmCsf-2 rescued cytokine response of Csf-2-deficient iNKT cells (Figure 4C). This functional rescue may perhaps be due to higher proportion of immature iNKT cells in 3- to 8-day-old but not in older thymocytes (Figure S4D). These data indicate that functional responsiveness to antigen is a property assumed during ontogeny that cannot be acquired once iNKT cells have completed their differentiation program in the thymus and have populated the peripheral lymphoid organs.

Autocrine Regulation of Functional iNKT Cell Ontogeny by Csf-2

Endothelial cells, stromal cells, macrophages, fibroblasts, NK cells, and activated T and iNKT cells can secrete Csf-2 in vivo (Enzler and Dranoff, 2003) and, hence, are potential sources of Csf-2 during iNKT cell ontogeny. To determine the source of Csf-2 that mediates functional iNKT cell ontogeny, we prepared a series of reciprocal bone marrow (BM) chimeras with Csf-2-deficient and Ja18-deficient (which develop conventional T cells but not iNKT cells [Cui et al., 1997]) mice. Because *Csf-2*$^{+/+}$→*Csf-2*$^{-/-}$ and *Csf-2*$^{+/+}$→*Csf-2*$^{+/+}$ radiation BM chimeras developed iNKT cells (Figure 5A) and reconstituted function (Figure 5B), we concluded that hematopoietic cell-derived Csf-2 mediates iNKT cell maturation. Thus, both conventional T and iNKT cells could be the source of thymic Csf-2 that promotes effector

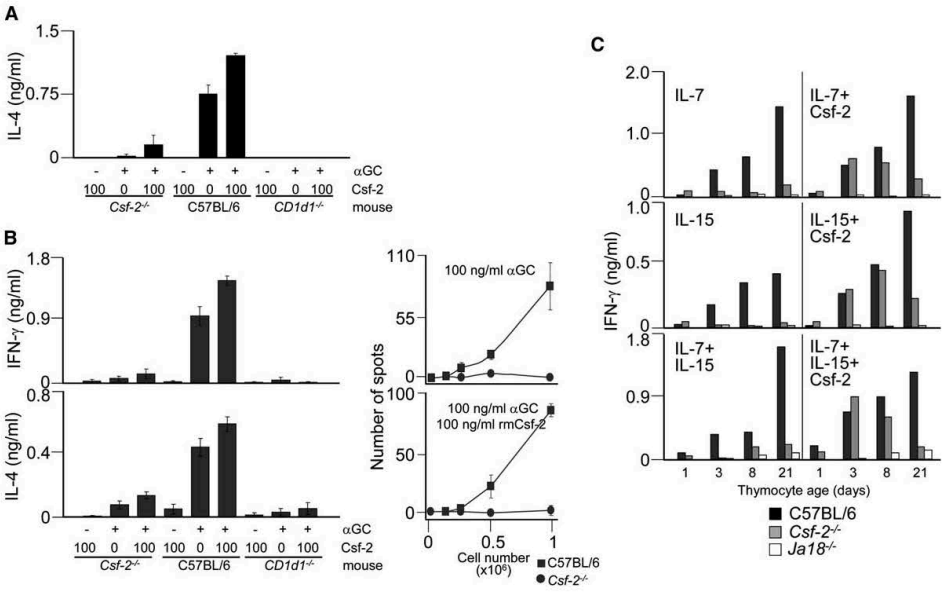

Figure 4. Administration of Csf-2 during Development but Not in the Periphery Rescues iNKT Cell Function

(A) C57BL/6, Csf-2-, and CD1d1-deficient mice were injected i.p. with vehicle or 5 μg αGC ± 100 ng of Csf-2. After 2 hr, serum IL-4 was measured by ELISA. Representative of two independent experiments; bars indicate mean ± SEM.

(B) Splenocytes from C57BL/6, Csf-2-, and CD1d1-deficient mice were stimulated with 100 ng/ml αGC+Csf-2 for 4 days. IL-4 and IFN-γ secreted by activated iNKT cells were measured by ELISA after 1, 2, 3, and 4 days. Representative results from 2-day culture are shown (left). Splenocytes from C57BL/6, Csf-2-deficient mice were similarly stimulated for 24 hr, and secreted IFN-γ was captured and detected by ELIspot assay (right). Representative of two independent experiments performed in triplicates; bars indicate mean ± SEM.

(C) Thymocytes from 3- to 21-day-old mice were cultivated for 14 days in vitro in the presence of 10 ng/ml rhIL-7, 100 ng/ml rhIL-15, and/or 100 ng/ml rmCsf-2. After 14 days, thymic cultures were stimulated overnight with vehicle- or αGC-loaded DCs in 1:100 DC:thymocyte ratio and secreted cytokines were monitored. Note that rhIL-7, rhIL-15, and rmCsf-2 were kept in cultures during the entire stimulation procedure. One representative experiment of two independent ones is shown; bars indicate mean of triplicate measurement for each condition.

differentiation of iNKT cells. To identify the source of thymic Csf-2, we generated mixed *Csf-2*$^{-/-}$+*Ja18*$^{-/-}$ → *Csf-2*$^{-/-}$ and *Csf-2*$^{-/-}$+*Ja18*$^{-/-}$ → *Ja18*$^{-/-}$ BM chimeras. In this system, *Ja18*$^{-/-}$ BM should be a source of T cell-derived Csf-2. We found that the mixed BM chimeras did not reconstitute iNKT cell function (Figure 5B). Note that all chimeras successfully reconstituted iNKT cell numbers (Figure 5A) as well as early features of glycolipid antigen recognition, as measured by CD69 upregulation on αGC-activated chimeric iNKT cells (Figure 5C). Thus, Csf-2 plays a cell-autonomous role in iNKT cell effector differentiation.

Csf-2 Controls the Acquisition of Secretory Function in iNKT Cells

Next, we investigated the mechanism by which Csf-2 instructs iNKT cell effector differentiation. The response of iNKT cells to antigen results in immediate translation of preformed cytokine mRNA and rapid cytokine secretion (Matsuda et al., 2003; Stetson et al., 2003) and proliferation (Crowe et al., 2003; Wilson et al., 2003) in vivo and ex vivo. Csf-2-deficient iNKT cells proliferated efficiently to antigen ex vivo (Figure S5A), suggesting that proximal TCR signaling is intact. Thus, the defect in Csf-2-deficient iNKT cells might reflect a block in cytokine transcription, translation, and/or secretion. Transcription of cytokine genes in Csf-2-deficient iNKT cells appeared unaffected because 4get Csf-2-deficient iNKT cells have similar eGFP expression as wt 4get iNKT cells (Figure S1A). To distinguish between the remaining two possibilities, iNKT cells were activated by αGC in vivo or in vitro and intracellular IL-4 and IFN-γ were monitored. We found that Csf-2-deficient iNKT cells expressed wt amounts of intracellular IL-4 and IFN-γ in response to αGC in vivo (Figure 6A) and in vitro (Figure 6B). Yet, Csf-2-deficient iNKT cells failed to secrete these cytokines into the serum (Figure 2C) and the culture supernatant (Figure S5B). Similar results were obtained when wt and Csf-2-deficient iNKT cells were activated in vitro with PMA+ionomycin (Figure S5C). Thus, we conclude that cytokine transcription and translation are intact whereas secretion is impaired in Csf-2-deficient iNKT cells.

Csf-2-Deficient iNKT Cells Have Defects in the Fusion of Secretory Vesicles with the Plasma Membrane

Current evidence suggests that cytokine-containing vesicles, akin to cytolytic granules (Bossi and Griffiths, 2005), are polarized toward the immune synapse prior to release by activated T cells (Morales-Tirado et al., 2004). Therefore, to test whether cytokine polarization is intact, freshly purified wt and Csf-2-deficient splenic

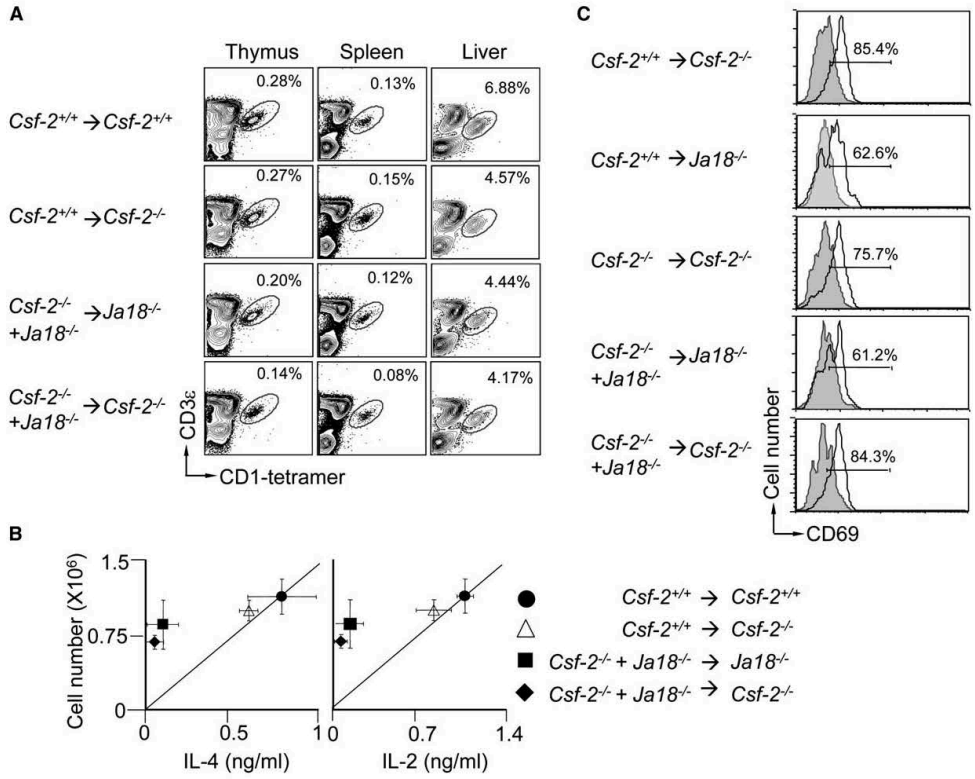

Figure 5. Csf-2 Controls Functional Maturation of iNKT Cells in a Cell-Intrinsic Manner

(A) Radiation BM chimeras were generated as indicated, and 8 weeks after transplantation, iNKT cell numbers were monitored in the thymus, spleen, and liver. Numbers within plots represent % iNKT cells among total lymphocytes. Representative of two independent experiments.

(B) 8 weeks after radiation, BM chimeras were generated and mice were injected with 5 μg αGC or vehicle i.p. and analyzed as described in Figure 2C. Data show mean of three independent experiments ± SEM.

(C) 8 weeks after transplantation, chimeras were injected i.p. with vehicle (gray histograms) or 5 μg αGC (open histograms). After 2 hr, CD69 upregulation was monitored on gated $CD3^+$tetramer$^+$ splenic iNKT cells. Numbers within plots represent % $CD69^+$ iNKT cells. Representative of two independent experiments.

iNKT cells were activated ex vivo with αGC-pulsed wt DC. iNKT cell-DC conjugates were visualized by confocal microscopy. Strikingly, Csf-2-deficient iNKT cells were just as fast and successful in polarizing cortical actin and IFN-γ to the plasma membrane at the site of the immune synapse as were their wt counterparts (Figure 7A). Thus, the early features of the regulated secretory pathway, i.e., formation and polarization of

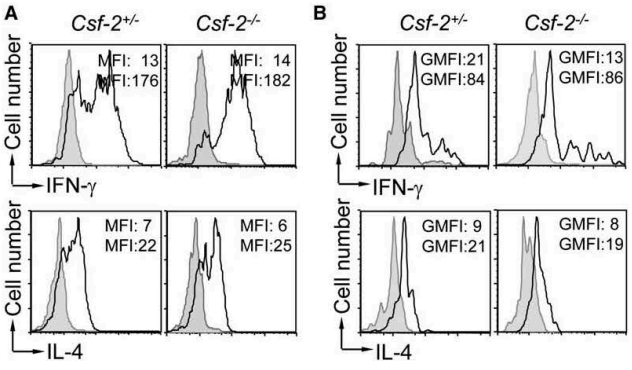

Figure 6. Csf-2 Controls Development of Rapid Cytokine Secretion by Activated iNKT Cells

(A) *Csf-2*$^{+/-}$ and *Csf-2*$^{-/-}$ mice were injected i.p. with 5 μg αGC (open histograms) or vehicle (gray histograms). After 2 hr, $B220^{lo}CD3^+$ tetramer$^+$ cells were electronically gated and intracellular IFN-γ (top), and IL-4 (bottom) expression was monitored. Numbers refer to MFI. Representative of three independent experiments. Numbers represent MFI.

(B) Splenocytes from *Csf-2*$^{+/-}$ and *Csf-2*$^{-/-}$ mice were incubated with vehicle (gray histograms) or 100 ng/ml of αGC (open histograms) for 5 days. $CD3^+$tetramer$^+$ iNKT lymphocytes were identified and analyzed as described in (A). Representative of two independent experiments. Numbers represent geometric MFI.

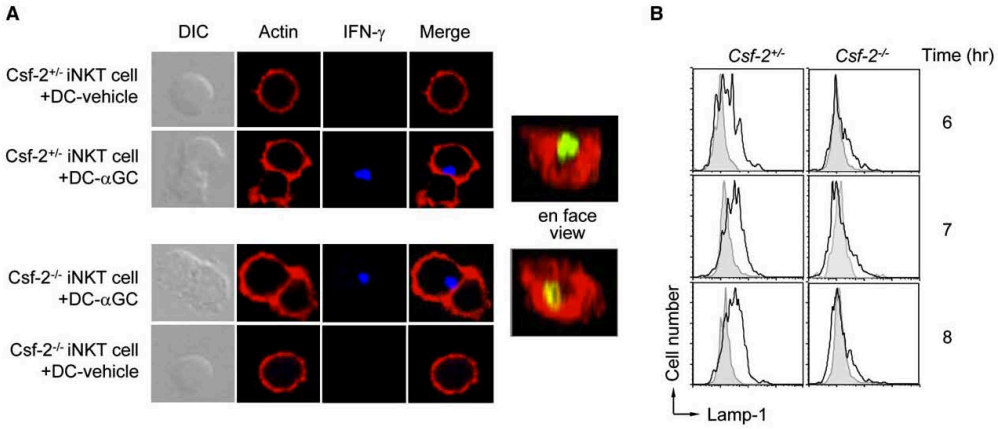

Figure 7. Fusion of Secretory Vesicles with iNKT Cell Plasma Membrane Requires Csf-2

(A) Purified, splenic iNKT cells from 4get;*Csf-2*$^{+/-}$ or 4get;*Csf-2*$^{-/-}$ mice were stimulated with vehicle- (rows 1 and 4) or αGC- (rows 2 and 3) pulsed DC as described in Experimental Procedures. Cells were adhered to cover slips, fixed, made permeable, and reacted with IFN-γ-Alexa647 Ab and phalloidin-rhodamine. Images were visualized by confocal microscopy. z axis image reconstitution over the iNKT cells-DC contact area are far right. Representative images obtained from three independent experiments are shown.

(B) Splenocytes from *Csf-2*$^{+/-}$ and *Csf-2*$^{-/-}$ mice were cultivated with vehicle (gray histograms) or 100 ng/ml αGC (open histograms). iNKT cells were identified as B220^{lo}CD3^{+}tetramer^{+} cells and cell-surface Lamp-1 expression determined. Representative of three independent experiments.

cytokine-containing vesicles, are intact in Csf-2-deficient iNKT cells.

The final release of cytokines from the secretory vesicles requires fusion of the vesicular and plasma membranes. This is a tightly regulated, signal-dependent process (Bossi and Griffiths, 2005). We hypothesized that the fusion of secretory vesicles with the plasma membrane is blocked in Csf-2-deficient iNKT cells. In conventional T lymphocytes, secretory vesicles express lysosomal markers: e.g., Lamp-1, which is normally not found on the cell surface, but appears there transiently upon T cell activation (Peters et al., 1991), an event that can be visualized by flow cytometry of intact cells. Thus, wt and Csf-2-deficient splenocytes were incubated in vitro with αGC, and Lamp-1 expression on gated tetramer^{+} cells was monitored at different times. We found that, although virtually all wt iNKT cells exposed Lamp-1 on the cell surface shortly upon activation (Figure 7B), only a few Csf-2-deficient iNKT cells did so (Figure 7B), despite similar expression patterns of cell surface (Figure S6A) and intracellular (Figure S6B) Lamp-1 on naive wt and Csf-2-deficient iNKT cells. This lack of cell-surface Lamp-1 expression on activated Csf-2-deficient iNKT cells was consistent with the inability of these cells to secrete cytokines. Thus, the cytokine secretion defect in Csf-2-deficient iNKT cells results from the failure to fuse cytokine-containing secretory vesicles with the plasma membrane.

Discussion

Csf-2 is generally recognized as a myeloid growth factor in vitro (Enzler and Dranoff, 2003). Nonetheless, Csf-2 deficiency does not impair myelopoiesis (Dranoff et al., 1994; Stanley et al., 1994), suggesting compensatory roles for other myelopoietic factors. Here we have described a previously unrecognized role for Csf-2 in the immune system, i.e., Csf-2 is critical for the effector differentiation of iNKT cells. Therefore, Csf-2 deficiency during thymic ontogeny results in the generation of iNKT cells that acquire all the attributes of a mature T lymphocyte, yet fail to secrete lineage-specific cytokines. This finding highlights the acquisition of cytokine secretory function as a terminal differentiation step toward the generation of immunocompetent iNKT cells.

iNKT cells share several properties common to NK and conventional T cells. Notwithstanding these similarities, functions of iNKT, NK, and conventional T cells in the immune system are distinct, suggesting that effector differentiation of these cells might require distinct signaling mechanisms. In support of this idea, T-box transcription factor eomesodermin is known to promote effector differentiation of CD8^{+} T and NK, but not CD4^{+} T or iNKT cells (Intlekofer et al., 2005; Pearce et al., 2003; Townsend et al., 2004). Therefore, whether effector differentiation is uniquely regulated in the iNKT cell lineage hitherto remained an unanswered question. Our data suggest that Csf-2 is an iNKT cell lineage-specific effector differentiation signal because Csf-2 deficiency did not alter conventional T or NK cell functions.

Effector differentiation is a process by which committed cells acquire their unique functional properties. It entails unique gene activation programs as observed during Th1 versus Th2 differentiation, translational regulation as seen in NK cells, and, in certain immune cells, the final act of effector molecule release (e.g., mast cells and eosinophils). Effector differentiation of conventional T cells occurs in the periphery upon antigen encounter and, hence, is a postdevelopmental process. In contrast, we found that effector differentiation of iNKT cells regulated by Csf-2 is an ontogenetic process, perhaps because their first encounter with

antigen, i.e., cellular isoglobotrioasylceramide (iGb_3), occurs within the thymus itself (Zhou et al., 2004). Thus, in contrast to conventional T cells, iNKT cell *Il4* and *Ifng* gene loci are transcriptionally active shortly after lineage commitment and positive selection (Matsuda et al., 2003; Stetson et al., 2003), suggesting that iNKT cell effector function is posttranscriptionally regulated. NK1.1$^-$ iNKT cells have already acquired the capacity to secrete IL-4 upon agonistic ligation of their TCR (Benlagha et al., 2002; Pellicci et al., 2002). Our data indicate that Csf-2-deficient thymic and splenic iNKT cells do not secrete IL-4 to agonistic signals, suggesting that (1) iNKT cell effector differentiation occurs at an early stage, shortly after lineage commitment and positive selection, and (2) the acquisition of secretory function regulated by Csf-2 is a terminal step during iNKT cell effector differentiation. Such tight, multilevel regulation of iNKT cell effector function might have evolved to protect this autoreactive, innate lymphocyte against overt reactivity and activation-induced negative selection in the thymus. In addition, this mechanism may have evolved to prevent overt reactivity of peripheral iNKT cells to CD1d-expressing cells that display iGb_3.

Reciprocal BM chimera experiments demonstrated that Csf-2 functions in an iNKT cell-intrinsic manner. We previously discovered that inhibition of NF-κB signaling blocks iNKT cell ontogeny at an immature stage due to the lack of survival signals (Stanic et al., 2004a). Surprisingly, we found that Bcl-x_L transgenesis, which fully reconstitutes what appears to be mature iNKT cells, does not restore iNKT cell function (Stanic et al., 2004b). This finding suggests that NF-κB signaling not only regulates survival but also functional maturation of iNKT cells. Importantly, Csf-2 is an NF-κB-regulated gene (Thomas et al., 1997), and as demonstrated here, Csf-2 partially acts by activating NF-κB. Moreover, 4get transgene introgressed into both IκBΔN and Csf-2-deficient mice yield iNKT cells that fluoresce green due to eGFP expression. Therefore, NF-κB and Csf-2 signaling are dispensable for transcription of the *Il4* locus. Nonetheless, only Csf-2 but not IκBΔN (Stanic et al., 2004b) iNKT cells translate the *Il4* transcript. Therefore, we propose a working model in which NF-κB controls functional maturation of iNKT cell precursors by inducing at least two regulators. The first, identified here as Csf-2, regulates cytokine secretion and the second one, yet to be identified, regulates translation of pretranscribed cytokine mRNA.

Our first glimpse of the iNKT cell-DC synapse reveals that Csf-2 deficiency prevents cytokine release from mature iNKT cells. Therefore, signals emanating from the Csf-2R could be acting on molecules essential for cellular secretion. Within lymphocytes, signal-induced secretion of cytolytic molecules appears to follow the principles of regulated secretion akin to neurotransmitters and hormones (Bossi and Griffiths, 2005; Burgoyne and Morgan, 2003). Secreted molecules packed into vesicles are transported to the synapse, via actin and tubulin cytoskeleton, where vesicles dock at the plasma membrane. Upon receiving agonistic signals, fusion of the secretory and plasma membrane lipid bilayers occurs, resulting in rapid release of the bioactive content into the exocytic space (Morales-Tirado et al., 2004; Murray et al., 2005). Our data place the Csf-2-dependent step at the terminal stage of this complex process. Csf-2-deficient iNKT cells synthesize cytokines and polarize them toward the immune synapse, yet fail to secrete them due to an intrinsic defect in the fusion of secretory vesicles with the plasma membrane. Because activated Csf-2-deficient iNKT cells polarize cortical actin and cytokine-containing vesicles toward the immune synapse, it is unlikely that WASp, Arp2/3, dynamin, and Rab27a, molecules required for vesicle polarization (Burgoyne and Morgan, 2003), mediate Csf-2 action. Moreover, we demonstrated that exogenous Csf-2 provided to activated, peripheral Csf-2-deficient iNKT cells does not restore secretion. Together, these data suggest that Csf-2 is unlikely to act as a direct activation signal for the assembly of the fusion complex. Instead, Csf-2 mediates its activity during ontogeny, as demonstrated here, by either inducing de novo synthesis of protein(s) required for vesicular fusion or by signaling their proper subcellular localization. The nature of the Csf-2-induced factor that regulates secretion and whether it is iNKT cell lineage specific currently remain unanswered questions.

In summary, in studies directed toward understanding when and how iNKT cells attain functional competence, we discovered that Csf-2 plays a novel, critical role in the effector differentiation of these cells. Csf-2 acts at the early thymic iNKT cell precursor stage after lineage commitment and positive selection by regulating the acquisition of secretory function for synapse-directed release of key immunoregulatory cytokines.

Experimental Procedures

Mice

C57BL/6, 129/SvJ, BALB/c-*4get* (4get), and B6.129-*IL-4*$^{-/-}$ (*IL-4*$^{-/-}$) were purchased from the Jackson Laboratory. B6.129-*CD1d1*$^{-/-}$ (*CD1*$^{-/-}$) and B6.129-*Ja18*$^{-/-}$ (*Ja18*$^{-/-}$) mice have been described (Cui et al., 1997; Mendiratta et al., 1997). B6.129-*Csf-2*$^{-/-}$ (Csf-2$^{-/-}$) mice (Stanley et al., 1994), generously provided by Dr. L.J. Old (Ludwig Institute for Cancer Research, NY), were generated by backcrosses to C57BL/6 for 5–6 generations. For sorting of iNKT cells, 4get mice were backcrossed once with Csf-2-deficient mice and the F1 animals were intercrossed; *Csf-2*$^{+/+}$, *Csf-2*$^{+/-}$, and *Csf-2*$^{-/-}$ littermates were used for experiments. All mouse experiments complied with Vanderbilt's IACUC regulations.

Antibodies and Reagents

All Abs, recombinant cytokines, ELISA, cell-surface, and intracellular staining reagents were from BD Pharmingen (Bezbradica et al., 2006), unless stated otherwise. Purified Csf-2Rα-, IκBα- (Santa Cruz Biotechnologies), phospho-IκBα- (Cell Signaling Technologies) specific Abs, anti-rabbit Ig-Alexa 670 (Invitrogen), anti-mouse Ig-IRDye (Rockland Immunochemicals), rhodamine-phalloidin (Invitrogen), and streptavidin-rhodamine (Jackson Immunoresearch Laboratories) were purchased from the indicated sources. Kirin Brewery Company (Gunma, Japan) generously provided αGC. Preparation and use of tetramer are described elsewhere (Bezbradica et al., 2006).

Flow Cytometry

Splenocytes of individual, age (6–10 weeks)-matched mice treated with αGC or vehicle (0.1% Tween 20 in PBS) as control were stained for four-color flow cytometric analysis. Abs and procedures are described elsewhere (Bezbradica et al., 2006). iNKT cells were identified as CD3$^+$tetramer$^+$ cells among B220^{lo} splenocytes and hepatocytes or CD8^{lo} thymocytes. Four-color flow cytometry was performed with a FACSCalibur instrument (Becton Dickinson), and the data were analyzed with FlowJo software (Treestar Inc.). Absolute iNKT cell numbers were calculated from % tetramer$^+$ cells and total number of cells recovered from the organ. Standard error of mean

(SEM) was calculated as the ratio of standard deviation to the square root of n, where n equals sample size.

Intracellular Staining

Splenocytes from mice treated with αGC or vehicle control were blocked with anti-CD16+CD32 (FcγIII/IIR). Cells were first stained for CD3ε and DX5 for NK cells or with anti-CD3ε and tetramer for iNKT cells, and then for IFN-γ, IL-4, or the intracellular domain of Csf-2Rα after fixing and permeabilizing with Cytofix+Cytoperm solution (BD Pharmingen) according to the manufacturer's protocol. Most experiments did not include brefeldin A in any of the steps. Experiments with PMA+ionomycin ± brefeldin A+monensin were performed as described (Stanic et al., 2004b).

ELISA

Each mouse was injected i.p. with 5 μg of αGC or with vehicle as the control. After 2, 4, and 6 hr, sera were collected and sandwich ELISA was performed as described (Bezbradica et al., 2006).

CTL Priming and ELIspot Assay

C57BL/6 and Csf-2-deficient mice were immunized with ~10^7 129 splenocytes in 0.1 ml PBS. A week later, 2.5 × 10^5 immune splenocytes were stimulated with $H2K^b$-restricted peptides (H60 [LTFNYRNL], $H4^b$ [SGIVYIHL], or SV40 epitope IV [VVYDFLKL] [Yoshimura et al., 2004]) in nitrocellulose microtitre plates (Millipore) precoated with anti-IFN-γ Ab (4 μg/ml). After 48 hr at 37°C, plates were washed with PBS containing 0.05% Tween and incubated with biotinylated anti-IFN-γ Ab (2 μg/ml; eBiosciences) for 4 hr at 37°C. After washing, spots were developed by sequential incubation with Vectastain ABC peroxidase (Vector Laboratories) and 3-amino-9-ethyl carbazole (Sigma) and counted with ELISPOT Reader (Zeiss).

Cell Sorting and Adoptive Transfer

Preparation of DCs

Splenic DCs were purified by auto-MACS sorting (Miltenyi Biotec) and pulsed with 0.1–1 μg/ml of αGC overnight. After extensive washes, 6–10 × 10^5 αGC-pulsed DCs were adoptively transferred i.v. into C57BL/6 or Csf-2-deficient mice. Control mice received the same number of vehicle-pulsed DCs. After 6 hr, cytokine response was measured by ELISA.

Enrichment of iNKT Cells

Splenic iNKT cells were enriched as described elsewhere (Bezbradica et al., 2006); average iNKT cell enrichment was up to ~15%.

Purification of iNKT Cells by FACS

Taking advantage of strong green fluorescence, naive, 4get (Matsuda et al., 2003; Stetson et al., 2003) iNKT cells were isolated by FACS. 4get thymocytes were reacted with CD8α and splenocytes with $H2IA^b$, B220, CD8α, and CD11c-specific beads. Labeled cells were removed with auto-MACS sorter and the negative fraction was used immediately for FACS. Granular cells were electronically gated out and $eGFP^+$ cells from a lymphocyte gate were sorted under low (20 psi) pressure at 4°C with FACSAria (Becton Dickinson). Purity of sorted cells was determined with tetramer and anti-CD3ε Ab; purity ranged between 95% and 99%.

Generation of Radiation BM Chimeras

Chimeras were generated as described previously (Bezbradica et al., 2005a) and analyzed 8 or more weeks after transplantation.

CFSE Dilution Assay

Freshly isolated C57BL/6 and Csf-2-deficient splenocytes were labeled with carboxy fluorescein succinimidyl ester (CFSE; Invitrogen) and cultivated with 100 ng/ml αGC or vehicle. After 5 days, cells were stained for B220 (B cells), CD3ε (T and iNKT cells), and tetramer (iNKT cells) and analyzed by flow cytometry.

Western Blot

Purified, primary iNKT cells were treated for 30 min with 1 μM epoxomycin (Sigma) to inhibit proteasome activity prior to activation by 100 ng/ml PMA+2 μM ionomycin (Sigma), 100 ng/ml LPS (Sigma), or 100 ng/ml rmCsf-2 (BD Pharmingen). After 15 min, addition of chilled PBS stopped the reaction. Cells were solubilized in RIPA buffer containing protease and phosphatase inhibitors. Proteins were separated by SDS-PAGE and transferred onto nitrocellulose membrane. Membrane was incubated with rabbit IκBα- and mouse phospho-IκBα-specific Abs followed by anti-rabbit Ig-Alexa670 and anti-mouse Ig-IRDye. Proteins were visualized by infrared imaging (Odyssey, LI-COR).

Csf-2 Complementation Experiments

Ex Vivo Thymic Csf-2 Complementation

Thymocytes of 2- to 42-day-old mice were cultivated for 14 days in vitro in the presence of 10 ng/ml rhIL-7, 100 ng/ml rhIL-15, and 100 ng/ml rmCsf-2 (BD Biosciences) individually or in combination as indicated. Cultures were supplemented with fresh medium and cytokines every 2 days. After 14 days, thymic cultures were stimulated overnight with vehicle- or αGC-loaded DCs in 1:100 DC:thymocyte ratio. Secreted cytokines were monitored in culture supernatant by ELISA.

In Vivo Csf-2 Complementation

Doses of 50–1000 ng of rmCsf-2 were coinjected with αGC into 6- to 8-week-old C57BL/6 or Csf-2-deficient mice. After 2, 4, and 6 hr, sera were collected for ELISA.

Ex Vivo Splenic Csf-2 Complementation

Splenocytes were cultivated in vitro with 10–500 ng/ml αGC ± 100 ng rmCsf-2 for 5 days. Every 24 hr, 100 μl of supernatant was collected for ELISA.

Confocal Microscopy

Splenic iNKT cells from 4get;$Csf\text{-}2^{+/-}$ or 4get;$Csf\text{-}2^{-/-}$ mice were purified by FACS and expanded in vitro for 3–5 days in the presence of 10 ng/ml rhIL-7 and 100 ng/ml rhIL-15. iNKT cells (~1–2 × 10^6) were stimulated with ~10^5 vehicle- or αGC-pulsed DCs in suspension for 30 min at 37°C to form conjugates, layered over poly-L-lysine-coated glass cover slips, and incubated for an additional 20–30 min to adhere. Cells were fixed with 3.7% paraformaldehyde for 10 min at room temperature (RT). After washes with PBS, cells were made permeable for intracellular staining and reacted with anti-IFN-γ-Alexa647 (BD Pharmingen) and phalloidin-rhodamine. After 1 hr at RT, cells on cover slips were fixed with 2% paraformaldehyde for 10 min and washed. The cover slips were mounted on slides and sealed with Aqua PolyMount (Polysciences, Inc.). Images were viewed with 63× oil objective on LSM 510 META inverted confocal microscope and captured with Zeiss LSM Image software. About 20–30 images per sample were scored per experiment. z-axis image reconstitution of the iNKT cell-DC contact area was visualized with Zeiss LSM5 Image Examiner Software.

Supplemental Data

Six Supplemental Figures can be found with this article online at http://www.immunity.com/cgi/content/full/25/3/487/DC1/.

Acknowledgments

We thank L.J. Old for Csf-2-deficient mice; N. Matsuki for the initial characterization of Csf-2-deficient mice; Kirin Brewery Co., Ltd., for αGC; S. Schaffer (Cell Imaging Shared Resource Core), J. Higginbotham (Flow Cytometry Core/Ingram Cancer Center), C. Alford (VA Flow Cytometry Special Resource Center, Nashville, VA), and A.J. Joyce for technical assistance; and M.R. Boothby, W.N. Khan, B. Cotter, and N. Shinners for helpful discussions. Supported by grants (AI042284 and AI061721 to S.J., HL069542 and HL068744 to J.H., AI054206 to D.U., and AI050953 and NS044044 to L.V.K.) from the NIH, The Juvenile Diabetes Research Foundation (S.J.), and Human Frontier Science Program (S.J.).

Received: January 5, 2006
Revised: May 26, 2006
Accepted: June 16, 2006
Published online: August 31, 2006

References

Benlagha, K., Kyin, T., Beavis, A., Teyton, L., and Bendelac, A. (2002). A thymic precursor to the NK T cell lineage. Science *296*, 553–555.

Benlagha, K., Wei, D.G., Veiga, J., Teyton, L., and Bendelac, A. (2005). Characterization of the early stages of thymic NKT cell development. J. Exp. Med. *202*, 485–492.

Bezbradica, J.S., Hill, T., Stanic, A.K., Van Kaer, L., and Joyce, S. (2005a). Commitment toward the natural T (iNKT) cell lineage occurs at the $CD4^+8^+$ stage of thymic ontogeny. Proc. Natl. Acad. Sci. USA *102*, 5114–5119.

Bezbradica, J.S., Stanic, A.K., Matsuki, N., Bour-Jordan, H., Bluestone, J.A., Thomas, J.W., Unutmaz, D., Van Kaer, L., and Joyce, S. (2005b). Distinct roles of dendritic cells and B cells in Va14Ja18 natural T cell activation in vivo. J. Immunol. *174*, 4696–4705.

Bezbradica, J.S., Stanic, A.K., and Joyce, S. (2006). Characterization and functional analysis of mouse invariant natural T (iNKT) cells. Curr. Protocols Immunol. 14.13.11–14.13.27.

Bossi, G., and Griffiths, G.M. (2005). CTL secretory lysosomes: biogenesis and secretion of a harmful organelle. Semin. Immunol. *17*, 87–94.

Brigl, M., Bry, L., Kent, S.C., Gumperz, J.E., and Brenner, M.B. (2003). Mechanism of CD1d-restricted natural killer T cell activation during microbial infection. Nat. Immunol. *4*, 1230–1237.

Burdin, N., Brossay, L., and Kronenberg, M. (1999). Immunization with α-galactosylceramide polarizes CD1-reactive NK T cells towards Th2 cytokine synthesis. Eur. J. Immunol. *29*, 2014–2025.

Burgoyne, R.D., and Morgan, A. (2003). Secretory granule exocytosis. Physiol. Rev. *83*, 581–632.

Carnaud, C., Lee, D., Donnars, O., Park, S.H., Beavis, A., Koezuka, Y., and Bendelac, A. (1999). Cross-talk between cells of the innate immune system: NKT cells rapidly activate NK cells. J. Immunol. *163*, 4647–4650.

Chung, B., Aoukaty, A., Dutz, J., Terhorst, C., and Tan, R. (2005). Signaling lymphocytic activation molecule-associated protein controls NKT cell functions. J. Immunol. *174*, 3153–3157.

Crowe, N.Y., Uldrich, A.P., Kyparissoudis, K., Hammond, K.J., Hayakawa, Y., Sidobre, S., Keating, R., Kronenberg, M., Smyth, M.J., and Godfrey, D.I. (2003). Glycolipid antigen drives rapid expansion and sustained cytokine production by NK T cells. J. Immunol. *171*, 4020–4027.

Cui, J., Shin, T., Kawano, T., Sato, H., Kondo, E., Toura, I., Kaneko, Y., Koseki, H., Kanno, M., and Taniguchi, M. (1997). Requirement for Vα14 NKT cells in IL-12-mediated rejection of tumors. Science *278*, 1623–1626.

Dranoff, G., Crawford, A.D., Sadelain, M., Ream, B., Rashid, A., Bronson, R.T., Dickersin, G.R., Bachurski, C.J., Mark, E.L., Whitsett, J.A., et al. (1994). Involvement of granulocyte-macrophage colony-stimulating factor in pulmonary homeostasis. Science *264*, 713–716.

Eberl, G., Lowin-Kropf, B., and MacDonald, H.R. (1999). NKT cell development is selectively impaired in Fyn-deficient mice. J. Immunol. *163*, 4091–4094.

Ebner, K., Bandion, A., Binder, B.R., de Martin, R., and Schmid, J.A. (2003). GMCSF activates NF-κB via direct interaction of the GMCSF receptor with IκB kinase β. Blood *102*, 192–199.

Egawa, T., Eberl, G., Taniuchi, I., Benlagha, K., Geissmann, F., Hennighausen, L., Bendelac, A., and Littman, D.R. (2005). Genetic evidence supporting selection of the Vα14i NKT cell lineage from double-positive thymocyte precursors. Immunity *22*, 705–716.

Enzler, T., and Dranoff, G. (2003). Granulocyte-macrophage colony-stimulating factor. In The Cytokine Handbook, A.W. Thomson and M.T. Lotze, eds. (San Diego: Academic Press), pp. 503–524.

Fujii, S., Shimizu, K., Smith, C., Bonifaz, L., and Steinman, R.M. (2003). Activation of natural killer T cells by α-galactosylceramide rapidly induces the full maturation of dendritic cells in vivo and thereby acts as an adjuvant for combined CD4 and CD8 T cell immunity to a coadministered protein. J. Exp. Med. *198*, 267–279.

Gadue, P., and Stein, P.L. (2002). NK T cell precursors exhibit differential cytokine regulation and require Itk for efficient maturation. J. Immunol. *169*, 2397–2406.

Gadue, P., Morton, N., and Stein, P.L. (1999). The Src family tyrosine kinase Fyn regulates natural killer T cell development. J. Exp. Med. *190*, 1189–1196.

Gapin, L., Matsuda, J.L., Surh, C.D., and Kronenberg, M. (2001). NKT cells derive from double-positive thymocytes that are positively selected by CD1d. Nat. Immunol. *2*, 971–978.

Hermans, I.F., Silk, J.D., Gileadi, U., Salio, M., Mathew, B., Ritter, G., Schmidt, R., Harris, A.L., Old, L., and Cerundolo, V. (2003). NKT cells enhance $CD4^+$ and $CD8^+$ T cell responses to soluble antigen in vivo through direct interaction with dendritic cells. J. Immunol. *171*, 5140–5147.

Intlekofer, A.M., Takemoto, N., Wherry, E.J., Longworth, S.A., Northrup, J.T., Palanivel, V.R., Mullen, A.C., Gasink, C.R., Kaech, S.M., Miller, J.D., et al. (2005). Effector and memory CD8+ T cell fate coupled by T-bet and eomesodermin. Nat. Immunol. *6*, 1236–1244.

Kinjo, Y., Wu, D., Kim, G., Xing, G.W., Poles, M.A., Ho, D.D., Tsuji, M., Kawahara, K., Wong, C.H., and Kronenberg, M. (2005). Recognition of bacterial glycosphingolipids by natural killer T cells. Nature *434*, 520–525.

Lacorazza, H.D., Miyazaki, Y., Di Cristofano, A., Deblasio, A., Hedvat, C., Zhang, J., Cordon-Cardo, C., Mao, S., Pandolfi, P.P., and Nimer, S.D. (2002). The ETS protein MEF plays a critical role in perforin gene expression and the development of natural killer and NK-T cells. Immunity *17*, 437–449.

Matsuda, J.L., Gapin, L., Baron, J.L., Sidobre, S., Stetson, D.B., Mohrs, M., Locksley, R.M., and Kronenberg, M. (2003). Mouse Vα14i natural killer T cells are resistant to cytokine polarization in vivo. Proc. Natl. Acad. Sci. USA *100*, 8395–8400.

Mattner, J., Debord, K.L., Ismail, N., Goff, R.D., Cantu, C., III, Zhou, D., Saint-Mezard, P., Wang, V., Gao, Y., Yin, N., et al. (2005). Exogenous and endogenous glycolipid antigens activate NKT cells during microbial infections. Nature *434*, 525–529.

Mendiratta, S.K., Martin, W.D., Hong, S., Boesteanu, A., Joyce, S., and Van Kaer, L. (1997). CD1d1 mutant mice are deficient in natural T cells that promptly produce IL-4. Immunity *6*, 469–477.

Morales-Tirado, V., Johannson, S., Hanson, E., Howell, A., Zhang, J., Siminovitch, K.A., and Fowell, D.J. (2004). Selective requirement for the Wiskott-Aldrich syndrome protein in cytokine, but not chemokine, secretion by $CD4^+$ T cells. J. Immunol. *173*, 726–730.

Murray, R.Z., Kay, J.G., Sangermani, D.G., and Stow, J.L. (2005). A role for the phagosome in cytokine secretion. Science *310*, 1492–1495.

Pasquier, B., Yin, L., Fondaneche, M.C., Relouzat, F., Bloch-Queyrat, C., Lambert, N., Fischer, A., de Saint-Basile, G., and Latour, S. (2005). Defective NKT cell development in mice and humans lacking the adapter SAP, the X-linked lymphoproliferative syndrome gene product. J. Exp. Med. *201*, 695–701.

Pearce, E.L., Mullen, A.C., Martins, G.A., Krawczyk, C.M., Hutchins, A.S., Zediak, V.P., Banica, M., DiCioccio, C.B., Gross, D.A., Mao, C.A., et al. (2003). Control of effector CD8+ T cell function by the transcription factor Eomesodermin. Science *302*, 1041–1043.

Pellicci, D.G., Hammond, K.J., Uldrich, A.P., Baxter, A.G., Smyth, M.J., and Godfrey, D.I. (2002). A natural killer T (NKT) cell developmental pathway involving a thymus-dependent $NK1.1^-CD4^+$ CD1d-dependent precursor stage. J. Exp. Med. *195*, 835–844.

Peters, P.J., Borst, J., Oorschot, V., Fukuda, M., Krahenbuhl, O., Tschopp, J., Slot, J.W., and Geuze, H.J. (1991). Cytotoxic T lymphocyte granules are secretory lysosomes, containing both perforin and granzymes. J. Exp. Med. *173*, 1099–1109.

Sato, H., Nakayama, T., Tanaka, Y., Yamashita, M., Shibata, Y., Kondo, E., Saito, Y., and Taniguchi, M. (1999). Induction of differentiation of pre-NKT cells to mature Vα14 NKT cells by granulocyte/macrophage colony-stimulating factor. Proc. Natl. Acad. Sci. USA *96*, 7439–7444.

Schmidt-Supprian, M., Tian, J., Grant, E.P., Pasparakis, M., Maehr, R., Ovaa, H., Ploegh, H.L., Coyle, A.J., and Rajewsky, K. (2004). Differential dependence of $CD4^+CD25^+$ regulatory and natural killer-like T cells on signals leading to NF-κB activation. Proc. Natl. Acad. Sci. USA *101*, 4566–4571.

Schmieg, J., Yang, G., Franck, R.W., Van Rooijen, N., and Tsuji, M. (2005). Glycolipid presentation to natural killer T cells differs in an organ-dependent fashion. Proc. Natl. Acad. Sci. USA *102*, 1127–1132.

Silk, J.D., Hermans, I.F., Gileadi, U., Chong, T.W., Shepherd, D., Salio, M., Mathew, B., Schmidt, R.R., Lunt, S.J., Williams, K.J., et al. (2004). Utilizing the adjuvant properties of CD1d-dependent NK T cells in T cell-mediated immunotherapy. J. Clin. Invest. *114*, 1800–1811.

Singh, N., Hong, S., Scherer, D.C., Serizawa, I., Burdin, N., Kronenberg, M., Koezuka, Y., and Van Kaer, L. (1999). Activation of NK T cells by CD1d and α-galactosylceramide directs conventional T cells to the acquisition of a Th2 phenotype. J. Immunol. *163*, 2373–2377.

Sivakumar, V., Hammond, K.J., Howells, N., Pfeffer, K., and Weih, F. (2003). Differential requirement for Rel/nuclear factor kappa B family members in natural killer T cell development. J. Exp. Med. *197*, 1613–1621.

Smyth, M.J., Crowe, N.Y., Pellicci, D.G., Kyparissoudis, K., Kelly, J.M., Takeda, K., Yagita, H., and Godfrey, D.I. (2002). Sequential production of interferon-γ by NK1.1$^+$ T cells and natural killer cells is essential for the antimetastatic effect of α-galactosylceramide. Blood *99*, 1259–1266.

Sriram, V., Du, W., Gervay-Hague, J., and Brutkiewicz, R.R. (2005). Cell wall glycosphingolipids of *Sphingomonas paucimobilis* are CD1d-specific ligands for NKT cells. Eur. J. Immunol. *35*, 1692–1701.

Stanic, A.K., Bezbradica, J.S., Park, J.J., Matsuki, N., Mora, A.L., Van Kaer, L., Boothby, M.R., and Joyce, S. (2004a). NF-κB controls cell fate specification, survival, and molecular differentiation of immunoregulatory natural T lymphocytes. J. Immunol. *172*, 2265–2273.

Stanic, A.K., Bezbradica, J.S., Park, J.J., Van Kaer, L., Boothby, M.R., and Joyce, S. (2004b). The ontogeny and function of Va14Ja18 natural T lymphocytes require signal processing by protein kinase Cθ and NF-κB. J. Immunol. *172*, 4667–4671.

Stanley, E., Lieschke, G.J., Grail, D., Metcalf, D., Hodgson, G., Gall, J.A., Maher, D.W., Cebon, J., Sinickas, V., and Dunn, A.R. (1994). Granulocyte/macrophage colony-stimulating factor-deficient mice show no major perturbation of hematopoiesis but develop a characteristic pulmonary pathology. Proc. Natl. Acad. Sci. USA *91*, 5592–5596.

Stetson, D.B., Mohrs, M., Reinhardt, R.L., Baron, J.L., Wang, Z.E., Gapin, L., Kronenberg, M., and Locksley, R.M. (2003). Constitutive cytokine mRNAs mark natural killer (NK) and NK T cells poised for rapid effector function. J. Exp. Med. *198*, 1069–1076.

Thomas, R.S., Tymms, M.J., McKinlay, L.H., Shannon, M.F., Seth, A., and Kola, I. (1997). ETS1, NFκB and AP1 synergistically transactivate the human GM-CSF promoter. Oncogene *14*, 2845–2855.

Townsend, M.J., Weinmann, A.S., Matsuda, J.L., Salomon, R., Farnham, P.J., Biron, C.A., Gapin, L., and Glimcher, L.H. (2004). T-bet regulates the terminal maturation and homeostasis of NK and Vα14i NKT cells. Immunity *20*, 477–494.

Van Kaer, L. (2005). α-Galactosylceramide therapy for autoimmune diseases: prospects and obstacles. Nat. Rev. Immunol. *5*, 31–42.

Wada, H., Noguchi, Y., Marino, M.W., Dunn, A.R., and Old, L.J. (1997). T cell functions in granulocyte/macrophage colony-stimulating factor deficient mice. Proc. Natl. Acad. Sci. USA *94*, 12557–12561.

Walunas, T.L., Wang, B., Wang, C.R., and Leiden, J.M. (2000). The Ets1 transcription factor is required for the development of NK T cells in mice. J. Immunol. *164*, 2857–2860.

Wilson, M.T., Johansson, C., Olivares-Villagomez, D., Singh, A.K., Stanic, A.K., Wang, C.R., Joyce, S., Wick, M.J., and Van Kaer, L. (2003). The response of natural killer T cells to glycolipid antigens is characterized by surface receptor down-modulation and expansion. Proc. Natl. Acad. Sci. USA *100*, 10913–10918.

Yoshimoto, T., and Paul, W.E. (1994). CD4^{pos}, NK1.1^{pos} T cells promptly produce interleukin 4 in response to in vivo challenge with anti-CD3. J. Exp. Med. *179*, 1285–1295.

Yoshimura, Y., Yadav, R., Christianson, G.J., Ajayi, W.U., Roopenian, D.C., and Joyce, S. (2004). Duration of alloantigen presentation and avidity of T cell antigen recognition correlate with immunodominance of CTL response to minor histocompatibility antigens. J. Immunol. *172*, 6666–6674.

Zhou, D., Mattner, J., Cantu, C., III, Schrantz, N., Yin, N., Gao, Y., Sagiv, Y., Hudspeth, K., Wu, Y.P., Yamashita, T., et al. (2004). Lysosomal glycosphingolipid recognition by NKT cells. Science *306*, 1786–1789.